

**ASSESSING THE NITROGEN SATURATION STATUS OF APPALACHIAN FORESTS
USING STABLE ISOTOPES OF NITRATE**

by

Lucy Ann Rose

B.S. in Plant Biology, University of Illinois at Urbana-Champaign, 1998

M.S. in Natural Resources and Environmental Sciences, University of Illinois
at Urbana-Champaign, 2003

Submitted to the Graduate Faculty of

The Kenneth P. Dietrich School of Arts and Sciences in partial fulfillment

of the requirements for the degree of

Doctor of Philosophy

University of Pittsburgh

2014

UNIVERSITY OF PITTSBURGH

Kenneth P. Dietrich School of Arts and Sciences

This dissertation was presented

by

Lucy A. Rose

It was defended on

July 16, 2014

and approved by

Mary Beth Adams, Ph.D., Research Soil Scientist, USDA Forest Service

Daniel Bain, Ph.D., Assistant Professor, Department of Geology and Planetary Science

Brian Stewart, Ph.D., Associate Professor, Department of Geology and Planetary Science

Josef Werne, Ph.D., Associate Professor, Department of Geology and Planetary Science

Dissertation Advisor: Emily Elliott, Ph.D., Assistant Professor, Department of Geology and
Planetary Science

Copyright © by Lucy A. Rose

2014

**ASSESSING THE NITROGEN SATURATION STATUS OF APPALACHIAN
FORESTS USING STABLE ISOTOPES OF NITRATE**

Lucy A. Rose, PhD

University of Pittsburgh, 2014

Chronic elevated nitrogen (N) deposition can lead to ecosystem N saturation, which is theorized to occur when N supply exceeds biological demand and excess N leaches to receiving waters. This research examined the post-depositional fate and transport of atmospheric nitrate in Appalachian forests across spatial and temporal scales by characterizing the nitrate stable isotopic composition ($\delta^{15}\text{N}$, $\delta^{18}\text{O}$, and $\Delta^{17}\text{O}$) of precipitation, soil water, and streams. Data indicate that elevated N deposition does not saturate biological demand; rather, N processing becomes more extensive as N availability increases. Along a regional N deposition gradient (North Carolina to New Hampshire), mean proportions of atmospheric nitrate in streams were inversely related to long-term annual average nitrate deposition. Stream nitrate concentrations were also negatively correlated to the proportion of atmospheric nitrate in streams ($R^2=0.23$; $p<0.05$). Similar relationships occurred along an N saturation gradient in four watersheds at Fernow Experimental Forest (West Virginia). The most N-saturated watershed had the highest stream nitrate concentrations (mean=3.7 mg L⁻¹) but the lowest proportions of atmospheric nitrate in the stream (mean=5%). Conversely, the stream in the N-limited watershed had the lowest nitrate concentrations (mean=0.0 mg L⁻¹) and the highest proportions of atmospheric nitrate (mean=42% among samples with sufficient nitrate for isotope analysis). High spatial variability of nitrate sources in one watershed at Fernow (WS4) suggests a decoupling of source

dynamics across spatial scales. Proportions of atmospheric nitrate in soil solution ranged from zero to 96% across WS4, but consistently low proportions of atmospheric nitrate in the stream suggest that watershed areas with high proportions of atmospheric nitrate may not contribute significantly to the stream. Storm event water and nitrate isotope data support this idea, indicating transient hydrologic flowpaths from hillslopes to the stream during storms. Although these transient flowpaths resulted in a wide range of mean event water contributions to stormflow (6% to 34%) during events, the maximum proportion of atmospheric nitrate in stormflow was only 8%. These trends in nitrate source contributions to streams along gradients of space, time, N deposition, and N saturation suggest that the widely-accepted mechanisms of nitrogen saturation require reevaluation.

TABLE OF CONTENTS

PREFACE.....	XVIII
1.0 INTRODUCTION.....	1
1.1 STABLE ISOTOPES AS TRACERS OF BIOGEOCHEMICAL CYCLING.. ..	5
1.2 STUDY SITE.....	8
1.3 ATMOSPHERIC NITRATE PROCESSING AND T RANSPORT IN APPALACHIAN FORESTS	10
2.0 DRIVERS OF ATMOSPHERIC NITRATE PROCESSING IN FORESTED WATERSHEDS	13
2.1 INTRODUCTION	13
2.2 MAJOR DRIVERS INFLUENCING ATMOSPHERIC NITRATE TRANSPORT IN WATERSHEDS.....	17
2.2.1 Methodological Biases	22
2.2.1.1 Frequency, Seasonality, and Scale of Sample Collection	23
2.2.1.2 Analytical Biases	25
2.2.2 Biological Drivers	30
2.2.2.1 Terrestrial Nitrogen Processing.....	30

2.2.2.2	In-stream Nitrogen Processing	33
2.2.2.3	Phase of Nitrogen Deposition and Synchrony with Biological Processing	35
2.2.3	Physical Drivers	38
2.2.3.1	Hydrologic Regime.....	38
2.2.3.2	Landscape Characteristics	42
2.3	KNOWLEDGE GAPS AND NEXT STEPS WITH RESPECT TO FUTURE EXPERIMENTS, OBSERVATIONS, AND INTERDISCIPLINARY RESEARCH ..	44
2.3.1	High Resolution Temporal and Spatial Sampling of Nitrate Isotopes	46
2.3.2	Understanding Internal Water Cycling Dynamics at Relevant Catchment Scales... ..	46
2.3.3	Models to Conceptualize and Parameterize Distinctions among Nitrate and Water Sources	47
2.4	IMPLICATIONS	48
3.0	TEMPORAL TRENDS IN STREAM NITRATE SOURCES ACROSS A NITROGEN SATURATION GRADIENT	50
3.1	INTRODUCTION	50
3.2	STUDY SITE AND METHODS.....	53
3.2.1	Study Site.....	53
3.2.2	Sample Collection	54
3.2.3	Isotopic Analysis	56
3.2.4	Statistical Analysis.....	58
3.3	RESULTS	59

3.3.1	Nitrate Concentration	59
3.3.2	$\delta^{15}\text{N}$ of Nitrate	62
3.3.3	$\delta^{18}\text{O}$ of Nitrate.....	63
3.3.4	$\Delta^{17}\text{O}$ of Nitrate	64
3.4	DISCUSSION.....	65
3.4.1	Atmospheric Nitrate Processing and Export across a Nitrogen Saturation Gradient	65
3.4.2	Seasonal Variability of Stream Nitrate Isotopic Composition	70
3.4.3	Hydrologic Drivers of Watershed Atmospheric Nitrate Export	76
3.4.4	Implications for Nitrogen Saturation Theory	77
3.5	CONCLUSION	81
4.0	DECOUPLED NITRATE SOURCE DYNAMICS IN WATERSHEDS ACROSS SPATIAL SCALES.....	83
4.1	INTRODUCTION	83
4.2	STUDY SITE AND METHODS.....	86
4.2.1	Study Site.....	86
4.2.2	Sample Collection	87
4.2.3	Isotopic Analysis	88
4.2.4	Statistical Analysis.....	90
4.3	RESULTS	91
4.3.1	Soil Water Nitrate Concentrations	91
4.3.2	Soil Water Nitrate Isotopes.....	96
4.3.3	Soil Nitrogen and Carbon Isotopes	97

4.4	DISCUSSION	98
4.4.1	Intra-watershed Variability of Nitrate Sources	98
4.4.2	Decoupled Nitrate Biogeochemical Signals Across Spatial Scales	104
4.5	CONCLUSION	109
5.0	ISOTOPIC VARIABILITY OF PRECIPITATION NITRATE DURING GROWING SEASON STORM EVENTS	111
5.1	INTRODUCTION	111
5.2	STUDY SITE AND METHODS	115
5.2.1	Study Site	115
5.2.2	Sample Collection	116
5.2.3	Isotopic Analysis	117
5.2.4	Electricity-Generating Unit NO_x Quantification	120
5.2.5	Biogenic NO_x Quantification	121
5.2.6	Statistical Analysis	122
5.3	RESULTS	122
5.3.1	Precipitation Nitrate Concentrations	122
5.3.2	$\delta^{15}\text{N}$ of Precipitation Nitrate	126
5.3.3	$\delta^{18}\text{O}$ of Precipitation Nitrate	127
5.3.4	$\Delta^{17}\text{O}$ of Precipitation Nitrate	128
5.3.5	$\delta^{18}\text{O}$ of Water in Precipitation	128
5.3.6	Biogenic NO_x Flux Measurements and Mixing Model Results	129
5.4	DISCUSSION	130
5.4.1	Anthropogenic and Biogenic NO_x Sources	130

5.4.2	Atmospheric Oxidation Chemistry	135
5.4.3	Rainout/Washout Processes.....	136
5.5	CONCLUSION	137
6.0	HYDROLOGIC AND NITROGEN BIOGEOCHEMICAL SOURCE DYNAMICS DURING GROWING SEASON STORM EVENTS IN A NITROGEN-SATURATED WATERSHED.....	139
6.1	INTRODUCTION	139
6.2	STUDY SITE AND METHODS.....	143
6.2.1	Study Site.....	143
6.2.2	Sample Collection	144
6.2.3	Isotopic Analysis	145
6.2.4	End-Member Mixing Analysis	148
6.2.5	Statistical Analysis.....	150
6.3	RESULTS	151
6.3.1	Nitrate Concentrations in Precipitation and Stormflow.....	151
6.3.2	Nitrate Isotopic Compositions of Precipitation and Stormflow	153
6.3.3	$\delta^{18}\text{O}\text{-H}_2\text{O}$ in Precipitation, Stormflow, and Soil Water	155
6.4	DISCUSSION.....	157
6.4.1	Sources of Stream Nitrate in Watershed 4.....	157
6.4.2	Drivers of Nitrate Export During Storms	159
6.4.3	Variable Source Areas of Stream Water and Nitrate during Storms	162
6.5	CONCLUSION	165

7.0	ECOSYSTEM PROCESSING OF ATMOSPHERIC NITRATE ALONG A NITROGEN DEPOSITION GRADIENT	167
7.1	INTRODUCTION	167
7.2	STUDY SITES AND METHODS	171
7.2.1	Study Sites	171
7.2.2	Sample Collection	173
7.2.3	Isotopic Analysis	174
7.2.4	Statistical Analysis.....	176
7.3	RESULTS	176
7.4	DISCUSSION.....	184
7.4.1	Atmospheric Nitrate Processing and Export	184
7.4.2	Seasonal Patterns of Precipitation Nitrate Isotopes	188
7.5	CONCLUSION	190
8.0	CONCLUSIONS	192
	APPENDIX A	196
	APPENDIX B	205
	APPENDIX C	209
	APPENDIX D	212
	APPENDIX E	216
	BIBLIOGRAPHY	220

LIST OF TABLES

Table 2.1. Site descriptions, nitrogen deposition and precipitation characteristics, and methods of nitrate isotope determination.	18
Table 2.2. Nitrate end-member $\delta^{15}\text{N}$ and $\delta^{18}\text{O}$ values and estimation methods, and fraction of atmospheric nitrate in streams.	20
Table 3.1. Description of study watersheds.....	55
Table 3.2. Means and ranges of precipitation and stream nitrate concentration and triple nitrate isotope values in study watersheds.	61
Table 4.1. Monthly mean, range, and coefficient of variation of soil water nitrate concentration and triple nitrate isotopes in WS4.....	93
Table 4.2. Mean, range, and coefficient of variation of soil water nitrate concentration and triple nitrate isotopes on east- and south-facing aspects of WS4.....	96
Table 5.1. Characteristics of six storm events sampled at Fernow Experimental Forest during 2010.....	124
Table 6.1. Precipitation and discharge characteristics of the three growing season storms at Fernow Experimental Forest.....	145

Table 6.2. Volume-weighted mean precipitation and stormflow nitrate concentrations and isotopic compositions during three growing season storms	153
Table 7.1. Description of study watersheds	173
Table 7.2. Mean concentrations and isotope values of nitrate in precipitation and stream water for study watersheds at Coweeta (CWT), Fernow (FEF), and Hubbard Brook (HBR) Experimental Forests.	179
Table 7.3. Mean concentrations and isotope values of nitrate in precipitation and stream water at individual study sites.....	181
Table 7.4. Mean cool (November-April) and warm (May-October) seasons precipitation and stream nitrate concentrations and isotope values.....	183
Table A-1 Nitrate concentration, nitrate isotope, and water isotope data for weekly stream and precipitation samples	196
Table B-1 Nitrate concentration, nitrate isotope, and water isotope data for monthly soil solution samples.....	205
Table C-1 Precipitation amount, nitrate concentration, nitrate isotope, and water isotope data for hourly precipitation samples.....	209
Table D-1 Discharge amount, nitrate concentration, nitrate isotope, and water isotope data for hourly stream samples.....	212
Table E-1 Nitrate concentration, nitrate isotope, and water isotope data for monthly precipitation and stream samples	216

LIST OF FIGURES

Figure 1.1. Annual average wet nitrate (a, b, c) and inorganic nitrogen (d, e, f) deposition rates at National Atmospheric Deposition Program monitoring sites from 1985 to 2012.....	2
Figure 1.2. Commonly reported values of $\delta^{15}\text{N}$ and $\delta^{18}\text{O}$ of nitrate for various sources.....	7
Figure 1.3. Triple isotope plot of $\delta^{18}\text{O}$, $\delta^{17}\text{O}$, and $\Delta^{17}\text{O}$	8
Figure 1.4. Experimental watersheds within the larger boundary of the Fernow Experimental Forest (FEF).....	10
Figure 2.1. Percent atmospheric nitrate (NO_3^-/atm) in streams as reported in various catchment-scale isotope tracer studies.....	22
Figure 2.2. Relationship of average percent atmospheric nitrate in streams to (a) long-term (1984 to the study year) average total wet inorganic N deposition, (b) long-term (1984 to the study year) average total wet NO_3^-/N deposition, and (c) annual average total precipitation (for study years only) at sites across the northeastern U.S. and eastern Canada.....	24
Figure 2.3. Estimated $\delta^{18}\text{O}-\text{NO}_3^-$ means (black dots) and ranges (shaded areas) for (a) atmospheric and (b) microbial nitrate end-members using various analytical techniques.	28
Figure 2.4. Streamflow versus stream $\delta^{18}\text{O}-\text{NO}_3^-$ values during (a) baseflow and (b) stormflow/snowmelt events at multiple sites.....	40

Figure 2.5. Conceptual model of hydrological and topographic regulation of catchment-scale atmospheric nitrate export.....	45
Figure 3.1. Average monthly stream nitrate concentrations in the four study watersheds at Fernow Experimental Forest from 1980-2010.....	56
Figure 3.2. Boxplots of stream and precipitation nitrate concentrations, $\delta^{15}\text{N}$, $\delta^{18}\text{O}$, and $\Delta^{17}\text{O}$ isotopes.	60
Figure 3.3. Nitrate concentration and isotopic composition of weekly stream and precipitation samples collected at Fernow Experimental Forest during 2010.	62
Figure 3.4. Temporal trends in stream water nitrate isotopic composition in the hardwood-dominated watersheds.....	73
Figure 3.5. Conceptual model of atmospheric nitrate processing and export dynamics under N-limitation and N-saturation.	80
Figure 4.1. Map of lysimeters in Watershed 4 at Fernow Experimental Forest (FEF).....	87
Figure 4.2. Monthly soil water nitrate (a) concentration, (b) $\delta^{15}\text{N}$, (c) $\delta^{18}\text{O}$, and (d) $\Delta^{17}\text{O}$ in WS4.....	92
Figure 4.3. Nitrate (a) concentration, (b) $\delta^{15}\text{N}$, (c) $\delta^{18}\text{O}$, and (d) $\Delta^{17}\text{O}$ on the dominant aspects of WS4.....	95
Figure 4.4. Median A horizon soil water nitrate (a) concentrations, (b) $\delta^{15}\text{N}$, (c) $\Delta^{17}\text{O}$, and (d) A horizon soil C:N ratios at lysimeter locations across WS4.....	101
Figure 4.5. Median percent atmospheric nitrate in lysimeters across WS4.....	102
Figure 4.6. Percent of atmospheric nitrate in stream samples collected weekly at the base of WS4 (black circles).....	107

Figure 5.1. Means and ranges of precipitation (a) nitrate concentration, (b) $\delta^{15}\text{N}$ of nitrate, (c) $\delta^{18}\text{O}$ of nitrate, and (d) $\Delta^{17}\text{O}$ of nitrate during six storms sampled at Fernow Experimental Forest in 2010.	125
Figure 5.2. Intra-storm variation during six storms sampled at Fernow Experimental Forest during 2010.	127
Figure 5.3. Hourly precipitation $\delta^{18}\text{O}\text{-H}_2\text{O}$ values and precipitation amounts during six growing season storms sampled in 2010 at Fernow Experimental Forest.	129
Figure 5.4. Relationship between antecedent moisture conditions measured at the study site and biogenic NO_x flux as estimated by the two-endmember mixing model for six growing season storms at Fernow Experimental Forest.	134
Figure 6.1. $\delta^{18}\text{O}\text{-H}_2\text{O}$ values in stream samples collected weekly during 2010 in WS4 (solid black circles) and an adjacent watershed (WS5; open squares). The black line shows discharge in WS5; grey bars show precipitation measured in WS5.	149
Figure 6.2. Hourly precipitation (grey bars), discharge (grey line), and $\delta^{15}\text{N}$ (blue line), $\delta^{18}\text{O}$ (red line), and $\Delta^{17}\text{O}$ (black line) of nitrate values for the 9 July (a and b), 16 September (c and d), and 30 September (e and f) storms sampled in WS4 at Fernow Experimental Forest.	152
Figure 6.3. Map of WS4, A horizon $\delta^{18}\text{O}$ of soil water values at lysimeter locations sampled on 17 September (regular type) and October 1 (bold type), 2010.	156
Figure 7.1. (a) Location of study sites along a long-term (1982-2007) nitrate deposition gradient. (b) Maps of study watersheds.	172
Figure 7.2. Monthly concentrations (a and e), $\delta^{15}\text{N}$ (b and f), $\delta^{18}\text{O}$ (c and g), and $\Delta^{17}\text{O}$ (d and h) values of nitrate in precipitation (open circles) and streams (solid circles) at Coweeta (in red), Fernow (in blue), and Hubbard Brook (in black) Experimental Forests.	178

Figure 7.3. Proportions of atmospheric nitrate calculated using observed $\Delta^{17}\text{O}$ values and daily discharge in reference watersheds at (a) Coweeta, (b) Fernow and (c) Hubbard Brook Experimental Forests. 185

PREFACE

Completing a doctoral degree is no small thing, and I am incredibly thankful for all of the encouragement and support I've received from family, friends, and colleagues throughout this process.

This research was funded by the National Science Foundation (Grant #0910521), the Agriculture and Food Research Initiative of the U.S. Department of Agriculture National Institute of Food and Agriculture (Predoctoral Fellowship Grant #2012-67011-19663), the Geological Society of America, the University Of Pittsburgh Kenneth P. Dietrich School of Arts and Sciences, the Henry Leighton Fund, the Andrew Mellon Predoctoral Fellowship, and the Marie Curie Initial Training Network on Mass-Independent Isotope Fractionation.

I could not have asked for a better advisor than Emily Elliott. Her encouragement and mentoring were fundamental to my development as a scientist, and her amazing support made it possible for me to successfully complete this work while raising two children. I also thank the other members of my committee: Mary Beth Adams, Dan Bain, Brian Stewart, and Josef Werne for many insightful conversations as well as a truly enjoyable discussion during my dissertation defense. Mary Beth Adams' wealth of knowledge about the Fernow Experimental Forest in particular and ecosystem processes in general was especially helpful; I learned so much from our conversations. I am also incredibly grateful to Dan Bain for his patience and willingness to

mentor me in the lab, as the development of my skills in this area frequently involved trial and error.

Additional thanks go to the many collaborators who helped me complete this research. I am particularly grateful to the scientists and technicians working at the USDA Forest Service-managed study sites where this research took place. I owe Chris Cassidy a huge debt of gratitude for his assistance in the collection, processing, and shipment of so many samples collected at Fernow Experimental Forest. Frederica Wood and Thomas Schuler were also incredibly helpful in providing data necessary to complete the work I did at Fernow. Jim Vose, Chelcy Miniati, and Stephanie Lasseter at Coweeta Hydrologic Laboratory were very supportive of the research I conducted there and truly went above and beyond in sharing their knowledge of the site and helping me interpret data. Grateful thanks to Charles Marshall at Coweeta and Tammy Wooster at Hubbard Brook for collecting, processing, and shipping samples to me, and additional thanks to Mark Green, Don Buso, Scott Bailey, and Gene Likens for their collaboration on the work at Hubbard Brook and for providing additional data necessary to complete the project.

Thanks to the Biogeochemistry Lab Group, who helped me interpret data, prepare presentations, and keep the lab work moving forward. Special thanks go to Katherine Colwell, Dave Felix, Troy Ferland, Debb Glosser, Kassia Groszewski, Krissy Hopkins, Mollie Kish, Erin Pfeil-McCullough, Katie Redling, Rob Rossi, Marion Sikora, Katie Tuite, and Zhongjie Yu.

Finally, I would like to thank Steve, Sylvie, and Sawyer for being patient with me through periods of frustration and exasperation, and for being the best distractions from research I could ever imagine.

1.0 INTRODUCTION

Forested watersheds worldwide are currently exhibiting symptoms of nitrogen (N) saturation, largely due to decades of chronic elevated atmospheric N deposition [*Flum and Nodvin, 1995; Mitchell et al., 1997; Aber et al., 2003; Van der Salm et al., 2007; Dise et al., 2009; Koba et al., 2012*]. As nitrogen oxides ($\text{NO}_x = \text{NO} + \text{NO}_2$) from coal-fired power plants and vehicles are emitted to the atmosphere, oxidation reactions convert this NO_x to atmospheric nitrate (NO_3^-) which is deposited onto landscapes as wet and dry atmospheric deposition [*Elliott et al., 2007, 2009*]. Deposition of atmospheric nitrate is particularly prevalent in the eastern U.S., as NO_x emissions from coal-fired power plants concentrated in the Midwest and Ohio River Valley are oxidized to nitrate and carried eastward. Although atmospheric N deposition rates have been declining in recent decades (Figure 1.1), the legacy effects of long-term elevated N deposition can be significant. Indeed, while surface water acidity has decreased in some parts of the eastern U.S., surface water in other areas remains acidic despite significant reductions in sulfate and nitrate deposition [*Dewalle et al., 1988; Driscoll et al., 2001; Webb et al., 2004*].

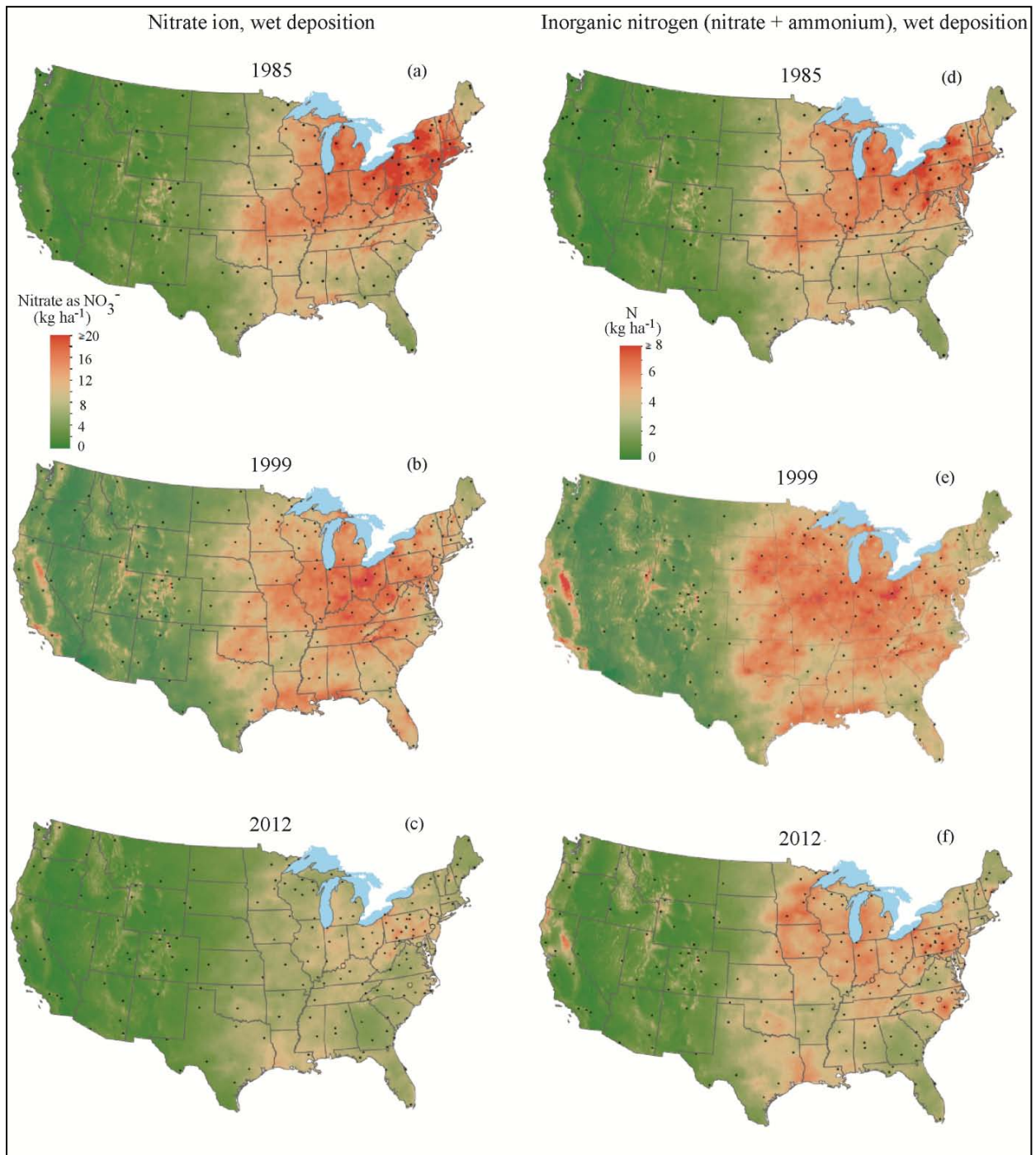


Figure 1.1. Annual average wet nitrate (a, b, c) and inorganic nitrogen (d, e, f) deposition rates at National Atmospheric Deposition Program monitoring sites from 1985 to 2012.

(maps accessed on 19 June 2014 [National Atmospheric Deposition Program, 2014]).

In forested systems, the two main sources of nitrate are atmospheric deposition and nitrate produced in the soil through microbial nitrification. Nitrate produced through nitrification does not necessarily represent a source of new N to ecosystems; rather, it results from the microbial conversion of organic N (from vegetation and microbial pools) to inorganic forms—first through mineralization to ammonium, then through subsequent oxidation to nitrate during nitrification. In contrast, atmospheric deposition constitutes a source of *external* N to an ecosystem, as it is derived from allochthonous sources (with the exception of biogenic NO_x emissions, which may also undergo oxidation to form atmospheric nitrate). While the addition of N via atmospheric deposition has been linked to elevated stream nitrate export in forested systems [Aber *et al.*, 2003], mineralization of organic N can be substantial, resulting in greater nitrate concentrations in streams relative to deposition [Stoddard, 1994]. The ability to distinguish between microbial and atmospheric contributions to stream nitrate export is therefore critical to understanding the biological and physical processes that affect N transport within terrestrial systems and from terrestrial to aquatic systems [Sebestyen *et al.*, 2008].

When vegetation and soil sinks cannot fully assimilate ecosystem N supply, nitrogen saturation can result, with excess nitrate leaching to streams [Ågren and Bosatta, 1988; Church, 1997; Aber *et al.*, 1998; Lovett and Goodale, 2011]. The early stages of N saturation can result in a “fertilizer effect”, yielding increased net primary productivity, increased foliar N concentrations, and increased N mineralization rates [Ågren and Bosatta, 1988; Aber *et al.*, 1998]. However, more severe symptoms of N saturation may develop as continued deposition adds more N to the system, including reduced soil C:N ratios and increased nitrification rates; these have been linked to elevated nitrate leaching to streams [Ågren and Bosatta, 1988; Aber *et al.*, 1998]. Increasing concentrations and decreased seasonality of stream nitrate are

characteristic signals that an ecosystem is approaching or has already become N-saturated [Stoddard, 1994].

Numerous studies have attempted to characterize ecosystem responses to chronic elevated N inputs [Mitchell *et al.*, 1997; Aber *et al.*, 2003; Driscoll *et al.*, 2003; Pardo *et al.*, 2006; Dise *et al.*, 2009; Argerich *et al.*, 2013]. These studies generally reported higher stream nitrate concentrations at sites receiving elevated rates of atmospheric N deposition. Long-term records of atmospheric N inputs at National Atmospheric Deposition Program (NADP) sites across the U.S. (e.g., Figure 1.1), paired with long-term records of watershed discharge and stream chemistry from a variety of long-term monitoring sites such as USDA Forest Service Experimental Forests have been essential to improving our understanding of watershed-scale biogeochemical responses to anthropogenic N inputs. In addition, intensive research at numerous sites has focused on N biogeochemical dynamics at the sub-watershed scale such as N mineralization and nitrification rates, soil C:N ratios, and N cycling in vegetation [Todd *et al.*, 1975; Peterjohn *et al.*, 1996; Gilliam *et al.*, 2001; Christ *et al.*, 2002; Magill *et al.*, 2004; Britto and Kronzucker, 2006; Clark and Tilman, 2008; Janssens *et al.*, 2010; Brookshire *et al.*, 2011; Argerich *et al.*, 2013]. While these studies and others have produced a wealth of information on biological nitrogen cycling in N-affected systems, fewer studies have focused on the processing and export of nitrate from different sources to aquatic systems. Characterization of atmospheric nitrate processing across spatial scales— and the biological and physical drivers affecting it— is necessary to accurately understand the effects of anthropogenic contributions to ecosystem N cycles. Clarification of these relationships has important implications for the mitigation of nutrient export from landscapes and the protection of sensitive receiving waters.

1.1 STABLE ISOTOPES AS TRACERS OF BIOGEOCHEMICAL CYCLING

Stable isotopes are often used in ecosystem studies to track the fate and transport of elements in natural systems. Small mass differences between isotopes of an element cause different reaction rates during physical (e.g., evaporation), chemical (e.g., precipitation reactions), and biological (e.g., nitrification and denitrification) processes. These differences affect the relative abundance of isotopes in substrates and their products. For example, nitrifying bacteria preferentially assimilate the lighter ^{14}N isotope of nitrogen rather than ^{15}N because the smaller mass is less energetically expensive to biologically process. This results in an isotopic fractionation between the ammonium substrate (which becomes enriched in ^{15}N) and the nitrate product (which becomes enriched in ^{14}N). Based on such mass-dependent fractionations, stable isotopic analysis is used to evaluate ecosystem processes and track changes across environmental gradients [Kendall *et al.*, 2007]. Stable isotopic compositions are typically reported as delta (δ) values (in parts per thousand, denoted by ‰) relative to a standard of known isotopic composition. Delta values for nitrogen and oxygen are calculated as:

$$\delta^{15}\text{N}, \delta^{18}\text{O}, \text{ and } \delta^{17}\text{O} (\text{‰}) = \left[\left(\frac{R_{\text{sample}}}{R_{\text{standard}}} \right) - 1 \right] \times 1000 \quad (\text{Eq. 1})$$

where R is the ratio of the heavy isotope to the light isotope (e.g., $^{15}\text{N}/^{14}\text{N}$, $^{18}\text{O}/^{16}\text{O}$, and $^{17}\text{O}/^{16}\text{O}$). As different sources often fractionate isotopes in unique ways, the isotopic composition of an element can be used alone or in combination with other elements to distinguish contributions from various sources (Figure 1.2).

Stable isotopes can also be fractionated via processes not dependent on mass; one such example is the anomalous enrichment of ozone (O_3) in the ^{17}O isotope [Cliff and Thiemens, 1997]. This enrichment, which deviates from the expected mass-dependent relationship between $\Delta^{17}O$ and $\delta^{18}O$ ($\Delta^{17}O = 0.52 * \delta^{18}O$), is denoted by $\Delta^{17}O$ (Figure 1.3). When NO_x is oxidized to nitric acid via ozone, the anomalous ^{17}O enrichment of ozone is passed on to the nitric acid product. The mass-independent $\Delta^{17}O$ isotope anomaly thus enters the nitrogen cycle through atmospheric nitrate, which has positive $\Delta^{17}O$ values. When atmospheric nitrate is affected by mass-dependent fractionating processes (such as biological uptake and cycling), the anomalous enrichment in ^{17}O is lost and the $\Delta^{17}O$ of nitrate value becomes 0‰ (or less). Thus, positive $\Delta^{17}O$ of nitrate values in natural waters indicate the presence of atmospheric nitrate that has not been biologically processed, making $\Delta^{17}O$ an unambiguous and conservative tracer of unprocessed atmospheric nitrate in terrestrial systems.

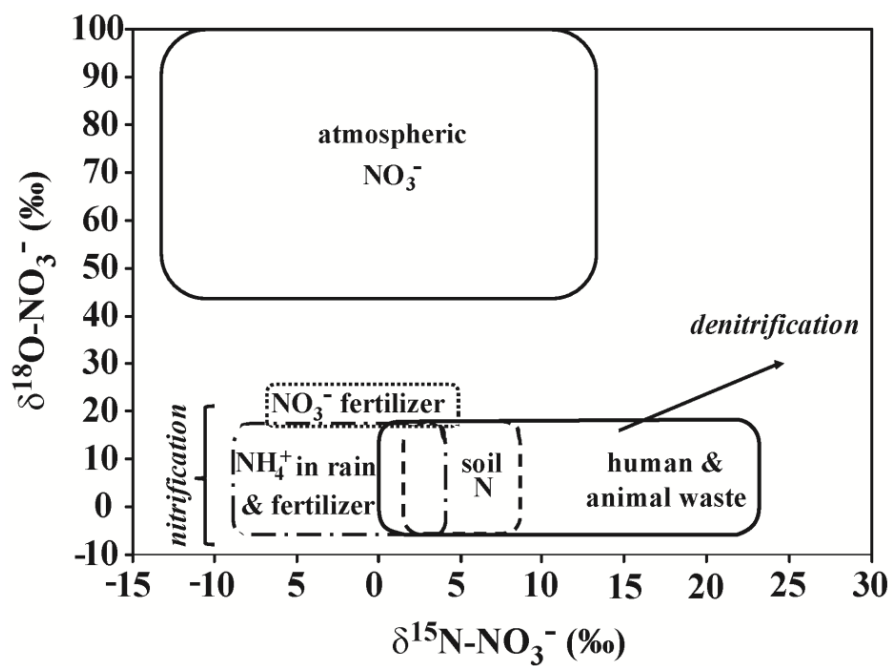


Figure 1.2. Commonly reported values of $\delta^{15}\text{N}$ and $\delta^{18}\text{O}$ of nitrate for various sources. Isotopic enrichment of the residual nitrate pool is depicted by the denitrification arrow. The $\delta^{18}\text{O}$ ranges for nitrified ammonium and organic N are shown as “nitrification” (modified from Kendall *et al.* [2007]).

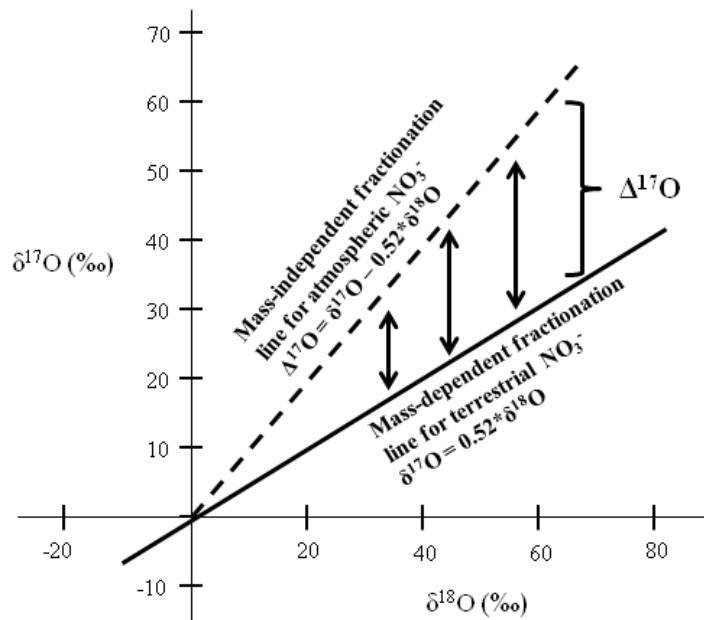


Figure 1.3. Triple isotope plot of $\delta^{18}\text{O}$, $\delta^{17}\text{O}$, and $\Delta^{17}\text{O}$.

The mass-dependent and mass-independent relationships between $\delta^{18}\text{O}$ and $\delta^{17}\text{O}$ are shown for different nitrate sources (modified from Michalski *et al.* [2004]).

1.2 STUDY SITE

The research presented in this dissertation was conducted at the USDA Forest Service Fernow Experimental Forest near Parsons, West Virginia (39°05' N, 79°40' W). This site has an extensive history of hydrological and ecological research, including numerous studies examining N dynamics across spatial scales. Fernow is located in the Allegheny Mountains portion of West Virginia (Figure 1.4), and elevations range from 670 to 930 m with slopes averaging ~20% [Taylor, 1999]. Bedrock on the western side of Fernow is primarily composed of hard sandstone and softer shale of the Upper Devonian Hampshire Formation; little water storage occurs in these strata [Reinhart *et al.*, 1963; Taylor, 1999; Kochenderfer, 2007]. Soils are channery silt loams of

the Calvin series (loamy-skeletal, mixed active, mesic typic Dystrudept), averaging 1 m in depth [Kochenderfer, 2007]. Infiltration rates in these soils are high and most precipitation reaches streams via subsurface flow [Reinhart *et al.*, 1963]. On the eastern side of Fernow, bedrock is composed of non-marine sandstone and shale of the Mauch Chunk Group and limestone of the Greenbriar Formation. The karst topography characterizing this portion of the Experimental Forest is unsuitable for watershed-scale water balance studies; the experimental watersheds are therefore concentrated on the western side of Fernow [Kochenderfer, 2007] (Figure 1.4).

The dominant forest type at Fernow is mixed hardwood. Common species include northern red oak (*Quercus rubra*), white oak (*Q. alba*), red maple (*Acer rubrum*), sugar maple (*A. saccharum*), tulip poplar (*Liriodendron tulipifera*) and black cherry (*Prunus serotina*). The growing season extends from May through October, with leaves emerging in late April. Precipitation is evenly distributed throughout the year, averaging 145 cm; significant snowpack does not accumulate over long periods. During high-intensity rain events, infiltration and streamflow are high, and streamflow falls off quickly during periods of low-intensity or no precipitation [Reinhart *et al.*, 1963]. Atmospheric deposition is an important source of nitrate at Fernow, and nitrate comprised approximately 60% of inorganic wet N deposition ($\text{NO}_3^- + \text{NH}_4^+$) in 2010 [National Atmospheric Deposition Program, 2011].

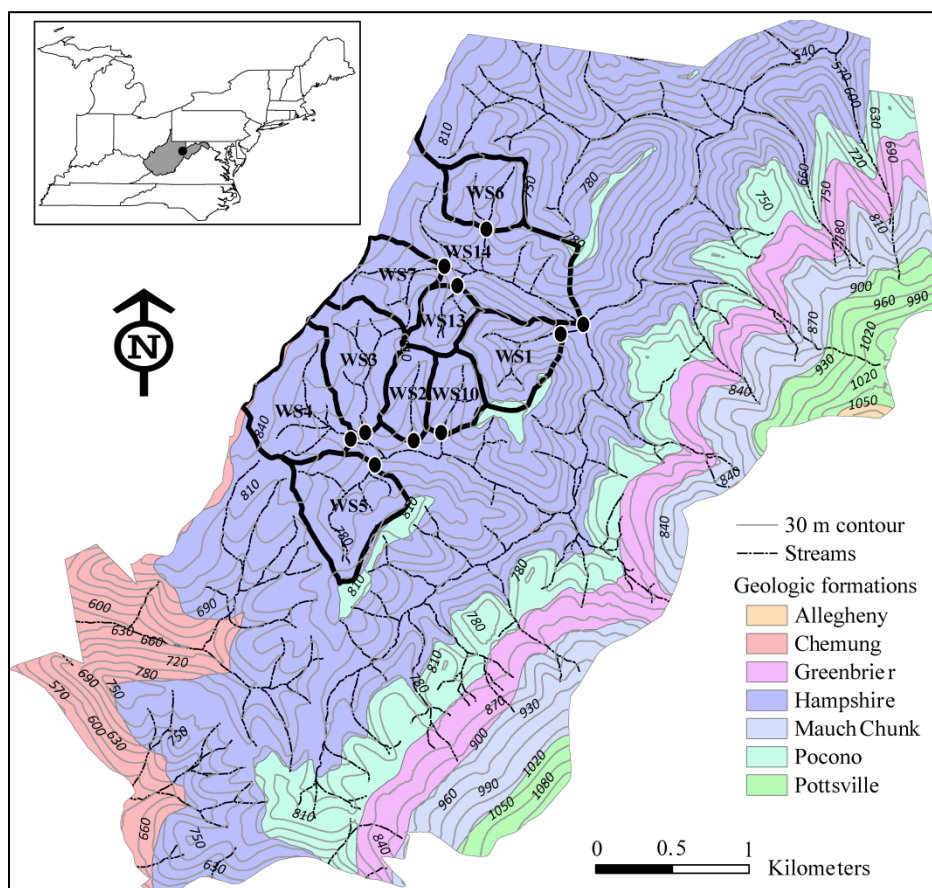


Figure 1.4. Experimental watersheds within the larger boundary of the Fernow Experimental Forest (FEF). Contours are at a 30-meter spacing and black dots show the locations of weirs in experimental watersheds. The black dot in the inset map shows the location of FEF in West Virginia (shown in grey).

1.3 ATMOSPHERIC NITRATE PROCESSING AND TRANSPORT IN APPALACHIAN FORESTS

This dissertation presents research examining the fate and transport of atmospheric nitrate deposition in forested watersheds of the Appalachian Mountain Range, using chemical and stable isotope analysis of precipitation, soil water, and stream water. Through a synthesis and review of nitrate stable isotope source apportionment studies, Chapter 2 explores the roles of hydrologic,

topographic, and biogeochemical processes in the cycling of atmospheric nitrate within watersheds. By influencing hydrologic flowpaths and landscape-stream connectivity, the hydrological and geomorphological characteristics of watersheds can play important— and perhaps underappreciated— roles in determining the extent to which unprocessed atmospheric nitrate is exported to streams. This chapter explores explanations for the small proportions of unprocessed atmospheric nitrate generally observed in baseflow in watersheds worldwide, identifies current knowledge gaps, and highlights areas where additional research is needed.

Chapter 3 presents a comparison of atmospheric nitrate export dynamics in four watersheds at Fernow Experimental Forest. Three hardwood-dominated stands and one conifer-dominated stand were compared, with each watershed representing a particular stage of nitrogen saturation, ranging from Stage 0 (N-limited) to Stage 3 (severely N-saturated) [*Aber et al.*, 1989].

In Chapter 4, spatially-distributed measurements of soil water nitrate concentration and isotopic composition ($\delta^{15}\text{N}$, $\delta^{18}\text{O}$, and $\Delta^{17}\text{O}$ of nitrate) are presented for Watershed 4 (WS4) at Fernow Experimental Forest. Samples collected during several months in 2010 demonstrate highly variable contributions from nitrate sources across this watershed. Potential drivers of the heterogeneous nitrate concentrations and sources observed in WS4 are explored in this chapter.

Chapter 5 examines the intra-storm variability of precipitation nitrate stable isotopic composition during six growing season storms sampled during 2010 at Fernow Experimental Forest. Hourly precipitation sampling facilitated this examination of high-temporal resolution variability in atmospheric nitrate isotopes. While much attention in recent decades has focused on the ecological effects of long-term declines and seasonal fluctuations in atmospheric deposition, few studies have explored event-based variability in wet nitrate deposition. The

research presented in Chapter 5 represents the first characterization of intra-event precipitation nitrate isotope dynamics using triple nitrate isotopes ($\delta^{15}\text{N}$, $\delta^{18}\text{O}$, and $\Delta^{17}\text{O}$).

As a corollary to the work presented in Chapter 5, Chapter 6 presents high-temporal resolution dynamics of stream nitrate export from various sources. Stormflow was sampled throughout the hydrograph during three growing season events in WS4 at Fernow Experimental Forest during 2010. In addition to characterizing the nitrate source dynamics in discharge during these storms, $\delta^{18}\text{O}\text{-H}_2\text{O}$ data provided important context on the role of hydrologic connectivity between watershed areas and the stream in facilitating nitrate export during storms.

Chapter 7 expands the examination of atmospheric nitrate transport and fate from the single-site level to a larger geographic context, spanning a ~ 1700 km nitrate deposition gradient along the Appalachian Mountain Range. Nitrate concentrations and stable isotopic composition ($\delta^{15}\text{N}$, $\delta^{18}\text{O}$, and $\Delta^{17}\text{O}$) were measured in precipitation and streams on a monthly basis from August 2012 through July 2013 in reference watersheds at Coweeta (North Carolina), Fernow (West Virginia), and Hubbard Brook (New Hampshire) Experimental Forests. These sites form a nitrogen deposition gradient with long-term (1982-2007) annual average nitrate deposition ranging from $11 \text{ kg ha}^{-1} \text{ yr}^{-1}$ to $17 \text{ kg ha}^{-1} \text{ yr}^{-1}$.

The research presented in this dissertation represents a novel examination of the effects of chronic elevated atmospheric nitrate deposition to forests and the variety of ecosystem responses observed in systems characterized as N-limited versus N-saturated. Insights into the variability of atmospheric nitrate processing and transport to streams resulting from this work can contribute practical guidance on the relative influence of anthropogenic and natural N inputs in forested systems.

2.0 DRIVERS OF ATMOSPHERIC NITRATE PROCESSING IN FORESTED WATERSHEDS

2.1 INTRODUCTION

Deposition of atmospheric nitrogen exceeds critical N loads in some ecosystems [Ågren and Bosatta, 1988; Fenn *et al.*, 2008; Galloway *et al.*, 2008; Pardo *et al.*, 2011], which has been linked to elevated nitrogen export from forests worldwide [Aber *et al.*, 1998; Galloway *et al.*, 2003]. Nitrogen saturation theory postulates that excess nitrate will leach from soils and landscapes when vegetation and soil sinks cannot assimilate additional N inputs [Ågren and Bosatta, 1988; Aber *et al.*, 1989; Stoddard, 1994; Lovett and Goodale, 2011]. When ecosystem sinks are full, this represents *capacity saturation*, whereas *kinetic saturation* occurs when the rate of N delivery exceeds the ability of active sinks to take up added N [Lovett and Goodale, 2011]. Several cross-site comparisons have examined the relationship between N deposition and nitrate export from forests [Mitchell *et al.*, 1997; Aber *et al.*, 2003; Driscoll *et al.*, 2003; Pardo *et al.*, 2006; Dise *et al.*, 2009; Argerich *et al.*, 2013]. These studies generally have reported higher stream nitrate concentrations at locations where atmospheric N deposition has been elevated relative to minimally polluted ecosystems. However, studies have rarely addressed the intra-catchment processes that affect the transport and fate of atmospheric nitrate after deposition onto the landscape. As mineralization of soil organic N is substantial in some systems, greater nitrate

concentrations in streams relative to deposition can occur [Stoddard, 1994], making the distinction between microbial and atmospheric nitrate sources in stream water important. Such source differentiation has implications for nitrogen saturation theory, particularly in identifying capacity versus kinetic saturation. Source differentiation can also provide novel detail about the biological and physical processes affecting N transport and fate within catchments [Sebestyen *et al.*, 2008]. For example, by influencing flowpaths and landscape-stream hydrologic connectivity, catchment structure and hydrology may play important— and perhaps underappreciated [Bain *et al.*, 2012]— roles in determining the extent of atmospheric source contributions to stream nitrate.

Previous studies have applied dual isotope ($\delta^{15}\text{N}$ and $\delta^{18}\text{O}$) approaches to assess catchment-scale processing of atmospheric nitrate. As significant overlap exists between the ranges of $\delta^{15}\text{N}$ values for microbial and atmospheric nitrate (the two main sources of nitrate to most forested systems), it has not been as useful in source apportionment [Kendall *et al.*, 2007]. Rather, $\delta^{15}\text{N-NO}_3^-$ has helped elucidate the importance of biological N processing (e.g. nitrification, denitrification, and uptake). In contrast, the oxygen isotopic signatures of microbial and atmospheric nitrate are more distinct, making $\delta^{18}\text{O-NO}_3^-$ a valuable tool for distinguishing between sources [Kendall *et al.*, 2007; Burns *et al.*, 2009; Ohte *et al.*, 2010]. Atmospheric $\delta^{18}\text{O-NO}_3^-$ can range from +45‰ to +100‰, whereas values from nitrification range from -10‰ to +15‰ [Kendall *et al.*, 2007]. When $\delta^{18}\text{O-NO}_3^-$ values in streams approach the range of $\delta^{18}\text{O-NO}_3^-$ in precipitation, this indicates that deposition inputs are not biologically cycled prior to export from the terrestrial system [Kendall *et al.*, 2007]. The proportion of unprocessed atmospheric nitrate in stream water can be calculated using a two end-member mixing model

$$\% \text{NO}_3^-_{\text{atm}} = \frac{\delta^{18}\text{O} - \text{NO}_3^-_{\text{str}} - \delta^{18}\text{O} - \text{NO}_3^-_{\text{nit}}}{\delta^{18}\text{O} - \text{NO}_3^-_{\text{atm}} - \delta^{18}\text{O} - \text{NO}_3^-_{\text{nit}}} \times 100 \quad (\text{Eq. 1})$$

where the subscripts $_{\text{str}}$, $_{\text{nit}}$, and $_{\text{atm}}$ refer to nitrate in the stream, from the nitrification end-member, and from the atmospheric end-member, respectively. In addition, a newer isotopic technique exploits inherent differences in $\Delta^{17}\text{O}$ (the ^{17}O isotope excess) of nitrate from atmospheric and terrestrial sources; this technique is increasingly being adopted in terrestrial N cycling studies [Michalski *et al.*, 2004; Tsunogai *et al.*, 2010; Costa *et al.*, 2011].

Previous studies of forested catchments in the U.S., Asia, and Europe have demonstrated positive relationships between stream nitrate concentrations and atmospheric N deposition [Mitchell *et al.*, 1997; Aber *et al.*, 2003; Dise *et al.*, 2009]. At some sites in the northeastern U.S., nitrate concentrations in streams and lakes increased significantly when N deposition rates exceeded $8 \text{ kg N ha}^{-1} \text{ yr}^{-1}$ [Aber *et al.*, 2003], whereas throughfall N in excess of $5 \text{ kg N ha}^{-1} \text{ yr}^{-1}$ resulted in elevated N leaching at 50 sites across China [Fang *et al.*, 2011a]. Higher thresholds were observed for European and Japanese forests, where N deposition rates in excess of $\sim 10 \text{ kg N ha}^{-1} \text{ yr}^{-1}$ resulted in elevated nitrate leaching at some sites [Grennfelt and Hultberg, 1986; Mitchell *et al.*, 1997]. While these relationships between N deposition and stream nitrate are noteworthy, these studies typically have not differentiated the contributions of atmospheric and microbial sources to stream nitrate.

In contrast to mass balance-based approaches, stable isotope-based investigations have not demonstrated the same association between atmospheric nitrate inputs and outputs at the catchment scale. Indeed, most isotope-based studies report only minor contributions of atmospheric nitrate to stream N export despite wide ranges in deposition fluxes (from 4 to 13 kg

$\text{N ha}^{-1} \text{ yr}^{-1}$), stream nitrate fluxes [Spoelstra *et al.*, 2001; Williard *et al.*, 2001; Burns and Kendall, 2002; Ohte *et al.*, 2004; Pardo *et al.*, 2004; Barnes *et al.*, 2008; Tobari *et al.*, 2010] and large proportions of atmospheric N observed in soil water [Templer and McCann, 2010]. These observations have implications for the current conceptualization of nitrogen saturation, as one of its central ideas holds that saturation occurs when N supply exceeds ecosystem demand [Aber *et al.*, 1989; Stoddard, 1994]. Thus, an examination of the factors driving nitrate export from forested catchments that considers both biological and physical processes is warranted. This review focuses primarily on nitrate export from forest ecosystems, as the N saturation concept has been most widely addressed in studies of forested catchments (this is particularly true of isotope-based studies). While the importance of biological factors (i.e. mineralization and nitrification rates, species composition, stand age) is well recognized, less emphasis has been placed on other potential drivers of atmospheric N export to streams including catchment hydrology, landscape characteristics, and the synchrony of atmospheric N inputs and exports. Here we explore major drivers that influence atmospheric nitrate transport in catchments via a review of the literature on nitrate source apportionment, and address knowledge gaps and highlight prospects for future experiments, observations, and interdisciplinary research.

2.2 MAJOR DRIVERS INFLUENCING ATMOSPHERIC NITRATE TRANSPORT IN WATERSHEDS

A number of isotope-based studies have examined nitrogen biogeochemical cycling in forests worldwide (Table 2.1; Table 2.2). Many of these studies have demonstrated that unprocessed atmospheric nitrate constitutes only a small proportion of the total nitrate (grand mean of all mean atmospheric nitrate percentages reported in Table 2 = 10%) measured in streams primarily during baseflow, regardless of deposition rates, nitrate export rates, or presumed degree of forest N saturation (Figure 2.1; Table 2.2). Notable exceptions to these low proportions of atmospheric nitrate in streams have been reported during sampling of higher streamflows such as snowmelt and storms [Williard *et al.*, 2001; Ohte *et al.*, 2004; Pellerin *et al.*, 2012; Sebestyen *et al.*, 2014]. The high retention of atmospheric deposition indicated by baseflow nitrate isotopic composition suggests that: 1) nitrate isotope data can be used to assess the extent of atmospheric N processing by biota with far less sampling and on much shorter time scales than traditional mass balance approaches; and 2) factors other than biological processing can influence atmospheric nitrate export to streams. While biological drivers do play an important role in determining the proportion of atmospheric nitrate present in streams, other influential factors include physical characteristics of catchments and methodological biases related to particular isotope analysis approaches.

Table 2.1. Site descriptions, nitrogen deposition and precipitation characteristics, and methods of nitrate isotope determination.
NA= data not available

Study	Site	Forest Type	Analytical Method for Isotope Determination	Total Wet NO ₃ ⁻ -N Deposition (kg ha ⁻¹ yr ⁻¹)	Total Annual Average Precipitation (mm)	% of Precip as Snow
Barnes 2008	CT & MA (USA)	HW/Conif	Denitrifier	1.4	1140	10
Buda 2009	Central PA (USA)	Mixed HW	Silver nitrate	NA	1043	NA
Burns 2002	Catskills NY (USA)	HW/Conif	Silver nitrate	4.2	1530	20-25
Campbell 2006	Adirondacks NY (USA)	Mixed HW	Silver nitrate	3.2	1035	47
Goodale 2009	Upper Susquehanna NY (USA)	HW/Conif	Denitrifier	3.6	932	NA
Mitchell 2006	Adirondacks NY (USA)	HW/Conif	Silver Nitrate	3.2	1010	47
Ohte 2004	Sleepers River VT (USA)	Mixed HW	Denitrifier	3.5	1323	20-30
Pardo 2004	Hubbard Brook NH (USA)	Mixed HW	Silver nitrate	3.6	1395	25-33
Pellerin 2012	Sleepers River VT (USA)	Mixed HW	Denitrifier	3.3	1323	20-30
Piatek 2005	Adirondacks NY (USA)	HW/Conif	Silver nitrate	3.2	1010	47
Sebestyen 2008	Sleepers River VT (USA)	Mixed HW	Denitrifier	3.5	1323	20-30
Sebestyen 2014	Sleepers River VT (USA)	Mixed HW	Denitrifier	3.5	1323	20-30
Spoelstra 2001	Turkey Lakes (Canada)	Mixed HW	Silver nitrate	NA	1239	35

Table 2.1 (continued)

Study	Site	Forest Type	Analytical Method	Total Wet NO ₃ ⁻ -N Deposition (kg ha ⁻¹ yr ⁻¹)	Total Annual Average Precipitation (mm)	% of Precip as Snow
Tobari 2010	Gomadansan Exper. For. (Japan)	Japanese cedar/cypress	Denitrifier	7.0	2650	NA
Tsunogai 2010	Rishiri Island (Japan)	HW/Conif	Cd/azide reduction to N ₂ O	4.5	NA	NA
Williard 2001	Fernow 4 WV (USA)	Mixed HW	Silver nitrate	4.6	1458	14
Williard 2001	Fernow 10 WV (USA)	Mixed HW	Silver nitrate	4.6	1458	14
Williard 2001	Otter Run WV (USA)	Mixed HW	Silver nitrate	4.6	1458	14
Williard 2001	Salamander Run WV (USA)	Mixed HW	Silver nitrate	4.6	1458	14
Williard 2001	W. Three Spring WV (USA)	Mixed HW	Silver nitrate	4.6	1458	14
Williard 2001	Karly Spring WV (USA)	Mixed HW	Silver nitrate	4.6	1458	14

Table 2.2. Nitrate end-member $\delta^{15}\text{N}$ and $\delta^{18}\text{O}$ values and estimation methods, and fraction of atmospheric nitrate in streams. Values represent reported mean (range); NA = data not available

Study	Nitrification End-member		Atmospheric End-member	$\delta^{15}\text{N}\text{-NO}_3^-$ (‰)		$\delta^{18}\text{O}\text{-NO}_3^-$ (‰)		% $\text{NO}_3^-_{\text{atm}}$ in streams
	$\delta^{18}\text{O}\text{-NO}_3^-$ Value (‰)	Estimation Method	$\delta^{18}\text{O}\text{-NO}_3^-$ Estimation Method	Atm	Stream	Atm	Stream	
Barnes 2008	-4	Lowest baseflow NO_3^- value	Avg. of storm event precipitation	-2	NA (0 to +6)	+71 (+50 to +84)	NA (-4 to +10)	12 (0 to 25)
Buda 2009	+5 (0 to +14)	Mean baseflow NO_3^- value	Avg. of storm event precipitation	0	NA	+44 (+12 to +70)	NA	NA (0 to 33)
Burns 2002	+15 (+13 to +16)	Incubated soil cores	Avg. of snowmelt, throughfall, wet deposition	0	+2 (-1 to +4)	+51 (+35 to +70)	+18 (+8 to +30)	8 (1 to 55)
Campbell 2006	0 to +3	$\delta^{18}\text{O}$ of soil water and O_2	Avg. of biweekly bulk precipitation	0	+1 (0 to +2)	+80 (+66 to +90)	NA (0 to +14)	<10
Goodale 2009	-6 to +2	$\delta^{18}\text{O}$ of soil water and O_2	Avg. of weekly bulk precipitation	-1 (-3 to +2)	NA (-2 to +6)	+77 (+71 to +81)	NA (-7 to +34)	NA (4 to 53)
Mitchell 2006	NA	NA	Throughfall	NA (-6 to +6)	NA (+1 to +4)	NA (+58 to +77)	NA (-5 to +4)	0
Ohte 2004	-11 to +21	Groundwater NO_3^- value	Weekly & event wet-only precipitation	NA	NA (+1 to +4)	NA (+78 to +89)	NA (-8 to +18)	9 (0.5 to 26)
Pardo 2004	-5 to +15	$\delta^{18}\text{O}$ of soil water and O_2	Weekly bulk precipitation	-2 (-5 to +2)	0 (-3 to +6)	+62 (+46 to +75)	+18 (+12 to +33)	NA (0 to 45)
Pellerin 2012	-3	Mean groundwater NO_3^- value from 2004	Avg. of snowmelt from 2004	NA	NA	+86 (+77 to +96)	+3 (-3 to +10)	7 (0 to 15)
Piatek 2005	NA	NA	Snowmelt, throughfall, wet deposition	+1 (-6 to +3)	+1 (-6 to +3)	+72 (+58 to +80)	+10 (+6 to +16)	NA
Sebestyen 2008	-2 to +2	Groundwater NO_3^- value	Weekly & event wet-only precipitation	NA (-4 to +3)	NA (0 to +7)	NA (+76 to +101)	NA (-5 to +43)	13 (0.4 to 48)

Table 2.2 (continued)

Study	Nitrification End-member		Atmospheric End-member	$\delta^{15}\text{N-NO}_3^-$ (‰)		$\delta^{18}\text{O-NO}_3^-$ (‰)		% $\text{NO}_3^-_{\text{atm}}$ in streams
	$\delta^{18}\text{O-NO}_3^-$ Value (‰)	Estimation Method	Estimation Method	Atm	Stream	Atm	Stream	
Sebestyen 2014	-4 to +1	Groundwater or soil water NO_3^- value	Event wet-only precipitation	NA	+2	NA (+70 to +101)	NA (-1 to +32)	NA (0 to 33)
Spoelstra 2001	-1 (-6 to +5)	$\delta^{18}\text{O}$ of soil water and O_2	Mass-wt. avg. of biweekly bulk precipitation	-2 (-4 to +1)	NA (+1 to +6)	+50 (+35 to +59)	NA (+3 to +15)	20 (8 to 30)
Tobari 2010	-16	Lowest baseflow NO_3^- value	Avg. of bulk rainfall	+3 (-7 to +15)	+3 (-3 to +10)	+64 (+43 to +76)	+5 (-16 to +38)	26 (11 to 45)
Tsunogai 2010	0	Assumed value for $\Delta^{17}\text{O}$ method	Avg. of daily wet deposition	-1	+2 (-4 to +9)	+87 $\Delta^{17}\text{O-NO}_3^- = +26$	+3 (-2 to +18)	7 (using $\Delta^{17}\text{O}$)
Williard 2001 (Fernow 4)	+10	Incubated Soil cores	Avg. of annual or monthly throughfall	NA	NA	+56 (+50 to +60)	+5 (+3 to +9)	3 (0 to 11)
Williard 2001 (Fernow 10)	+7	Incubated soil cores	Avg. of annual or monthly throughfall	NA	NA	+56 (+50 to +60)	+7 (+2 to +14)	7 (0 to 21)
Williard 2001 (Otter Run)	+14	Incubated soil cores	Avg. of annual or monthly throughfall	NA	NA	+56 (+50 to +60)	+10 (+2 to +15)	13 (0 to 23)
Williard 2001 (Salamander Run)	+12	Incubated soil cores	Avg. of annual or monthly throughfall	NA	NA	+56 (+50 to +60)	+10 (+6 to +12)	12 (5 to 19)
Williard 2001 (W. Three Spring)	+3	Incubated soil cores	Avg. of annual or monthly throughfall	NA	NA	+56 (+50 to +60)	+7 (+3 to +11)	7 (0 to 17)
Williard 2001 (Karly Run)	+8	Incubated soil cores	Avg. of annual or monthly throughfall	NA	NA	+56 (+50 to +60)	+4 (+1 to +6)	2 (0 to 7)

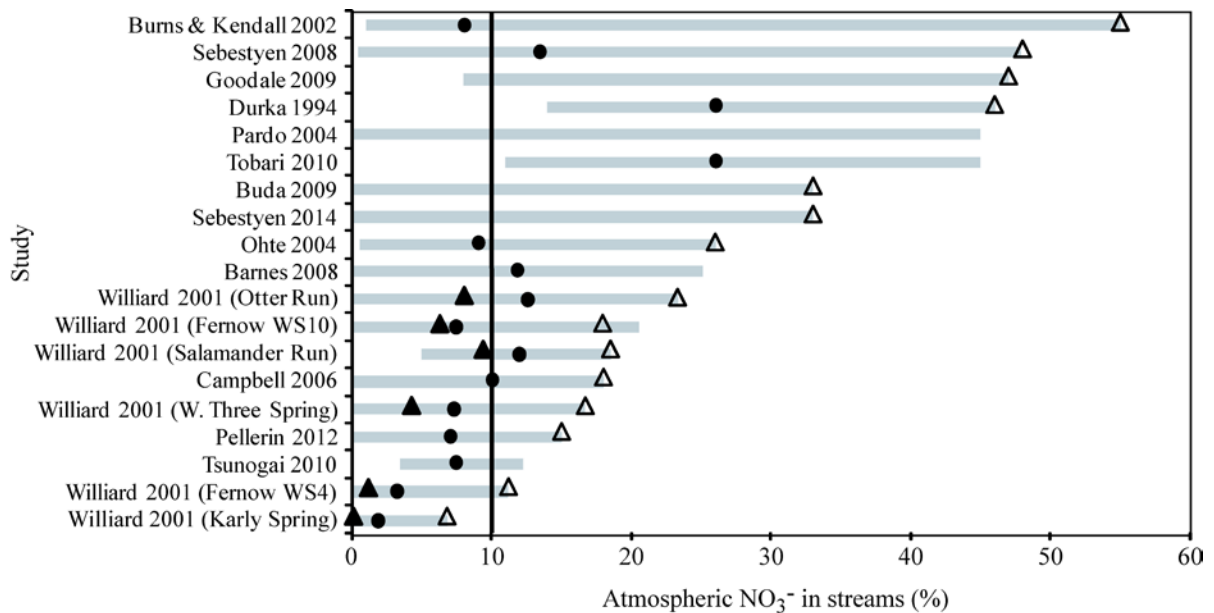


Figure 2.1. Percent atmospheric nitrate ($\text{NO}_3^-_{\text{atm}}$) in streams as reported in various catchment-scale isotope tracer studies.

Data were obtained from values reported in publications or were extracted from published figures using g3data software (<http://frantz.fi/software/g3data.php>; [Bauer and Reynolds, 2008; Snider et al., 2010]). Grey bars represent reported ranges of $\text{NO}_3^-_{\text{atm}}$ in streams for each study. Solid circles represent average % $\text{NO}_3^-_{\text{atm}}$ during the entire study period; this may represent a combination of baseflow and quickflow (snowmelt and stormflow). Solid triangles represent average % $\text{NO}_3^-_{\text{atm}}$ reported for baseflow only. Open triangles show the maximum reported % $\text{NO}_3^-_{\text{atm}}$ in quickflow. For emphasis, the bold line represents 10% $\text{NO}_3^-_{\text{atm}}$ in streams.

2.2.1 Methodological Biases

Due to the potential importance of this source of bias in interpreting atmospheric nitrate dynamics in catchments, we focus first on methodological biases. Examples of methodological biases include those related to the timing and frequency of sample collection, as well as analytical approaches that may influence estimated contributions of atmospheric nitrate to streams.

2.2.1.1 Frequency, Seasonality, and Scale of Sample Collection

Given that atmospheric N delivery to streams varies over time scales as short as individual hydrologic events, the frequency and seasonality of sample collection strongly influences data interpretation, particularly in catchments with fast hydrologic response times. Some studies have attributed the small amounts of unprocessed atmospheric nitrate in streams to low sampling frequency during snowmelt events [*Pardo et al.*, 2004; *Piatek et al.*, 2005]. In other cases, heterogeneity in atmospheric nitrate delivery to streams occurs on longer time scales. Indeed, the largest atmospheric nitrate inputs to streams have been measured during hydrologic conditions that are seasonal (e.g. snowmelt and monsoon events) [*Sebestyen et al.*, 2008; *Fang et al.*, 2011a; *Pellerin et al.*, 2012]. As a result, seasonal sampling biases can also influence the perceived importance of atmospheric nitrate export to streams.

Sampling scale and can also influence interpretations of atmospheric nitrate export dynamics. Analysis of a subset of the studies presented in Table 2.1 demonstrates this point (Figure 2.2). The data presented in Figure 2.2 are from forested catchments, undisturbed for at least 40 years prior to the study period, where sample collection occurred on a bi-monthly or monthly basis for at least one full year. While the studies shown in Figure 2.2 reflect relatively minor inorganic N and NO₃⁻-N deposition gradients, in both cases declining proportions of atmospheric nitrate in streams with increasing N deposition suggest that chronic elevated atmospheric N inputs may result in greater export of microbial nitrate in streams. Similarly, the proportion of atmospheric nitrate in streams decreases with increasing average

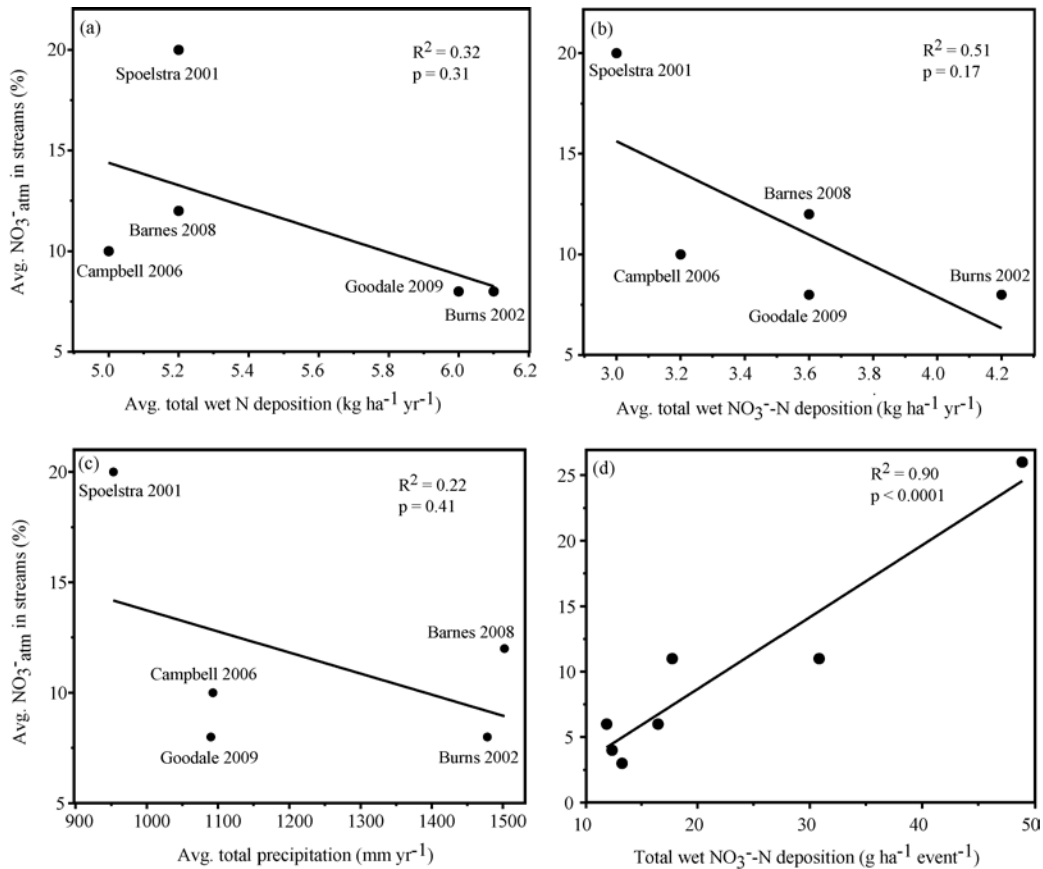


Figure 2.2. Relationship of average percent atmospheric nitrate in streams to (a) long-term (1984 to the study year) average total wet inorganic N deposition, (b) long-term (1984 to the study year) average total wet NO_3^- -N deposition, and (c) annual average total precipitation (for study years only) at sites across the northeastern U.S. and eastern Canada.

Average annual precipitation, total N, and total NO_3^- -N deposition were calculated from the nearest National Atmospheric Deposition Program site (less than 70 km away for all sites). Average values incorporate a range of hydrologic conditions, as all studies were conducted for more than one year (with bimonthly or monthly sampling). (d) The relationship between average percent atmospheric nitrate in streams and total wet NO_3^- -N deposition during individual storm events measured at Sleepers River Research Watershed.

total precipitation among these sites (Figure 2.2c). In contrast, examination of a similar relationship at a single site (Watershed 9 at Sleepers River Research Watershed) and over a shorter temporal scale (i.e. individual storm events) shows the opposite trend (Figure 2.2d).

Increasing proportions of atmospheric nitrate in the stream at Sleepers River with increasing wet NO_3^- -N deposition during storms may be due to the occurrence of saturated overland flow that has been observed at this site [Sebestyen *et al.*, 2008, 2014]. These examples demonstrate the potential dependence of perceived atmospheric nitrate export dynamics on the spatial and temporal scales at which the nitrate deposition-export relationship is examined.

It is not always possible to control for certain types of sampling biases across sites, but they should be acknowledged nevertheless. For example, snowmelt events account for a large proportion of annual water and nutrient budgets at some sites [Sebestyen *et al.*, 2008] but can be less important in other catchments [Barnes *et al.*, 2008]. The synchrony of seasonal patterns of atmospheric deposition and biological uptake also influences nitrate transport to streams. Seasonal differences in peak nitrate export among catchments (e.g., during dormant season snowmelt in the northeastern U.S. and the summer monsoon season in Japan) exemplify the reasons why timing and frequency of sampling must be considered. The paucity of nitrate isotope data from summer and autumn stormflow may particularly bias our assessment of unprocessed atmospheric nitrate contributions to streams. To date, few publications have documented substantial inputs of stream nitrate from unprocessed atmospheric sources outside of snowmelt [Williard *et al.*, 2001; Sebestyen *et al.*, 2014].

2.2.1.2 Analytical Biases

Multi-isotope approaches are emerging as new techniques for the estimation of unprocessed atmospheric nitrate export and evaluation of nitrogen processing in catchments. Until the last several years, natural abundance isotopic studies relied primarily on $\delta^{18}\text{O}-\text{NO}_3^-$ to differentiate atmospheric and microbial sources in natural waters. However, isotopic analyses that coupled

sample preparation using silver nitrate with sealed glass tube combustion analytical methods often resulted in abnormally high nitrification and low atmospheric $\delta^{18}\text{O}$ end-member values [Revesz and Böhlke, 2002]. Additionally, high concentrations of dissolved organic matter biased results using the silver nitrate method [Chang *et al.*, 1999; Casciotti *et al.*, 2002]. More recently, the bacterial denitrifier method has become a preferred and accepted approach for dual nitrate isotopic analysis; this method is not subject to the same biases as the combustion-based methods [Sigman *et al.*, 2001; Casciotti *et al.*, 2002]. Xue *et al.* [2010] compared $\delta^{18}\text{O}\text{-NO}_3^-$ values in surface waters analyzed using both techniques, and concluded that the silver nitrate- and denitrifier-derived results were highly correlated and generally statistically comparable. However, no precipitation samples were analyzed by Xue *et al.* [2010] and the range of $\delta^{18}\text{O}\text{-NO}_3^-$ values in their study was -19‰ to +31‰; it is unclear whether analysis of precipitation nitrate samples would show the same degree of correlation between analytical methods.

$\delta^{18}\text{O}\text{-NO}_3^-$ has frequently been used to differentiate atmospheric and microbial N sources, as their ranges are generally considered distinct. However, $\delta^{18}\text{O}\text{-NO}_3^-$ data from an increasing number of studies has widened the ranges of both microbial and atmospheric isotopic signatures, making $\delta^{18}\text{O}$ -based source apportionment more challenging. This is particularly evident when theoretical end-member isotopic values have been accepted to be true rather than directly measured. This often occurs with respect to designation of the nitrification end-member value, which has been variously estimated using baseflow, soil water, or groundwater $\delta^{18}\text{O}\text{-NO}_3^-$ values, or from an “expected” isotope value based on assumed or measured $\delta^{18}\text{O}$ values of soil water and O_2 and the assumed ratio of oxygen atoms contributed from each during nitrification (Table 2.2; Figure 2.3). Such differences in the method of estimation can lead to substantial uncertainties in the nitrification end-member value. Direct measurement of nitrate source

isotopic composition of both precipitation and nitrification end-members provides a higher degree of certainty that apportionment values represent reasonable estimates of unprocessed atmospheric nitrate inputs. Conversely, large ranges of microbial and atmospheric nitrate isotope values have resulted in greater uncertainties when isotope values have been assumed rather than measured [Michalski *et al.*, 2004]. Adding to this uncertainty is the potential influence of abiotic oxygen exchange between nitrite and soil water during nitrification. Depending on the degree to which it occurs in forest soils, abiotic oxygen exchange may alter the $\delta^{18}\text{O-NO}_3^-$ value of the microbial nitrate end-member [Snider *et al.*, 2010], potentially erroneously inflating estimates of microbial source contributions to stream nitrate. However, it is unclear to what extent abiotic oxygen exchange occurs in natural settings, as this process has so far only been evaluated in laboratory settings. In addition, Snider *et al.* [2010] observed decreasing fractions of abiotic oxygen exchange with increasing net nitrification in laboratory incubation experiments. Spatial variability in net nitrification rates (both within individual catchments and among different sites) may therefore also influence the degree to which this abiotic process affects microbial end-member $\delta^{18}\text{O-NO}_3^-$ values.

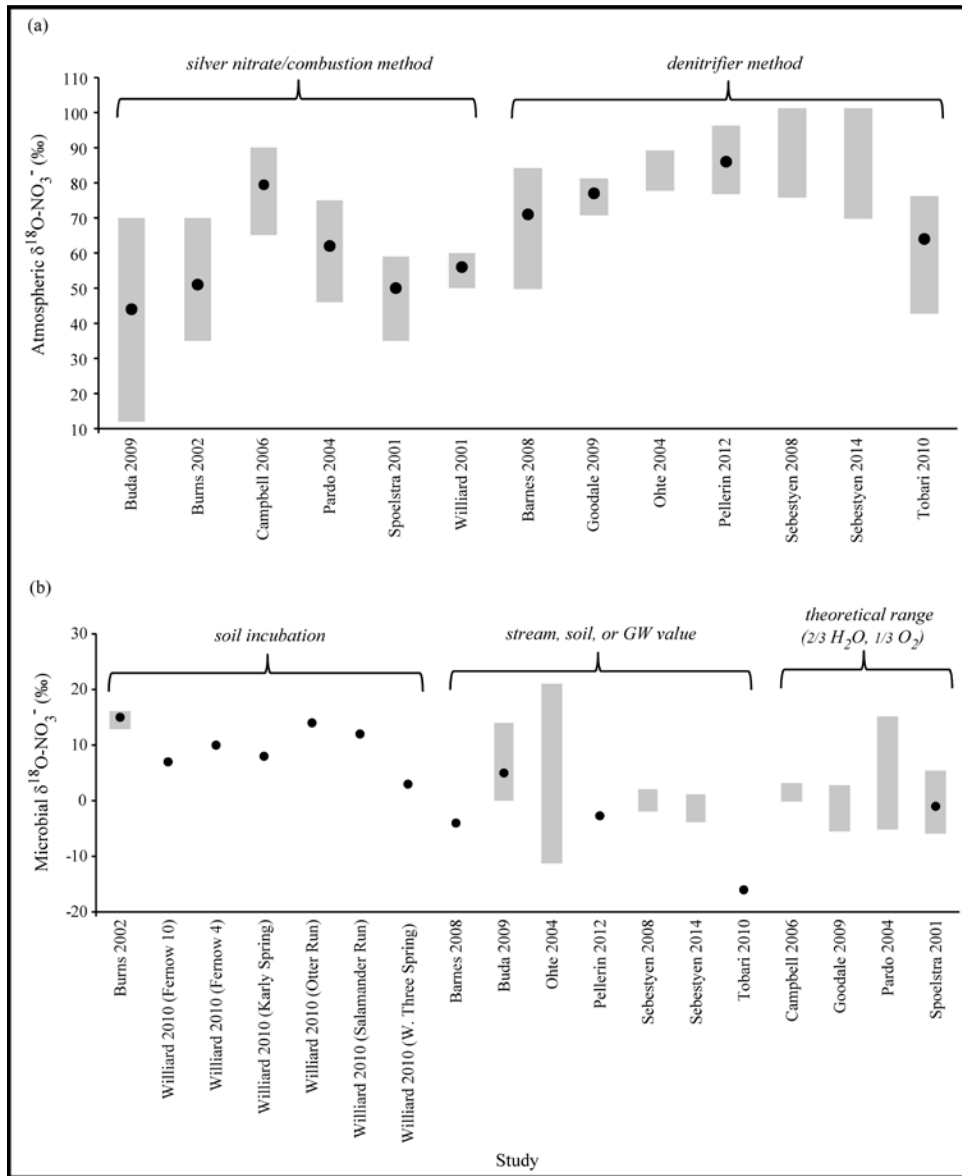


Figure 2.3. Estimated $\delta^{18}\text{O-NO}_3^-$ means (black dots) and ranges (shaded areas) for (a) atmospheric and (b) microbial nitrate end-members using various analytical techniques.

Studies using the silver nitrate/combustion method generally report lower atmospheric nitrate $\delta^{18}\text{O}$ values than studies using the denitrifier method. Soil incubation approaches to estimating microbial end-member $\delta^{18}\text{O-NO}_3^-$ values generally report higher values than studies that estimate the microbial end-member value using a stream, soil, or groundwater $\delta^{18}\text{O-NO}_3^-$ value or that calculate a theoretical end-member value based on the assumption of two oxygen atoms contributed to the nitrate molecule from soil water and one oxygen contributed from O_2 . The wide ranges of potential microbial and atmospheric nitrate end-member values presented in some studies can lead to considerable uncertainty in the calculated proportion of atmospheric nitrate in streams.

Source apportionment can be further complicated by mass-dependent fractionation of $\delta^{18}\text{O}-\text{NO}_3^-$, particularly during biological processes such as denitrification or coupled nitrification and denitrification. Such fractionating processes can enrich the $\delta^{18}\text{O}$ of residual nitrate pools, thereby complicating data interpretation [Kendall *et al.*, 2007]. As the fractionation due to biological transformation is often difficult to quantify and is not constant through time [Koba *et al.*, 1997, 2012], the isotopic fractionation inherent in such biological processes must be considered in interpretations of dual nitrate isotope data. More recently, $\Delta^{17}\text{O}-\text{NO}_3^-$ — a mass-independent tracer of atmospheric nitrate — has been increasingly adopted in addition to $\delta^{18}\text{O}$ analysis. Oxygen atom exchange during biological processes such as assimilation and denitrification erases the $\Delta^{17}\text{O}$ signature of the original atmospheric nitrate; $\Delta^{17}\text{O}$ is not fractionated by those processes. It therefore serves as a conservative tracer of unprocessed atmospheric nitrate contributions to streams. Indeed, one major advantage of combining $\delta^{18}\text{O}$ and $\Delta^{17}\text{O}$ analyses is the potential for a wealth of process-based information such an approach provides. The difference between stream $\delta^{18}\text{O}-\text{NO}_3^-$ values and the $\delta^{18}\text{O}-\text{NO}_3^-$ values of atmospheric deposition indicates the degree of atmospheric nitrate processing. In contrast, $\Delta^{17}\text{O}-\text{NO}_3^-$ values provide information about the proportion of unprocessed atmospheric nitrate present in stream water. The distinction between $\delta^{18}\text{O}$ - and $\Delta^{17}\text{O}$ -based interpretations is subtle, yet important to consider as each provides unique information about ecosystem processes. In addition, $\Delta^{17}\text{O}-\text{NO}_3^-$ analysis circumvents uncertainty in the estimation of microbial nitrification end-member values arising from differences in analytical approaches (i.e., silver nitrate/combustion versus bacterial denitrifier methods; Table 2.2), as the absence of mass-independent ^{17}O isotope enrichment in microbial nitrate sets this end-member $\Delta^{17}\text{O}$ value to zero.

As the $\Delta^{17}\text{O-NO}_3^-$ approach is relatively new, few studies have applied it to questions in catchment biogeochemistry. Based on $\Delta^{17}\text{O-NO}_3^-$ measurements in precipitation and discharge waters (spring, lake, and stream water), *Tsunogai et al.* [2010] estimated that ~9% of deposited atmospheric nitrate was exported without biological processing. *Costa et al.* [2011] used $\Delta^{17}\text{O-NO}_3^-$ measurements in a northern hardwood forest to determine that on average, 9% of soil solution nitrate originated from atmospheric deposition. In a semi-arid ecosystem, *Michalski et al.* [2004] reported large proportions of unprocessed atmospheric nitrate (20-40%) during stormflow, and smaller proportions (3-8%) in baseflow. They also quantified the difference in estimated atmospheric nitrate contributions to streams using both $\delta^{18}\text{O}$ and $\Delta^{17}\text{O}$ analyses. In that study, $\delta^{18}\text{O}$ -based estimates ranged from 40% less to 10% more than estimated contributions based on $\Delta^{17}\text{O}$ analysis. The disparity between $\delta^{18}\text{O}$ - and $\Delta^{17}\text{O}$ -based estimates of atmospheric nitrate export exemplifies the importance of careful interpretation of $\delta^{18}\text{O}$ and $\Delta^{17}\text{O}$ data to ensure that conclusions about the influence of biological versus depositional processes are accurate.

2.2.2 Biological Drivers

2.2.2.1 Terrestrial Nitrogen Processing

Most studies of atmospheric nitrate deposition to forested catchments have focused on the influence of biology, particularly uptake and cycling of atmospheric N by vegetation and microbes. Important insights have been gained from such work, including species-level responses to N deposition [*Templer and Dawson, 2004; Templer et al., 2005; McNeil et al., 2007; Clark and Tilman, 2008*], functional responses of microbial communities to atmospheric N

inputs [Tietema, 1998; Corre and Lamersdorf, 2004; Frey et al., 2004], and a better appreciation of the spatially heterogeneous response of these biological drivers to atmospheric N deposition [Lovett et al., 2002; McNeil et al., 2007; Costa et al., 2011].

Forest characteristics, such as stand age and species composition, play an important role in nitrogen transport from terrestrial to aquatic systems [Vitousek and Reiners, 1975; Lovett et al., 2002, 2004]. However, among the few studies comparing N dynamics in catchments with differing forest type (e.g., coniferous vs. deciduous), most have focused on nitrate concentrations rather than isotopic compositions of litterfall, soil solution, or stream water. Research approaches that employ only concentration measurements do not differentiate nitrate sources, the degree to which atmospheric N inputs are biologically cycled, or whether species composition influences atmospheric N uptake. In a comparison of N leaching in 21 deciduous and 37 coniferous forests across Europe, Van der Salm et al. [2007] found no effect of forest type on the relationship between N deposition and soil N leaching. Conversely, microbial nitrate production was nine times greater in a hardwood forest than a conifer forest at the Fernow Experimental Forest (West Virginia, USA), where the N deposition was $\sim 12 \text{ kg ha}^{-1}$ [Kelly et al., 2011]. However, neither study distinguished between atmospheric and within-catchment nitrate sources. Durka et al. [1994] conducted one of the few studies to employ a dual nitrate isotope approach to examine unprocessed atmospheric nitrate export from coniferous forests. Lower proportions of atmospheric nitrate were observed in streams draining healthy Norway spruce plantations than in stands that were already in a deposition-induced state of decline [Durka et al., 1994], but a direct comparison to hardwood forests was not possible because their study did not include deciduous species.

In some cases, forest age may exert a strong influence on ecosystem retention of atmospheric inputs and the proportion of atmospheric nitrate in streams. *Tobari et al.* [2010] observed greater proportions of atmospheric nitrate in streams draining stands of Japanese cedar (*Cryptomeria japonica*) and cypress (*Chamaecyparis obtusa*) older than 25 years. Low total N uptake in a younger stands led to higher nitrate concentrations and fractions of atmospheric nitrate exported to streams, while proportions of atmospheric nitrate in streams were lower in younger stands due to greater contributions from microbial sources [*Tobari et al.*, 2010].

The nutrient demands of microbes and vegetation, as well as abiotic incorporation into soil organic matter, influence how atmospheric N inputs are cycled and immobilized in catchments. Uptake and conversion of dissolved nitrogen from inorganic to organic forms by vegetation and microbes explains the high rates of nitrate retention in some systems [*Aber et al.*, 1998], while other studies have demonstrated that the plasticity of microbial C:N ratios can exert significant control on ecosystem N dynamics [*Perakis et al.*, 2005; *Taylor and Townsend*, 2010]. *Perakis et al.* [2005] calculated that the decrease in microbial biomass C:N ratios from 8.4 to 4.8 following experimental N additions would yield a 40% increase in soil organic matter N storage in a coastal old-growth forest in Chile. Other studies have also reported high rates of nitrate assimilation and sequestration in microbial biomass [*Davidson*, 1992; *Stark and Hart*, 1997], highlighting the importance of the overall N availability in catchments to nitrate retention in general, and retention of atmospheric N inputs in particular [*Ågren and Bosatta*, 1988].

Denitrification also influences catchment N retention and nitrate export to streams, and has been measured along subsurface flowpaths, as well as within streams and hyporheic zones [*Böhlke and Denver*, 1995; *Seitzinger et al.*, 2006; *Inamdar et al.*, 2009; *Osaka et al.*, 2010; *Zarnetske et al.*, 2011]. Denitrification is sensitive to the balance between hydrologic conditions

and redox state, and can be minimal even when the supply of nitrate is ample [Cirmo and McDonnell, 1997; Hedin *et al.*, 1998; Vidon *et al.*, 2010]. Hill *et al.* [2000] reported greater denitrification in riparian subsurface sediments where nitrate-rich groundwater flowed through pockets of dissolved organic carbon-rich microsites. Low denitrification rates have also been attributed to shorter water residence times and lower organic matter contents in coarser sediments [Vidon and Hill, 2004]. Thus, while vegetation and soil microbial communities consume nitrate, the importance of these biological controls may ultimately be regulated by hydrologic conditions.

The degree of biological processing varies with distance and depth along soil water and groundwater flowpaths [Gold *et al.*, 2001; Inamdar *et al.*, 2009]. Unprocessed atmospheric nitrate has been found in both shallow groundwater [Nolan *et al.*, 2002; Osaka *et al.*, 2010] and in the deeper groundwater of arid systems [Michalski *et al.*, 2004; Deiwakh *et al.*, 2012]. Durka *et al.* [1994] found unprocessed atmospheric nitrate in spring waters, suggesting the presence of unprocessed atmospheric nitrate along groundwater flowpaths. Osaka *et al.* [2010] reported decreasing nitrate concentrations and increasing $\delta^{15}\text{N-NO}_3^-$ with depth in a headwater catchment, suggesting more denitrification along deeper flowpaths. Interestingly, $\delta^{15}\text{N}$ values of stream nitrate fell between those of the shallow and deep groundwater nitrate, suggesting mixing from two different flowpaths and the imprint of denitrification on nitrate export to the stream [Koba *et al.*, 1997; Osaka *et al.*, 2010].

2.2.2.2 In-stream Nitrogen Processing

In-stream uptake and processing can strongly influence the amount of nitrate exported to the catchment outlet, and potentially the fraction of atmospheric nitrate observed in the stream.

Sebestyen et al. [2014] suggested that decreased in-stream nitrification coupled with greater heterotrophic nitrate uptake during autumn leaf fall contributed to declining nitrate concentrations and yields at the catchment outlet in W-9 at Sleepers River Research Watershed in Vermont (USA). *Campbell et al.* [2002] reported little change in the proportions of atmospheric and microbial nitrate in stream water during summer snowmelt in an alpine forest, despite a reduction in stream nitrate concentrations. The decline in stream nitrate concentrations was partially attributed to in-stream uptake; however, differential elution of snowpack solutes and temporal variability in soil nitrate flushing also reduced stream nitrate concentration while maintaining the relatively constant proportions of atmospheric and microbial nitrate in the stream.

The importance of in-stream uptake and processing on catchment-scale nitrate export is not limited to event or seasonal time scales, but has been observed on decadal time scales [*Bernhardt et al.*, 2005] and for several years following catastrophic disturbance [*Bernhardt et al.*, 2003]. Longitudinal variability of in-stream processes (such as denitrification), coupled with spatially variable nitrate inputs from groundwater, can also affect the magnitude and sources of nitrate export observed at the catchment outlet [*Burns*, 1998]. Indeed, *Burns* [1998] suggested that differential in-stream nitrate processing among catchments receiving similar amounts of atmospheric N deposition could contribute to differences in stream nitrate concentrations. Thus, the complexity of interactions among terrestrial and aquatic N biogeochemical cycles can influence catchment nitrate export in general and the proportion of atmospheric nitrate in streams specifically.

2.2.2.3 Phase of Nitrogen Deposition and Synchrony with Biological Processing

While the amount of atmospheric nitrate in wet deposition has often been implicated in the development of forest N saturation, the phase (wet vs. dry) and timing of atmospheric nitrate inputs may influence the degree to which it is biologically cycled within catchments. In a study of dry nitrate deposition in Ohio, Pennsylvania, and New York, *Elliott et al.* [2009] reported positive correlations between stationary source NO_x emissions (e.g., electricity generation) and particulate nitrate concentrations during all seasons except summer. Preferential formation of particulate nitrate at lower temperatures, combined with increased stationary source NO_x emission rates during colder months [*Elliott et al.*, 2009], may cause higher rates of dry nitrate deposition across the northeastern U.S. during the dormant season. The ways in which this potentially significant source of N— dry deposition constitutes up to 40% of the total N deposition in some areas [*Elliott et al.*, 2009]— interacts with hydrologic and climatic drivers may profoundly affect the degree to which atmospheric nitrate is biologically cycled or transported directly to streams.

Vegetation canopies are highly effective scavengers of dry N deposition, with nitric acid (HNO₃) vapor comprising nearly 50% of annual average atmospheric nitrate flux to canopies in the southeastern U.S. [*Lindberg et al.*, 1986]. Dry deposition is a particularly important N source in western U.S. forests, where it dominates total N deposition and is scavenged (i.e. deposited onto leaf surfaces) with great efficiency by conifer-dominated stands [*Bytnerowicz and Fenn*, 1996; *Fenn et al.*, 2003]. Such interactions between vegetation canopies and dry deposition often yield throughfall N inputs in excess of those observed in bulk deposition [*De Schrijver et al.*, 2007], potentially altering the temporal dynamics of N deposition and stream nitrate export.

Synchrony between atmospheric N deposition and biological uptake can influence nitrate isotopic values in stream water. In the U.S., dormant season hydrologic events associated with snowmelt runoff often contribute large proportions of unprocessed atmospheric nitrate to streams [Spoelstra *et al.*, 2001; Sebestyen *et al.*, 2008; Goodale *et al.*, 2009]. Catchment-scale studies in monsoonal climates such as Japan also report increased proportions of unprocessed atmospheric nitrate in streams during winter, but overall nitrate export is greatest during the growing season, when production and consumption of microbial nitrate is also greatest [Mitchell *et al.*, 1997; Ohte *et al.*, 2010; Fang *et al.*, 2011a; Nakamura *et al.*, 2011; Ohte, 2012; Kohzu *et al.*, 2013]. As the growing season coincides with the rainy season in Japan, the greater nitrate export observed during this season likely reflects the combined influence of increased microbial nitrate production and high water drainage [Mitchell *et al.*, 1997; Mitchell, 2001]. In a study of forested catchments near Tokyo, Tabayashi and Koba [2011] reported higher stream nitrate concentrations and $\delta^{18}\text{O-NO}_3^-$ values in areas receiving elevated N deposition inputs; however, maximum $\delta^{18}\text{O-NO}_3^-$ values only reached +6‰. They showed that microbial sources dominated stream nitrate, including catchments exporting the most nitrate. These studies point to increased rates of nitrate export from forests under conditions of greater microbial nitrate production (as regulated by factors such as soil temperature, moisture, and carbon and nitrogen availability [Stark and Firestone, 1995; Stark, 1996; Taylor and Townsend, 2010]), high atmospheric deposition rates, and peak precipitation inputs. Further investigations comparing $\delta^{15}\text{N}$ and $\delta^{18}\text{O}$ of nitrate in Asian, North American, and European catchments can help elucidate the roles that synchrony among N deposition, biology, and hydrology play in determining the proportion of atmospheric nitrate observed in forest streams. For example, it is possible that the coincidence of hydrologic events (e.g. monsoons) and biological activity in some catchments may result in

greater atmospheric N processing prior to N export. Conversely, short transit times of atmospheric deposition through terrestrial systems during the rainy season or asynchrony between biological activity and hydrologic events (e.g. snowmelt) may preclude extensive biological processing and yield greater proportions of unprocessed atmospheric nitrate in streams.

Other studies have reported no seasonal trends in atmospheric nitrate export. *Pardo et al.* [2004] observed similar proportions of atmospheric nitrate in streams during both the winter and non-winter months in a mixed hardwood catchment in the northeastern USA. The authors attributed this pattern to short hydrologic residence times on steep hillslopes and significant storage capacity in well-mixed subsurface reservoirs that dampened seasonal differences in stream water nitrate isotopic signatures. *Cirimo and McDonnell* [1997] suggested that increased litter decomposition at the end of the growing season could create a significant dissolved inorganic N pool in soils. Subsequent flushing during dormant season hydrologic events may result in elevated stream nitrate concentrations [*Ohte*, 2012], but not necessarily increased proportions of atmospheric nitrate. However, *Sebestyen et al.* [2014] reported a significant decline in stream nitrate concentrations during the end of the growing season, with assimilatory nitrate uptake and decreased rates of in-stream nitrification responsible for the retention of up to 72% of nitrate entering the stream.

2.2.3 Physical Drivers

A variety of physical factors can influence estimated contributions of atmospheric nitrate to streams draining N-polluted forests. The hydrologic regime of a catchment and its landscape characteristics are particularly important drivers of nitrate transport dynamics.

2.2.3.1 Hydrologic Regime

Given the commonality across many studies of low mean proportions of atmospheric nitrate in streams, particularly in baseflow (Table 2.2; Figure 2.1), it is important to consider the influence of catchment hydrologic regime on biological processing of deposition inputs. If processing is more rapid than transport, then only minor contributions of unprocessed atmospheric nitrate to streams can result [*Hales et al.*, 2007; *Osaka et al.*, 2010]. *Helliwell et al.* [2007] suggested that rapid hydrologic routing likely outweighs N retention in steep watersheds, whereas greater soil water residence times in watersheds with shallower slopes increase soil N pools and enhance nitrification. Lower saturated hydraulic conductivities and greater soil thickness resulted in greater hydrologic residence times in old (4.1 million years) Hawaiian soils, thereby impeding nitrate leaching and increasing the opportunity for biological uptake and retention [*Lohse and Matson*, 2005]. In contrast, short hydrologic residence times in a younger (300-year-old) Hawaiian soil facilitated rapid and large losses of added nitrate following precipitation events; limited contact time between soils and drainage waters prevented plant and microbial retention of added N [*Lohse and Matson*, 2005]. While this study did not characterize the sources of nitrate leached to streams specifically, the results demonstrate the potential for hydrologic residence times to influence the degree of biological processing and kinetic and/or capacity N

saturation within catchments, with implications for the export of unprocessed atmospheric nitrate.

Water and nitrate can be quickly routed to streams along preferential flowpaths during rain and snowmelt events in some systems [McGlynn *et al.*, 1999; Burns *et al.*, 2001; Sebestyen *et al.*, 2008] with the potential for elevated atmospheric nitrate export. In other systems, event water and nitrate may be initially incorporated into well-mixed groundwater reservoirs, with export to the stream delayed [Schiff *et al.*, 2002; Pardo *et al.*, 2004], although this speculation has not been validated through measurement of nitrate isotopes along deeper subsurface flowpaths. Burns and Kendall [2002] reported small proportions of atmospheric nitrate (< 9%) in baseflow from streams draining two forested catchments in the Catskill Mountains (USA), but the occurrence of a storm event with a 10-year recurrence interval during the study resulted in large contributions of atmospheric nitrate (55%) to stormflow. These results provide further evidence that variations in hydrologic flowpaths influence the connectivity of catchment areas to the stream and exert control on the export of atmospheric nitrate. The influence of catchment hydrologic condition on the proportion of unprocessed atmospheric nitrate in streams is demonstrated in Figure 2.1.

Relationships between streamflow and $\delta^{18}\text{O-NO}_3^-$ values during baseflow and stormflow/snowmelt periods at several sites are shown in Figure 2.4. While the relationship between baseflow discharge rate and $\delta^{18}\text{O-NO}_3^-$ values is positive for all catchments shown in Figure 2.4a, the catchments show a variety of trends in $\delta^{18}\text{O-NO}_3^-$ values with increasing

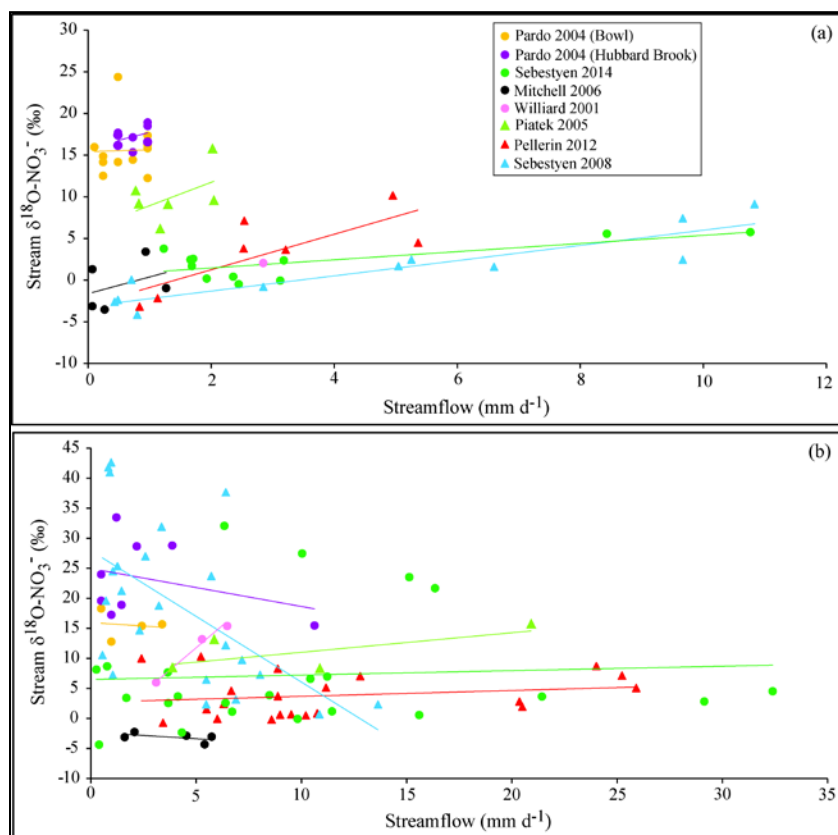


Figure 2.4. Streamflow versus stream $\delta^{18}\text{O-NO}_3^-$ values during (a) baseflow and (b) stormflow/snowmelt events at multiple sites.

Circles represent rainfall events and triangles represent snowmelt events. Data were obtained either from published tables or were extracted from published figures using g3data software (<http://frantz.fi/software/g3data.php>; [Bauer and Reynolds, 2008; Snider et al., 2010]). Direct comparison of trends across studies should be done with caution, as differences in the analytical method used for $\delta^{18}\text{O-NO}_3^-$ determination (i.e., silver nitrate/combustion method versus denitrifier method) may confound direct comparisons in some cases.

discharge during stormflow/snowmelt conditions (Figure 2.4b). For example, *Sebestyen et al.* [2008] and *Pellerin et al.* [2012] attributed high nitrate concentrations and $\delta^{18}\text{O-NO}_3^-$ values during relatively low flows to preferential flowpaths and the presence of melting snow in the stream channel during two snowmelt events at Sleepers River Research Watershed. Such direct routing of high-concentration meltwater resulted in high proportions of atmospheric nitrate (up to

48%) during early snowmelt, with decreasing proportions of atmospheric nitrate in the stream thereafter [Sebestyen *et al.*, 2008]. In contrast to the atmospheric nitrate-streamflow dynamics observed at Sleepers River, other studies have shown increasing stream nitrate concentrations and $\delta^{18}\text{O}$ values with increasing discharge during snowmelt and storm events [Williard *et al.*, 2001; Piatek *et al.*, 2005; Hales *et al.*, 2007]. These positive trends have been attributed to flushing of accumulated soil N pools with increasing stormflow [Creed *et al.*, 1996; Williard *et al.*, 2001; Piatek *et al.*, 2005]. While positive trends in stormflow/snowmelt $\delta^{18}\text{O}\text{-NO}_3^-$ occur for some studies shown in Figure 2.4b (e.g., Piatek *et al.* [2005] and Williard *et al.* [2001]), the reported $\delta^{18}\text{O}\text{-NO}_3^-$ values are nonetheless within the theoretical source range of microbial nitrate (-5‰ to +16‰; [Kendall *et al.*, 2007]). Thus, although $\delta^{18}\text{O}\text{-NO}_3^-$ values may increase slightly in streams as soils are flushed during hydrologic events (particularly flushing of upper soil layers [Williard *et al.*, 2001])— possibly due to increased contributions of atmospheric nitrate in some cases— most nitrate mobilized by increasing discharge comes from a microbial source. This is also the case during baseflow for all catchments shown in Figure 2.4a. While it is noteworthy that stream $\delta^{18}\text{O}\text{-NO}_3^-$ values increase with increasing baseflow at all sites in Figure 2.4a, $\delta^{18}\text{O}\text{-NO}_3^-$ values in the microbial source range suggest that any contributions of atmospheric nitrate to streams are minor under baseflow regimes.

Our understanding of hydrologic controls on catchment N export has been highly influenced by coupled hydro-ecological models [Creed *et al.*, 1996; Creed and Band, 1998] that have advanced our understanding of nitrate transport during hydrologic events (i.e. snowmelt and rainfall) when stream nitrate responses are most dynamic. Runoff processes include some combination of overland flow and subsurface flow [Dunne and Black, 1970, 1971; Hibbert and Troendle, 1988], and the hydrological and biogeochemical processes that control atmospheric

nitrate export are rarely discernible from measurements at the catchment outlet alone. As such, the catchment sciences community still faces the challenge of elucidating similarities and differences among rainfall-runoff processes and N deposition-runoff dynamics. This represents a striking example of the double paradox in catchment hydrology [Kirchner, 2003], wherein streams respond rapidly to precipitation inputs, but the precipitation itself is not a large contributor to stormflow and the chemical composition of stormflow varies with flow regime. Making progress on this front is particularly important for better constraining mechanisms responsible for the low proportions of atmospheric nitrate in streams during baseflow and dynamic variation during stormflow.

2.2.3.2 Landscape Characteristics

While catchment hydrology and topography can be important drivers of overall forest nitrate export, the factors affecting unprocessed atmospheric nitrate delivery to streams are more nuanced. The hydrologic regime of a catchment is often closely related to its landscape characteristics, including geological, pedological, and topographical features [Dunne and Black, 1970; Jencso *et al.*, 2009]. Topography can exert a first-order control on the source areas of water that affect streamflow variation, meaning that landform acts as the primary determinant of streamflow characteristics [Dunne and Black, 1970; Jencso *et al.*, 2009]. Topographic characteristics such as slope steepness and aspect, upslope accumulated area (UAA), bedrock and soil type, and soil thickness influence the capacity for water and nitrogen storage and movement [Creed *et al.*, 1996; Creed and Band, 1998; Jencso *et al.*, 2009; Speiran, 2010]. Topographic influences on the hydrologic storage capacity of various reservoirs (e.g., in hillslopes, riparian areas, and bedrock) may also affect the degree of atmospheric nitrate

processing by controlling water transit times and opportunities for biological uptake and cycling [Inamdar *et al.*, 2009]. As biological processing resets the $\delta^{18}\text{O}$ of atmospheric nitrate from a range of +45 to +100‰ to the range of -10 to +15‰, the residence time of water in various catchment reservoirs can influence the isotopic expression of unprocessed atmospheric nitrate inputs to streams [Pardo *et al.*, 2004; Hales *et al.*, 2007; Osaka *et al.*, 2010]. For example, landscape and soil characteristics that promote rapid water movement facilitate greater atmospheric nitrate delivery to streams in some catchments [Durka *et al.*, 1994]. Similarly, exposed rock surfaces can quickly transport water and nitrate inputs past plant and microbial pools, resulting in greater unprocessed atmospheric nitrate export [Curtis *et al.*, 2011]. Conversely, groundwater reservoirs may store nitrate for longer periods than shallower soil layers, potentially influencing the timing of nitrate export to streams while allowing more time for microbial processing of atmospheric inputs [Burns *et al.*, 1998; Schiff *et al.*, 2002; Pardo *et al.*, 2004].

Interactions between catchment topography and hydrologic regime are highly dynamic through space and time, as variations in seasonal and event-scale precipitation cause expansion or contraction of the effective streamflow source area [Dunne and Black, 1970, 1971]. The concept of variable source areas and spatio-temporal heterogeneity of hillslope-riparian-stream connectivity has clear implications for the delivery of atmospheric nitrate to streams. For example, areas of topographic concavity (e.g. convergent hillslope hollows) may have more persistent connectivity to streams and exert greater influence on the composition of stream nitrate than areas of topographic convexity (e.g. tops of slopes) [Dunne and Black, 1970]. Topographic lows in near-stream areas (e.g. wetlands) are often characterized by low nitrate export and high denitrification rates due to greater soil water content and carbon-rich sediments

[Groffman and Tiedje, 1989; Gold et al., 2001; Ogawa et al., 2006; Inamdar et al., 2009]. Conversely, Durka et al. [1994] reported greater proportions of atmospheric nitrate in streams draining forested catchments with waterlogged soils, suggesting that surface flow can facilitate direct routing of atmospheric nitrate to streams. Still other studies have reported considerable differences in overall nitrate export but only minor differences in the proportion of unprocessed atmospheric nitrate in streams draining catchments with widely differing topographic characteristics [Schiff et al., 2002].

2.3 KNOWLEDGE GAPS AND NEXT STEPS WITH RESPECT TO FUTURE EXPERIMENTS, OBSERVATIONS, AND INTERDISCIPLINARY RESEARCH

A better conceptual, functional, and observational understanding of the factors regulating atmospheric nitrate transfer to streams is needed, particularly as it relates to catchment-scale hydrologic and topographic drivers of N biogeochemistry (Figure 2.5). While studies on the importance of biological factors are prevalent in the N saturation literature, less research has focused on catchment hydrology and landscape topography as related to N processing and transport. A fundamental challenge of catchment-scale biogeochemistry is the integration of hydrologic processes and landscape form and function into conceptual and computational models optimized for biological parameterization. In order to establish a more comprehensive view of “catchment processes”, we suggest some potential areas of future research.

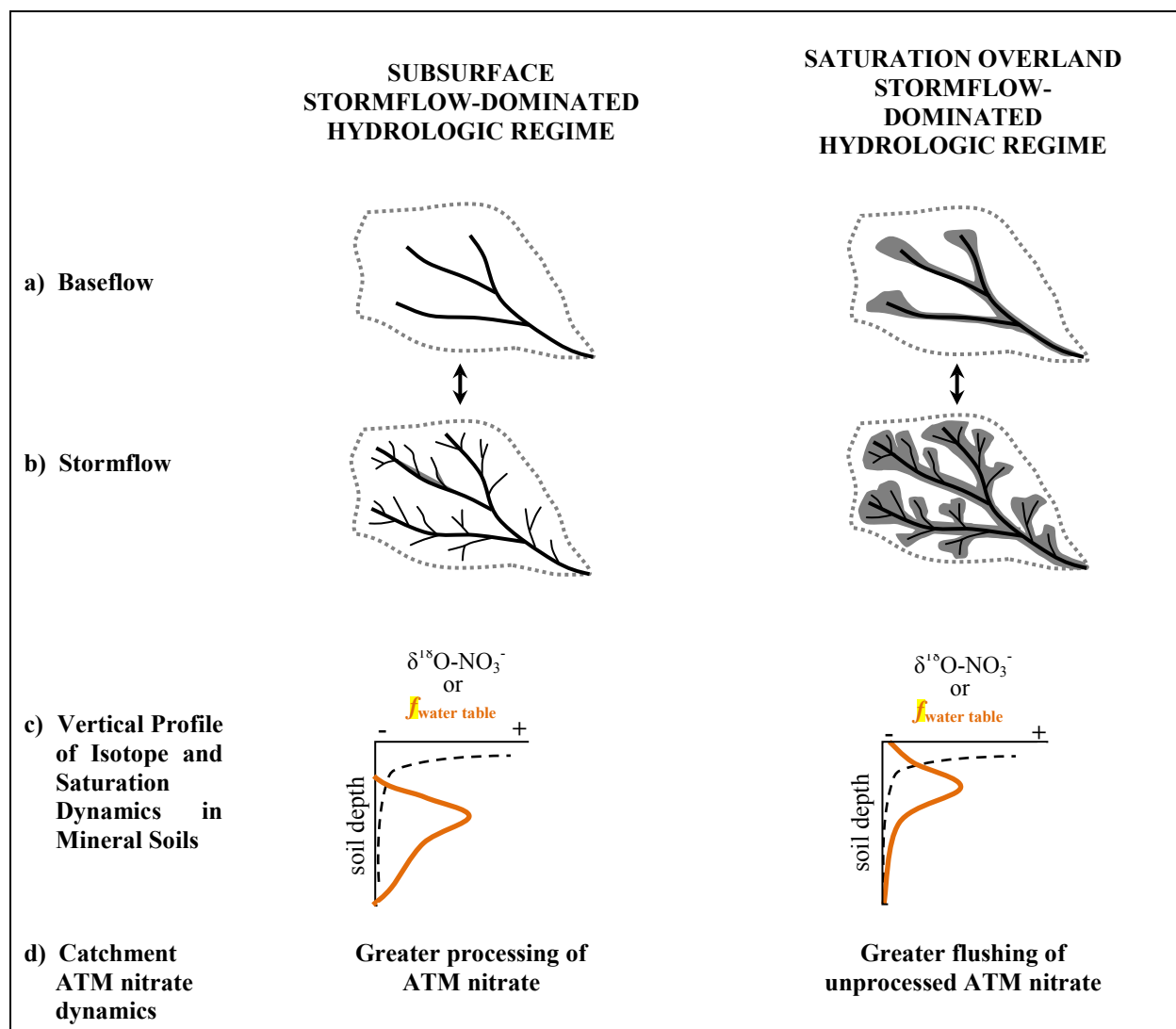


Figure 2.5. Conceptual model of hydrological and topographic regulation of catchment-scale atmospheric nitrate export.

a) During baseflow, subsurface stormflow-dominated systems (SSF) maintain little hydrologic connectivity between hillslope surficial soils and streams, whereas saturation overland stormflow-dominated systems (SOF) maintain more extensive hydrologic connectivity between catchment areas and streams. b) Under stormflow conditions, channel networks and hydrologic connectivity of surficial soils to streams expand from topographic lows and near-stream areas in SSF-dominated catchments; larger areas of hydrologic connectivity to surficial soils and source areas develop during storms in SOF-dominated systems. c) $\delta^{18}\text{O}-\text{NO}_3^-$ reflects the proportion of unprocessed atmospheric nitrate in soils; under baseflow conditions, $\delta^{18}\text{O}-\text{NO}_3^-$ decreases with soil depth in both SSF- and SOF-dominated systems (dashed line). However, the degree of atmospheric nitrate flushing from upper soil layers to streams during storms depends on the dominant hydrologic regime of the catchment and the depth of the water table (solid orange line; this represents the relative frequency of water table depth within the soil profile). In SSF-dominated systems, the water table

does not intersect the land surface and also might not intersect upper soil layers (i.e. frequency goes to zero), keeping atmospheric nitrate in upper soil layers hydrologically disconnected from the stream. In SOF-dominated systems, the water table may periodically intersect the land surface during hydrologic events, resulting in SOF and flushing of atmospheric nitrate in upper soil layers to the stream. The vertical $\delta^{18}\text{O}-\text{NO}_3^-$ profile is therefore particularly dynamic in SOF-dominated systems. As the water table intersects upper soil layers, $\delta^{18}\text{O}-\text{NO}_3^-$ values temporarily decrease as microbial nitrate from deeper soil layers is transported upward and atmospheric nitrate is flushed to the stream. Subsequent atmospheric deposition inputs gradually increase the $\delta^{18}\text{O}-\text{NO}_3^-$ values of upper soil layers again. d) Greater flushing of unprocessed atmospheric nitrate is therefore expected from SOF-dominated catchments, whereas more extensive processing of atmospheric nitrate inputs is expected in soils of SSF-dominated catchments. These saturation and isotope dynamics are expected to be particularly relevant in flatter near-stream areas.

2.3.1 High Resolution Temporal and Spatial Sampling of Nitrate Isotopes

Hydrologic connectivity and N transport between terrestrial and aquatic systems can be highly transient in space and time, creating “hotspots” and “hot moments” within catchments [Vidon *et al.*, 2010]. Frequent, spatially-intensive sampling for isotopic analysis of N sources and sinks across a range of hydrologic conditions is critical to advancing our understanding of the influence of topographic and hydrologic factors on atmospheric N transport. With the capacity for high-throughput sample analysis, the bacterial denitrifier method for nitrate isotope analysis makes such high resolution sampling and analysis a viable option.

2.3.2 Understanding Internal Water Cycling Dynamics at Relevant Catchment Scales

Heterogeneity of flowpath characteristics across landscapes can result in some areas serving as nutrient sources while others function as nutrient sinks [Fortescue, 1980; Sebestyen *et al.*, 2008;

Inamdar et al., 2009]. Investigating the relative magnitude of N transport along various flowpaths and the biological processes taking place along them would better constrain the importance of biological versus physical drivers in atmospheric nitrate delivery to streams. Additional research on the ways these biological and physical dynamics differ under baseflow and event conditions would provide critical details about the processes by which catchment hydrology and topography facilitate atmospheric nitrate export.

2.3.3 Models to Conceptualize and Parameterize Distinctions among Nitrate and Water

Sources

Catchment-scale hydrologic models can be powerful tools for hypothesis testing and evaluating the sensitivity of ecosystem responses to changes in hydrologic parameters. In order to better understand how hydrology, topography, and biogeochemistry interact across a range of spatial and temporal scales to influence the transport and fate of atmospheric N, new and more integrated models are needed. In addition, existing spatially-explicit hydro-ecological process models such as the Regional Hydro-Ecologic Simulation System (RHESSys) [*Band et al.*, 1993; *Tague and Band*, 2004] are also useful for examining catchment-scale N dynamics. Although most existing biogeochemical models do not explicitly simulate isotope dynamics within ecosystem compartments, coupling mass-balance models with software packages such as the Non-Equilibrium Stable Isotope Simulator (NESIS) [*Rastetter et al.*, 2005] may facilitate such calculations. Future biogeochemical models should also emphasize the incorporation of parameters that capture the spatio-temporal influence of landscape topography and vegetation on

both water and N dynamics, as well as the incorporation of biogeochemical and hydrologic isotope parameters.

2.4 IMPLICATIONS

Determining the factors that most influence atmospheric nitrate processing in and transport through forests has important implications for the study and management of these systems. The concept of N saturation as a condition where ecosystem N supply exceeds biological demand may be too simplistic [*Lovett and Goodale, 2011*], given the overwhelming contributions of microbially-derived N to stream nitrate export observed in many systems (Table 2.2; Figure 2.1). Indeed, observations that demonstrate the greatest percentage of atmospheric nitrate in streams during periods of hydrologic extremes (e.g. snowmelt and storm events) suggest a direct role of catchment hydrology and, perhaps less directly, topography in atmospheric nitrate export to streams. Coupled isotopic analyses of water and nitrate can also inform the parameterization of hydrologic models, as the pathways and processing of the two may not always be the same .

With respect to land management, understanding the role of catchment hydrology in linking atmospheric N inputs and export: 1) provides a basic understanding of how atmospheric pollutants directly affect forests and streams, 2) may inform practices to maximize the potential for N retention through plant uptake or denitrification within landscapes, and 3) offers valuable information to regulators and management agencies to consider when evaluating critical loads, nutrient criteria, and emission regulations. In addition, the importance of seasonal variability in hydrologic regime (e.g. snowmelt and monsoon events) on both total N export as well as the

delivery of atmospheric nitrate in particular to streams can help focus management efforts to mitigate the effects of episodic acidification during those times when N export is likely to be greatest.

3.0 TEMPORAL TRENDS IN STREAM NITRATE SOURCES ACROSS A NITROGEN SATURATION GRADIENT

3.1 INTRODUCTION

Since the Industrial Revolution, anthropogenic nitrogen (N) sources have more than doubled the bioavailable N cycled through the environment [Vitousek *et al.*, 1997]. Increased N deposition can lead to ecosystem N saturation, causing significant harm to terrestrial and aquatic systems. Nitrogen saturation occurs when N inputs exceed vegetation and soil uptake capacities and excess N leaches from landscapes to surface and ground waters, typically as nitrate (NO₃⁻) [Ågren and Bosatta, 1988; Aber *et al.*, 1989; Lovett and Goodale, 2011]. Nitrate can be added to forests via atmospheric deposition, and can also be produced through microbial nitrification in forest soils; increased microbial nitrification rates are one hypothesized symptom of ecosystem N saturation [Aber *et al.*, 1989; Peterjohn *et al.*, 1996]. Elevated nitrate in forest soils can increase nitrate and base cation leaching, leading to soil acidification [Adams *et al.*, 2007]. Excess nitrate leached to surface waters can cause acidification and eutrophication in aquatic systems, resulting in toxic algae blooms, “dead zones”, and degraded drinking water quality [Vitousek *et al.*, 1997; Galloway *et al.*, 2003]. As anthropogenic additions to the global N cycle will likely continue unabated for the foreseeable future [Galloway *et al.*, 2003], it is important to understand the post-depositional processes influencing the transport and fate of atmospheric nitrate in forests.

Aber et al. [1989] proposed a conceptual model detailing various ecosystem responses to elevated N deposition. In this model, ecosystem N saturation progresses through four stages, ranging from N-limited (Stage 0) to severely N-saturated (Stage 3). Long-term increases in nitrate leaching to streams are one hypothesized indicator of N saturation [*Aber et al.*, 1989]. While long-term stream chemistry changes provide a framework for investigating ecosystem health under N-saturated conditions, these data provide little detail about the extent of N cycling prior to its export from the watershed. For example, it is unclear whether the extent to which atmospheric N inputs are cycled differs in N-limited versus N-saturated systems. Stream nitrate concentrations alone provide little information about the biological processes and transport mechanisms affecting atmospheric nitrate in watersheds.

Stable isotopes of nitrate ($\delta^{15}\text{N}$, $\delta^{18}\text{O}$, and $\Delta^{17}\text{O}$) elucidate the influence of biotic and abiotic factors on the fate and transport of atmospheric nitrate deposited to forests. Small mass differences between isotopes of an element cause different reaction rates during physical, chemical, and biological processes. These differences impart unique isotopic signatures (denoted by δ) to various sources, making stable isotopes useful for differentiating among ecosystem nitrate sources (Figure 1.2).

Previous studies have used nitrogen and oxygen stable isotopes to track spatio-temporal changes in atmospheric and microbial nitrate pools and to differentiate between them [*Pardo et al.*, 2004; *Barnes et al.*, 2008; *Sebestyen et al.*, 2008, 2014; *Goodale et al.*, 2009]. For example, preferential biological uptake of lighter isotopes (termed *mass-dependent fractionation*) can lead to enrichment of soil and stream $\delta^{15}\text{N}$ compared to $\delta^{15}\text{N}$ values in precipitation [*Barnes et al.*, 2008]. Temporal trends in $\delta^{15}\text{N}$ values across dormant and growing seasons can thus provide information about biological nitrate processing. However, mass-dependent fractionation also

confounds nitrate source apportionment when biological processes (such as denitrification) act as permanent sinks for nitrate (Figure 1.2).

Differences in nitrate $\delta^{18}\text{O}$ values have also been used to distinguish atmospheric and soil sources and to calculate their relative contributions to ecosystem nitrate pools [Williard *et al.*, 2001; Pardo *et al.*, 2004; Goodale *et al.*, 2009; Sebestyen *et al.*, 2014]. While $\delta^{18}\text{O}$ of nitrate has proven useful in many previous studies, it is also susceptible to mass-dependent fractionation and may therefore lead to imprecise source apportionment. However, isotopic source signatures can also result from processes not dependent on mass; these mass-independent signatures— such as $\Delta^{17}\text{O}$ of nitrate— are not fractionated by biological processes [Michalski *et al.*, 2004]. Positive $\Delta^{17}\text{O}$ of nitrate values result from the creation of atmospheric nitrate anomalously enriched in the ^{17}O isotope [Cliff and Thiemens, 1997]. Because the nitrate $\Delta^{17}\text{O}$ anomaly only forms in the atmosphere, its presence identifies a nitrate molecule as atmospherically-derived. This makes $\Delta^{17}\text{O}$ a robust tool for differentiating atmospheric from microbially-derived nitrate, which lacks the $\Delta^{17}\text{O}$ anomaly. The $\Delta^{17}\text{O}$ signature is altered only when an atmospheric nitrate molecule ceases to exist—i.e., when it is biologically assimilated and converted to organic N. The $\Delta^{17}\text{O}$ of atmospheric nitrate is not fractionated by biological processes; rather, biological processing resets the $\Delta^{17}\text{O}$ value to zero. Thus, $\Delta^{17}\text{O}$ serves as a conservative and unambiguous tracer of atmospheric nitrate in ecosystems. The presence of positive $\Delta^{17}\text{O}$ values in forest streams implies that some proportion of atmospheric nitrate deposition has not undergone biological processing prior to export, potentially signaling N-saturated conditions.

In this study, we characterized the triple nitrate isotopic composition ($\delta^{15}\text{N}$, $\delta^{18}\text{O}$, and $\Delta^{17}\text{O}$) of streams sampled weekly from four watersheds in the Fernow Experimental Forest (Figure 1.4). These watersheds differ with respect to long-term patterns of stream nitrate export,

suggesting that they represent unique stages of N saturation. Here we present the results of triple nitrate isotope analysis and discuss the implications of our findings for N saturation theory.

3.2 STUDY SITE AND METHODS

3.2.1 Study Site

Fernow Experimental Forest is located in the Allegheny Mountains portion of West Virginia, on the unglaciated Allegheny Plateau (Figure 1.4). Elevations in the study watersheds range from 720 to 865 m, and slopes average ~20%. Bedrock is primarily composed of hard sandstone and softer shale of the Upper Devonian Hampshire Formation (Canon Hill and Rowlesburg Members); little water storage occurs in these strata [Reinhart *et al.*, 1963; Kochenderfer, 2007]. Soils are well-drained loams and silt loams of the Calvin and Dekalb series (loamy-skeletal, mixed active, mesic typic Dystrudepts), averaging 1 m in depth. Mixed hardwoods are the dominant forest type, with northern red oak (*Quercus rubra*), sugar maple (*Acer saccharum*), red maple (*Acer rubrum*), black cherry (*Prunus serotina*), and yellow poplar (*Liriodendron tulipifera*) the most abundant species. The growing season at Fernow extends from late April through October, and precipitation is evenly distributed throughout the year, with an annual average of 1450 mm; significant snowpack does not accumulate over long periods. During high-intensity rain events, streamflow is high and falls off quickly during periods of low-intensity or no precipitation [Reinhart *et al.*, 1963]. Infiltration rates are high and most precipitation reaches the streams via subsurface flow [Reinhart *et al.*, 1963].

We sampled stream water from three hardwood-dominated stands and one Norway spruce (*Picea abies*) stand. These four watersheds share similar site characteristics (e.g., climate, discharge patterns, geology, soils, elevation) but vary with respect to stream nitrate concentrations, treatment history, and dominant overstory composition (Table 3.1). The N saturation status of each study watershed was determined based on long-term stream nitrate concentrations (Table 3.1); this metric has been cited as one indicator of N saturation stage [Aber *et al.*, 1989; Stoddard, 1994]. Indeed, Stoddard [1994] identified the Stage 2 watershed in this study (WS4) as one of the best examples of an N-saturated watershed based on long-term trends in stream nitrate concentration in this watershed (Figure 3.1).

3.2.2 Sample Collection

From January through December 2010, 1 L stream samples were collected weekly in high density polyethylene bottles at the base of each watershed when streams were flowing. Samples were vacuum-filtered through 0.22 μm polyethersulfone membrane filters to remove suspended solids and biological material. All samples were processed at the US Forest Service Timber and Watershed Laboratory in Parsons, West Virginia within 24 hours of collection. Filtered samples were frozen and transported to the University of Pittsburgh, where they remained frozen until isotopic analysis. Weekly samples of wet-only deposition were also collected at a National Atmospheric Deposition Program (NADP) National Trends Network site located approximately 2 km from the study watersheds from February through December 2010. These samples were filtered through 0.45 μm polyethersulfone membrane filters and archived at 4°C at the NADP

Central Analytical Laboratory in Champaign, IL, USA. Precipitation samples were shipped to the University of Pittsburgh and frozen until isotopic analysis.

Table 3.1. Description of study watersheds

N saturation stage	Water-shed #	Size (ha)	Dominant canopy species	Forest age (yrs)	Aspect	Treatment history	Mean stream [NO ₃] (mg L ⁻¹) 1980-2010
0	6	22	<i>Picea abies</i>	40	S	Lower half clearcut 1964; upper half clearcut 1967-68; maintained barren until 1969. Planted <i>P. abies</i> 1973	0.9
1	5	36	<i>Acer rubrum</i> , <i>Acer saccharum</i>	Uneven	NE	Selective cut (~10% of basal area > 27.9cm dbh removed every 10 yrs.)	1.7
2	4	39	<i>Quercus rubra</i> , <i>Acer rubrum</i>	110	SE	Control, no treatment	3.4
3	7	24	<i>Liriodendron tulipifera</i> , <i>Acer rubrum</i> , <i>Quercus rubra</i>	44	E	Upper half clearcut 1963; lower half clearcut 1966; kept barren until 1969, natural regeneration	5.1

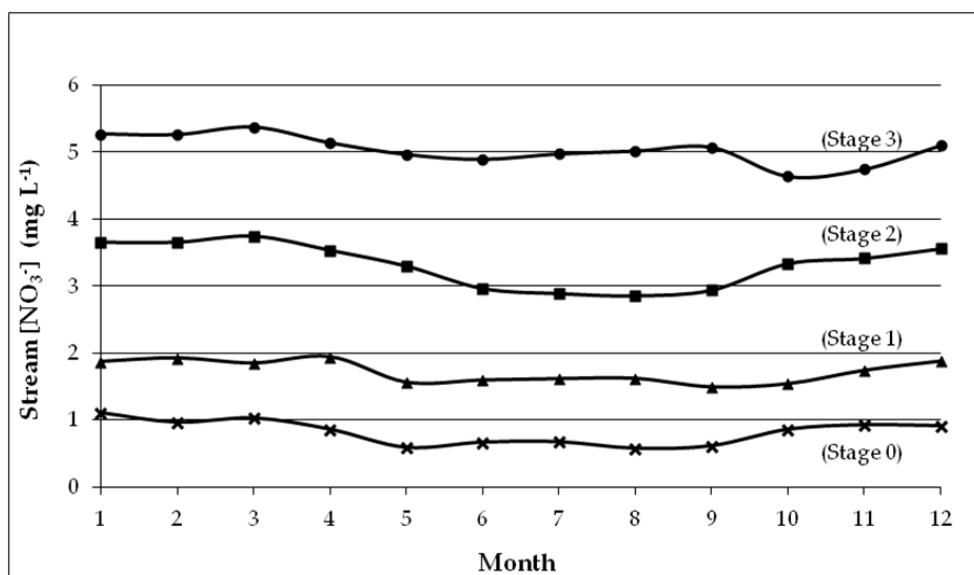


Figure 3.1. Average monthly stream nitrate concentrations in the four study watersheds at Fernow Experimental Forest from 1980-2010.

3.2.3 Isotopic Analysis

Nitrate concentrations for all samples were measured by ion chromatography (Dionex ICS-2000) at the University of Pittsburgh. For isotopic analysis, a denitrifying bacteria, *Pseudomonas aureofaciens*, was used to convert aqueous nitrate into gaseous N_2O which was then introduced into the mass spectrometer [Sigman *et al.*, 2001; Casciotti *et al.*, 2002]. For $\Delta^{17}O$ analysis, this N_2O was thermally decomposed at $800^\circ C$ into N_2 and O_2 prior to isotopic analysis following the method described by Kaiser *et al.* [2007]. Duplicate samples were analyzed for $\delta^{15}N$ and $\delta^{18}O$ of nitrate (and separately for $\Delta^{17}O$ of nitrate during $\Delta^{17}O$ analysis) on an Isoprime Trace Gas and Gilson GX-271 autosampler coupled with an Isoprime Continuous Flow Isotope Ratio Mass Spectrometer (CF-IRMS) at the *Regional Stable Isotope Laboratory for Earth and*

Environmental Science at the University of Pittsburgh. Isotope values are reported in parts per thousand relative to nitrate standards as follows:

$$\delta^{15}\text{N}, \delta^{18}\text{O}, \text{ and } \delta^{17}\text{O} (\text{‰}) = \left[\left(\frac{R_{\text{sample}}}{R_{\text{standard}}} \right) - 1 \right] \times 1000 \quad (\text{Eq. 1})$$

where $R = {}^{15}\text{N}/{}^{14}\text{N}$, ${}^{18}\text{O}/{}^{16}\text{O}$, or ${}^{17}\text{O}/{}^{16}\text{O}$. The mass-independent oxygen isotope anomaly of nitrate ($\Delta^{17}\text{O}\text{-NO}_3^-$) is likewise reported in parts per thousand and calculated using the equation:

$$\Delta^{17}\text{O} (\text{‰}) = \delta^{17}\text{O} - 0.52 \times \delta^{18}\text{O} \quad (\text{Eq. 2})$$

Samples with low nitrate concentrations were pre-concentrated prior to bacterial conversion to N_2O . Pre-concentration was accomplished by calculating the sample volume necessary to obtain a final concentration of 20 nmol (for $\delta^{15}\text{N}$ and $\delta^{18}\text{O}$ analysis) or 200 nmol (for $\Delta^{17}\text{O}$ analysis) in a 5 mL sample. Appropriate sample volumes were measured into 10% hydrochloric acid-washed Pyrex or Teflon beakers and placed in a drying oven at 60°C until all liquid evaporated. The interior of each beaker was then rinsed with 10mL of 18 M Ω water to reconstitute duplicate samples to the appropriate concentration. Samples were prepared for isotopic analysis following the bacterial denitrifier method as previously described. International reference standards were similarly pre-concentrated and used for correction of pre-concentrated samples.

$\delta^{15}\text{N}$ and $\delta^{18}\text{O}$ values were corrected using international reference standards USGS-32, USGS-34, USGS-35, and N3; USGS-34 and USGS-35 were used to correct $\Delta^{17}\text{O}$ values. These

standards were also used to correct for linearity and instrument drift. Standard deviations for international reference standards were 0.2‰, 0.5‰, and 0.2‰ for $\delta^{15}\text{N}$, $\delta^{18}\text{O}$, and $\Delta^{17}\text{O}$, respectively.

There is the potential for isobaric interference of the $\delta^{15}\text{N}$ signal in samples with high $\Delta^{17}\text{O}$ values. Corrections for mass-independent contributions of $\Delta^{17}\text{O}$ to m/z 45 were evaluated following the relationship described in *Coplen et al.* [2004], where a 1‰ increase in $\delta^{15}\text{N}$ corresponds to an 18.8‰ increase in $\Delta^{17}\text{O}$. Corrected $\delta^{15}\text{N}$ values were zero to 1.3‰ lower than uncorrected values, depending on the mass-independent contribution of $\Delta^{17}\text{O}$ in the sample. Because $\Delta^{17}\text{O}$ of nitrate values were low in most samples and because we could not apply the correction to some samples due to a lack of $\Delta^{17}\text{O}$ data (particularly in the Stage 0 stand), the $\delta^{15}\text{N}$ values presented here do not include the mass-independent $\Delta^{17}\text{O}$ correction. While values of corrected $\delta^{15}\text{N}$ data are slightly lower than those presented here, the temporal and spatial trends of $\delta^{15}\text{N}$ values presented here are not strongly influenced by the omission of the mass-independent $\Delta^{17}\text{O}$ correction.

3.2.4 Statistical Analysis

We used analysis of variance to test for significant differences in mean nitrate concentrations, $\delta^{15}\text{N}$, $\delta^{18}\text{O}$, and $\Delta^{17}\text{O}$ values. When significant differences were indicated, we applied Tukey's Honestly Significant Difference test to determine which means were significantly different ($\alpha=0.05$). The experiment-wise error rate was held at $\alpha=0.05$ for multiple comparisons. All statistical analyses were conducted using SAS [*SAS Institute, Inc.*, 2011].

3.3 RESULTS

3.3.1 Nitrate Concentration

Intermittent streamflow in all study watersheds precluded sample collection during much of July through October in the Stage 0, 1, and 2 watersheds and August through October in the Stage 3 watershed. In addition, stream nitrate concentrations were frequently below the detection limit in the Stage 0 watershed, precluding isotopic analysis. Discharge-weighted mean nitrate concentrations in the Stage 0, 1, 2, and 3 watersheds were 0.0, 1.1, 2.1, and 3.7 mg L⁻¹, respectively. The volume-weighted mean nitrate concentration in precipitation was 0.7 mg L⁻¹ (<http://nadp.isws.illinois.edu/data/ntndata.aspx>). Stream nitrate concentrations ranged from zero to 8.4 mg L⁻¹ (Figure 3.2; Table 3.2) and mean nitrate concentration increased significantly with increasing N saturation stage ($p < 0.0001$; Table 2). Nitrate concentrations were seasonally variable in the Stage 1 and Stage 2 watersheds (Figure 3.3), with significantly lower concentrations during the growing season than the dormant season in the Stage 1 ($p < 0.0001$) and 2 ($p = 0.0004$) watersheds. No seasonality in nitrate concentrations was observed in the Stage 0 or 3 watersheds or in precipitation.

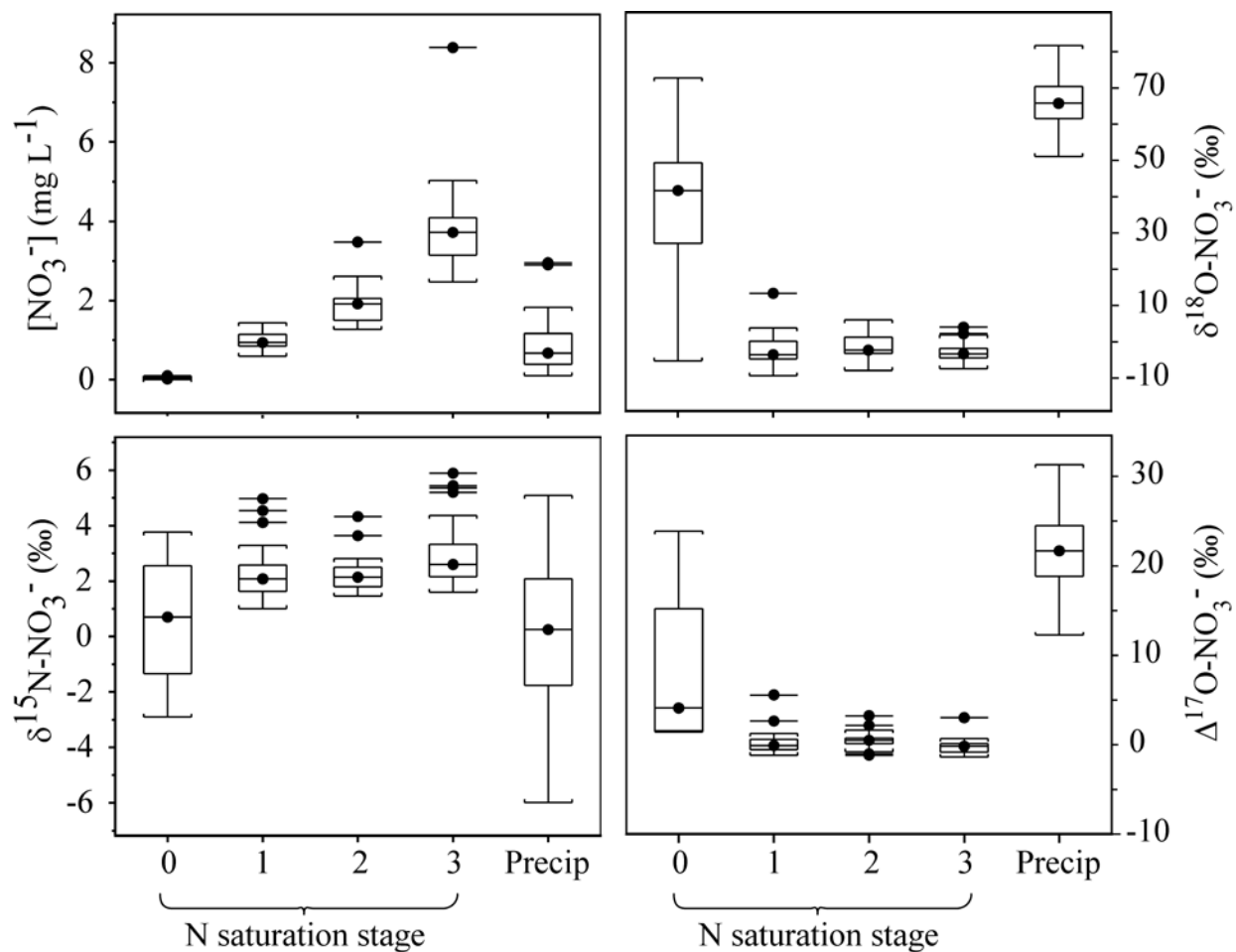


Figure 3.2. Boxplots of stream and precipitation nitrate concentrations, $\delta^{15}\text{N}$, $\delta^{18}\text{O}$, and $\Delta^{17}\text{O}$ isotopes. Boxes represent upper and lower quartiles; whiskers extend to ± 1.5 times the interquartile range. Circles with a line inside the boxes represent median values. Outliers are shown as circles with lines through them.

Table 3.2. Means and ranges of precipitation and stream nitrate concentration and triple nitrate isotope values in study watersheds.

Nitrogen saturation stage means followed by different letters are significantly different at $p < 0.05$.

N saturation stage	[NO ₃ ⁻] (mg L ⁻¹)		δ ¹⁵ N-NO ₃ ⁻ (‰)		δ ¹⁸ O-NO ₃ ⁻ (‰)		Δ ¹⁷ O-NO ₃ ⁻ (‰)	
	<i>Mean</i>	<i>Range</i>	<i>Mean</i>	<i>Range</i>	<i>Mean</i>	<i>Range</i>	<i>Mean</i>	<i>Range</i>
0	0.0 ^d	0.0 to 0.1	+0.5 ^b	-2.9 to +3.8	+38.6 ^b	-5.3 to +72.8	+8.4 ^b	-1.4 to +23.9
1	1.0 ^c	0.6 to 1.4	+2.2 ^a	+1.0 to +5.0	-2.4 ^c	-9.4 to +13.4	+0.2 ^c	-1.2 to +5.6
2	1.9 ^b	1.3 to 3.5	+2.2 ^a	+1.5 to +4.3	-1.5 ^c	-7.9 to +6.1	+0.5 ^c	-1.2 to +3.2
3	3.7 ^a	2.5 to 8.4	+2.9 ^a	+1.6 to +5.9	-2.9 ^c	-7.5 to +4.0	-0.3 ^c	-1.4 to +3.0
Precip	0.8 ^c	0.1 to 2.9	+0.1 ^b	-6.0 to +5.1	+65.2 ^a	+51.1 to +81.7	+20.9 ^a	+12.3 to +29.1

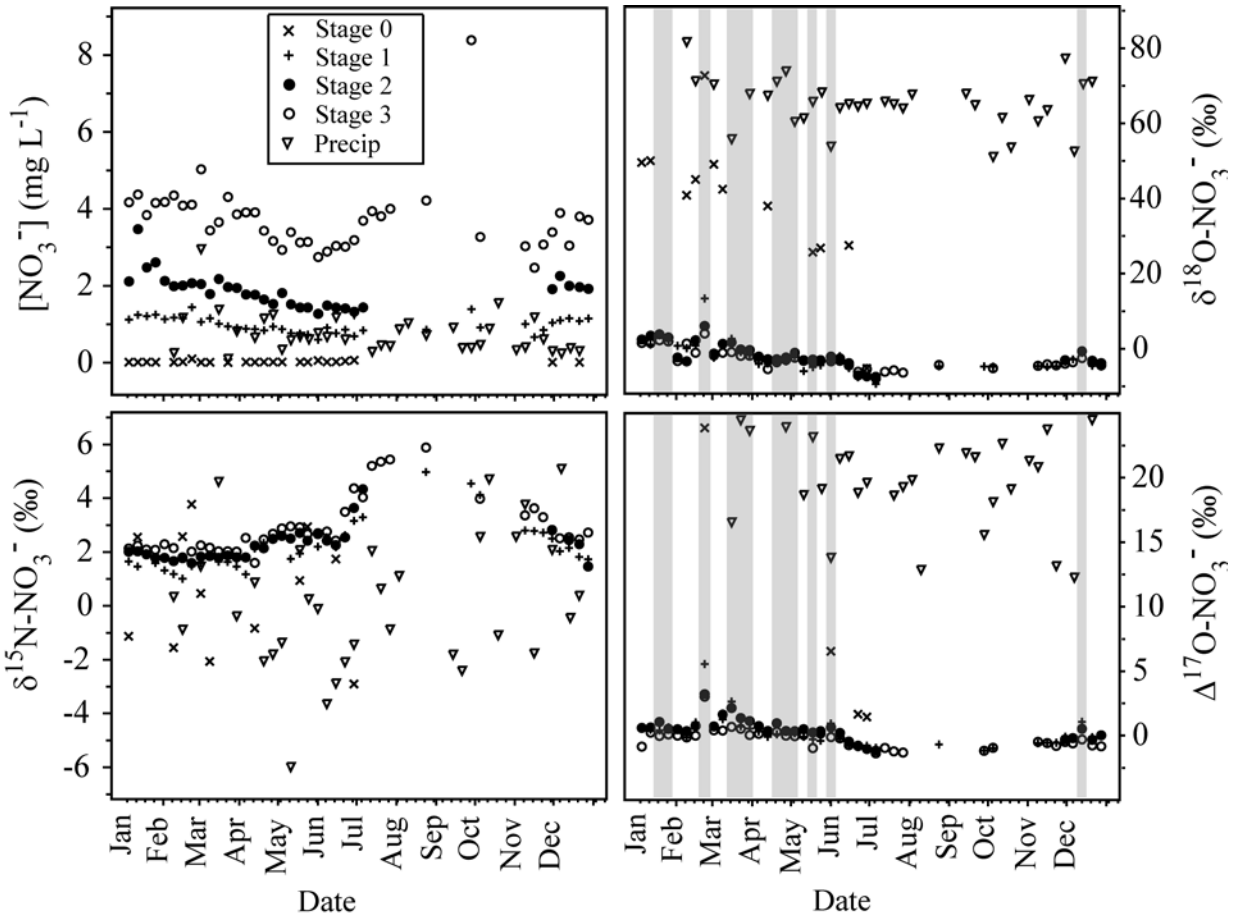


Figure 3.3. Nitrate concentration and isotopic composition of weekly stream and precipitation samples collected at Fernow Experimental Forest during 2010.

Grey bars in $\delta^{18}\text{O}$ and $\Delta^{17}\text{O}$ of nitrate plots indicate samples collected during stormflow.

3.3.2 $\delta^{15}\text{N}$ of Nitrate

Across all watersheds, stream nitrate $\delta^{15}\text{N}$ values ranged from -2.9‰ to +5.9‰; precipitation values ranged from -6.0‰ to +5.1‰ (Figure 3.2; Table 3.2). Mean $\delta^{15}\text{N}$ was significantly lower in the Stage 0 watershed than in the other watersheds ($p < 0.0001$), but mean $\delta^{15}\text{N}$ values were higher in all watersheds than in precipitation (Table 3.2).

Seasonally, mean stream nitrate $\delta^{15}\text{N}$ values were significantly higher during the growing season than the dormant season in the Stage 1, 2, and 3 watersheds and also in precipitation ($p < 0.0001$ for stream water; $p = 0.02$ for precipitation). This seasonal trend may partially explain the lower mean $\delta^{15}\text{N}$ values in the Stage 0 watershed, as streamflow was absent in this watershed during the growing season, when $\delta^{15}\text{N}$ values were highest in the hardwood-dominated stands (Figure 3.3). Seasonal isotope dynamics were not evaluated in the Stage 0 watershed due to the small number of samples collected during the growing season ($n=4$).

3.3.3 $\delta^{18}\text{O}$ of Nitrate

The range of stream nitrate $\delta^{18}\text{O}$ values across all watersheds was -9.4‰ to $+72.8\text{‰}$ whereas precipitation nitrate $\delta^{18}\text{O}$ values ranged from $+51.1\text{‰}$ to $+81.7\text{‰}$ (Figure 3.2; Table 3.2). The highest mean stream nitrate $\delta^{18}\text{O}$ value ($+38.6 \pm 19.0\text{‰}$) occurred in the Stage 0 watershed ($p < 0.0001$; Table 3.2). Although this value was higher than those observed in the other watersheds, it was significantly lower than the mean precipitation value ($+65.2 \pm 6.8\text{‰}$; $p < 0.0001$).

Seasonal trends in stream nitrate $\delta^{18}\text{O}$ were similar among the Stage 1, 2, and 3 watersheds (Figure 3.3), with higher mean values during the dormant season and lower mean values during the growing season ($p < 0.0007$ for all watersheds). While there was no statistically significant difference in seasonal mean $\delta^{18}\text{O}$ values of precipitation nitrate, weekly precipitation samples showed higher dormant season values and lower growing season values (Figure 3.3).

3.3.4 $\Delta^{17}\text{O}$ of Nitrate

The $\Delta^{17}\text{O}$ in stream nitrate ranged from -1.4‰ to +23.9‰ across all watersheds (Figure 3.2; Table 3.2), with a significantly higher mean in the Stage 0 watershed ($p < 0.0001$). Precipitation nitrate $\Delta^{17}\text{O}$ ranged from +12.3‰ to +29.1‰ and the mean ($+20.9 \pm 4.3\%$) was significantly higher than means for all streams ($p < 0.0001$). Values of $\Delta^{17}\text{O}$ in precipitation nitrate were generally lower during the growing season and higher during the dormant season (Figure 3.3), but this trend was not statistically significant. Patterns in stream nitrate $\Delta^{17}\text{O}$ values were opposite that of precipitation (Figure 3.3), with significantly higher means in the Stage 1, 2, and 3 watersheds during the dormant season ($p \leq 0.0135$ for all watersheds).

3.4 DISCUSSION

3.4.1 Atmospheric Nitrate Processing and Export across a Nitrogen Saturation Gradient

A central tenet of nitrogen saturation theory is that N saturation occurs when N supply exceeds the capacity of vegetation and soil pools [Ågren and Bosatta, 1988; Aber *et al.*, 1989; Stoddard, 1994; Lovett and Goodale, 2011]. This theory also posits that excess N supply reduces seasonal variability and leads to a long-term increase in stream nitrate concentration [Aber *et al.*, 1989; Stoddard, 1994]. While these N saturation characteristics have been previously recognized in the Stage 2 and 3 watersheds [Peterjohn *et al.*, 1996; Gilliam *et al.*, 2001], stream nitrate concentration data alone are inadequate to assess biological N demand. Stream nitrate source contributions cannot be determined solely based on temporal trends in concentration, and such source characterization is essential for quantifying the balance between ecosystem N supply and demand. This has important implications for N saturation theory, as elevated rates and/or decreased seasonality of nitrate export may not necessarily indicate saturation of biological demand; the isotope data presented here are a case in point. Although long-term mean stream nitrate concentrations in the Stage 1, 2, and 3 watersheds span a nearly three-fold range (Table 3.1), similarity in their nitrate isotopic compositions (Table 3.2) suggests that atmospheric nitrate inputs are extensively biologically cycled in these watersheds. In contrast, while persistently low nitrate concentrations in the Stage 0 watershed stream suggest N-limitation, $\delta^{18}\text{O}$ and $\Delta^{17}\text{O}$ values of stream nitrate indicate that most of the atmospheric nitrate deposited in this watershed bypasses biological assimilation prior to export.

Differences in atmospheric nitrate processing among watersheds may be related to N saturation stage or may result from other characteristics. The Stage 0 watershed is a Norway spruce monoculture, which is entirely different in terms of plant physiology from the other mixed hardwood-dominated watersheds. This difference in species composition may contribute to the observed atmospheric nitrate export patterns. For example, stream nitrate $\delta^{15}\text{N}$ values were lower and more similar to precipitation $\delta^{15}\text{N}$ values in the Norway spruce-dominated Stage 0 watershed than in the hardwood-dominated stands (Table 3.2). This may be partially attributable to preferential uptake of ammonium over nitrate by Norway spruce, resulting in less enrichment of soil nitrate $\delta^{15}\text{N}$. In an N-saturated forest in Germany, [Gessler *et al.*, 1998] observed minimal nitrate uptake by Norway spruce, particularly in the presence of ammonium. [Marschner *et al.*, 1991] similarly reported ammonium uptake rates 3-4 times higher than nitrate in Norway spruce. During 2010, ammonium-N and nitrate-N deposition rates were 1.7 and 2.5 kg N ha⁻¹, respectively [National Atmospheric Deposition Program, 2014] at Fernow, thus ammonium should be available for uptake, particularly in the Stage 0 watershed where nitrification rates are low [Kelly *et al.*, 2011]. Nitrate comprises only about 1% of soil solution total dissolved N (TDN) in the Stage 0 watershed, with the majority of TDN occurring as dissolved organic N [Kelly, 2010]. In contrast, nitrate is approximately 60% of soil solution TDN in the Stage 3 watershed [Kelly, 2010]. This difference is noteworthy, as these watersheds have identical treatment histories aside from conversion of the Stage 0 watershed to Norway spruce following clearcutting (Table 3.1). These watersheds also differ markedly in microbial nitrate production rates, being nine times higher in the Stage 3 versus Stage 0 watershed [Kelly *et al.*, 2011]. The wide disparity in nitrate source contributions in these two watersheds is reflected in their stream nitrate isotopic compositions. Most of the atmospheric nitrate deposited on the

Stage 0 watershed is retained (as demonstrated by perpetually low stream nitrate concentrations), but high proportions of atmospheric deposition in exported nitrate suggest that nitrate supply exceeds the capacity of biological sinks. This contrasts with the low proportions of atmospheric deposition present in the Stage 3 stream, indicating extensive biological processing. Low rates of microbial nitrate production and potentially lower rates of nitrate uptake by Norway spruce in the presence of ammonium offer one explanation for the higher proportions of atmospheric nitrate in the Stage 0 stream, as well as the similarity between $\delta^{15}\text{N}$, $\delta^{18}\text{O}$, and $\Delta^{17}\text{O}$ values of stream nitrate and precipitation in this watershed.

The range of stream nitrate $\delta^{15}\text{N}$ values across all watersheds (-2.9‰ to +5.9‰) was similar to that reported for microbial nitrate (+2‰ to +8‰) [Kendall *et al.*, 2007]. However, exclusion of Stage 0 watershed data reduces the range of stream nitrate $\delta^{15}\text{N}$ values to +1.0‰ to +5.9‰ in the hardwood-dominated stands; these values are almost fully encompassed by the microbial source range. Enrichment of mean stream nitrate $\delta^{15}\text{N}$ values in the Stage 1, 2, and 3 watersheds versus that of precipitation may be due to preferential biological uptake of the ^{14}N isotope in these watersheds [Pardo *et al.*, 2004; Barnes *et al.*, 2008; Koba *et al.*, 2012]. This mass-dependent fractionation would enrich the soil nitrate pool in ^{15}N , which could subsequently leach to streams. Conversely, similar mean $\delta^{15}\text{N}$ values in precipitation and stream nitrate in the Stage 0 watershed suggest a lesser degree of biological cycling and potentially greater inputs of unprocessed atmospheric nitrate to the stream; this is also confirmed by $\delta^{18}\text{O}$ and $\Delta^{17}\text{O}$ values.

Similar to $\delta^{15}\text{N}$, the range of stream nitrate $\delta^{18}\text{O}$ values across all watersheds (-9.4‰ to +72.8‰) was large, but when the Stage 0 watershed was excluded, the range was greatly reduced (-9.4‰ to +13.4‰). Stream nitrate $\delta^{18}\text{O}$ values in the Stage 1, 2, and 3 watersheds fell within the microbial source range (-10‰ to +15‰; [Kendall *et al.*, 2007]), indicating that microbial

nitrification was the primary nitrate source in these hardwood-dominated watersheds throughout the year. Using an isotope mixing model, we calculated the mean fraction of atmospheric nitrate exported from each watershed (Equation 3):

$$f_{\text{atm}} = \frac{\chi_{\text{stream}} - \chi_{\text{nitrification}}}{\chi_{\text{atm}} - \chi_{\text{nitrification}}} \quad (\text{Eq. 3})$$

where χ is $\delta^{18}\text{O}$ or $\Delta^{17}\text{O}$ of nitrate. We used the lowest measured stream nitrate $\delta^{18}\text{O}$ value in each watershed as the nitrification end-member and the minimum and maximum $\delta^{18}\text{O}$ of nitrate values of precipitation as the atmospheric end-member to calculate the range of atmospheric nitrate export from each watershed [Barnes *et al.*, 2008]. This $\delta^{18}\text{O}$ -based approach indicates that atmospheric nitrate accounts for an average of 8 to 12%, 7 to 11%, and 5 to 8% of nitrate in streams draining the Stage 1, 2, and 3 watersheds, respectively. These low proportions are in agreement with $\delta^{18}\text{O}$ -based results of other studies in the northeastern U.S. that have generally observed minor contributions of atmospheric nitrate to streams draining forested watersheds [Williard *et al.*, 2001; Burns and Kendall, 2002; Barnes *et al.*, 2008; Sebestyen *et al.*, 2008, 2014; Goodale *et al.*, 2009]. In contrast to the hardwood-dominated stands, the Norway spruce-dominated Stage 0 watershed displayed very different patterns in $\delta^{18}\text{O}$ of nitrate. Using Equation 3, atmospheric nitrate contributions to the Stage 0 stream ranged from 50 to 78%.

While mixing model estimates based on $\delta^{18}\text{O}$ of nitrate values have previously been used to quantify the extent of biological N cycling [Williard *et al.*, 2001; Burns and Kendall, 2002; Barnes *et al.*, 2008; Sebestyen *et al.*, 2008; Goodale *et al.*, 2009], the potential for mass-dependent fractionation of $\delta^{18}\text{O}$ during assimilation and denitrification can enrich the residual

soil nitrate pool over time and lead to overestimation of atmospheric source contributions. $\Delta^{17}\text{O}$ of nitrate more conservatively estimates the proportion of atmospheric nitrate in streams because it is not susceptible to mass-dependent fractionation. Values of $\Delta^{17}\text{O}$ for terrestrial sources (e.g., nitrification) are typically zero or less, whereas values for atmospheric nitrate can range from +20‰ to +30‰ [Michalski *et al.*, 2004]. In the hardwood-dominated stands, stream nitrate $\Delta^{17}\text{O}$ values ranged from -1.4‰ to +5.6‰, suggesting minor atmospheric nitrate contributions to streams draining these watersheds. In contrast, $\Delta^{17}\text{O}$ values in the Norway spruce stand ranged from +1.5‰ to +23.9‰ (Figure 3.2). It should be noted, however, that $\Delta^{17}\text{O}$ data from this watershed were extremely limited (n=4) due to low nitrate concentrations in most stream samples. Using the lowest $\Delta^{17}\text{O}$ value in each watershed as the nitrification end-member (this value was set to 0‰ in the Stage 0 watershed, as all measured stream nitrate values were positive) and the minimum and maximum $\Delta^{17}\text{O}$ of nitrate values of precipitation as the atmospheric end-member, we substituted the corresponding $\Delta^{17}\text{O}$ values into Equation 3 to calculate atmospheric nitrate contributions to streams. $\Delta^{17}\text{O}$ -based estimates of atmospheric nitrate in the Stage 0, 1, 2, and 3 watershed streams are 29-68%, 5-10%, 6-12%, and 4-8%, respectively. Thus, $\delta^{18}\text{O}$ and $\Delta^{17}\text{O}$ data both indicate that as stream nitrate concentrations increase (suggesting increasing nitrogen saturation), microbial nitrification becomes an increasingly important stream nitrate source. This is in agreement with results of other nitrate isotope studies that reported extensive biological processing of atmospheric N in forests across a range of N deposition rates [Spoelstra *et al.*, 2001; Williard *et al.*, 2001; Michalski *et al.*, 2004; Pardo *et al.*, 2004; Barnes *et al.*, 2008; Sebestyen *et al.*, 2008; Tsunogai *et al.*, 2010]. Therefore, while mean stream nitrate concentrations differ among the Stage 0, 1, 2, and 3 N-saturated watersheds, nitrate concentrations alone cannot serve as a basis for inferences about the presence

of nitrate in excess of biological demand. Indeed, the combined concentration- and isotope-based approaches presented here indicate that nitrogen supply does not exceed biological demand in any of these watersheds and that microbial nitrate production may even increase in response to elevated atmospheric N deposition.

3.4.2 Seasonal Variability of Stream Nitrate Isotopic Composition

A clear seasonal pattern in stream nitrate $\delta^{15}\text{N}$ was observed in the hardwood-dominated watersheds (Figure 3.3). The sharp increase in $\delta^{15}\text{N}$ values from early April through late August may be due to mass-dependent fractionation during nitrification and/or plant uptake. While mineralization of organic N to ammonium does not produce large isotopic fractionations [Kendall, 1998], oxidation of ammonium to nitrate can result in fractionations ranging from $\epsilon = -12\text{‰}$ to -29‰ [Shearer and Kohl, 1986]. Thus, as the ratio of net nitrification to net mineralization increases, the $\delta^{15}\text{N}$ of nitrate in soils should approach that of the original soil ammonium pool [Spoelstra *et al.*, 2007]. Increasing rates of net nitrification relative to net N mineralization from early April through late August may have resulted in this seasonal increase of $\delta^{15}\text{N}$ values in the hardwood-dominated watersheds. Alternatively, greater N uptake by plants could have produced the same temporal $\delta^{15}\text{N}$ trend. In N-limited forests, available soil N pools are depleted during the growing season as plants maximize N uptake [Stoddard, 1994]. By contrast, net nitrification rates in the Stage 2 and 3 watersheds are highest during the growing season and soil N pools remain well above $0 \text{ g NO}_3^- \text{-N m}^{-2}$ throughout the year, indicating that microbial nitrate production exceeds plant uptake [Gilliam *et al.*, 2001]. Greater nitrate supply during the growing season may facilitate preferential uptake of the lighter ^{14}N isotope, yielding

an isotopically-enriched residual soil nitrate pool [Högberg, 1997; Templer *et al.*, 2007] that could then be leached to streams. Although plant N demand decreases sharply at the end of the growing season, soil microbial processes such as nitrification can continue throughout the dormant season under an insulating snowpack [Campbell *et al.*, 2005]. Persistent microbial activity coupled with decreased N demand during the dormant season would result in less isotopic fractionation of soil water nitrate, yielding lower $\delta^{15}\text{N}$ of nitrate values in streams at the end of the growing season and throughout the dormant season. Similarly, the generally lower $\delta^{15}\text{N}$ values observed in the Stage 0 watershed throughout the study period may indicate lower N cycling rates in that watershed relative to the more N-saturated stands. Indeed, previous studies in the Stage 0, 2, and 3 watersheds confirm that net nitrification rates are lower in the Stage 0 Norway spruce stand than in the Stage 2 and 3 hardwood-dominated stands [Gilliam *et al.*, 2001; Kelly, 2010].

In contrast to the seasonal enrichment in stream nitrate $\delta^{15}\text{N}$ values, trends in stream $\delta^{18}\text{O}$ of nitrate were flat or declined during the growing season (Figure 3.3). Patterns in stream $\delta^{18}\text{O}$ of nitrate may be disproportionately influenced by varying contributions of atmospheric nitrate, that has high $\delta^{18}\text{O}$ values [Michalski *et al.*, 2004]; this can obscure temporal signals resulting from biological activity. It is therefore helpful to remove the atmospheric component from nitrate $\delta^{18}\text{O}$ values when examining temporal trends that may be due to biological processes [Dejwakh *et al.*, 2012]. Because the two primary sources of nitrate at Fernow are atmospheric deposition and nitrification, a simple mixing model can be used to subtract the atmospheric nitrate contribution, yielding the $\delta^{18}\text{O}$ value of the microbial end-member (Equation 4):

$$\delta^{18}\text{O}_{\text{microbial}} = \delta^{18}\text{O}_{\text{stream}} - f_{\text{atm}} \times \delta^{18}\text{O}_{\text{atm}} \quad (\text{Eq. 4})$$

The f_{atm} term is calculated using $\Delta^{17}\text{O}$ of nitrate values in Equation 3 because $\Delta^{17}\text{O}$ is a conservative tracer of atmospheric nitrate in ecosystems [Dejwakh *et al.*, 2012]. Assigning $\Delta^{17}\text{O}$ values of 0‰ to the nitrification end-member and +19.8‰ to the precipitation end-member (representing the volume-weighted $\Delta^{17}\text{O}$ value of precipitation nitrate during 2010) we calculated the proportion of atmospheric nitrate (f_{atm}) in each stream sample. Substituting this f_{atm} value and a $\delta^{18}\text{O}_{\text{atm}}$ value of +60.8‰ (representing the volume-weighted $\delta^{18}\text{O}$ value of precipitation nitrate during 2010) into Equation 4, we estimated the $\delta^{18}\text{O}$ of microbial nitrate ($\delta^{18}\text{O}_{\text{microbial}}$) for all stream samples. Because the Stage 0 watershed only had four data points for $\Delta^{17}\text{O}$ of nitrate, $\delta^{18}\text{O}_{\text{microbial}}$ was not calculated for this watershed.

After removing the atmospheric nitrate contribution, a temporal shift occurs between untransformed $\delta^{18}\text{O}$ and $\delta^{18}\text{O}_{\text{microbial}}$ values of stream nitrate (Figure 3.4). Although $\delta^{18}\text{O}_{\text{microbial}}$ values still decrease during the early growing season, the timing of this trend is shifted, such that the lowest $\delta^{18}\text{O}_{\text{microbial}}$ values occur in March and April rather than July and August. This seasonal timing is more consistent with the expected increase in microbial activity (which would yield lower nitrate $\delta^{18}\text{O}$ values) as ambient temperatures increase during the early growing season [Norton and Stark, 2011].

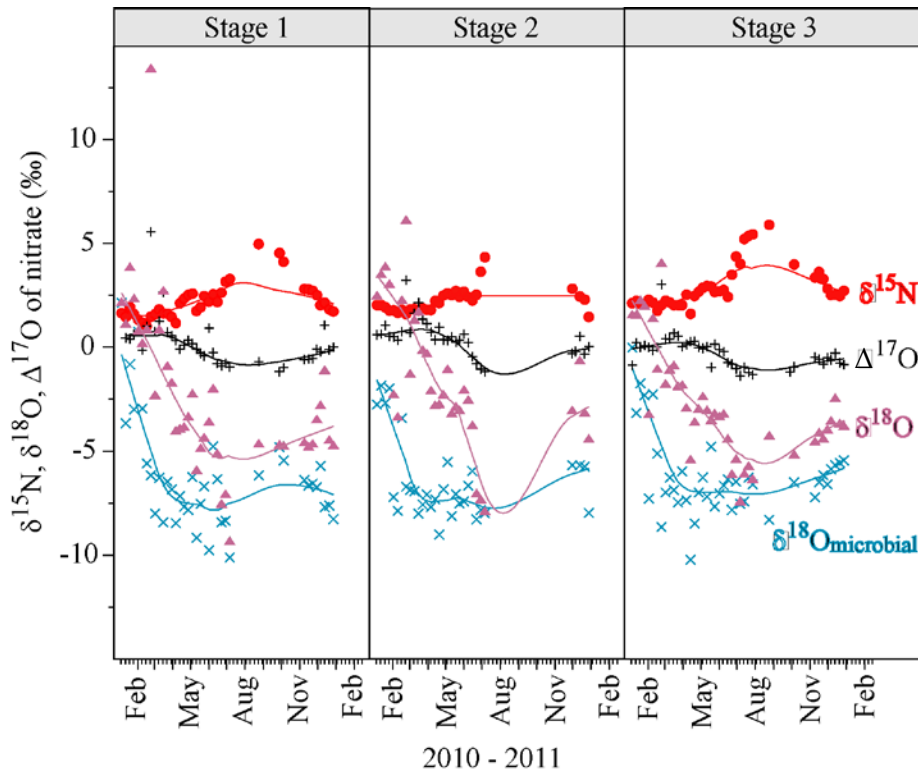


Figure 3.4. Temporal trends in stream water nitrate isotopic composition in the hardwood-dominated watersheds.

Data for $\delta^{18}\text{O}_{\text{microbial}}$ represent stream nitrate $\delta^{18}\text{O}$ data that have been transformed using Equation 4 to remove the influence of atmospheric nitrate. Removal of the atmospheric influence allows temporal trends due to biological processes (e.g., nitrification, denitrification, assimilation) to be more clearly visualized. Trendlines for data series were generated using a local regression (LOESS) smoothing curve to emphasize the temporal shift between untransformed $\delta^{18}\text{O}$ and $\delta^{18}\text{O}_{\text{microbial}}$ values.

The absence of a seasonal enrichment in stream nitrate $\delta^{18}\text{O}$ values similar to that observed for $\delta^{15}\text{N}$ is not unexpected, as the $^{18}\text{O}/^{16}\text{O}$ ratio of microbial nitrate is not influenced by nitrogen substrate availability [Spoelstra et al., 2007]. Rather, the $\delta^{18}\text{O}$ values of stream nitrate in the hardwood-dominated stands were likely influenced by the oxygen isotopic compositions of soil water and O_2 , as microbial nitrification was the dominant stream nitrate source in the Stage

1, 2, and 3 watersheds. During microbial nitrification, oxygen atoms are contributed to the nitrate molecule in varying proportions by atmospheric O₂ ($\delta^{18}\text{O-O}_2 = +23\text{‰}$) and soil water [Buchwald and Casciotti, 2010]. While $\delta^{18}\text{O}$ values of soil O₂ could have increased with increasing respiration rates, previous research in temperate forests suggests these fractionations are minor (+0.08‰ to +0.47‰ relative to $\delta^{18}\text{O}$ of atmospheric O₂; [Spoelstra et al., 2007]). In contrast, $\delta^{18}\text{O}$ values of soil water can be highly spatially and temporally variable at Fernow (L. Rose, unpublished data), potentially affecting the oxygen isotopic composition of stream nitrate. The influence of soil water isotopic composition on the $\delta^{18}\text{O}$ of stream nitrate depends on several factors, including spatial and temporal variability of microbial nitrification rates and hydrologic connectivity between watershed areas and the stream. This complicates efforts to determine the specific factors responsible for the temporal trends in $\delta^{18}\text{O}$ of nitrate observed in streams.

While trends in both $\delta^{15}\text{N}$ and $\delta^{18}\text{O}$ can provide insight into the role of biological processes in stream nitrate export, temporal $\Delta^{17}\text{O}$ of nitrate dynamics highlight the seasonal variability of atmospheric nitrate contributions to streams. Mean $\Delta^{17}\text{O}$ values were significantly higher during the dormant season than the growing season in all watersheds ($p < 0.0135$ for all watersheds). Lower biological N demand during the dormant season may partially explain the elevated atmospheric nitrate export during the dormant season. However, stream $\Delta^{17}\text{O}$ of nitrate was low compared to precipitation even during the dormant season, indicating little atmospheric nitrate in streams. Mean stream nitrate $\Delta^{17}\text{O}$ values during the dormant season were $+0.6 \pm 1.4\text{‰}$, $+0.8 \pm 0.8\text{‰}$, and $0.0 \pm 0.8\text{‰}$ for the Stage 1, 2, and 3 N-saturated watersheds, respectively. In comparison, the mean dormant season precipitation nitrate $\Delta^{17}\text{O}$ value was $+22.4 \pm 5.5\text{‰}$. Substituting into Equation 3 and using the lowest $\Delta^{17}\text{O}$ value measured in each watershed for the nitrification end-member, mean dormant season contributions of atmospheric nitrate to streams

in the Stage 1, 2, and 3 N-saturated watersheds were 8%, 8%, and 6%, respectively. Thus, despite generally higher stream nitrate $\Delta^{17}\text{O}$ values during the dormant season, overall contributions of atmospheric nitrate to streams during this period of lower biological demand remained small.

The low proportions of atmospheric nitrate in streams draining the hardwood-dominated stands may be due to persistent microbial activity in these watersheds, perhaps facilitated periodically by an insulating snowpack [Campbell *et al.*, 2005]. Hydrologic characteristics of the study watersheds may also influence atmospheric nitrate export to streams. [Pardo *et al.*, 2004] suggested that short hydrologic residence times on hillslopes and significant storage capacity in well-mixed subsurface reservoirs may dampen seasonal signals of stream nitrate isotopes. Increased litter decomposition at the end of the growing season could also create a significant soil N pool that, if flushed during a dormant season hydrologic event, could elevate stream nitrate concentrations, but not necessarily increase proportions of atmospheric nitrate [Cirimo and McDonnell, 1997]. However, [Sebestyen *et al.*, 2014] observed the opposite trend during an autumn storm event, attributing lower stream nitrate concentrations to heterotrophic uptake following leaf fall, and elevated atmospheric nitrate export during storm events to increased hydrologic connectivity and rapid transport. Without directly measuring changes in hydrologic connectivity between landscape areas and streams, it is difficult to determine how biological versus hydrologic drivers influenced the seasonal trends and magnitudes of atmospheric nitrate export we observed at Fernow. However, there is evidence to support the idea that hydrologic status influenced atmospheric nitrate export in these watersheds.

3.4.3 Hydrologic Drivers of Watershed Atmospheric Nitrate Export

Stream nitrate $\delta^{18}\text{O}$ and $\Delta^{17}\text{O}$ values were higher in samples collected during stormflow in all watersheds (Figure 3.3). Additionally, the largest proportion of atmospheric nitrate exported from all watersheds occurred during a snowmelt event on 23 February. Using the highest precipitation nitrate $\Delta^{17}\text{O}$ value measured during the study period (+29.1‰) and the lowest $\Delta^{17}\text{O}$ value measured in each watershed (and 0‰ for the Stage 0 watershed) for the nitrification end-member in Equation 3, atmospheric nitrate contributed 82%, 22%, 15%, and 14% to total stream nitrate in the Stage 0, 1, 2, and 3 N-saturated watersheds, respectively, on 23 February. That the greatest proportions of atmospheric nitrate in all streams occurred on the same day suggests a common factor influencing atmospheric nitrate export.

Prior to 21 February, the maximum daily temperature remained below 0°C for 26 days while total precipitation ranged from 88 mm in the Stage 2 watershed to 112 mm in the Stage 1 watershed (snow water equivalent). When ambient temperatures rose above freezing from 21-23 February, the resulting snowmelt event produced peak discharges of 2.9 mm, 1.7 mm, and 2.1 mm on 24 February in the Stage 1, 2, and 3 watersheds and 0.96 mm on 3 March in the Stage 0 watershed. Sample collection on 23 February coincided with the rising limb of this hydrologic event in each watershed. Rapid routing of melt water and decreased biological activity during this time may have facilitated greater export of atmospheric nitrate to streams. Other studies have reported greater proportions of atmospheric nitrate in streams during snowmelt events [Burns and Kendall, 2002; Sebestyen et al., 2008; Goodale et al., 2009], suggesting that watershed hydrologic status can be an important regulator of atmospheric nitrate export. However, it is important to reiterate that the proportion of atmospheric nitrate exported from

these watersheds is generally small throughout the year. Indeed, much larger discharges than those observed on 23 February were recorded in all of the watersheds during the study period but these occurred during the growing season, resulting in only marginal increases in the proportion of atmospheric nitrate in streams. Although hydrologic status can influence atmospheric nitrate export, extensive biological N cycling— particularly in the hardwood-dominated watersheds— outweighs the influence of hydrologic extremes (e.g., storm events) in these watersheds.

3.4.4 Implications for Nitrogen Saturation Theory

Various mechanisms have been proposed to explain the development of N saturation in forests, including interactions between soil and vegetation pools [Ågren and Bosatta, 1988; Lovett and Goodale, 2011]. These models hypothesize that soil N accumulates over time due to low net N mineralization rates relative to N input from litterfall (assuming constant litter production rates), eventually saturating the soil N pool [Ågren and Bosatta, 1988; Lovett and Goodale, 2011]. The rate at which the soil N pool saturates (termed *kinetic saturation* by [Lovett and Goodale, 2011]) is a function of several factors, including litterfall quality, the rate of litter addition to the forest floor, and the C:N ratio and community composition of the soil microbial pool [Ågren and Bosatta, 1988; Magill et al., 1997; Compton et al., 2004; Lovett and Goodale, 2011]. These factors, combined with rates of allochthonous N additions from atmospheric deposition, regulate the degree of kinetic N saturation in soils.

Under N-limited conditions, strong competition exists between vegetation and microbial sinks for available N, with plants generally out-competing nitrifying bacteria [Kaye and Hart, 1997]. Increased ecosystem N availability can reduce this competition, leading to greater

microbial nitrate production and lower ratios of mineralization to nitrification [Magill *et al.*, 1997; Compton *et al.*, 2004]. Previous studies have reported higher microbial nitrification rates at sites with elevated N deposition [Magill *et al.*, 1997; Lovett and Rueth, 1999; Jordan *et al.*, 2005]; when microbial nitrate production exceeds plant N demand, excess nitrate can leach to streams, signaling ecosystem N saturation. This appears to be occurring in the Stage 2 and 3 N-saturated watersheds examined in our study. Net nitrification is nearly 100% of net N mineralization in these watersheds, and soil inorganic N pools remain above 0 g NO₃⁻-N m⁻² throughout the growing season [Gilliam *et al.*, 2001] suggesting that N supply exceeds plant demand. In contrast, net nitrification is only approximately 20% of net N mineralization in the Stage 0 (N-limited) watershed [Kelly, 2010], indicating stronger competition between vegetation and microbial sinks for available ammonium.

The idea put forth in previous descriptions of N saturation— that stream nitrate export represents the fraction of N inputs in *excess* of biological demand [Aber *et al.*, 1989; Stoddard, 1994]— may not apply to all (or even most) forests exhibiting symptoms of N saturation. Our study and others employing nitrate stable isotopes [Williard *et al.*, 2001; Barnes *et al.*, 2008; Sebestyen *et al.*, 2008, 2014] highlight a critical aspect of ecosystem N cycling with important implications for N saturation theory: while the capacity for biological N cycling is large in some forests, the capacity for N retention is often smaller, particularly in forests exhibiting symptoms of N saturation.

The conceptual model in Figure 3.5 shows potential differences in vegetation and microbial processing of atmospheric nitrate inputs and ecosystem N retention in N-limited versus N-saturated forests. While nitrate uptake can occur in N-limited systems, nitrate assimilation is typically low in vegetation when soil nitrate availability is limited [Gessler *et al.*, 1998; Collier

et al., 2003]. In contrast, greater soil nitrate supply (such as in N-saturated systems) can induce nitrate uptake in vegetation [*Gessler et al.*, 1998; *Min et al.*, 1998; *Collier et al.*, 2003], leading to greater biological cycling of atmospheric nitrate inputs. Additionally, decreased competition between vegetation and microbial pools for soil N may increase biological N cycling in both vegetation and microbial pools, further elevating biological N processing in already N-saturated forests. Increased vegetative uptake of N (including atmospheric nitrate), along with greater microbial nitrate production, is manifested at the watershed outlet as elevated stream nitrate concentrations, greater proportions of microbial nitrate, and lower proportions of atmospheric nitrate in streams (Figure 3.5). The roles of vegetation and soil microbial communities in ecosystem N processing suggested by this conceptual model have been confirmed by a variety of studies showing induction of nitrate uptake by vegetation with increasing soil nitrate availability [*Gessler et al.*, 1998; *Min et al.*, 1998; *Collier et al.*, 2003] and increasing nitrification relative to N mineralization under elevated N deposition [*Aber et al.*, 1998]. Thus, the more extensive biological processing of atmospheric nitrate inputs associated with elevated stream nitrate concentrations in the current study suggests that rather than exceeding biological demand, elevated atmospheric nitrate inputs may actually stimulate both vegetative demand and microbial production of nitrate.

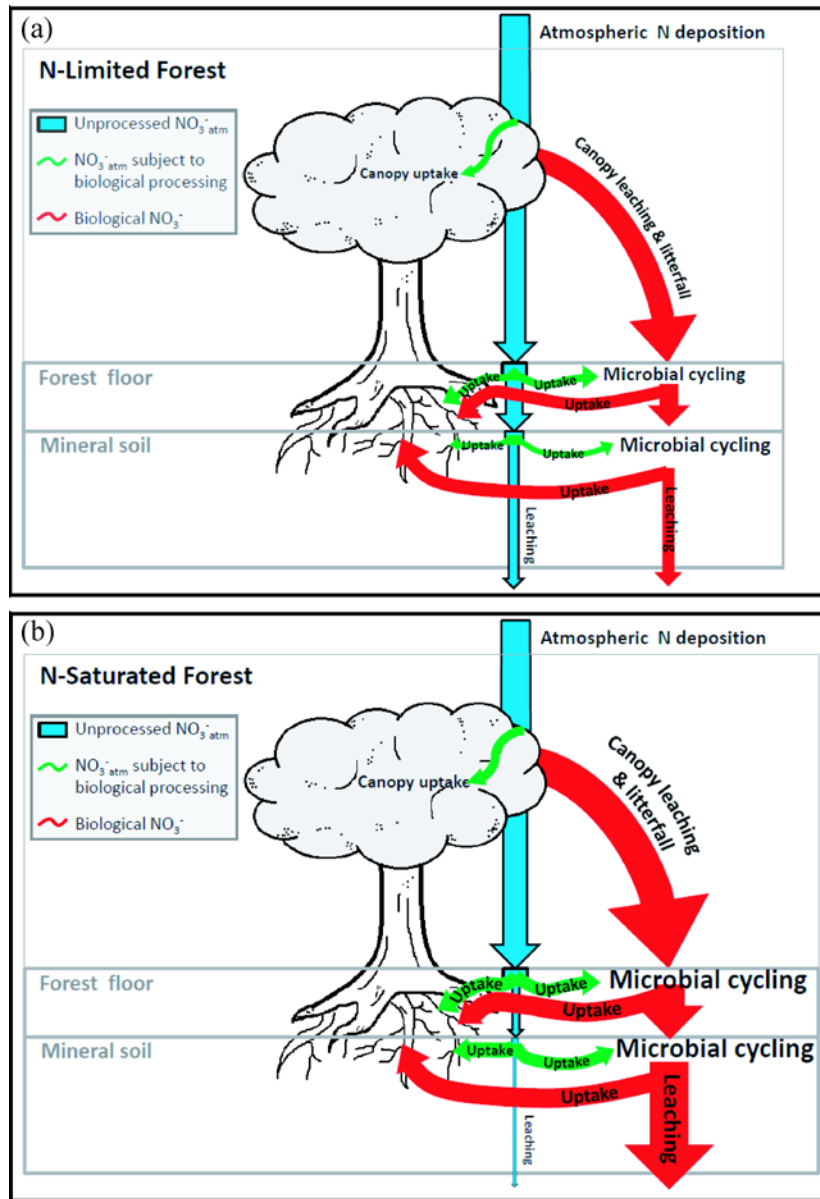


Figure 3.5. Conceptual model of atmospheric nitrate processing and export dynamics under N-limitation and N-saturation.

Text and arrow sizes reflect the relative importance of N sources and fluxes. (a) In N-limited systems, nitrate uptake by vegetation and microbial nitrate production are limited, facilitating greater export of unprocessed atmospheric nitrate. (b) Chronic elevated nitrate deposition induces nitrate uptake by vegetation and decreases competition between vegetation and microbes for N, encouraging microbial nitrate production, elevated nitrate leaching, and ecosystem N saturation.

Given the large capacity of soil to serve as both a source and sink for ecosystem N, improved understanding of the ways that chronic N additions (in all forms) alter the capacity of ecosystem sinks to cycle and retain N will facilitate better predictions of N saturation development in forests. The stable isotope data presented here demonstrate that elevated stream nitrate export does not necessarily signal N supply in excess of biological demand, and that microbial nitrate production can exert significant control on the degree of watershed nitrate export.

3.5 CONCLUSION

Our results indicate that while vegetation and microbial sinks assimilate atmospheric N inputs to a great extent at Fernow, their ability to retain N inputs is often limited. These observations are in agreement with the conceptual models of ecosystem nitrogen saturation put forward by [Ågren and Bosatta, 1988] and [Lovett and Goodale, 2011], which emphasize the importance of balance among soil N production, plant demand, and atmospheric deposition in regulating ecosystem N export. By quantifying the direct contributions of atmospheric deposition to stream nitrate export in multiple watersheds characterized by differing long-term stream nitrate concentrations, we have demonstrated that stream nitrate concentrations alone do not reflect the capacity of forests to cycle and retain atmospheric N inputs. While this study focused on nitrate export dynamics in forested watersheds, other forms of N input—such as ammonium and dissolved organic N—exert additional influence on the degree of biological N cycling and ecosystem N retention. Improved understanding of the ways that various forms of chronic N addition alter the

capacity of biological sinks to cycle and retain N will facilitate better predictions of N saturation development in forested systems.

4.0 DECOUPLED NITRATE SOURCE DYNAMICS IN WATERSHEDS ACROSS SPATIAL SCALES

4.1 INTRODUCTION

Decades of chronic elevated atmospheric nitrogen (N) deposition have led to the N saturation of forested systems throughout the eastern U.S. [Aber *et al.*, 1998; Galloway *et al.*, 2003]. The theory of N saturation holds that as N availability exceeds the retention capacity of ecosystem sinks (e.g., vegetation and soils), excess nitrate (NO_3^-) is leached to surface and ground waters [Aber *et al.*, 1989; Stoddard, 1994; Lovett and Goodale, 2011]. Common metrics used to assess the extent of ecosystem N saturation include long-term concentration increases [Edwards and Helvey, 1991; Peterjohn *et al.*, 1996; Adams, 1999] and decreased seasonal variability [Stoddard, 1994; Peterjohn *et al.*, 1996; Adams, 1999] of stream nitrate concentrations. However, concentration measurements taken at the watershed outlet alone provide little information about the heterogeneity of intra-watershed N cycling processes. The potential decoupling of terrestrial and stream nitrate dynamics across spatial scales has been previously observed in eastern forests [Goodale *et al.*, 2009; Sebestyen *et al.*, 2014].

Spatio-temporal variability of intra-watershed atmospheric N processing and transport may influence the nitrate signals observed at the watershed outlet. Stream nitrate is generally positively correlated with atmospheric N deposition [Mitchell *et al.*, 1997; Aber *et al.*, 2003;

Driscoll et al., 2003; *Pardo et al.*, 2006; *Dise et al.*, 2009], but N mineralization and nitrification rates can be substantial in some systems, potentially complicating this relationship. For example, nitrification rates are highly spatially variable in several watersheds at Fernow Experimental Forest [*Gilliam et al.*, 2001] but the effect of this spatial variability on nitrate source contributions to streams is poorly constrained, particularly across a continuum of hydrologic states. Nitrate concentrations measured at the watershed outlet may therefore obscure N processing heterogeneity at the sub-watershed scale. Outlet measurements represent the integration of all nitrate sources in watershed areas that are hydrologically connected to the stream. As the extent of landscape-stream hydrologic connectivity can vary spatially and temporally [*Hibbert and Troendle*, 1988; *Creed and Band*, 1998; *Jencso et al.*, 2009], it is important to characterize nitrate biogeochemical indicators (e.g., concentration and stable isotopic composition) at a variety of spatial scales to identify the drivers of nitrate export from individual landscape units to the watershed outlet.

Isotopic approaches employing $\delta^{15}\text{N}$, $\delta^{18}\text{O}$, and $\Delta^{17}\text{O}$ of nitrate can be useful for differentiating nitrate sources (Figure 1.2) and assessing N source dynamics across spatial scales. The presence of atmospheric nitrate isotopic signatures in soil water and streams indicates that some proportion of N deposition inputs is not biologically cycled. However, several studies reported only minor contributions of unprocessed atmospheric nitrate to streams, despite a wide range of deposition and stream N fluxes [*Spoelstra et al.*, 2001; *Burns and Kendall*, 2002; *Ohte et al.*, 2004; *Pardo et al.*, 2004; *Barnes et al.*, 2008]. If landscape units vary in their contributions to streamflow— or if contributing areas change through time—this can have serious implications for the interpretation of N dynamics as assessed at the watershed outlet.

Thus, a closer examination of the N saturation concept and the roles of hydrologic connectivity and dynamic contributing areas in nitrate export is warranted.

Understanding the roles of hydrology and topography in determining the source areas, magnitude, and timing of N transport to aquatic systems is essential, as effective management and mitigation of N pollution effects requires a clear understanding of the drivers of biogeochemical signals observed at the watershed outlet. Characterizing the influences of hydrology and topography on nitrate export can also clarify the extent to which stream nitrate concentrations are reflective of physical (e.g., hydrology- and mixing-driven) versus biological processes.

Here we use nitrate concentration and stable isotope measurements to address the spatio-temporal variability of nitrate sources across Watershed 4 (WS4) at Fernow Experimental Forest, as measured in A horizon (0-10 cm) soil water from January 2010 through February 2011. We consider potential drivers of intra-watershed nitrate source heterogeneity, contrast these observations with patterns of nitrate source contributions to the stream at the outlet of WS4, and discuss the implications for N saturation theory of decoupled nitrate source dynamics across spatial scales.

4.2 STUDY SITE AND METHODS

4.2.1 Study Site

This study was conducted in Watershed 4 (WS4) at the Fernow Experimental Forest (39°05' N, 79°40' W; Figure 1.4). Fernow is located in the Allegheny Mountains portion of West Virginia. Elevations in WS4 range from 720 to 865 m, and slopes average ~20%. Bedrock is primarily composed of hard sandstone and softer shale of the Upper Devonian Hampshire Formation (Rowlesberg Member); little water storage occurs in these strata [Reinhart *et al.*, 1963; Kochenderfer, 2007]. Soils are channery silt loams of the Calvin series (loamy-skeletal, mixed active, mesic typic Dystrudept), averaging 1 m in depth [Kochenderfer, 2007]. Infiltration rates in these soils are high and most precipitation reaches the stream via subsurface flow [Reinhart *et al.*, 1963]. Mixed hardwoods are the dominant forest type in WS4; northern red oak (*Quercus rubra*), sugar maple (*Acer saccharum*), red maple (*Acer rubrum*), and black cherry (*Prunus serotina*) are the most abundant species [Peterjohn *et al.*, 1999]. The growing season at Fernow extends from late April through October, and precipitation is evenly distributed throughout the year, with an annual average of 1450 mm; significant snowpack does not accumulate over long periods. Nitrate comprised approximately 60% of inorganic wet N deposition ($\text{NO}_3^- + \text{NH}_4^+$) to Fernow in 2010 [National Atmospheric Deposition Program, 2011].

4.2.2 Sample Collection

Fifteen sets of nested zero-tension pan lysimeters collected soil water draining the A horizon throughout WS4 (Figure 4.1). When soil water was present in lysimeters, we collected samples monthly from January 2010 through February 2011. During the growing season there is generally insufficient soil water present in lysimeters; in addition, sample collections did not occur in February and December 2010 or January 2011.

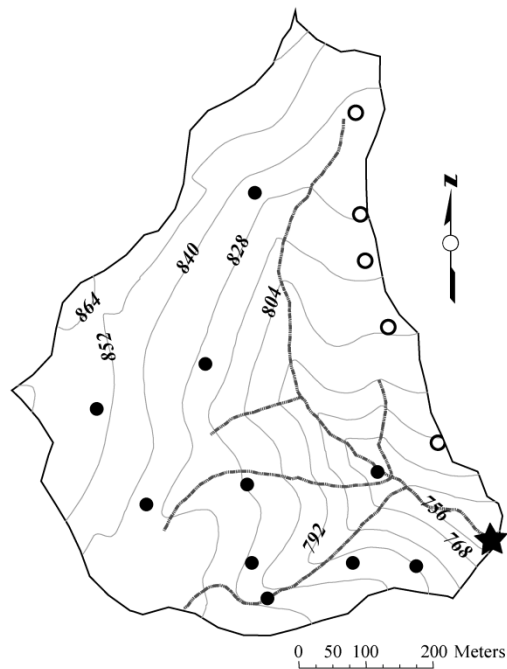


Figure 4.1. Map of lysimeters in Watershed 4 at Fernow Experimental Forest (FEF).

Lysimeters located on the east-facing aspect are shown as solid black circles; lysimeters on the south-facing aspect are shown as open circles. The black star indicates the location of the weir at the base of the watershed. Elevation contours are in meters (12-meter interval).

In October 2011, soil samples were collected from the A horizon immediately upslope of each lysimeter location. At each location, five mineral soil samples were collected to a depth of 5 cm using a hand trowel. Samples at each lysimeter were composited in plastic bags, thoroughly mixed, and transported to the University of Pittsburgh where they were frozen until isotopic analysis. Soil subsamples from each lysimeter location were subsequently freeze-dried, ground with a mortar and pestle, and packed into tin capsules for isotopic analysis.

4.2.3 Isotopic Analysis

Isotopic analysis of soil samples was conducted using a EuroVector high temperature elemental analyzer connected to a GV Instruments Isoprime Continuous Flow Isotope Ratio Mass Spectrometer (CF-IRMS) at the *Regional Stable Isotope Laboratory for Earth and Environmental Science* at the University of Pittsburgh. Precisions were 0.3‰ for $\delta^{13}\text{C}$ and 0.5‰ for $\delta^{15}\text{N}$ on duplicate samples.

Nitrate concentrations for all soil water samples were measured by ion chromatography (Dionex ICS-2000) at the University of Pittsburgh. For $\delta^{15}\text{N}$, $\delta^{18}\text{O}$, and $\Delta^{17}\text{O}$ analysis of soil water nitrate, a denitrifying bacteria, *Pseudomonas aureofaciens*, was used to convert aqueous nitrate into gaseous N_2O which was then introduced into the mass spectrometer [Sigman *et al.*, 2001; Casciotti *et al.*, 2002]. For $\Delta^{17}\text{O}$ analysis, this N_2O was thermally decomposed at 800°C into N_2 and O_2 prior to isotopic analysis following the method described by Kaiser *et al.* [2007]. Duplicate samples were analyzed for $\delta^{15}\text{N}$ and $\delta^{18}\text{O}$ of nitrate (and separately for $\Delta^{17}\text{O}$ of nitrate during $\Delta^{17}\text{O}$ analysis) on an Isoprime Trace Gas and Gilson GX-271 autosampler coupled with

an Isoprime Continuous Flow Isotope Ratio Mass Spectrometer (CF-IRMS). Isotope values are reported in parts per thousand relative to nitrate standards as follows:

$$\delta^{15}\text{N}, \delta^{17}\text{O}, \text{ and } \delta^{18}\text{O} (\text{‰}) = \left[\left(\frac{R_{\text{sample}}}{R_{\text{standard}}} \right) - 1 \right] \times 1000 \quad (\text{Eq. 1})$$

where $R = {}^{15}\text{N}/{}^{14}\text{N}$, ${}^{18}\text{O}/{}^{16}\text{O}$, or ${}^{17}\text{O}/{}^{16}\text{O}$. The mass-independent oxygen isotope anomaly of nitrate ($\Delta^{17}\text{O}\text{-NO}_3^-$) is likewise reported in parts per thousand and calculated using the equation:

$$\Delta^{17}\text{O} (\text{‰}) = \delta^{17}\text{O} - 0.52 \times \delta^{18}\text{O} \quad (\text{Eq. 2})$$

Samples with low nitrate concentrations were pre-concentrated prior to bacterial conversion to N_2O . For pre-concentration, the sample volume necessary to obtain a final concentration of 20 nmol (for $\delta^{15}\text{N}$ and $\delta^{18}\text{O}$ analysis) or 200 nmol (for $\Delta^{17}\text{O}$ analysis) in a 5 mL sample was calculated. Appropriate sample volumes were measured into 10% hydrochloric acid-washed Pyrex or Teflon beakers and placed in a drying oven at 60°C until all liquid evaporated. The interior of each beaker was then rinsed with 10mL of 18 M Ω water to reconstitute duplicate samples to the appropriate concentration. Samples were prepared for isotopic analysis following the bacterial denitrifier method described above. International reference standards were similarly pre-concentrated and used for correction of pre-concentrated samples. Precisions for all soil water samples were 0.2‰, 0.5‰, and 0.2‰ for $\delta^{15}\text{N}$, $\delta^{18}\text{O}$, and $\Delta^{17}\text{O}$, respectively.

There is the potential for isobaric interference of the $\delta^{15}\text{N}$ signal in samples with high $\Delta^{17}\text{O}$ values. Corrections for mass-independent contributions of $\Delta^{17}\text{O}$ to m/z 45 were evaluated following the relationship described in *Coplen et al.* [2004], where a 1‰ increase in $\delta^{15}\text{N}$ corresponds to an 18.8‰ increase in $\Delta^{17}\text{O}$. Corrected $\delta^{15}\text{N}$ values were zero to 1.7‰ lower than uncorrected values, depending on the mass-independent contribution of $\Delta^{17}\text{O}$ in the sample. Because this correction factor is small relative to the range of soil water $\delta^{15}\text{N}$ values observed and because we could not apply the correction to some samples due to a lack of $\Delta^{17}\text{O}$ data, the $\delta^{15}\text{N}$ values presented here do not include the mass-independent $\Delta^{17}\text{O}$ correction. While values of corrected $\delta^{15}\text{N}$ data are slightly lower than the data presented here, the temporal and spatial trends of $\delta^{15}\text{N}$ values presented here are not strongly influenced by the omission of the mass-independent $\Delta^{17}\text{O}$ correction.

4.2.4 Statistical Analysis

Data were analyzed using the Proc GLM procedure in SAS [*SAS Institute, Inc.*, 2011]; mean values were not volume-weighted. Nitrate concentration data for March 2010 and February 2011 were log-transformed prior to means comparisons among months to meet the assumption of normality and equality of variances. Nitrate concentration data for east- and south-facing aspects were similarly log-transformed prior to means comparisons between aspects.

4.3 RESULTS

4.3.1 Soil Water Nitrate Concentrations

Soil water nitrate concentrations showed a high degree of spatial and temporal variability across WS4. Nitrate concentrations ranged from zero to 11.4 mg L⁻¹ over the entire study period, with the highest monthly mean concentrations in March (2.5±3.3 mg L⁻¹) and the lowest monthly value in the single sample collected in July (0.2 mg L⁻¹) (Figure 4.2; Table 4.1). It should be noted that the soil water samples collected in October 2010 represent soil water from a single storm event whereas soil water collected during all other months had accumulated since the previous monthly collection. The large coefficients of variation during most months (Table 4.1) demonstrate the high degree of spatial variability observed across WS4 throughout the study period. Due to this variability, there were no statistically significant differences in mean nitrate concentration among months, despite a five-fold difference between the highest and lowest mean monthly nitrate concentrations (Figure 4.2; Table 4.1).

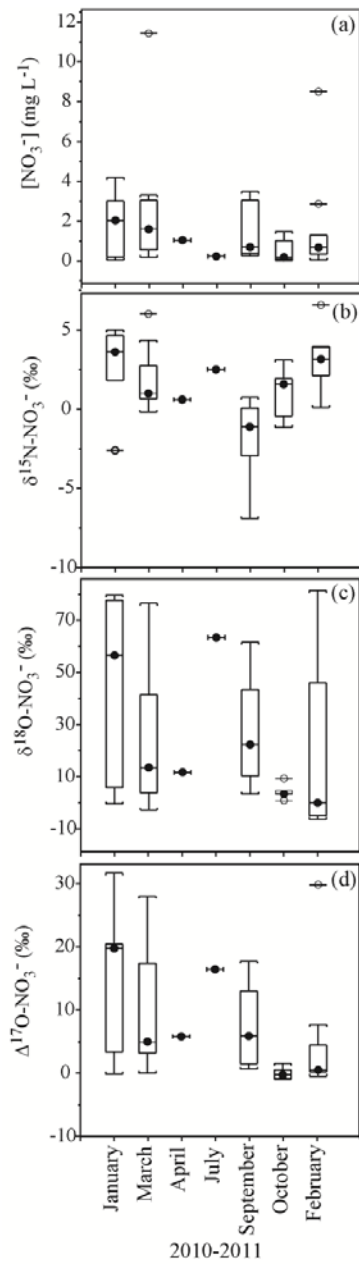


Figure 4.2. Monthly soil water nitrate (a) concentration, (b) $\delta^{15}\text{N}$, (c) $\delta^{18}\text{O}$, and (d) $\Delta^{17}\text{O}$ in WS4
Boxplots for nitrate concentration show untransformed data. Boxes represent upper and lower quartiles; whiskers extend to ± 1.5 times the interquartile range. Circles and lines inside boxes represent median values. Outliers are shown as open circles with lines.

Table 4.1. Monthly mean, range, and coefficient of variation of soil water nitrate concentration and triple nitrate isotopes in WS4.

NA=Unable to calculate range and CV due to n=1 (April and July 2010), or negative mean yielded negative CV% (September and October 2010).

*Nitrate concentration mean, range, and CV are reported for back-transformed data. CVs were calculated following [Koopmans *et al.*, 1964].

Month	$[\text{NO}_3^-]$			$\delta^{15}\text{N-NO}_3^-$			$\delta^{18}\text{O-NO}_3^-$			$\Delta^{17}\text{O-NO}_3^-$		
	<i>Mean</i> (mg L^{-1})	<i>Range</i> (mg L^{-1})	<i>CV (%)</i>	<i>Mean</i> (mg L^{-1})	<i>Range</i> (mg L^{-1})	<i>CV</i> (%)	<i>Mean</i> (mg L^{-1})	<i>Range</i> (mg L^{-1})	<i>CV</i> (%)	<i>Mean</i> (mg L^{-1})	<i>Range</i> (mg L^{-1})	<i>CV</i> (%)
Jan 2010	1.7 (n=7)	0.0 to 4.2	94	+2.7 (n=6)	-2.6 to +5.0	105	+46.0 (n=6)	-0.5 to +79.7	77	+15.0 (n=5)	-0.1 to +31.6	88
Mar 2010*	1.3 (n=10)	0.2 to 12.6	183	+1.8 (n=10)	-0.2 to +6.0	113	+25.0 (n=10)	-2.8 to +76.5	121	+10.0 (n=9)	0.0 to +28.0	104
Apr 2010	1.0 (n=1)	<i>NA</i>	<i>NA</i>	+0.6 (n=1)	<i>NA</i>	<i>NA</i>	+11.7 (n=1)	<i>NA</i>	<i>NA</i>	+5.8 (n=1)	<i>NA</i>	<i>NA</i>
Jul 2010	0.2 (n=1)	<i>NA</i>	<i>NA</i>	+2.5 (n=1)	<i>NA</i>	<i>NA</i>	+63.4 (n=1)	<i>NA</i>	<i>NA</i>	+16.4 (n=1)	<i>NA</i>	<i>NA</i>
Sept 2010	1.5 (n=8)	0.3 to 3.5	96	-1.8 (n=8)	-6.9 to +0.8	<i>NA</i>	+27.1 (n=8)	+3.4 to +61.6	76	+7.4 (n=8)	+0.7 to +17.7	87
Oct 2010	0.5 (n=9)	0.0 to 1.5	110	+1.0 (n=5)	-1.1 to +3.1	169	+4.3 (n=5)	+0.9 to +9.3	72	-0.05 (n=6)	-1.0 to +1.5	<i>NA</i>
Feb 2011*	0.6 (n=10)	0.0 to 8.0	238	+3.1 (n=8)	+0.1 to +6.6	60	+19.6 (n=8)	-6.4 to +81.4	190	+5.0 (n=8)	-0.5 to +29.8	209

Previous work on this watershed has demonstrated a significant influence of aspect on biogeochemical attributes such as soil water nitrate concentration, net nitrification rate, and overstory vegetation species composition [*Peterjohn et al.*, 1999; *Gilliam et al.*, 2001; *Christ et al.*, 2002]. In agreement with these previous studies, we observed a higher mean soil water nitrate concentration on the east-facing aspect (1.10 ± 0.49) than the south-facing aspect (0.20 ± 0.41) following log-transformation of nitrate concentrations (Figure 4.3; Table 4.2).

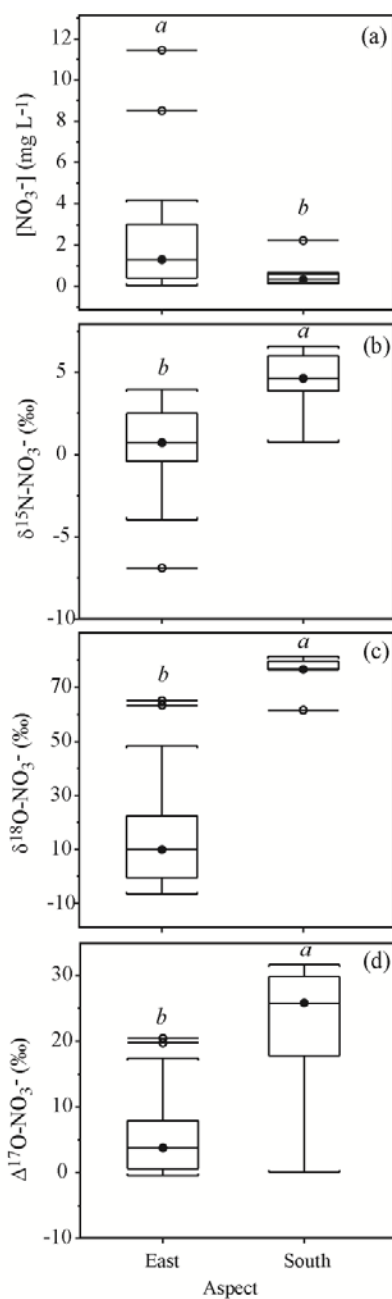


Figure 4.3. Nitrate (a) concentration, (b) $\delta^{15}\text{N}$, (c) $\delta^{18}\text{O}$, and (d) $\Delta^{17}\text{O}$ on the dominant aspects of WS4. Boxplots for nitrate concentration show untransformed data. Boxes represent upper and lower quartiles; whiskers extend to ± 1.5 times the interquartile range. Solid circles and lines inside boxes represent median values. Outliers are shown as open circles with lines. Boxplots labeled with different letters were significantly different at $\alpha=0.05$.

Table 4.2. Mean, range, and coefficient of variation of soil water nitrate concentration and triple nitrate isotopes on east- and south-facing aspects of WS4.

Nitrate concentration mean, range, and CV values are reported for back-transformed data. CV values for were calculated following [Koopmans *et al.*, 1964].

Aspect	$[\text{NO}_3^-]$			$\delta^{15}\text{N-NO}_3^-$			$\delta^{18}\text{O-NO}_3^-$			$\Delta^{17}\text{O-NO}_3^-$		
	Mean (mg L^{-1})	Range (mg L^{-1})	CV (%)	Mean (mg L^{-1})	Range (mg L^{-1})	CV (%)	Mean (mg L^{-1})	Range (mg L^{-1})	CV (%)	Mean (mg L^{-1})	Range (mg L^{-1})	CV (%)
East	1.1 (n=33)	0.1 to 11.5	157	+0.7 (n=32)	-6.9 to +4.0	351	+14.6 (n=32)	-6.4 to +65.1	136	+5.0 (n=31)	-1.0 to +20.4	130
South	0.3 (n=10)	0.1 to 2.2	119	+4.5 (n=7)	0.8 to +6.6	42	+75.7 (n=7)	+61.6 to +81.4	9	+18.8 (n=7)	+0.1 to +31.6	71

4.3.2 Soil Water Nitrate Isotopes

As with nitrate concentrations, the isotopic composition of soil water nitrate was also highly variable across WS4, particularly for $\delta^{18}\text{O}$ and $\Delta^{17}\text{O}$. The total range of $\delta^{18}\text{O}$ values was -6.4‰ to +81.4‰ during the study period; the lowest monthly mean $\delta^{18}\text{O}$ value of $+4.3 \pm 3.1$ ‰ occurred in October and the highest monthly value of +63.4‰ occurred in the single sample collected in July (Figure 4.2; Table 4.1). Soil water nitrate $\Delta^{17}\text{O}$ values were similarly variable, ranging from -1.0‰ to +31.6‰ during the study period. The highest monthly mean $\Delta^{17}\text{O}$ value occurred in July (+16.4‰) and the lowest monthly mean value occurred in October (-0.05 ± 0.9 ‰) (Figure 4.2; Table 4.1). There were no statistically significant differences in monthly mean $\delta^{18}\text{O}$ or $\Delta^{17}\text{O}$ of nitrate due to the highly variable isotopic compositions of soil water nitrate throughout the study. Temporal trends in the nitrogen isotopic composition of soil water nitrate were similar to

those observed for oxygen isotopes. Overall, $\delta^{15}\text{N}$ values ranged from -6.9‰ to $+8.2\text{‰}$ (Figure 4.2; Table 4.1); the highest monthly mean value of $+2.9\pm 1.9\text{‰}$ occurred in February and the lowest value of $-1.8\pm 2.6\text{‰}$ occurred in September. As with oxygen isotopes, there were no statistically significant differences in mean $\delta^{15}\text{N}$ among months due to the high degree of variability in soil water nitrate isotopic compositions.

Mean $\delta^{18}\text{O}$, $\Delta^{17}\text{O}$, and $\delta^{15}\text{N}$ values for the entire study period were all significantly higher on the south-facing aspect ($p \leq 0.0003$ for all; Figure 4.3; Table 4.2). $\delta^{18}\text{O}$ and $\Delta^{17}\text{O}$ values were also higher on the south-facing aspect during every month, but the differences among means were only statistically significant in September ($p=0.01$; Table 4.2). $\delta^{15}\text{N}$ values were higher on the south-facing aspect during every month but due to the high degree of spatial variability across WS4, none of the monthly mean values were significantly different between aspects (Table 4.2).

4.3.3 Soil Nitrogen and Carbon Isotopes

Nitrogen and carbon isotopic compositions of A horizon soils varied little across the watershed. The range of $\delta^{13}\text{C}$ values was small (-27.4‰ to -26.8‰) and the range of $\delta^{15}\text{N}$ values was slightly greater ($+1.9\text{‰}$ to $+3.4\text{‰}$), but means for neither were significantly different on east- versus south-facing aspects. However, the mean soil C:N ratio was significantly higher on the south-facing aspect (16.72 ± 1.87) compared to the east-facing aspect (13.61 ± 0.29).

4.4 DISCUSSION

Soil water nitrate concentrations and isotopic compositions were highly spatially variable across the watershed, indicating that nitrate source contributions also varied across WS4. Indeed, this high degree of spatial heterogeneity, combined with small sample sizes during individual months and inconsistent availability of soil water at any given lysimeter from month to month preclude meaningful analysis of temporal trends in soil water nitrate sources. Given these limitations, we focus our discussion on two important aspects of nitrate source dynamics in WS4: 1) persistent spatial variability of nitrate sources across the watershed and, 2) differences in nitrate source contributions observed across spatial scales.

4.4.1 Intra-watershed Variability of Nitrate Sources

The two main sources of nitrate in soil water and streams at Fernow are atmospheric deposition and microbial nitrification. Interpretation of the $\delta^{18}\text{O}$ and $\Delta^{17}\text{O}$ isotopic signatures of nitrate allows the relative contributions from these two sources to be quantified. Characteristic $\delta^{18}\text{O}$ and $\Delta^{17}\text{O}$ ranges for atmospheric nitrate are high (+60‰ to +100‰ and +20‰ to +35‰ for $\delta^{18}\text{O}$ and $\Delta^{17}\text{O}$, respectively) whereas the ranges for microbial nitrate are lower (-10‰ to +15‰ for $\delta^{18}\text{O}$ and a maximum of 0‰ for $\Delta^{17}\text{O}$) [Michalski *et al.*, 2004; Kendall *et al.*, 2007]. Due to significant overlap in the ranges of $\delta^{15}\text{N}$ values for atmospheric and microbial nitrate (Figure 1.2), these data are not typically used for source differentiation. Rather, they can provide insight into the relative extent of biological nitrate uptake and processing.

Nitrate concentrations showed a negative relationship with both $\delta^{18}\text{O}$ and $\Delta^{17}\text{O}$ during all months; significantly so in September ($p=0.01$ for $\delta^{18}\text{O}$ and $\Delta^{17}\text{O}$) and October ($p=0.04$ for $\delta^{18}\text{O}$ and $p=0.05$ for $\Delta^{17}\text{O}$). This indicates that greater proportions of microbial nitrate were associated with higher soil water nitrate concentrations. Previous studies have also documented the importance of microbial nitrification as a nitrate source in WS4 [*Peterjohn et al.*, 1999; *Gilliam et al.*, 2001; *Christ et al.*, 2002]. *Gilliam et al.* [2001] reported high percentages of relative nitrification in WS4, with 92% of mineralized N converted to nitrate. However, that study and others also observed a high degree of spatial variability in net nitrification rates and nitrate concentrations in A horizon soil water [*Peterjohn et al.*, 1999; *Gilliam et al.*, 2001]. The spatial distribution of net nitrification rates and nitrate concentrations reported in these studies agree with the spatial trends in $\delta^{18}\text{O}$ and $\Delta^{17}\text{O}$ values we observed. The lowest median nitrate concentrations and highest oxygen isotope values were observed on the south-facing aspect of WS4 (Figure 4.4), corresponding to the highest proportions of unprocessed atmospheric nitrate in soil water. Indeed, the median soil water nitrate concentration on this part of the watershed was only 0.20 mg L^{-1} and the median $\Delta^{17}\text{O}$ value was $+23.6\text{‰}$. Applying the two end-member mixing model

$$f_{\text{atm}} = \frac{\Delta^{17}\text{O}_{\text{soil water}} - \Delta^{17}\text{O}_{\text{nitrification}}}{\Delta^{17}\text{O}_{\text{atm}} - \Delta^{17}\text{O}_{\text{nitrification}}} \quad (\text{Eq. 3})$$

we calculated the median fraction of atmospheric nitrate in soil water (f_{atm}). Using a nitrification end-member $\Delta^{17}\text{O}$ value of -1.0‰ (representing the lowest soil solution nitrate $\Delta^{17}\text{O}$ value observed during the study period) and an atmospheric end-member $\Delta^{17}\text{O}$ value of $+31.3\text{‰}$

(representing the highest $\Delta^{17}\text{O}$ value observed in precipitation samples collected weekly at Fernow from February 2010 through February 2011), the median contribution of atmospheric deposition to soil water nitrate was 62% on the south-facing aspect. This indicates that the majority of soil water nitrate on this part of the watershed was atmospherically-derived. These results agree with those of previous studies that reported microbial nitrification rates near zero on the south-facing aspect [Gilliam *et al.*, 2001], and explain the greater importance of atmospheric nitrate and lower overall nitrate concentrations on this part of the watershed. In contrast, lower median nitrate $\Delta^{17}\text{O}$ isotope values, higher median concentrations, and low proportions of atmospheric nitrate (range=0 to 67%; median=6%) on the east-facing portion of the watershed (Figure 4.4 and Figure 4.5) indicate that atmospheric nitrate inputs are biologically cycled to a greater extent and microbial nitrification contributes more substantially to the soil N pool in these areas.

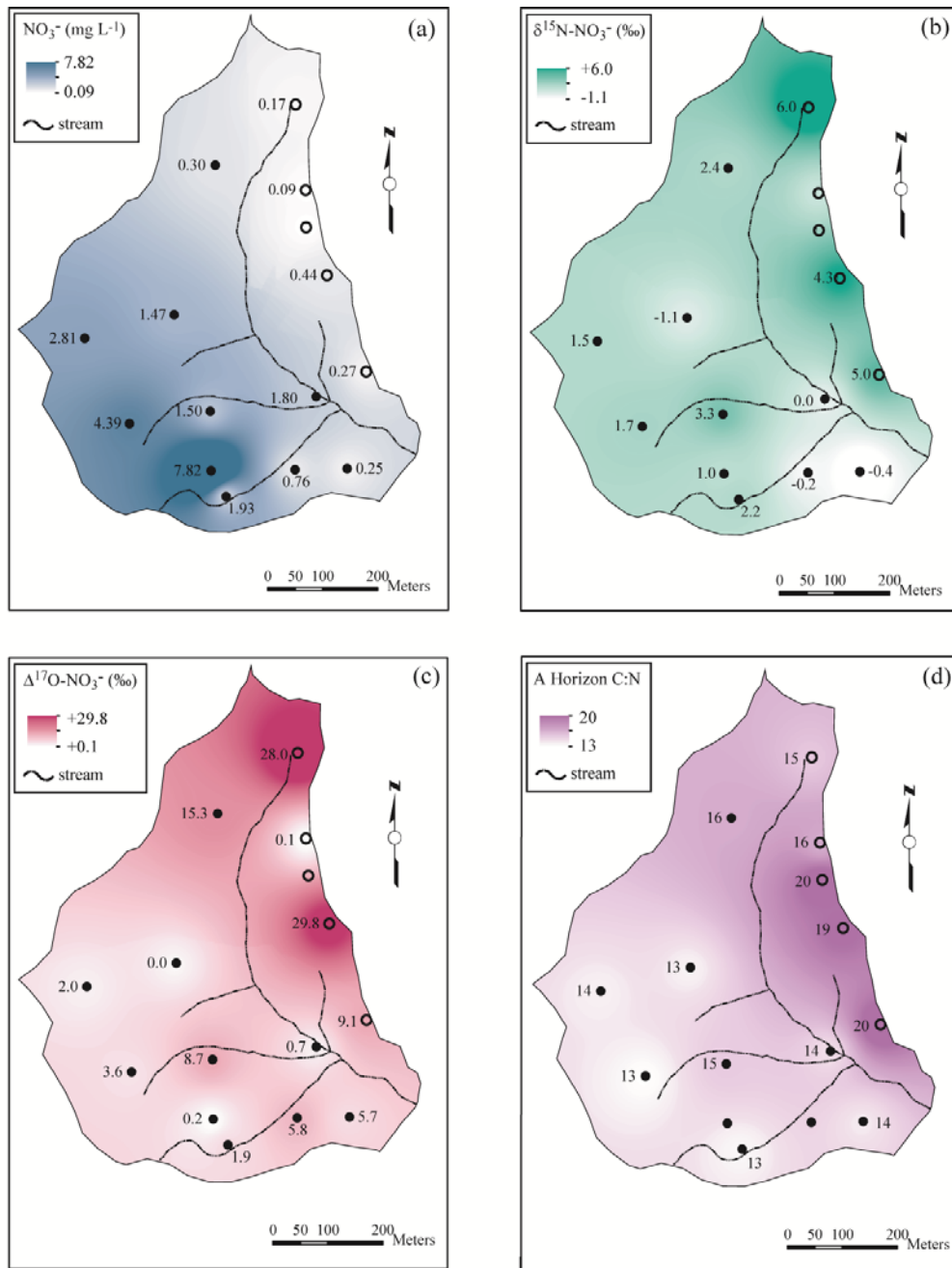


Figure 4.4. Median A horizon soil water nitrate (a) concentrations, (b) $\delta^{15}\text{N}$, (c) $\Delta^{17}\text{O}$, and (d) A horizon soil C:N ratios at lysimeter locations across WS4.

Lysimeters located on the east-facing aspect are shown as solid black circles; lysimeters on the south-facing aspect are shown as open circles.

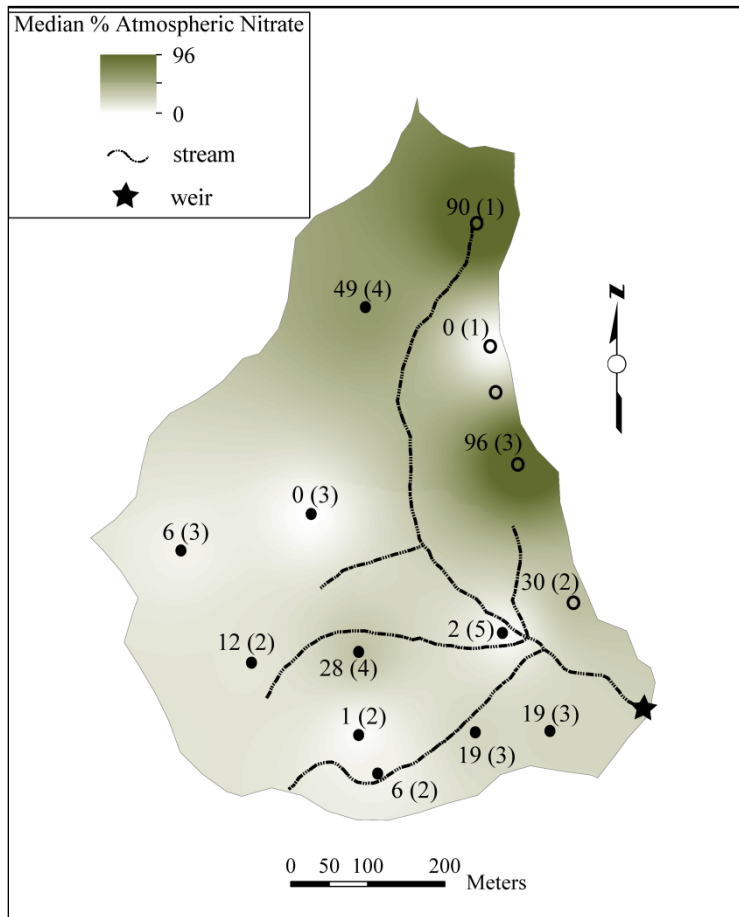


Figure 4.5. Median percent atmospheric nitrate in lysimeters across WS4.

Lysimeters located on the east-facing aspect are shown as solid black circles; lysimeters on the south-facing aspect are shown as open circles. Values in parentheses denote the number of monthly samples used to calculate median $\Delta^{17}\text{O}$ values at each lysimeter.

Previous efforts to understand the spatial variability in soil water nitrate across WS4 have focused on the relationship between vegetation composition and soil N dynamics [*Peterjohn et al.*, 1999; *Gilliam et al.*, 2001; *Christ et al.*, 2002]. However, these studies have often presented conflicting ideas. *Peterjohn et al.* [1999] hypothesized that higher net nitrification rates and soil water nitrate concentrations observed on the east-facing aspect were due to greater abundances

of sugar maple (*Acer saccharum*) and black cherry (*Prunus serotina*) on that part of the watershed, while lower N cycling rates on the south-facing aspect were due to the presence of species with more recalcitrant litter such as northern red oak (*Quercus rubra*) and American beech (*Fagus grandifolia*). Similarly, *Christ et al.* [2002] reported higher N processing rates associated with overstory sugar maple and lower rates with oak species in WS4. *Piatek et al.* [2010] also reported greater total N immobilization and lower rates of N mineralization in oak litter versus litter from a mixture of species, suggesting that overstory species composition influences soil N dynamics at Fernow. In contrast to these studies, *Gilliam et al.* [2001] found no relationship between soil water nitrate concentration or nitrification potential and overstory species composition in WS4. Rather, they suggested that more extensive soil weathering and greater abundance of the ericaceous shrub hillside blueberry (*Vaccinium vacillans*) on the south-facing aspect may have inhibited nitrification activity on this part of the watershed, resulting in lower soil water nitrate concentrations. As the root exudates of hillside blueberry are capable of inhibiting the activity of nitrifying bacteria [*Gilliam et al.*, 2001], the absence of this species on the east-facing aspect and its dense cover on the south-facing aspect (up to 30% in some areas sampled by *Gilliam et al.* [2001]) suggests that the species composition of vegetation exerts some influence on microbial N processing across WS4.

The spatial differences in $\delta^{15}\text{N}$ values observed in our study support the idea that biological nitrate processing is variable across the watershed. Mean $\delta^{15}\text{N}$ values for the entire study period were significantly lower on the east-facing versus south-facing aspect ($+0.7\pm 2.4\text{‰}$ and $+4.5\pm 2.1\text{‰}$ for east- and south-facing aspects, respectively; Table 4.2). This relationship also held during individual months, although differences were only significant in March ($+0.9\pm 0.9\text{‰}$ and $+5.2\pm 1.2\text{‰}$ for east- and south-facing aspects, respectively). Lower mean $\delta^{15}\text{N}$

values on the east-facing aspect could be the result of greater microbial nitrate production on this part of the watershed relative to the south-facing aspect, consistent with results from *Peterjohn et al.* [1999] and *Gilliam et al.* [2001]. Higher rates of mineralization and nitrification of ^{14}N -rich organic matter (e.g., plant litter) would result in an isotopically depleted forest floor and mineral soil on the east-facing portion of the watershed. Significantly different nitrification rates on the east- and south-facing aspects [*Gilliam et al.*, 2001] may therefore explain the spatial differences in $\delta^{15}\text{N}$, as well as $\delta^{18}\text{O}$ and $\Delta^{17}\text{O}$ of nitrate observed in our study (Figure 4.4).

Research at Fernow and other forested sites has additionally demonstrated negative relationships between soil C:N ratios and microbial nitrification potential [*Christ et al.*, 2002; *Ross et al.*, 2004]. The spatial differences in A horizon C:N ratios observed in our study also support this idea. Mean A horizon C:N ratios were significantly higher on the south-facing portion of WS4 (18.22 ± 2.41) compared to the east-facing aspect (14.00 ± 1.07), coincident with generally higher mean nitrogen and oxygen isotope values (Figure 4.4). Taken together, the patterns in soil water nitrate concentration and isotopic composition across WS4 suggest that microbial nitrification is a more important source of nitrate on the east-facing portion of the watershed while atmospheric deposition is the main source of nitrate on the south-facing aspect.

4.4.2 Decoupled Nitrate Biogeochemical Signals Across Spatial Scales

Soil water nitrate concentrations and isotopic compositions across WS4 demonstrate that the biogeochemical characteristics of a watershed can be highly variable even across small spatial scales. As this variability is often not reflected in stream water measurements integrated over an

entire watershed (i.e., at the watershed outlet), it is important to consider the factors that may influence the coupling (or decoupling) of N biogeochemical cycles at different spatial scales.

One watershed attribute that is particularly important in linking biogeochemical cycles across spatial and temporal scales is hydrologic regime. Hydrologic connectivity and transit time of water between specific landscape areas (e.g., uplands, hillslopes, and riparian areas) and the stream can influence the biogeochemical signal that is ultimately observed at the watershed outlet [Evans *et al.*, 2005; Gardner *et al.*, 2011]. For example, in a 212 km² mixed land-use watershed in Montana (USA), Gardner *et al.* [2011] found that while 98-99% of N inputs were retained in upland areas or by in-stream processing, fast transit times of water to the stream from a portion of the watershed dominated by wastewater inputs resulted in its disproportionate influence on nitrate export measured at the watershed outlet. Similarly, variation in the degree of landscape-stream hydrologic connectivity can result in low nitrate export during periods of slow water transit and greater export via overland flow during storms [Evans *et al.*, 2005]. Such hydrologic drivers also appear to operate at Fernow, where consistently low $\Delta^{17}\text{O}$ of nitrate values observed in stream samples collected at the base of WS4 (Figure 3.3) could indicate that 1) areas on the south-facing aspect of the watershed are minimally hydrologically connected to the stream, 2) these areas are hydrologically connected to the stream, but unprocessed atmospheric nitrate undergoes biological processing before reaching the watershed outlet, or 3) these areas are hydrologically connected to the stream, but low soil water nitrate concentrations in these areas (potentially linked to high soil C:N ratios) result in little unprocessed atmospheric nitrate reaching the watershed outlet.

The highly variable contributions of microbial and atmospheric nitrate across space and time in WS4 are not reflected at the watershed outlet. Rather, low $\Delta^{17}\text{O}$ of nitrate values in

stream water collected weekly at the base of the watershed demonstrate that microbial nitrification is the dominant nitrate source in the stream draining WS4 (Figure 3.3). Using (Equation 3) and $\Delta^{17}\text{O}$ values of -1.2‰ for the nitrification end-member (representing the lowest $\Delta^{17}\text{O}$ of nitrate value measured in stream samples collected at the base of the watershed during 2010) and $+29.1\text{‰}$ for the atmospheric end-member (representing the highest $\Delta^{17}\text{O}$ of nitrate value measured in precipitation at Fernow during 2010), atmospheric deposition contributed a maximum of 15% to stream nitrate during 2010 (Figure 4.6). This indicates that the majority of nitrate export at the whole-watershed scale derives from microbial nitrification. These results are in stark contrast to the high contributions of atmospheric nitrate to soil water (often greater than 90%) observed in some areas of WS4 (Figure 4.5), suggesting a decoupling of N biogeochemical dynamics across spatial scales in WS4.

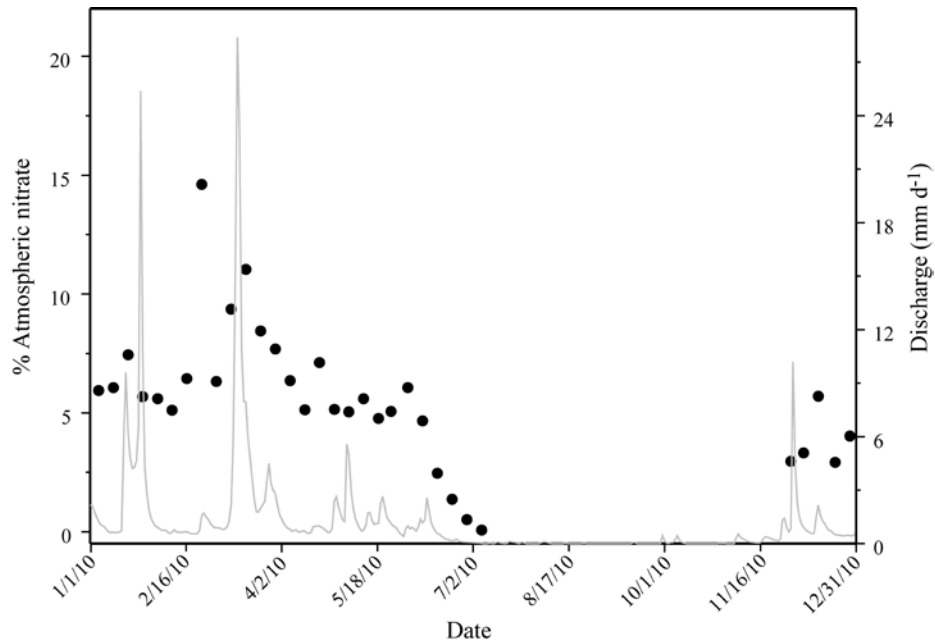


Figure 4.6. Percent of atmospheric nitrate in stream samples collected weekly at the base of WS4 (black circles).

Daily discharge is shown on the secondary axis to highlight the greater atmospheric nitrate export in samples collected during stormflow. The area shaded in grey represents a snowmelt event sampled at the end of February 2010.

Previous research has emphasized the importance of landscape-stream hydrologic connectivity as a driver of nitrate source contributions to watershed nitrate export [Dunne and Black, 1970; Goodale et al., 2009; Gardner et al., 2011; Sebestyen et al., 2014]. These studies and others [Dunne and Black, 1970; Jencso et al., 2009; Pacific et al., 2010] demonstrate that all areas within a watershed do not contribute equally to streamflow at all times; this finding has direct applications to nitrogen biogeochemical cycling and nitrogen saturation across spatial scales in watersheds at Fernow. For example, the greatest export of atmospheric nitrate generally occurred on sampling dates that coincided with stormflow (Figure 4.6). Indeed, the highest percentage of atmospheric nitrate in the stream observed during 2010 occurred during a

snowmelt event in late February (Figure 4.6). While the dominant nitrate source in the stream throughout 2010 was microbial nitrification, temporal relationships between atmospheric nitrate export and discharge suggest that variable hydrologic connectivity between watershed areas and the stream may influence the degree of atmospheric nitrate export. The difference in nitrate sources on the east- and south-facing aspects of WS4 represents an ideal setting for future work investigating the influence of variable hydrologic source areas on nitrate export dynamics.

The idea that the fate and transport of atmospheric nitrate in watersheds is mediated not only by biological activity, but also by watershed hydrology has implications for our conceptualization of nitrogen saturation across spatial scales. While WS4 has been cited as one of the best examples of an N-saturated watershed in North America [*Stoddard, 1994; Peterjohn et al., 1996; Gress et al., 2007*], this characterization is based on long-term trends in stream nitrate concentration measured at the watershed outlet alone. Such a sampling scheme integrates the N cycling dynamics of the entire watershed, reducing them to a single value. The disparity between the proportions of atmospheric nitrate in soil water across WS4 and those observed at the base of the watershed demonstrates that stream-based characterizations of nitrate sources and export may not entirely reflect the complexities of nitrate source dynamics occurring within a watershed.

In-stream N processing can also exert some influence on nitrate source contributions and export measured at the watershed outlet [*Sebestyen et al., 2014*] and deserves further study in WS4; in-stream N cycling is currently not well characterized in this watershed. However, our results also suggest that characterizations of a watershed's apparent nitrogen saturation status can be scale-dependent. At the whole-watershed scale, nitrate deposition in WS4 appears to exceed the retention capacities of vegetation and soil pools, suggesting a nitrogen-saturated system

[Stoddard, 1994; Aber *et al.*, 1998; Lovett and Goodale, 2011]. However, the soil water nitrate isotope results presented here demonstrate that this is not the case for all areas of WS4. Rather, our data suggest that the portions of WS4 that appear most saturated (i.e., those that with the highest nitrate concentrations in soil water) are also the areas with the greatest biological nitrate production. In contrast, watershed areas that leach the smallest amounts of nitrate to soil water are more strongly influenced by atmospheric nitrate inputs. This decoupling of N biogeochemical indicators across spatial scales is an important feature of watershed-scale biogeochemical cycling and should be considered in the development of forest management plans aimed at mitigating the negative effects of chronic, elevated N deposition.

4.5 CONCLUSION

The disparity between nitrate source contributions at differing spatial scales in WS4 has implications for our understanding of nitrogen saturation. This decoupling of biogeochemical indicators across spatial scales illustrates the importance of not only biological drivers but also physical factors that influence the fate and transport of nitrate from landscapes to streams.

The results presented here demonstrate that atmospheric deposition inputs are biologically processed to varying degrees across WS4. Little unprocessed atmospheric nitrate occurs in soil solution on the east-facing portion of the watershed, while nitrate in soil solution on the south-facing slope is dominated by an atmospheric source. While these results support the conclusions of previous studies of microbial nitrification in WS4 [Peterjohn *et al.*, 1996; Gilliam *et al.*, 2001], the atmospheric source dynamics presented here for soil solution and stream water

nitrate provide additional insight into the variable importance of atmospheric deposition when considered across spatial scales. Our results further suggest that hydrologic and topographic factors may be important in regulating the degree of atmospheric nitrate export from WS4. When watershed outlet-based characterizations of nitrogen saturation status do not reflect the heterogeneous N cycling dynamics observed at the intra-watershed scale, it is important to understand the basis for this difference in order to most effectively manage for improved forest health and water quality. The results of this study emphasize the need to consider N saturation mechanisms at a variety of spatial and temporal scales, as well as their relationships to other watershed attributes such as hydrologic regime and geomorphology, which operate across spatial scales.

5.0 ISOTOPIC VARIABILITY OF PRECIPITATION NITRATE DURING GROWING SEASON STORM EVENTS

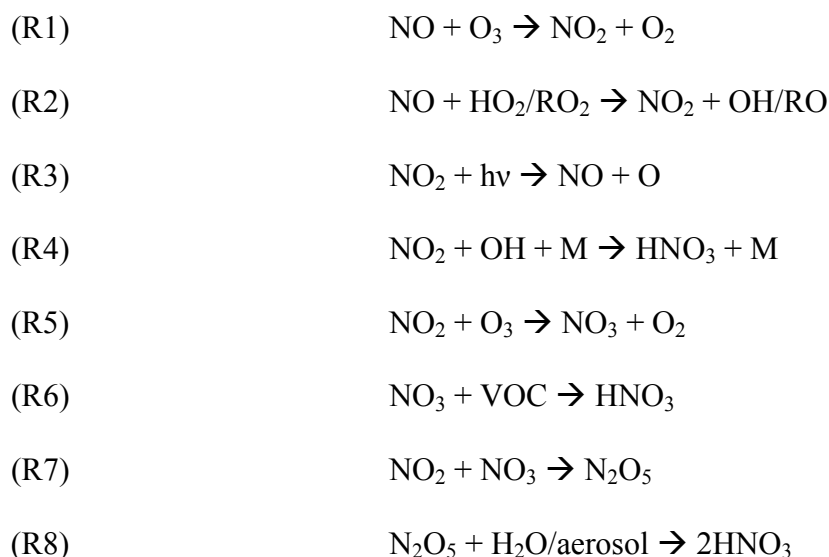
5.1 INTRODUCTION

Since their passage in 1990, the Clean Air Act Amendments have resulted in markedly decreased acidic deposition across the northeastern United States [Burns *et al.*, 2011]. While the greatest reductions occurred in sulfate (SO_4^{2-}) deposition (a 43% decrease from 1989-2009 across the region), reductions of up to 27% were also observed in regional wet inorganic nitrogen (N) deposition over the same time period [Burns *et al.*, 2011]. Recent attention has focused on the ecological effects of seasonal and long-term fluctuations in atmospheric deposition [Driscoll *et al.*, 2003; Galloway *et al.*, 2008], but few studies have explored the variable nature of nitrate (NO_3^-) deposition on short time scales, such as storm events. As wet deposition of nitrate during storms represents an important mode of N transfer from the atmosphere to terrestrial systems, examination of nitrate deposition dynamics during storms can improve constraints on nitrate inputs from natural and anthropogenic sources, improving our understanding of terrestrial N cycling.

Atmospheric nitrate is generated through the oxidation of NO_x ($\text{NO} + \text{NO}_2$) precursors by a variety of atmospheric oxidants [Alexander *et al.*, 2009]. Identifying the sources of NO_x precursors and the atmospheric processes that convert those emissions to atmospheric nitrate

deposition is important for our understanding of ecosystem nitrogen biogeochemistry. It is particularly important to examine NO_x source dynamics and oxidation processes on very short time scales (e.g., during individual storm events) as contributions from NO_x sources such as lightning and biogenic emissions are transitory.

Following emission, NO is oxidized to NO₂ by ozone (R1) or peroxy radicals (R2). During the daytime, this NO₂ is rapidly converted back to NO (R3); rapid interconversion between NO and NO₂ results in a steady state equilibrium during the day. The lifetime of NO₂ in the atmosphere is 1 to 2 days; conversion of NO₂ to nitric acid (HNO₃) can proceed via a 3-body reaction with OH (R4), or NO₂ can be oxidized by ozone to form the nitrate radical (NO₃) (R5). The nitrate radical can react further with volatile organic compounds (VOC) to form nitric acid (R6) or with NO₂ to form N₂O₅ (R7); these reactions are only important at night because the nitrate radical is readily photolyzed during the day. N₂O₅ can then react slowly with gas phase water or more rapidly with wetted aerosol surfaces to form nitric acid (R8).



The oxygen isotopic compositions ($\delta^{18}\text{O}$ and $\Delta^{17}\text{O}$) of NO_x and nitrate have been used in many previous studies to infer the relative importance of these oxidation pathways to atmospheric nitrate formation [Savarino *et al.*, 2007; Alexander *et al.*, 2009; Morin *et al.*, 2009; Michalski *et al.*, 2013; Vicars *et al.*, 2013]. For example, ozone has both high $\delta^{18}\text{O}$ (+80‰ to +120‰) and $\Delta^{17}\text{O}$ (+30‰ to +50‰) values [Michalski *et al.*, 2013], and these isotopic enrichments are imparted to atmospheric nitrate when NO_x oxidation proceeds via ozone. In contrast, atmospheric nitrate formed via oxidation by the hydroxyl radical has lower $\delta^{18}\text{O}$ and $\Delta^{17}\text{O}$ values, more closely reflecting the oxygen isotopic composition of OH ($\delta^{18}\text{O}\text{-OH} = -30‰$ to +2‰ and $\Delta^{17}\text{O}\text{-OH} = 0‰$; [Hastings *et al.*, 2003]). These differences in the isotopic compositions of O_3 and OH have been used to infer their relative importance in the formation of atmospheric nitrate [Hastings *et al.*, 2003; Michalski *et al.*, 2003]. Indeed, the typical $\delta^{18}\text{O}$ values of atmospheric nitrate ($\delta^{18}\text{O} = +63‰$ to +94‰ and $\Delta^{17}\text{O} = +20‰$ to +30‰; [Michalski *et al.*, 2003; Kendall *et al.*, 2007]) demonstrate the importance of ozone in the oxidation of NO_x to nitrate.

Throughout these oxidation reactions, nitrogen atoms are conserved. Thus, $\delta^{15}\text{N}$ of nitrate can be used to trace the contributions of NO_x sources to atmospheric nitrate formation. However, variation in ambient conditions (e.g., relative humidity, atmospheric ozone levels) can alter the equilibrium between atmospheric NO_x pools, with consequences for their isotopic compositions [Freyer *et al.*, 1993; Morino *et al.*, 2006; Wankel *et al.*, 2010]. While these factors are important to consider when using $\delta^{15}\text{N}$ values to infer source dynamics, they may be less important during storm events when short-term fluctuations in relative humidity and temperature are minor. Similarly, while seasonal variability in ozone levels can lead to fractionation of

nitrogen isotopes [Morin *et al.*, 2009], this is not likely to be important on the time scale of individual storm events.

Many previous studies have used $\delta^{15}\text{N}$ of nitrate to identify NO_x sources in the environment and to quantify their relative contributions to atmospheric N pools [Heaton, 1990; Elliott *et al.*, 2007, 2009; Felix *et al.*, 2012]. $\delta^{15}\text{N}$ is well-suited to such source differentiation, as the isotopic signatures of anthropogenic and biogenic NO_x are distinct. $\delta^{15}\text{N}$ - NO_x values for electricity-generating units (EGUs) range from +9‰ to +26‰, depending on the type of emissions control technology employed [Felix *et al.*, 2012], while reported values for vehicle NO_x range from -13‰ to +10‰ [Heaton, 1990; Ammann *et al.*, 1999] and those for biogenic NO_x range from -49‰ to -20‰ [Li and Wang, 2008]. However, few studies have attempted to identify the role of NO_x source dynamics in atmospheric nitrate formation during storm events. Freyer [1991] reported a negligible influence of source contributions on seasonal variability in precipitation nitrate isotopes during storms in Europe. Instead, lower mean precipitation $\delta^{15}\text{N}$ of nitrate values in summer versus winter were attributed to differences in nitrate formation pathways and nitrate species (i.e., particulate vs. gas phase); variability within individual storms was not discussed. In contrast, higher mean $\delta^{15}\text{N}$ and lower mean $\delta^{18}\text{O}$ of nitrate were reported during warm season events in Bermuda [Hastings *et al.*, 2003]. While the seasonal isotopic variability observed in this study was attributed to varying NO_x sources, source dynamics within individual storm events were not addressed. In one of the few studies that examined within-storm variability in nitrate isotopic composition, Buda and DeWalle, [2009b] reported significant $\delta^{15}\text{N}$ and $\delta^{18}\text{O}$ variability during six storms in central Pennsylvania. Among the six storms sampled, the largest within-storm $\delta^{15}\text{N}$ and $\delta^{18}\text{O}$ ranges were 8.8‰ and 30.0‰, respectively;

both intra-storm and seasonal variability were attributed to changing air mass back trajectories and atmospheric oxidation chemistry [Buda and DeWalle, 2009b].

Here we present the results of triple nitrate isotope analyses ($\delta^{15}\text{N}$, $\delta^{18}\text{O}$, and $\Delta^{17}\text{O}$) of precipitation samples collected during six growing season storms at Fernow Experimental Forest (West Virginia, USA). We discuss possible explanations for the wide variation in isotopic composition observed over short time periods and address the potential importance of anthropogenic and biogenic NO_x sources and atmospheric oxidation pathways to atmospheric nitrate formation. This research highlights the dynamic nature of intra-event atmospheric nitrate isotopic composition, with implications for our understanding of N source-sink relationships in forested watersheds.

5.2 STUDY SITE AND METHODS

5.2.1 Study Site

This study was conducted at the USDA Fernow Experimental Forest (39°05' N, 79°40' W; Figure 1.4). Fernow is located in the Allegheny Mountains portion of West Virginia. Elevations in WS4 range from 670 to 930 m, and slopes average ~20%. Bedrock in the study area is primarily composed of hard sandstone and softer shale of the Upper Devonian Hampshire Formation (Rowlesberg Member); little water storage occurs in these strata [Reinhart *et al.*, 1963; Kochenderfer, 2007]. Soils are channery silt loams of the Calvin series (loamy-skeletal, mixed active, mesic typic Dystrudept), averaging 1 m in depth [Kochenderfer, 2007]. Infiltration

rates in these soils are high and most precipitation reaches the stream via subsurface flow [Reinhart *et al.*, 1963]. Mixed hardwoods are the dominant forest type at Fernow; northern red oak (*Quercus rubra*), sugar maple (*Acer saccharum*), red maple (*Acer rubrum*), and black cherry (*Prunus serotina*) are the most abundant species [Peterjohn *et al.*, 1999]. The growing season extends from late April through October, and precipitation is evenly distributed throughout the year, with an annual average of 1450 mm; significant snowpack does not accumulate over long periods. Nitrate comprised approximately 60% of inorganic wet N deposition ($\text{NO}_3^- + \text{NH}_4^+$) to the Fernow in 2010 [National Atmospheric Deposition Program, 2011].

5.2.2 Sample Collection

We sampled six growing season storms during July and September 2010. Hourly precipitation samples were collected in a clearing adjacent to Watersheds (WS) 3, 4, and 5 during each storm (Figure 1.4). For the 9 July event, hourly precipitation samples were collected using a plastic funnel (area of funnel top = 1200 cm²) clamped to a pole at a height of 2 m, which drained into a 1 L HDPE sample bottle also clamped to the pole. Sample bottles were replaced hourly. For subsequent storms, a Teledyne ISCO autosampler collected hourly precipitation samples. Two rectangular plastic containers (total area = 4756 cm²) were arranged in series and angled downslope, with a hole drilled into the downslope corner. Precipitation collected in these containers drained into a 1 L HDPE sample bottle, held in place by a clamp beneath the downslope container. The ISCO autosampler suction tube was secured so that it rested in the bottom of the sample bottle. Once per hour, the autosampler collected all accumulated precipitation. Immediately prior to all storms, the funnel, plastic containers, sample bottles, and

all autosampler bottles were triple-rinsed with 18 M Ω water. On 16 September, the first precipitation sample was collected approximately four hours after rainfall onset. For the 11 and 26 September events, the first sample represents a composite of all precipitation since the onset of rainfall. All precipitation samples were processed at the U.S. Forest Service Timber and Watershed Laboratory in Parsons, WV within 24 hours. Samples were vacuum-filtered through 0.22 μm polyethersulfone (PES) membrane filters to remove suspended solids and biological material. Samples were frozen and transported to the University of Pittsburgh, where they remained frozen until further analysis.

5.2.3 Isotopic Analysis

Concentrations of nitrate for all samples were measured by ion chromatography (Dionex ICS-2000) at the University of Pittsburgh. For isotopic analysis, a denitrifying bacteria, *Pseudomonas aureofaciens*, was used to convert aqueous nitrate into gaseous N_2O which was then introduced into the mass spectrometer [Sigman *et al.*, 2001; Casciotti *et al.*, 2002]. For $\Delta^{17}\text{O}$ analysis, this N_2O was thermally decomposed at 800°C into N_2 and O_2 prior to isotopic analysis following the method described by Kaiser *et al.* [2007]. Duplicate samples were analyzed for $\delta^{15}\text{N}$ and $\delta^{18}\text{O}$ of nitrate (and separately for $\Delta^{17}\text{O}$ of nitrate during $\Delta^{17}\text{O}$ analysis) on an Isoprime Trace Gas and Gilson GX-271 autosampler coupled with an Isoprime Continuous Flow Isotope Ratio Mass Spectrometer (CF-IRMS) at the *Regional Stable Isotope Laboratory for Earth and Environmental Science* at the University of Pittsburgh. Isotope values are reported in parts per thousand relative to nitrate standards as follows:

$$\delta^{15}\text{N}, \delta^{18}\text{O}, \text{ and } \delta^{17}\text{O} (\text{‰}) = \left[\left(\frac{R_{\text{sample}}}{R_{\text{standard}}} \right) - 1 \right] \times 1000 \quad (\text{Eq. 1})$$

where $R = {}^{15}\text{N}/{}^{14}\text{N}$, ${}^{18}\text{O}/{}^{16}\text{O}$, or ${}^{17}\text{O}/{}^{16}\text{O}$. The mass-independent oxygen isotope anomaly of nitrate ($\Delta^{17}\text{O}\text{-NO}_3^-$) is likewise reported in parts per thousand and calculated using the equation:

$$\Delta^{17}\text{O} (\text{‰}) = \delta^{17}\text{O} - 0.52 \times \delta^{18}\text{O} \quad (\text{Eq. 2})$$

Samples with low nitrate concentrations were pre-concentrated prior to bacterial conversion to N_2O . Pre-concentration was accomplished by calculating the sample volume necessary to obtain a final concentration of 20 nmol (for $\delta^{15}\text{N}$ and $\delta^{18}\text{O}$ analysis) or 200 nmol (for $\Delta^{17}\text{O}$ analysis) in a 5 mL sample. Appropriate sample volumes were measured into 10% hydrochloric acid-washed Pyrex or Teflon beakers and placed in a drying oven at 60°C until all liquid evaporated. The interior of each beaker was then rinsed with 10mL of 18 M Ω water to reconstitute duplicate samples to the appropriate concentration. Samples were prepared for isotopic analysis following the bacterial denitrifier method as previously described. International reference standards were similarly pre-concentrated and used for correction of pre-concentrated samples.

$\delta^{15}\text{N}$ and $\delta^{18}\text{O}$ values were corrected using international reference standards USGS-32, USGS-34, USGS-35, and N3; USGS-34 and USGS-35 were used to correct $\Delta^{17}\text{O}$ values. These standards were also used to correct for linearity and instrument drift. Standard deviations for international reference standards were 0.2‰, 0.5‰, and 0.2‰ for $\delta^{15}\text{N}$, $\delta^{18}\text{O}$, and $\Delta^{17}\text{O}$, respectively.

Water isotope analyses were carried out at the University of Maryland, Baltimore County (UMBC) and at the Cornell Isotope Laboratory (COIL) at Cornell University. Sample analyses at UMBC were carried out on a Picarro water isotope cavity ring-down spectrometer. $\delta^{18}\text{O}\text{-H}_2\text{O}$ values for these samples represent an average of five sample injections and samples were corrected using reference standards USGS-46 and USGS-48, with a standard deviation of 0.2‰. Samples analyses at COIL were carried out on a Thermo Delta V isotope ratio mass spectrometer interfaced to a Gas Bench II. These samples were analyzed in duplicate and corrected against Vienna Standard Mean Ocean Water and in-house standards, with a standard deviation of 0.2‰.

There is the potential for isobaric interference of the $\delta^{15}\text{N}$ signal in samples with high $\Delta^{17}\text{O}$ values. Corrections for mass-independent contributions of $\Delta^{17}\text{O}$ to m/z 45 were evaluated following the relationship described in *Coplen et al.* [2004], where a 1‰ increase in $\delta^{15}\text{N}$ corresponds to an 18.8‰ increase in $\Delta^{17}\text{O}$. Corrected $\delta^{15}\text{N}$ values were 0.6‰ to 1.6‰ lower than uncorrected values, depending on the mass-independent contribution of $\Delta^{17}\text{O}$ in the sample. Because this correction factor is small relative to the range of precipitation $\delta^{15}\text{N}$ values observed and because we could not apply the correction to some samples due to a lack of $\Delta^{17}\text{O}$ data, the $\delta^{15}\text{N}$ values presented here do not include the mass-independent $\Delta^{17}\text{O}$ correction. However, given that the magnitude of $\delta^{15}\text{N}$ variability is much greater than the correction for isobaric interference by ~12 times, omission of the mass-independent $\Delta^{17}\text{O}$ correction does not influence the observed $\delta^{15}\text{N}$ trends and our interpretation of storm dynamics.

5.2.4 Electricity-Generating Unit NO_x Quantification

To quantify EGU NO_x source inputs to the study site, we used the National Oceanographic and Atmospheric Administration (NOAA) Hybrid Single Particle Lagrangian Integrated Trajectory (HYSPLIT) model to calculate a 48-hour back trajectory for each hourly precipitation sample collected during storm events. We chose a back trajectory duration of 48 hours because it approximates the lifetime of NO_x in the near-surface troposphere [Seinfeld and Pandis, 2006; Alexander *et al.*, 2009]. Back trajectories were calculated at 500 m above ground level using the Eta Data Assimilation System (EDAS, 40 km resolution). Hourly NO_x emission data from the U.S. EPA Air Markets Program were used to characterize NO_x emissions along each back trajectory; emissions from all EGUs located within a 100 km radius of the back trajectory were included. A radius of 100 km was chosen based on evaluation of the relationship between bimonthly $\delta^{15}\text{N}$ and EGU NO_x emissions summed within varying radial source areas of NTN sites as shown in Elliott *et al.* [2007]. As the current study focuses on NO_x source dynamics at much shorter time scales than those evaluated in Elliott *et al.* [2007] (i.e., hourly as opposed to bimonthly time scales) and improvements in R² values were minimal at radii greater than 100 km [Elliott *et al.*, 2007], we chose a radius of 100 km in this study. Total NO_x emissions were calculated by summing all emissions occurring within this 100 km radius during each hour. Emissions were categorized by the reported NO_x control technology in use at the time of emission: selective catalytic reduction (SCR), selective non-catalytic reduction (SNCR) or low-NO_x burner (LNB); emissions from EGUs using both SCR and SNCR were categorized as SCR. The proportions of total NO_x contributed by each control technology along a back-trajectory were used to calculate a representative EGU $\delta^{15}\text{N}$ -NO_x value for each hour, where $\delta^{15}\text{N}$ -NO_x

values of +20‰, +14‰, and +10‰ were used for SCR, SNCR, and LNB facilities, respectively [Felix *et al.*, 2012]. To account for fractionations between the estimated EGU $\delta^{15}\text{N-NO}_x$ and $\delta^{15}\text{N}$ of nitrate, we applied a fractionation factor of $\alpha=0.997$ to all $\delta^{15}\text{N}$ values [Freyer, 1991].

5.2.5 Biogenic NO_x Quantification

To estimate biogenic NO_x contributions to precipitation, we assumed a biogenic $\delta^{15}\text{N-NO}_x$ isotopic signature of -27‰ [Felix and Elliott, 2013] and applied the same $\alpha=0.997$ fractionation factor described above, yielding a nitrate $\delta^{15}\text{N}$ value of -30‰. Using measured precipitation nitrate $\delta^{15}\text{N}$ values and the estimated nitrate $\delta^{15}\text{N}$ values for EGU and biogenic NO_x emissions as described above, we created a two-endmember isotope mixing model to estimate contributions of biogenic NO_x emissions to precipitation nitrate:

$$f_{\text{biogenic}} = \frac{\delta^{15}\text{N} - \text{NO}_3^-_{\text{precip}} - (f_{\text{EGU}} \times \delta^{15}\text{N} - \text{NO}_3^-_{\text{EGU}})}{\delta^{15}\text{N} - \text{NO}_3^-_{\text{biogenic}}} \quad (\text{Eq. 3})$$

where f_{biogenic} is the fraction of precipitation N from biogenic NO_x . Our model did not consider mobile NO_x emissions (e.g., vehicles) due to the remoteness of the study area; the only roads in the vicinity are U.S. Forest Service roads that receive minimal automobile traffic. Previous research suggests that NO_2 fluxes decline rapidly with distance from roadways [Ammann *et al.*, 1999; Cape *et al.*, 2004; Kirchner *et al.*, 2005; Redling *et al.*, 2013]; one study reported a 90% reduction in NO_2 concentrations at distances greater than 15 m from the roadway [Cape *et al.*,

2004]. As the nearest public road is ~1.5 km from the study site, we therefore assumed negligible contributions from vehicle NO_x emissions.

5.2.6 Statistical Analysis

We used analysis of variance to test for significant differences among storm event nitrate concentration and mean $\delta^{15}\text{N}$ and $\delta^{18}\text{O}$ of nitrate. When significant differences were indicated, we applied Tukey's Honestly Significant Difference test to determine which storm means were significantly different ($\alpha=0.05$). To evaluate the relationships between NO_x emissions, storm characteristics, and precipitation isotope values, we used Pearson Correlation Coefficients. Linear regression was used to evaluate the relationship between $\delta^{15}\text{N}$ and $\delta^{18}\text{O}$ of nitrate during individual storms. All statistical analyses were conducted using SAS [SAS Institute, Inc., 2011].

5.3 RESULTS

5.3.1 Precipitation Nitrate Concentrations

Storm event characteristics are presented in Table 5.1. Volume-weighted mean nitrate concentrations ranged from 0.1 to 1.6 mg/L. Within-storm nitrate concentrations also varied, with some events showing large ranges (Figure 5.1). With the exception of the 9 July event, volume-weighted mean precipitation nitrate concentrations among events generally decreased with time (Figure 5.1). Storms differed in duration and pattern of precipitation input, including short, intense downpours and moderate, steady rainfall (Table 5.1), but precipitation intensity

was not correlated with nitrate concentration. While this relationship was not statistically significant during any storm, nitrate concentrations did decrease sharply during periods of very high intensity precipitation on 16 September and 30 September.

Table 5.1. Characteristics of six storm events sampled at Fernow Experimental Forest during 2010

Date	Antecedent precip. (mm in past month)	Days since rain >5mm	Total precip. (mm)	Mean intensity (mm hr ⁻¹)	Volume-weighted mean				Total NO _x emissions (metric tons)			Estimated mean biogenic flux (µg N m ⁻² h ⁻¹)	Estimated mean biogenic fraction (%)
					<i>[NO₃⁻]</i>	<i>δ¹⁵N-</i>	<i>δ¹⁸O-</i>	<i>Δ¹⁷O-</i>	<i>SCR</i>	<i>SNCR</i>	<i>LNB</i>		
					(mg L ⁻¹)	<i>NO₃⁻ (‰)</i>	<i>NO₃⁻ (‰)</i>	<i>NO₃⁻ (‰)</i>					
9 July	61.7	14	17.7	2.2	0.6	+1.1	+65.5	+18.4	784	198	1047	69.5	17
11 Sept	47.5	3	5.5	0.9	1.6	-3.5	+54.5	+16.8	110	36	59	124.0	36
16 Sept	44.2	9	47.7	4.8	0.5	-3.2	+61.0	+14.9	141	64	317	195.1	36
26 Sept	65.3	10	8.6	0.7	0.7	-0.4	+69.7	+23.3	183	34	361	27.7	32
28 Sept	67.3	1	7.8	1.1	0.2	-3.7	+70.2	+24.8	160	89	199	17.8	29
30 Sept	81.5	2	56.2	3.5	0.1	+2.3	+67.5	+22.5	659	230	785	9.9	19

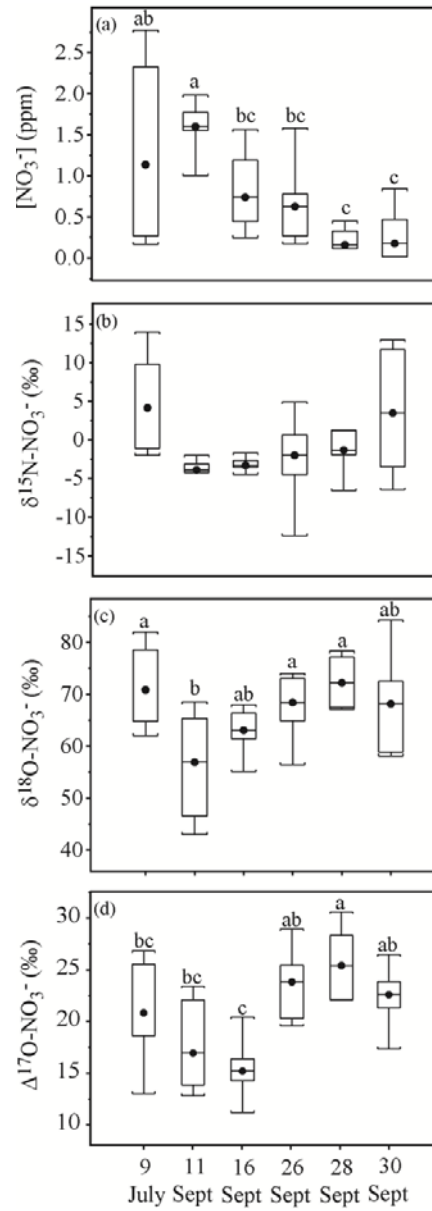


Figure 5.1. Means and ranges of precipitation (a) nitrate concentration, (b) $\delta^{15}\text{N}$ of nitrate, (c) $\delta^{18}\text{O}$ of nitrate, and (d) $\Delta^{17}\text{O}$ of nitrate during six storms sampled at Fernow Experimental Forest in 2010.

Storm means are indicated by a black circle. Box limits represent the interquartile range; whisker limits denote the entire data range. Storms with different letters are significantly different at $p < 0.05$ based on Tukey's HSD test.

Among NO_x emissions control types, LNB showed the strongest relationship to nitrate concentrations ($R^2=0.17$, $p=0.0008$). This may be due in part to the lower efficiency of LNB among the three NO_x control types considered here [Felix *et al.*, 2012], yielding higher NO_x fluxes from stacks employing this technology. Interestingly, SCR emissions showed a significantly positive relationship to precipitation sulfate concentrations ($R^2=0.27$, $p<0.0001$) despite the greater efficiency of this emissions control type. LNB emissions were also positively related to sulfate concentrations, but the relationship was slightly weaker ($R^2=0.14$, $p=0.0024$).

5.3.2 $\delta^{15}\text{N}$ of Precipitation Nitrate

Precipitation nitrate $\delta^{15}\text{N}$ values ranged from -12.4 to +13.9‰ across all storms; volume-weighted mean $\delta^{15}\text{N}$ for individual events ranged from -3.7‰ to +2.3‰ (Table 5.1). Mean $\delta^{15}\text{N}$ did not differ among storms (Figure 5.1). However, large intra-storm variations in $\delta^{15}\text{N}$ did occur during some events. For example, $\delta^{15}\text{N}$ values increased by nearly 16‰ over two hours on 9 July and by 12‰ over three hours on 30 Sept (Figure 5.2). Temporal trends in $\delta^{15}\text{N}$ of nitrate varied among storms (Figure 5.2). On some dates (9 July, 26 September), values were low at the beginning of the storm, increased during the middle, then decreased toward the end. During others (30 September), $\delta^{15}\text{N}$ values began high, decreased sharply within a few hours, then increased again shortly thereafter. Still other events (11 September, 16 September) showed only minor trends in $\delta^{15}\text{N}$ values.

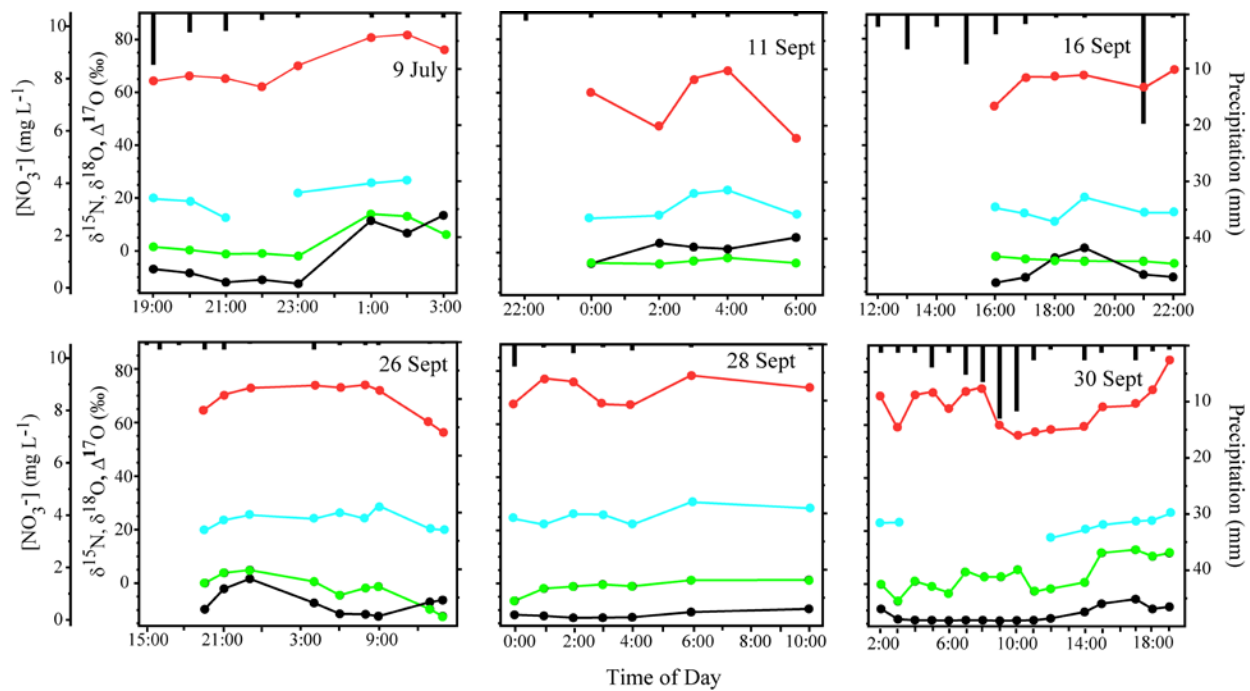


Figure 5.2. Intra-storm variation during six storms sampled at Fernow Experimental Forest during 2010. Precipitation intensity is shown by black bars, nitrate concentration by black circles, $\delta^{15}\text{N}$ of nitrate by green circles, $\delta^{18}\text{O}$ of nitrate by red circles, and $\Delta^{17}\text{O}$ of nitrate by blue circles. Storm date is indicated in the top right corner of each plot.

5.3.3 $\delta^{18}\text{O}$ of Precipitation Nitrate

$\delta^{18}\text{O}$ of nitrate values ranged from +43.0‰ to +84.3‰. Volume-weighted mean $\delta^{18}\text{O}$ ranged from +54.5‰ to +70.2‰ (Table 5.1), with significant differences in mean $\delta^{18}\text{O}$ among events (Figure 5.1). As with $\delta^{15}\text{N}$, intra-storm $\delta^{18}\text{O}$ values were highly variable, and storms differed in temporal $\delta^{18}\text{O}$ trends (Figure 5.2). For example, $\delta^{18}\text{O}$ values were lowest during the early part of the storm on 9 July, whereas values were highest and decreased sharply at the end of the storm

on 26 September. On other dates, trends in $\delta^{18}\text{O}$ were both positive and negative within storm events.

5.3.4 $\Delta^{17}\text{O}$ of Precipitation Nitrate

Due to low nitrate concentrations and insufficient sample volume for pre-concentration, $\Delta^{17}\text{O}$ data are lacking for eight samples during the 30 September storm. During all storms, the temporal dynamics of nitrate $\Delta^{17}\text{O}$ values were similar to those of $\delta^{18}\text{O}$ of nitrate. $\Delta^{17}\text{O}$ values spanned a wide range across all storms, from +11.2‰ to +30.6‰. Volume-weighted mean $\Delta^{17}\text{O}$ of nitrate values ranged from +14.9‰ to +24.8‰ (Table 5.1), with significant differences among events (Figure 5.1). Within individual storms, $\Delta^{17}\text{O}$ values were highly variable and temporal trends differed among storms (Figure 5.2).

5.3.5 $\delta^{18}\text{O}$ of Water in Precipitation

$\delta^{18}\text{O}\text{-H}_2\text{O}$ values ranged from -22.8‰ to -4.5‰ across all storms. Volume-weighted mean $\delta^{18}\text{O}\text{-H}_2\text{O}$ ranged from -20.7‰ to -5.4‰. Intra-storm $\delta^{18}\text{O}\text{-H}_2\text{O}$ values were highly variable, and storms differed in temporal trends (Figure 5.3). For example, $\delta^{18}\text{O}\text{-H}_2\text{O}$ values showed generally decreasing trends throughout the event on 9 July and 30 September, whereas values showed a positive trend on 26 September. On other dates, trends in $\delta^{18}\text{O}$ were both positive and negative within storm events.

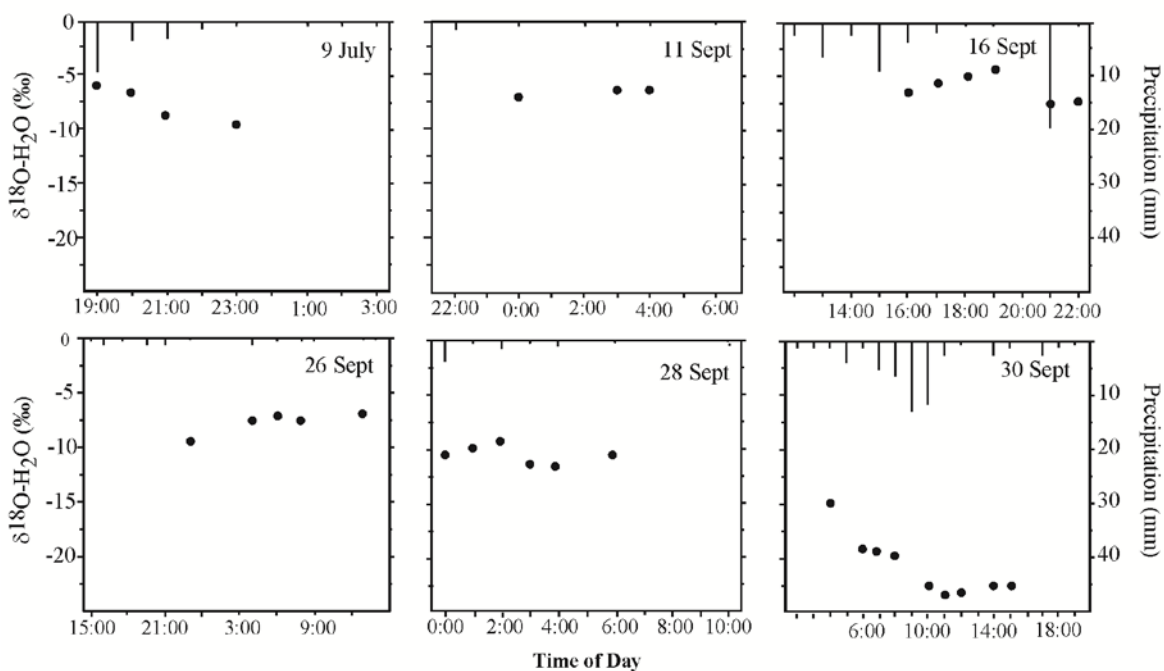


Figure 5.3. Hourly precipitation $\delta^{18}\text{O-H}_2\text{O}$ values and precipitation amounts during six growing season storms sampled in 2010 at Fernow Experimental Forest.

5.3.6 Biogenic NO_x Flux Measurements and Mixing Model Results

Based on the two endmember mixing model in Eq. 3, mean biogenic NO_x flux estimates ranged from 9.9 to 195.1 $\mu\text{g N m}^{-2} \text{h}^{-1}$ for the six storms (Table 5.1). Using Eq. 4, we calculated mean biogenic NO_x contributions to wet nitrate deposition ranging from 17% to 36%

$$\% \text{ biogenic} = \frac{[(\delta^{15}\text{N} - \text{NO}_3^-)_{\text{precip}} - (\delta^{15}\text{N} - \text{NO}_3^-)_{\text{EGU}}]}{[(\delta^{15}\text{N} - \text{NO}_3^-)_{\text{biogenic}} - (\delta^{15}\text{N} - \text{NO}_3^-)_{\text{EGU}}]} \times 100 \quad (\text{Eq. 4})$$

for the six storms (Table 5.1); hourly estimates ranged from -7% to 59%.

5.4 DISCUSSION

5.4.1 Anthropogenic and Biogenic NO_x Sources

The high degree of variability in $\delta^{15}\text{N}$ of nitrate during storms was surprising. Because the nitrogen isotopic composition of the NO_x source is generally retained during atmospheric nitrate formation [Wankel *et al.*, 2010], we attribute this intra-storm variability in precipitation nitrate $\delta^{15}\text{N}$ values to contributions from two NO_x sources—emissions from local biogenic sources and regional EGUs.

Various NO_x emissions controls may operate at an EGU, as well as along an air mass back trajectory. Each emissions control technology fractionates $\delta^{15}\text{N}$ -NO_x differently (mean SCR= +20‰, mean SNCR= +14‰, mean LNB= +10‰; [Felix *et al.*, 2012]) and efficiencies vary through time. Potential rainout and recharge of EGU-derived atmospheric nitrate along back trajectories may also influence the isotopic composition of precipitation. However, these factors alone cannot explain the large number of isotopically depleted $\delta^{15}\text{N}$ values observed during storms. The majority (59%) of hourly precipitation samples had negative $\delta^{15}\text{N}$ values, whereas a small fraction (10%) had $\delta^{15}\text{N}$ values greater than +7‰ (representing the lowest measured EGU $\delta^{15}\text{N}$ -NO_x value from Felix *et al.* [2012] with an $\alpha=0.997$ fractionation factor applied). This strongly suggests that another N source— with a much lower $\delta^{15}\text{N}$ signature— influences precipitation nitrate isotopes. The highly dynamic fluctuations in $\delta^{15}\text{N}$ over short time periods (Figure 5.2) also suggest another NO_x source. Lightning may have contributed to NO_x formation along air mass back trajectories, although the $\delta^{15}\text{N}$ of NO_x range for this source (-0.5 to +1.4‰; [Hoering, 1957]) cannot account for the much lower $\delta^{15}\text{N}$ of nitrate values observed

during many storms. Biomass burning was also not significant NO_x source during this time, as no large fires were reported in any of the states through which air mass back trajectories passed [National Oceanic and Atmospheric Administration (NOAA), 2010a, 2010b]. Vehicle NO_x emissions produced along air mass back trajectories likely had minimal effect on the δ¹⁵N values observed during storms because most of these NO_x emissions (in some cases up to 90% [Cape et al., 2004]) are deposited within a short distance of roadways [Ammann et al., 1999; Cape et al., 2004; Kirchner et al., 2005; Redling et al., 2013] and the closest public road to the Fernow study site is ~ 1km away. Instead, we propose that biogenic NO_x emissions from the soils at Fernow served as an additional NO_x source during storms. If these isotopically-depleted emissions were rapidly oxidized and deposited as wet nitrate deposition during storms, this could partially explain the highly variable isotopic composition observed in precipitation samples during storms.

Plumes of microbial NO_x following soil wetting have been widely reported [Davidson and Kinglerlee, 1997; Davidson et al., 2000; Jaeglé et al., 2004; Ghude et al., 2010; Zhang et al., 2011; Hudman et al., 2012], with large NO fluxes often occurring with the first wetting event after a dry period [Stark et al., 2002]. Because of the low δ¹⁵N values associated with biogenic NO_x (-49‰ to -20‰ [Li and Wang, 2008]; -27‰ [Felix and Elliott, 2013]), even a small contribution from this source could lower δ¹⁵N of nitrate values substantially. NO flux increases of 12-2200% have been reported within 10 minutes after the addition of 2 cm of water to forest soils in the western US [Stark et al., 2002]; these fluxes were positively correlated with net nitrification rates and soil nitrate content. At sites where nitrate is the dominant form of soil inorganic N, NO and N₂O emissions are also high [Davidson et al., 2000]. High nitrification rates and the predominance of nitrate in the soil inorganic N pool in watersheds adjacent to our study site Gilliam et al. [2001] suggest the potential for large soil NO fluxes. In addition,

negative correlations between soil moisture content and NO flux have been reported [Horváth *et al.*, 2006], indicating a soil moisture threshold for nitrification. Threshold soil water contents of 59% and 53% were observed in oak and spruce forests, respectively [Horváth *et al.*, 2006]. Beyond these thresholds, denitrification exceeded nitrification and N₂O flux was greater than NO flux. Other studies confirm this negative relationship between nitrification and soil moisture [Stark and Firestone, 1995; Ullah and Moore, 2009].

Accordingly, in this study, early decreases in $\delta^{15}\text{N}$ during some storms may have resulted in part from increasing nitrification rates during soil wet-up. During periods of intense rainfall or long events (e.g., 9 July and 30 September), sharp increases in $\delta^{15}\text{N}$ of nitrate may signify a threshold soil water content beyond which nitrification rates and/or diffusion of NO_x from the soil decreased. Precipitation nitrate deposited after this time would have been influenced primarily by EGU NO_x, yielding higher $\delta^{15}\text{N}$ values.

Based on Eq. 4, mean biogenic NO_x contributions to wet nitrate deposition ranged from 17 to 36% for individual storms (Table 5.1). These estimates encompass those reported elsewhere using satellite observations and atmospheric chemistry models [Jaeglé *et al.*, 2005; Steinkamp *et al.*, 2008]. Globally, soil NO_x is estimated to contribute 22% to surface NO_x emissions based on satellite observations [Jaeglé *et al.*, 2005]. Similarly, the ECHAMS/MESSy atmospheric chemistry (EMAC) model showed a 25% decrease in estimated global HNO₃ deposition during the summer months when soil NO_x was removed from the model [Steinkamp *et al.*, 2008]. Our estimates of mean biogenic NO_x fluxes (9.9 $\mu\text{g N m}^{-2} \text{ h}^{-1}$ to 195.1 $\mu\text{g N m}^{-2} \text{ h}^{-1}$) encompass measured NO fluxes reported by Venterea *et al.* [2004] on an N-amended watershed (WS3) at Fernow. In that study, maximum soil NO fluxes during August were approximately 33

$\mu\text{g N m}^{-2} \text{ h}^{-1}$ and $14 \mu\text{g N m}^{-2} \text{ h}^{-1}$ at low and high elevations, respectively, suggesting potentially high rates and high spatial heterogeneity in local biogenic NO_x emissions.

While the highly variable $\delta^{15}\text{N}$ values over short time periods indicate that biogenic NO_x may be an important source of wet nitrate deposition at Fernow, negative estimates in the range of biogenic NO_x contributions (range = -7% to 59%) based on our mixing model demonstrate that further constraints to our mixing model are necessary. For example, we held the biogenic $\delta^{15}\text{N}$ of nitrate value fixed at -30‰ in our mixing model. While this value is based on empirical measurements [Freyer, 1991; Felix and Elliott, 2013], it may differ at Fernow and likely varies through time. Indeed, $\delta^{15}\text{N-NO}_x$ values are reported to vary temporally, ranging from -49‰ to -20‰ over 11 days in one study [Li and Wang, 2008]. To better constrain our understanding of biogenic NO_x fluxes, future work should address temporal variability in $\delta^{15}\text{N-NO}_x$. Additional model refinements should include biological processes such as canopy scavenging through stomatal uptake, which can be an important regulator of soil NO_x emissions [Ganzeveld *et al.*, 2002]. Changes in soil moisture during storms can also influence microbial activity [Linn and Doran, 1984; Davidson *et al.*, 2000], however, the lack of high-temporal resolution data precluded evaluation of precipitation-soil-microbial interactions and their effects on precipitation nitrate dynamics. A comparison of average estimated biogenic NO_x flux derived from Eq. 4 with total precipitation at the study site during the 30 days prior to each storm indicates a significantly negative relationship ($p=0.01$; $R^2=0.84$; Figure 5.4). Length of antecedent drying period is a controlling factor in the magnitude of soil N gas flux; the longer dry conditions persist, the larger the biogenic NO_x flux following precipitation [Davidson, 1992]. Our results confirm that larger estimated biogenic NO_x fluxes occurred during storms with drier antecedent moisture conditions. Similarly, the effect of precipitation intensity on soil moisture should be better constrained.

Nitrification rates increase when water-filled pore space (WFPS) is between ~25 and 60%; beyond this threshold, nitrification drops sharply and approaches zero at 80% WFPS [Linn and Doran, 1984; Davidson *et al.*, 2000]. Given the highly significant relationship between antecedent moisture and the NO_x flux estimated by our mixing model (Figure 5.4), further investigation of the mechanisms relating precipitation intensity, soil moisture, and biogenic NO_x flux is warranted. Future work in this area should focus on constraining the dynamics of soil moisture change and nitrification rates under varying precipitation intensities and durations.

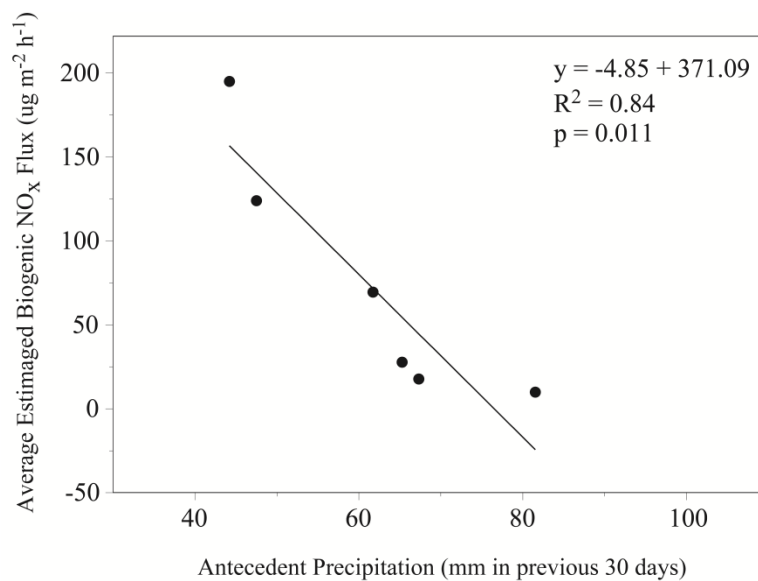


Figure 5.4. Relationship between antecedent moisture conditions measured at the study site and biogenic NO_x flux as estimated by the two-endmember mixing model for six growing season storms at Fernow Experimental Forest.

5.4.2 Atmospheric Oxidation Chemistry

Variability in $\delta^{18}\text{O}$ and $\Delta^{17}\text{O}$ of nitrate has been used to interpret changes in oxidation pathways of atmospheric nitrate [Hastings *et al.*, 2003; Michalski *et al.*, 2003]. The relative importance of ozone (O_3) and the hydroxyl radical (OH) in the oxidation of NO_x to nitrate varies both seasonally [Hastings *et al.*, 2003; Michalski *et al.*, 2003] and diurnally [Brown *et al.*, 2004; Alexander *et al.*, 2009; Morin *et al.*, 2011]. As the lifetime of NO_x in the troposphere is 1-2 days [Seinfeld and Pandis, 2006; Alexander *et al.*, 2009], diurnal variations in NO_x oxidation pathways along air mass back trajectories could have contributed to the temporal variability in precipitation $\delta^{18}\text{O}$ and $\Delta^{17}\text{O}$ we observed.

Ozone is characterized by high values of $\delta^{18}\text{O}$ (+80‰ to +120‰) and $\Delta^{17}\text{O}$ (+30‰ to +50‰) [Michalski *et al.*, 2013], and ozone imparts this enrichment in heavy isotopes to atmospheric nitrate during NO_x oxidation [Michalski *et al.*, 2003], resulting in $\delta^{18}\text{O}$ and $\Delta^{17}\text{O}$ of nitrate values ranging from +63‰ to +94‰ and +20‰ to +30‰, respectively [Michalski *et al.*, 2003; Kendall *et al.*, 2007]. In contrast, the oxygen isotopic compositions of other atmospheric oxidants— such as OH and peroxy radicals— are much lower than that of ozone [Michalski and Xu, 2010]. Consequently, atmospheric nitrate formed via these pathways has lower $\delta^{18}\text{O}$ and $\Delta^{17}\text{O}$ values than that formed via pathways involving ozone. Michalski and Xu, [2010] used an isotope mass balance model (ISO-RACM) to predict atmospheric $\Delta^{17}\text{O}$ of nitrate values resulting from various NO_x oxidation pathways. Their model predicted that $\Delta^{17}\text{O}$ values below +15‰ would occur under atmospheric conditions of low ozone and high biogenic VOC mixing ratios; however, the authors suggested that such conditions were unlikely to be observed in the troposphere. On three dates (9 July, 11 and 16 September) we observed $\Delta^{17}\text{O}$ of nitrate values

less than +15‰; these low values occurred during both day and night (Figure 5.2). As ozone production involves photolytic reactions, cloudy conditions during these storm events may have suppressed ozone production to some extent, resulting in low ozone mixing ratios. Low ozone mixing ratios coupled with potentially high biogenic VOC mixing ratios due to the densely-forested surroundings at the study site could have resulted in the low $\Delta^{17}\text{O}$ of nitrate values we observed during some storms. While we did not measure ozone or VOC mixing ratios at Fernow during the storm events, future research focusing on such episodic atmospheric chemistry dynamics during would provide novel detail about the sources and processes that drive the formation and deposition of atmospheric nitrate in forested systems.

5.4.3 Rainout/Washout Processes

Rainout/washout processes can be important modes of N transport from the atmosphere to terrestrial systems; this is particularly true of nitrate, which is highly soluble in water [*Seinfeld and Pandis*, 2006]. Rainout occurs when atmospheric constituents (such as nitrate) are fixed by raindrops or ice crystals as clouds form (i.e., before raindrops begin to drop), whereas washout occurs when constituents are scavenged from the surrounding atmosphere as raindrops fall [*Burch et al.*, 1996]. In the current study, precipitation intensity was not correlated with nitrate concentration during any storm; however, nitrate concentrations did decrease sharply during periods of high-intensity precipitation on 16 September and 30 September, possibly due to rainout/washout of atmospheric nitrate (Figure 5.3). In addition, rainout/washout of atmospheric nitrate during the beginning of the 9 July event may have contributed to the greater proportion of atmospheric nitrate observed in the stream on this date. In an analysis of intra-storm variation in

rain chemistry during 230 events, *Burch et al.* [1996] found that during short events, the highest nitrate concentrations typically occurred during the beginning of the storm, followed by a rapid decrease in concentrations. The authors attributed this pattern to strong initial washout of atmospheric nitrate by raindrops. It is also possible that evidence of rainout/washout processes during the storms sampled at Fernow may have been confounded by continuous recharge of NO_x from EGUs along trajectories during all but the highest precipitation intensities.

The temporal dynamics we observed in the precipitation $\delta^{18}\text{O}\text{-H}_2\text{O}$ of precipitation suggest that rainout/washout processes along 48-hour back trajectories were important during some events (Figure 5.3). For example, sharply decreasing $\delta^{18}\text{O}\text{-H}_2\text{O}$ values coincided with periods of high-intensity rainfall during the 16 and 30 September storms. These lower values may have resulted from the preferential rainout of heavier oxygen isotopes along air mass back trajectories, leaving the subsequent rainfall that occurred over Fernow isotopically lighter (i.e., depleted in the heavier isotope).

5.5 CONCLUSION

This study demonstrates the highly variable nature of intra-storm nitrate stable isotopes and represents the first attempt to quantify the importance of biogenic NO_x emissions and NO_x oxidation pathways to nitrate deposition during storm events, using $\delta^{15}\text{N}$, $\delta^{18}\text{O}$, and $\Delta^{17}\text{O}$ of nitrate. Our results suggest that biogenic sources may contribute up to 59% of NO_x emissions that are the precursors to precipitation nitrate and subsequent deposition and that NO_x oxidation pathways may be highly variable over short time scales during storms. Biogenic emissions are

often underestimated or overlooked in terrestrial N budgets due to the paucity of data and difficulty in obtaining measurements. We have shown that this source may contribute significantly to atmospheric nitrate formation, particularly on short time scales. Understanding the magnitude of transient biogenic N inputs will further clarify the importance of this source during episodic acidification events. This may be particularly important in rapidly industrializing countries such as India and China, where large biogenic NO_x plumes occur in the spring, facilitated by the monsoonal climate [Wang *et al.*, 2007; Ghude *et al.*, 2010]. Indeed, in eastern China, increased wet nitrate deposition in spring coincides with large biogenic NO_x pulses [Wang *et al.*, 2007].

Identifying the sources of atmospheric nitrate— and understanding the oxidation pathways leading to its formation— clarifies the influence of natural and anthropogenic inputs to the biogeochemical N cycle. We have demonstrated that nitrate stable isotope analysis can provide valuable information on source differentiation and dynamics on short temporal scales. The results of this study can serve as a catalyst for constraints on the importance of autochthonous and allochthonous NO_x emissions to atmospheric nitrate formation in forested systems. Such dynamics may be important in N-saturated systems, particularly if “priming” [Guenet *et al.*, 2010] of microbial communities under N saturation results in greater nitrification and biogenic NO_x production. In addition, elucidating the interactions among nitrate sources, atmospheric nitrate formation pathways, and hydrologic regime on short temporal scales will lead to more effective mitigation of both chronic and episodic acidification events.

6.0 HYDROLOGIC AND NITROGEN BIOGEOCHEMICAL SOURCE DYNAMICS DURING GROWING SEASON STORM EVENTS IN A NITROGEN-SATURATED WATERSHED

6.1 INTRODUCTION

In forested watersheds, water and nitrate typically originate from either the atmosphere (e.g., precipitation and atmospheric nitrate deposition) or the landscape (e.g., groundwater and microbial nitrate). Nitrogen additions from atmospheric deposition can alter terrestrial biogeochemical cycles in a number of ways, including increased nitrification in soils and elevated nitrate export in streams [Christ *et al.*, 2002; Aber *et al.*, 2003; Adams *et al.*, 2007]. Pinpointing the sources and processes that drive nitrate export from forested systems is therefore essential, particularly during transient yet hydrologically dynamic periods such as storm and snowmelt events, when variable sources and source areas can contribute to elevated nitrate export and episodic acidification [Murdoch and Stoddard, 1992].

Stable isotopes of nitrate ($\delta^{15}\text{N}$, $\delta^{18}\text{O}$, and $\Delta^{17}\text{O}$) and water ($\delta^{18}\text{O}\text{-H}_2\text{O}$) can clarify the importance of these biogeochemical and hydrological sources in natural systems and the processes affecting them. Variations in $\delta^{18}\text{O}\text{-H}_2\text{O}$ values of stream water on both long and short time scales have been used to quantify precipitation and groundwater inputs to streams and to estimate hydrologic transit times in watersheds [DeWalle *et al.*, 1997; McGlynn *et al.*, 1999;

McDonnell et al., 2010]. Spatially-distributed measurements of water isotopic composition in the subsurface can also be coupled with stream water isotopic compositions to understand source area dynamics under different hydrologic conditions [*McGlynn et al.*, 1999]. Similarly, nitrate stable isotopes have been used to quantify source contributions to aquatic systems and to identify biological processes, such as nitrification and denitrification, that influence ecosystem N retention and export [*Michalski et al.*, 2004; *Barnes et al.*, 2008; *Sebestyen et al.*, 2008; *Goodale et al.*, 2009; *Koba et al.*, 2012].

If the characteristic delta values of hydrologic and biogeochemical sources are distinct, then source contributions can be distinguished using end-member mixing analysis. For example, $\delta^{18}\text{O}\text{-H}_2\text{O}$ values of deep groundwater are often consistent through time because this well-mixed reservoir integrates precipitation inputs over long periods. Groundwater $\delta^{18}\text{O}$ values can be compared to those of precipitation and soil water, which are typically more temporally variable, and the relative contributions of these sources to streamflow can be determined [*McGlynn et al.*, 1999]. Similarly, $\delta^{18}\text{O}$ values of atmospheric and microbial nitrate are relatively distinct (Figure 1.2) and have been widely used in end-member mixing analysis to quantify contributions of nitrate from atmospheric and microbial sources [*Burns and Kendall*, 2002; *Pardo et al.*, 2004; *Barnes et al.*, 2008; *Sebestyen et al.*, 2008; *Goodale et al.*, 2009]. However, while the $\delta^{18}\text{O}$ of nitrate approach has been used to characterize nitrate source contributions in many forested systems, there are a number of limitations to this approach that should be considered. As $\delta^{18}\text{O}$ of nitrate continues to be characterized for an increasing variety of systems, the reported source ranges for atmospheric and microbial nitrate also continue to expand and become more similar. In addition, recent studies of variable oxygen exchange between nitrite and soil water during nitrification have highlighted the difficulty in pinpointing the isotopic composition of the

nitrification end-member [Buchwald and Casciotti, 2010; Casciotti et al., 2010; Snider et al., 2010]. Indeed, many studies simply estimate the $\delta^{18}\text{O}$ value of the nitrification end-member rather than directly measure it, which adds further uncertainty to source apportionment estimates [Sebestyen et al., 2014]. Perhaps the most widely recognized limitation the $\delta^{18}\text{O}$ -based approach for nitrate source apportionment is the issue of mass-dependent fractionation during biological processes such as denitrification and assimilation. Preferential uptake of lighter isotopes during biological processes alters the isotopic composition of the residual soil nitrate pool; it is precisely this effect that makes $\delta^{15}\text{N}$ a useful tracer of biological processing, as described below. However, increasing $\delta^{18}\text{O}$ values due to enrichment of the residual soil nitrate pool can lead to the assignment of an erroneous nitrification end-member value in isotope mixing models, thereby increasing the potential for inaccurate source apportionment of nitrate in streams.

To overcome these limitations of $\delta^{18}\text{O}$ -based mixing model approaches, $\Delta^{17}\text{O}$ of nitrate is increasingly used to quantify nitrate source contributions to streams. The ranges of atmospheric and microbial $\Delta^{17}\text{O}$ values are distinct; $\Delta^{17}\text{O}$ values of atmospheric nitrate range from +20‰ to +35‰ [Morin et al., 2009] while those of microbial nitrate are zero or less [Michalski et al., 2004]. Unlike $\delta^{18}\text{O}$ of nitrate, $\Delta^{17}\text{O}$ is not subject to mass-dependent fractionation during biological processing, making it a conservative tracer of atmospheric nitrate.

When the delta value ranges of two sources overlap, end-member mixing analysis cannot be used to distinguish source contributions; such is the case for $\delta^{15}\text{N}$ ranges of atmospheric and microbial nitrate (Figure 1.2). Instead, examination of temporal trends in $\delta^{15}\text{N}$ can provide information about the extent of biological processing in ecosystems [Robinson, 2001; Koba et al., 2012]. For example, consumption of soil nitrate during denitrification results in a

characteristic isotopic enrichment of the residual soil nitrate pool (Figure 1.2). A analysis of temporal trends in $\delta^{15}\text{N}$ values of nitrate in soil water or streams may therefore be useful in determining the importance of this N cycling process within watersheds at a variety of time scales.

While many previous studies have used nitrate stable isotopes to track changes in the relative contributions of atmospheric and microbial nitrate in streams, much of this research has occurred on monthly, seasonal, and inter-annual time scales [*Burns and Kendall, 2002; Pardo et al., 2004; Barnes et al., 2008; Sebestyen et al., 2008*]. Investigations of stream nitrate source contributions over shorter periods are less common, and those which have examined event-scale dynamics have often occurred in snowmelt-dominated systems [*Campbell et al., 2002; Ohte et al., 2004; Sebestyen et al., 2008*]. In this paper, we present stable isotope analyses for nitrate ($\delta^{15}\text{N}$, $\delta^{18}\text{O}$, and $\Delta^{17}\text{O}$) and water ($\delta^{18}\text{O}$) in precipitation and stream samples collected hourly during three growing season storm events at Fernow Experimental Forest (West Virginia, USA). Coupled observation of nitrate and water isotope dynamics provides important insights into the biogeochemical and hydrological processes regulating atmospheric nitrate export on the time scale of individual storm events in a nitrogen-polluted watershed.

6.2 STUDY SITE AND METHODS

6.2.1 Study Site

This study was conducted on Watershed 4 (WS4) at the Fernow Experimental Forest (39°05' N, 79°40' W; Figure 1.4). Fernow is located in the Allegheny Mountains portion of West Virginia. Elevations in WS4 range from 720 to 865 m, and slopes average ~20%. Bedrock is primarily composed of hard sandstone and softer shale of the Upper Devonian Hampshire Formation (Rowlesberg Member); little water storage occurs in these strata [Reinhart *et al.*, 1963; Kochenderfer, 2007]. Soils are channery silt loams of the Calvin series (loamy-skeletal, mixed active, mesic typic Dystrudept), averaging 1 m in depth [Kochenderfer, 2007]. Infiltration rates in these soils are high and most precipitation reaches the stream via subsurface flow [Reinhart *et al.*, 1963]. During high-intensity rain events, streamflow is high and falls off quickly during periods of low-intensity or no precipitation [Reinhart *et al.*, 1963]. Infiltration rates are high and most precipitation reaches the streams via subsurface flow [Reinhart *et al.*, 1963]. Mixed hardwoods are the dominant forest type in WS4; northern red oak (*Quercus rubra*), sugar maple (*Acer saccharum*), red maple (*Acer rubrum*), and black cherry (*Prunus serotina*) are the most abundant species [Peterjohn *et al.*, 1999]. The growing season at Fernow extends from late April through October, and precipitation is evenly distributed throughout the year, with an annual average of 1450 mm; significant snowpack does not accumulate over long periods. Nitrate comprised approximately 60% of inorganic wet N deposition ($\text{NO}_3^- + \text{NH}_4^+$) to the Fernow in 2010 [National Atmospheric Deposition Program, 2011].

From 1980 to 2010, the annual average stream nitrate concentration in WS4 was 3.4 mg L⁻¹. Stream nitrate concentrations show some seasonal variability, with a maximum monthly average of 3.8 mg L⁻¹ in March and the lowest monthly average of 2.9 mg L⁻¹ in August. Annual average discharge from 1980 to 2010 was 1.8 mm. Discharge from this watershed is highly dynamic on both event and seasonal time scales; the stream draining WS4 is ephemeral, but responds quickly to precipitation inputs. Seasonally, maximum monthly average discharge occurs in March (3.4 mm), while the lowest monthly average discharge in September is nearly an order of magnitude lower (0.4 mm).

6.2.2 Sample Collection

Hourly precipitation and stream samples were collected during storm events on 9 July, 16 September, and 30 September 2010. Precipitation was collected hourly in a clearing located 180 m from the bottom of WS4 using an automated sampler. Precipitation was intercepted by two plastic basins arranged in series (total area = 0.48 m²) that drained into a 1 L plastic sample collection bottle. An autosampler evacuated all precipitation from the collection bottle once per hour. Stream samples were also collected hourly using an automated sampler. At the base of WS4, all streamflow is diverted through a plastic culvert routed beneath a shed. A door in the shed's floor allows access to a large plastic tub, into which a portion of streamflow drains via holes drilled into the bottom of the culvert. The autosampler was manually triggered to collect the first stream sample from the tub when a sufficient volume of water was judged to have accumulated to obtain a 1 L sample. All subsequent samples were collected on an hourly basis

by the autosampler, and collection continued until cessation of streamflow. Table 6.1 provides additional information about each storm event.

Table 6.1. Precipitation and discharge characteristics of the three growing season storms at Fernow Experimental Forest

Event date	Precipitation			Stormflow		
	<i>Duration (h)</i>	<i>Mean (mm h⁻¹)</i>	<i>Total (mm)</i>	<i>Duration (h)</i>	<i>Mean (mm h⁻¹)</i>	<i>Total (mm)</i>
9 July	8	2.21	17.66	23	0.04	0.96
16 Sept	10	4.77	47.67	19	0.17	3.22
30 Sept	17	3.51	56.23	27	0.48	16.35

All precipitation and stream samples were taken to the U.S. Forest Service Timber and Watershed Laboratory in Parsons, WV within 24 hours for processing. Samples were vacuum filtered through 0.22 μm polyethersulfone membrane filters to remove suspended solids and biological material. Samples were then frozen and transported to the University of Pittsburgh, where they remained frozen until analysis.

6.2.3 Isotopic Analysis

Nitrate concentrations for all samples were measured by ion chromatography (Dionex ICS-2000) at the University of Pittsburgh. For isotopic analysis, a denitrifying bacteria, *Pseudomonas aureofaciens*, was used to convert aqueous nitrate into gaseous N_2O which was then introduced

into the mass spectrometer [Sigman *et al.*, 2001; Casciotti *et al.*, 2002]. For $\Delta^{17}\text{O}$ analysis, this N_2O was thermally decomposed at 800°C into N_2 and O_2 prior to isotopic analysis following the method described by Kaiser *et al.* [2007]. Duplicate samples were analyzed for $\delta^{15}\text{N}$ and $\delta^{18}\text{O}$ of nitrate (and separately for $\Delta^{17}\text{O}$ of nitrate during $\Delta^{17}\text{O}$ analysis) on an Isoprime Trace Gas and Gilson GX-271 autosampler coupled with an Isoprime Continuous Flow Isotope Ratio Mass Spectrometer (CF-IRMS) at the *Regional Stable Isotope Laboratory for Earth and Environmental Science* at the University of Pittsburgh. Isotope values are reported in parts per thousand relative to nitrate standards as follows:

$$\delta^{15}\text{N}, \delta^{18}\text{O}, \text{ and } \delta^{17}\text{O} (\text{‰}) = \left[\left(\frac{R_{\text{sample}}}{R_{\text{standard}}} \right) - 1 \right] \times 1000 \quad (\text{Eq. 1})$$

where $R = {}^{15}\text{N}/{}^{14}\text{N}$, ${}^{18}\text{O}/{}^{16}\text{O}$, or ${}^{17}\text{O}/{}^{16}\text{O}$. The mass-independent oxygen isotope anomaly of nitrate ($\Delta^{17}\text{O}\text{-NO}_3^-$) is likewise reported in parts per thousand and calculated using the equation:

$$\Delta^{17}\text{O} (\text{‰}) = \delta^{17}\text{O} - 0.52 \times \delta^{18}\text{O} \quad (\text{Eq. 2})$$

Samples with low nitrate concentrations were pre-concentrated prior to bacterial conversion to N_2O . Pre-concentration was accomplished by calculating the sample volume necessary to obtain a final concentration of 20 nmol (for $\delta^{15}\text{N}$ and $\delta^{18}\text{O}$ analysis) or 200 nmol (for $\Delta^{17}\text{O}$ analysis) in a 5 mL sample. Appropriate sample volumes were measured into 10% hydrochloric acid-washed Pyrex or Teflon beakers and placed in a drying oven at 60°C until all liquid evaporated. The interior of each beaker was then rinsed with 10mL of 18 M Ω water to

reconstitute duplicate samples to the appropriate concentration. Samples were prepared for isotopic analysis following the bacterial denitrifier method as previously described. International reference standards were similarly pre-concentrated and used for correction of pre-concentrated samples.

$\delta^{15}\text{N}$ and $\delta^{18}\text{O}$ values were corrected using international reference standards USGS-32, USGS-34, USGS-35, and N3; USGS-34 and USGS-35 were used to correct $\Delta^{17}\text{O}$ values. These standards were also used to correct for linearity and instrument drift. Standard deviations for international reference standards were 0.2‰, 0.5‰, and 0.2‰ for $\delta^{15}\text{N}$, $\delta^{18}\text{O}$, and $\Delta^{17}\text{O}$, respectively.

Water isotope analyses were carried out at the University of Maryland, Baltimore County (UMBC) and at the Cornell Isotope Laboratory (COIL) at Cornell University. Sample analyses at UMBC were carried out on a Picarro water isotope cavity ring-down spectrometer. $\delta^{18}\text{O}\text{-H}_2\text{O}$ values for these samples represent an average of five sample injections and samples were corrected using reference standards USGS-46 and USGS-48, with a standard deviation of 0.2‰. Sample analyses at COIL were carried out on a Thermo Delta V isotope ratio mass spectrometer interfaced to a Gas Bench II. These samples were analyzed in duplicate and corrected against Vienna Standard Mean Ocean Water and in-house standards, with a standard deviation of 0.2‰.

There is the potential for isobaric interference of the $\delta^{15}\text{N}$ signal in samples with high $\Delta^{17}\text{O}$ values. Corrections for mass-independent contributions of $\Delta^{17}\text{O}$ to m/z 45 were evaluated following the relationship described in *Coplen et al.* [2004], where a 1‰ increase in $\delta^{15}\text{N}$ corresponds to an 18.8‰ increase in $\Delta^{17}\text{O}$. Corrected $\delta^{15}\text{N}$ values were zero to 0.1‰ lower than uncorrected values, depending on the mass-independent contribution of $\Delta^{17}\text{O}$ in the sample. Because this correction factor is small relative to the range of stream $\delta^{15}\text{N}$ values observed and

because we could not apply the correction to some samples due to a lack of $\Delta^{17}\text{O}$ data, the $\delta^{15}\text{N}$ values presented here do not include the mass-independent $\Delta^{17}\text{O}$ correction. However, given that the magnitude of $\delta^{15}\text{N}$ variability is much greater than the correction for isobaric interference, omission of the mass-independent $\Delta^{17}\text{O}$ correction does not influence the observed $\delta^{15}\text{N}$ trends and our interpretation of stormflow dynamics.

6.2.4 End-Member Mixing Analysis

The two main sources of stream water in WS4 are precipitation and subsurface flow [DeWalle *et al.*, 1997], and atmospheric deposition and microbial nitrification are the two sources of stream nitrate (see Chapter 3). Because the isotopic compositions of these water and nitrate sources are distinct, two end-member isotope mixing models can be used to quantify the relative contributions of each source to water and nitrate in streams. We calculated the fractions of event water and atmospheric nitrate in hourly stormflow samples using the mixing model

$$f_{\text{event}} = \frac{\chi_{\text{sf}} - \chi_{\text{bf}}}{\chi_{\text{atm}} - \chi_{\text{bf}}} \quad (\text{Eq. 3})$$

where f_{event} is the fraction of event water or atmospheric nitrate in stormflow, and χ_{sf} , χ_{bf} , and χ_{atm} represent the $\delta^{18}\text{O}\text{-H}_2\text{O}$ or $\Delta^{17}\text{O}$ of nitrate isotopic composition of stormflow, baseflow, and precipitation water or nitrate, respectively. For the baseflow end-member on 9 July, we used a $\delta^{18}\text{O}\text{-H}_2\text{O}_{\text{bf}}$ value of -10.3‰ measured during baseflow conditions in WS4 on 6 July. Because streamflow was absent in WS4 during routine weekly sampling from August through October 2010, we used a $\delta^{18}\text{O}\text{-H}_2\text{O}_{\text{bf}}$ end-member value of -8.1‰ for the two September storms, based on

a baseflow sample collected on 28 September from an adjacent watershed (WS5). This end-member value is justified based on the general agreement between growing season baseflow $\delta^{18}\text{O}\text{-H}_2\text{O}$ values measured in WS4 and WS5 during 2010 (Figure 6.1). For $\delta^{18}\text{O}\text{-H}_2\text{O}_{\text{atm}}$, we used the incremental mean method described by *McDonnell et al.* [1990] to calculate a volume-weighted mean based on precipitation samples collected hourly during each storm.

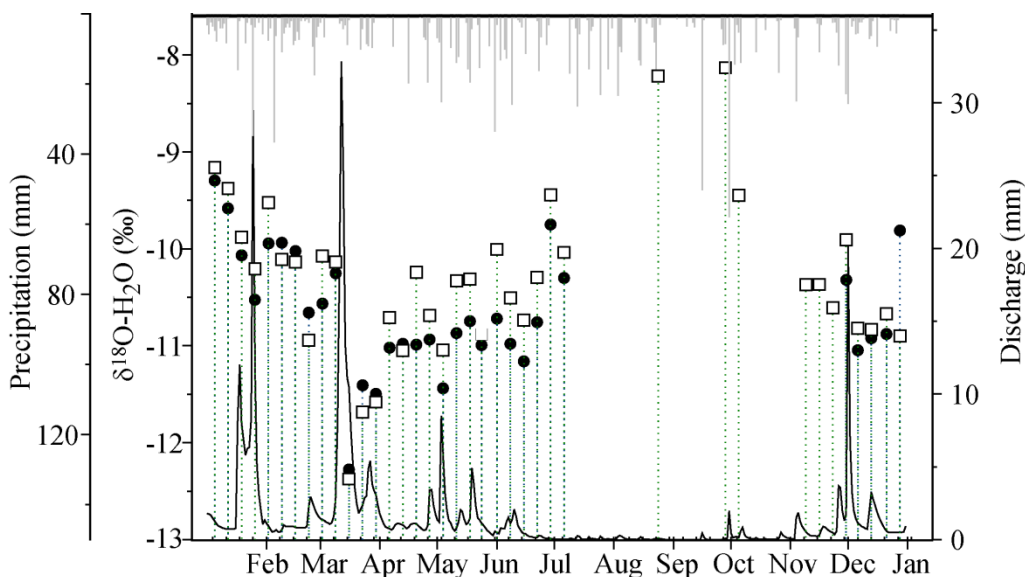


Figure 6.1. $\delta^{18}\text{O}\text{-H}_2\text{O}$ values in stream samples collected weekly during 2010 in WS4 (solid black circles) and an adjacent watershed (WS5; open squares). The black line shows discharge in WS5; grey bars show precipitation measured in WS5.

We chose a $\Delta^{17}\text{O}$ -based approach for nitrate source apportionment because, unlike $\delta^{18}\text{O}$ of nitrate, this isotope tracer is not affected by mass-dependent fractionation during biological processes such as assimilation and denitrification. Biological processing does not incrementally

bias $\Delta^{17}\text{O}$ of nitrate values; rather, the $\Delta^{17}\text{O}$ value of atmospheric nitrate becomes zero (or negative) following biological processing. The $\Delta^{17}\text{O}$ values for the two nitrate sources at Fernow— atmospheric deposition and nitrification— are therefore distinct. To calculate the fraction of atmospheric nitrate in each stormflow sample, we used a baseflow nitrate $\Delta^{17}\text{O}$ value ($\Delta^{17}\text{O}\text{-NO}_3^-_{\text{bf}}$) of zero to represent microbial nitrate [Michalski *et al.*, 2004]. The atmospheric end-member value for each storm ($\Delta^{17}\text{O}\text{-NO}_3^-_{\text{atm}}$) was calculated using the incremental mean method [McDonnell *et al.*, 1990]. The absence of $\Delta^{17}\text{O}$ data for several precipitation nitrate samples during the 30 September storm may have biased the atmospheric nitrate fractions calculated using the incremental mean method toward the $\Delta^{17}\text{O}$ values of the first two precipitation nitrate samples on this date. The atmospheric nitrate contributions to stormflow should therefore be interpreted cautiously for this storm event.

6.2.5 Statistical Analysis

We used Pearson's Correlation Coefficients to evaluate the relationships among hydrologic and biogeochemical variables during storms. Variables were significantly correlated at $p < 0.05$. All statistical analyses were conducted using SAS [SAS Institute, Inc., 2011].

6.3 RESULTS

6.3.1 Nitrate Concentrations in Precipitation and Stormflow

Hourly precipitation, discharge, and nitrate concentrations during storms are shown in Figure 6.2. Precipitation samples were not collected during the first four hours of the 16 September storm. Total precipitation amounts were 18 mm, 48 mm, and 56 mm, whereas peak discharges reached 0.1 mm, 1.0 mm, and 2.1 mm on 9 July, 16 September, and 30 September, respectively (Table 6.2). Volume-weighted mean nitrate concentrations in precipitation were 0.7 mg L⁻¹, 0.5 mg L⁻¹, and 0.1 mg L⁻¹; corresponding discharge-weighted mean nitrate concentrations in the stream were 1.9, 8.6, and 2.5 mg L⁻¹ for the 9 July, 16 September, and 30 September storms, respectively. Differences in mean precipitation and stormflow nitrate concentrations indicate much higher nitrate concentrations in stormflow than precipitation (Table 6.2). During the 9 July and 30 September events, nitrate concentrations were highest immediately following peak discharge; on 16 September, nitrate concentrations were highest prior to and immediately after peak discharge, with substantially lower concentrations thereafter (Figure 6.2).

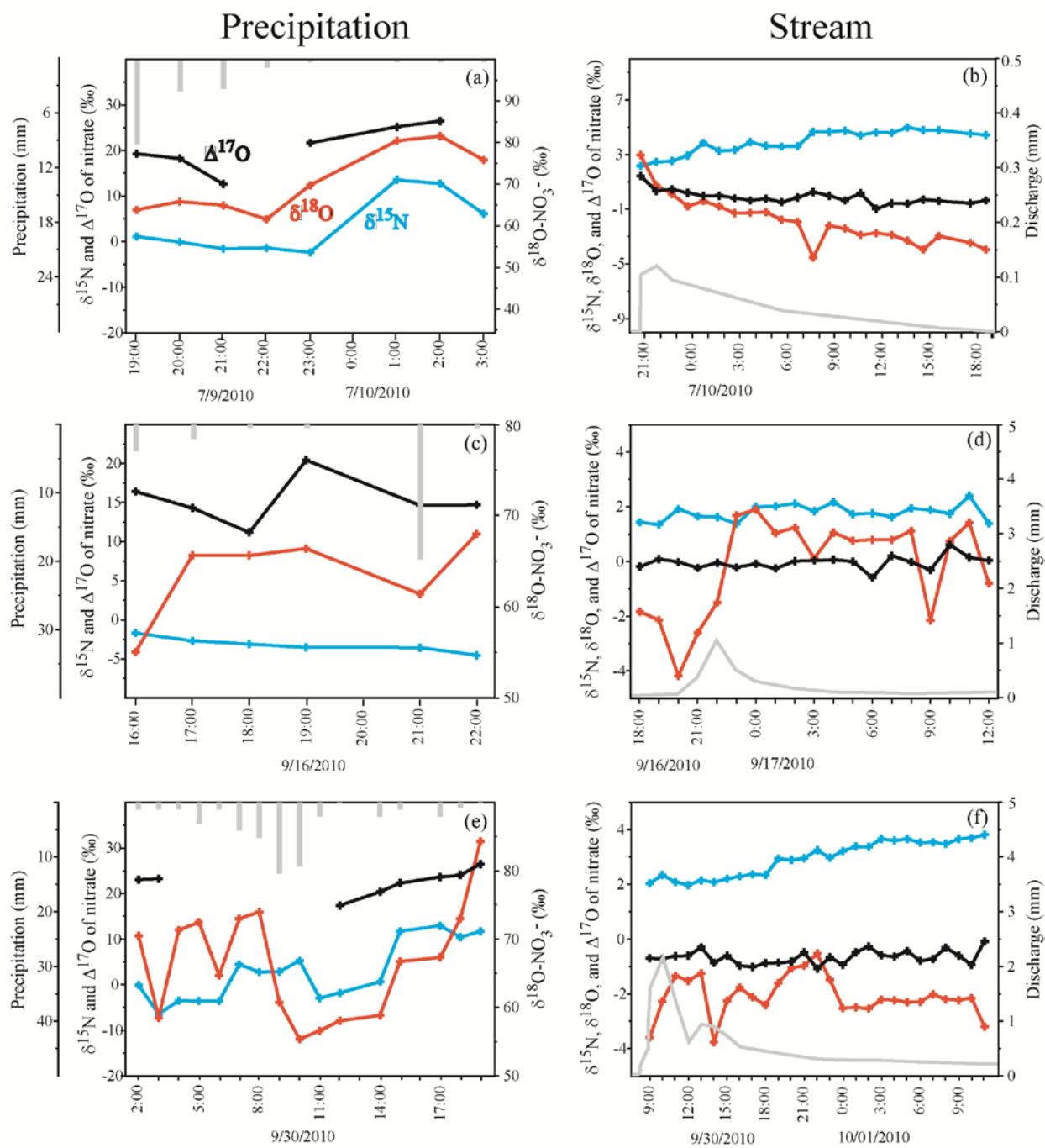


Figure 6.2. Hourly precipitation (grey bars), discharge (grey line), and $\delta^{15}\text{N}$ (blue line), $\delta^{18}\text{O}$ (red line), and $\Delta^{17}\text{O}$ of nitrate values for the 9 July (a and b), 16 September (c and d), and 30 September (e and f) storms sampled in WS4 at Fernow Experimental Forest.

Table 6.2. Volume-weighted mean precipitation and stormflow nitrate concentrations and isotopic compositions during three growing season storms

Event date	Precipitation					Stormflow				
	$[NO_3^-]$	$\delta^{15}N$	$\delta^{18}O$	$\Delta^{17}O$	$\delta^{18}O$	$[NO_3^-]$	$\delta^{15}N$	$\delta^{18}O$	$\Delta^{17}O$	$\delta^{18}O$
	($mg L^{-1}$)	NO_3^-	NO_3^-	NO_3^-	H_2O	($mg L^{-1}$)	NO_3^-	NO_3^-	NO_3^-	H_2O
	(‰)	(‰)	(‰)	(‰)		(‰)	(‰)	(‰)	(‰)	
9 July	0.7	+1.1	+65.5	+18.4	-7.2	1.9	+3.4	-0.6	+0.2	-10.1
16 Sept	0.5	-3.2	+61.0	+14.9	-7.1	8.6	+1.7	-0.2	-0.1	-7.6
30 Sept	0.1	+2.3	+67.5	+22.5	-20.7	2.5	+2.5	-2.2	-0.7	-11.7

6.3.2 Nitrate Isotopic Compositions of Precipitation and Stormflow

The range of precipitation nitrate $\delta^{15}N$ values (-6.5‰ to +14.0‰) was much larger than the range observed in stream samples during all storms (+1.4‰ to +5.0‰; Figure 6.2). Volume-weighted mean $\delta^{15}N$ values in precipitation were +1.1‰, -3.2‰, and +2.3‰ on 9 July, 16 September, and 30 September, respectively. Stream nitrate $\delta^{15}N$ values were much less variable than those measured in precipitation (Figure 6.2), and discharge-weighted means were +3.0‰, +1.7‰, and +2.0‰ on 9 July, 16 September, and 30 September, respectively. $\delta^{15}N$ was lowest in early discharge and increased slightly over time during all events (Figure 6.2). On 9 July, $\delta^{15}N$ values ranged from +2.2‰ at the onset of discharge to +5.0‰ near the end. On 16 September, the lowest $\delta^{15}N$ value of +1.4‰ occurred one hour after discharge onset; the highest value of +2.4‰ occurred one hour before the cessation of discharge. Similarly, stream $\delta^{15}N$ values spanned a

small range on 30 September, from +1.98‰ in early discharge to +3.81‰ during the final hour of streamflow.

Precipitation $\delta^{18}\text{O}$ of nitrate ranged from +55.1‰ to +82.0‰ for the three storms (Figure 6.2), and volume-weighted mean $\delta^{18}\text{O}$ values were +65.5‰, +61.0‰, and +67.5‰ on 9 July, 16 September, and 30 September, respectively (Table 6.2). These values are in stark contrast to the discharge-weighted mean $\delta^{18}\text{O}$ values of stormflow nitrate: -1.0‰, -0.1‰, and -2.1‰ on 9 July, 16 September, and 30 September, respectively (Table 6.2). The range of stream nitrate $\delta^{18}\text{O}$ values was small, from -4.2‰ to +3.0‰ across all storms, and temporal trends in stream nitrate $\delta^{18}\text{O}$ values differed among storms (Figure 6.2). On 9 July, the highest value (+3.0‰) occurred at the onset of stormflow and values decreased steadily to -3.9‰ at the end of discharge. In contrast, $\delta^{18}\text{O}$ of nitrate values on 16 September were lowest in early discharge (-4.2‰), increased to +1.9‰ during the rising limb of the hydrograph, and remained elevated for the next 12 hours before decreasing again in the last hours of discharge. Stream nitrate $\delta^{18}\text{O}$ values also increased during the rising limb of the 30 September hydrograph, but alternating negative and positive trends in isotopic composition occurred following peak discharge.

As with $\delta^{18}\text{O}$ of nitrate, precipitation nitrate $\Delta^{17}\text{O}$ values spanned a wide range (+11.2‰ to +26.8‰; Figure 6.2), and volume-weighted mean $\Delta^{17}\text{O}$ values were +17.3‰, +14.9‰, and +22.5‰ on 9 July, 16 September, and 30 September, respectively (Table 6.2). Stream nitrate $\Delta^{17}\text{O}$ values showed a much smaller range— from only -1.1‰ to +1.5‰ across all storms (Figure 6.2). Discharge-weighted mean $\Delta^{17}\text{O}$ values were +0.1‰, -0.1‰, and -0.6‰ on 9 July, 16 September, and 30 September, respectively. On 9 July, the highest $\Delta^{17}\text{O}$ value (+1.5‰) occurred at discharge onset and steadily decreased thereafter; in contrast, $\Delta^{17}\text{O}$ of nitrate values showed no temporal trends during the two September storms (Figure 6.2).

6.3.3 $\delta^{18}\text{O}\text{-H}_2\text{O}$ in Precipitation, Stormflow, and Soil Water

The range of precipitation $\delta^{18}\text{O}\text{-H}_2\text{O}$ values was wide across all storms, from -23.1‰ to -4.5‰ (Figure 6.2). In general, lower isotope values corresponded to periods of higher intensity rainfall, suggesting rainout of heavier isotopes during storms. Mean precipitation $\delta^{18}\text{O}\text{-H}_2\text{O}$ values for the July and September storms did not follow the general seasonal trend of higher values in July and lower values in September reported by *DeWalle et al.* [1997] at Fernow. Rather, volume-weighted mean precipitation $\delta^{18}\text{O}\text{-H}_2\text{O}$ values were -7.2‰, -7.1‰, and -20.4‰ on 9 July, 16 September, and 30 September, respectively (Table 6.2).

The $\delta^{18}\text{O}\text{-H}_2\text{O}$ in streams ranged from -15.0‰ to -7.3‰ across all events, and showed very little variability within the 9 July and 16 September events (Figure 6.2). Discharge-weighted mean $\delta^{18}\text{O}\text{-H}_2\text{O}$ values were -10.1‰, -7.6‰, and -11.7‰ on 9 July, 16 September, and 30 September, respectively (Table 6.2).

On 17 September and 1 October, soil water samples were collected from lysimeters draining the A horizon at several locations across WS4 (Figure 6.3); no soil water was present in lysimeters following the 9 July event. Values of $\delta^{18}\text{O}\text{-H}_2\text{O}$ in these distributed soil water samples were used to characterize the hydrologic connectivity between upslope areas in WS4 and the stream during storm events. The samples collected on 17 September had accumulated over the previous two weeks; $\delta^{18}\text{O}\text{-H}_2\text{O}$ values in these samples ranged from -6.8‰ to -5.8‰ (Figure 6.3). Lysimeters were emptied on 29 September to ensure that samples collected on 1 October contained only soil water that had accumulated during the 30 September event. The range of soil water $\delta^{18}\text{O}\text{-H}_2\text{O}$ values for this event was -17.8‰ to -10.4‰ (Figure 6.3).

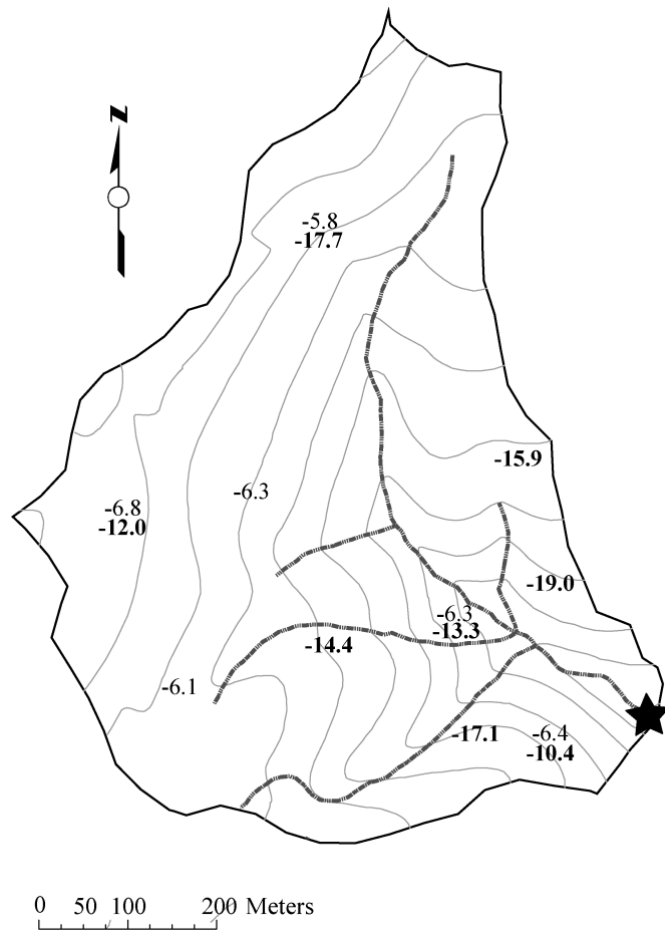


Figure 6.3. Map of WS4, A horizon $\delta^{18}\text{O}$ of soil water values at lysimeter locations sampled on 17 September (regular type) and October 1 (bold type), 2010. The location of the weir in WS4 is shown by the star.

6.4 DISCUSSION

6.4.1 Sources of Stream Nitrate in Watershed 4

The highly variable isotopic composition of precipitation nitrate was not reflected in the nitrate stable isotopic composition of stormflow (Figure 6.2). The low values and small range of stream $\delta^{18}\text{O}$ and $\Delta^{17}\text{O}$ of nitrate across all storms (-3.9 to +3.0‰ and -1.1‰ to +1.5‰, respectively) indicate that microbial nitrification was the dominant nitrate source in stormflow. In addition, the lack of coincident increasing trends in stream nitrate $\delta^{15}\text{N}$ and $\delta^{18}\text{O}$ values during storm events suggests that denitrification was not an important N cycling process during these storms.

Using Equation 3 (with the minimum and maximum precipitation nitrate $\Delta^{17}\text{O}$ values during each storm representing $\Delta^{17}\text{O-NO}_3^-_{\text{atm}}$ and a value of zero for $\Delta^{17}\text{O-NO}_3^-_{\text{bf}}$), atmospheric nitrate contributions to hourly stormflow ranged from 0 to 12%, 0 to 5%, and 0% during the 9 July, 16 September, and 30 September events, respectively. These proportions of atmospheric nitrate in stormflow are smaller than those reported for other watersheds [*Spoelstra et al.*, 2001; *Williard et al.*, 2001; *Burns and Kendall*, 2002; *Campbell et al.*, 2006; *Sebestyen et al.*, 2008, 2014; *Buda and DeWalle*, 2009a; *Goodale et al.*, 2009]. In many of these previous studies, larger proportions of atmospheric nitrate occurred during snowmelt; these dynamics are not represented by the growing season storms sampled in this study at Fernow. In other studies of nitrate export during non-snowmelt events, large proportions of atmospheric nitrate in stormflow were attributed to a variety of factors. *Buda and DeWalle* [2009a] reported maximum atmospheric nitrate contributions ranging from 19 to 100% during peakflow of five storms sampled from March through November. The authors suggested that direct channel interception

of precipitation and wash-off of dry atmospheric nitrate deposition to streams was responsible for the high proportions of atmospheric nitrate in streams during small storms. Similarly, *Michalski et al.* [2004] attributed the nearly 40% of atmospheric nitrate in stormflow at the onset of the southern California rainy season to wash-off of dry nitrate deposition which had accumulated on plant and soil surfaces during the dry season. Although the largest contribution of atmospheric nitrate observed in our study (12%) was smaller than those reported by others, it occurred at the beginning of the smallest storm on 9 July (18 mm total precipitation and 2 mm total discharge). Direct channel interception of precipitation nitrate is unlikely due to dense canopy cover over the stream channel during this time of year; however wash-off of dry atmospheric nitrate deposition in throughfall may have facilitated direct routing of atmospheric nitrate to the stream early in this event.

Other studies attributed significant atmospheric nitrate export (up to 33% in some cases) to the establishment of saturation overland flow during summer and autumn storms [*Sebestyen et al.*, 2014]. Under such hydrologic conditions, atmospheric nitrate deposited to the land surface may be rapidly transported to streams along surficial flowpaths, bypassing opportunities for extensive biological processing [*Sebestyen et al.*, 2014]. Such nitrate transport mechanisms are not likely to occur at Fernow, as overland flow has not been observed in WS4 [*Reinhart et al.*, 1963]. High rates of N mineralization and nitrification in WS4 [*Peterjohn et al.*, 1999; *Gilliam et al.*, 2001], coupled with stormflow generation occurring primarily along subsurface flowpaths, may explain the predominance of microbial nitrification as a nitrate source in stormflow.

Gilliam et al. [2001] reported that soil N pools remain well above $0 \text{ g NO}_3^- \text{-N m}^{-2}$ in WS4 throughout the year, indicating that microbial nitrate production consistently exceeds plant and microbial demand. N et nitrification rates in WS4 also demonstrate a strong response to

increasing ambient temperature and soil moisture ($R^2 = 0.66$; [Gilliam *et al.*, 2001]). Such conditions likely facilitated high rates of microbial nitrification during the period of storm sampling, as the mean minimum temperature at the study site during the month prior to 16 September was 13°C and the antecedent moisture for the same period was 44.2 mm. Indeed, the low $\delta^{18}\text{O}$ and $\Delta^{17}\text{O}$ of nitrate values observed in stormflow (Figure 6.2) are consistent with large contributions of nitrate from a microbial source.

6.4.2 Drivers of Nitrate Export During Storms

Direct channel interception and routing of precipitation along preferential flowpaths during storms can result in contributions of event water to stormflow, and atmospheric nitrate can also be routed along these pathways [Sebestyen *et al.*, 2008]. Mean proportions of event water in stormflow were 6, 34, and 28% for the 9 July, 16 September, and 30 September storms, respectively. Unfortunately, sample vials for several water isotope samples collected during the 16 September event broke during transport (including those collected at peakflow), so the proportion of event water in stormflow calculated for this date may be underestimated. In contrast to event water, mean contributions of atmospheric deposition to stormflow nitrate were negative for all storms, indicating greater proportions of event water than event nitrate in stormflow during all storms. This difference indicates that factors other than precipitation inputs regulate nitrate export during storms. Greater nitrate deposition did not correspond to increased stream nitrate export during storms ($p=0.44$). Although stream nitrate export showed no significant relationship to discharge amount ($p=0.11$), the greater nitrate yields observed with

greater discharge suggests that event size may have influenced overall nitrate export during storms, possibly from flushing of the stored soil nitrate pool from source areas throughout WS4.

Nitrate export dynamics during the 16 September event provide a good example of nitrogen flushing. Concentrations in the stream prior to and including peak discharge on 16 September ranged from 9.0 mg L⁻¹ to 10.8 mg L⁻¹; samples collected after peak discharge had lower nitrate concentrations (Figure 6.2). Prior to this storm, antecedent moisture during the previous month was 44.2 mm and the average temperature was 13°C; the last rainfall event of at least 5 mm occurred 9 days prior. These conditions, along with increased inputs of labile organic nitrogen from litterfall during this time of year, could have facilitated microbial nitrate production in soils. Indeed, high stream nitrate concentrations during the onset of stormflow and low $\delta^{18}\text{O}$ and $\Delta^{17}\text{O}$ of nitrate values throughout the event (Figure 6.2) suggest that soil N flushing was the main source of nitrate to the stream. In addition, high proportions of event water in stormflow relative to atmospheric nitrate during this event lend further support to the idea that precipitation inputs facilitated soil nitrate flushing rather than directly contributing nitrate to the stream. Similar soil nitrate flushing dynamics have been described in other storm response studies in forested watersheds [Creed *et al.*, 1996; Mitchell *et al.*, 2006; Inamdar *et al.*, 2009].

The stream responses we observed at Fernow are comparable to patterns of water and nitrate source contributions to stormflow reported elsewhere, but with some important differences. Buda and DeWalle [2009a] reported greater fractions of event nitrate than event water in stormflow during small events (> 35 mm of precipitation) in a forested watershed. During larger storms, the authors invoked a similar nitrate export mechanism as we hypothesized here for WS4, whereby event water mobilizes stored soil nitrate and transports it along shallow

subsurface flowpaths to the stream [Buda and DeWalle, 2009a]. While contributions of event water exceeded those of atmospheric nitrate in all stormflow samples collected in WS4, the greatest proportion of atmospheric nitrate export (12%) occurred in the first sample collected during the smallest event on 9 July. During this time, direct routing of precipitation and atmospheric nitrate to the stream (perhaps via throughfall) may have been an important pathway for direct routing of atmospheric nitrate to the stream. Buda and DeWalle [2009a] similarly attributed high proportions of atmospheric nitrate in stormflow during small events (<35 mm precipitation) to wash-off of dry-deposited nitrate from vegetation surfaces to the stream. Vegetation canopies can be highly effective scavengers of wet and dry atmospheric N deposition [Lovett and Lindberg, 1986; Johnson and Lindberg, 1992], with throughfall nitrate concentrations in excess of bulk precipitation concentrations in areas of high N deposition [Parker, 1983; Grennfelt and Hultberg, 1986; Lovett and Lindberg, 1986]. Fernow has historically received some of the highest rates of atmospheric N deposition in the U.S. [Adams et al., 2007], and dry inorganic N deposition represents nearly 25% of bulk inorganic N deposition at this site [National Atmospheric Deposition Program, 2011; U.S. EPA CASTNET, 2012]). Dry nitrate deposition accumulated on vegetation surfaces since the previous storm event (14 days prior) could have been transported to the stream as throughfall; this atmospheric nitrate transport process seems feasible given that the most intense rainfall period (9 mm h⁻¹) occurred during the first hour of the 9 July event. Alternatively, rainout/washout of atmospheric nitrate during the beginning of the 9 July event may have contributed to the greater proportion of atmospheric nitrate observed in the stream on this date. In an analysis of intra-storm variation in rain chemistry during 230 events, Burch et al. [1996] found that during short events, the highest nitrate concentrations typically occurred during the beginning of the storm, followed by rapid

decrease in concentrations. The authors attributed this pattern to strong initial washout of the atmosphere by raindrops. These atmospheric source contributions notwithstanding, the overwhelming contributions of microbial nitrate to the stream across all storms (92 to 100%) emphasize the dominant role of microbial nitrification in watershed nitrate export, regardless of the hydrologic pathway responsible for nitrate transport to the stream.

6.4.3 Variable Source Areas of Stream Water and Nitrate during Storms

The storms sampled in this study represent a wide range of hydrologic and biogeochemical characteristics. There was a 17-fold difference in peak discharge measured during the smallest event (0.1 mm on 9 July) versus the largest event (2.1 mm on 30 September), and the timing of the stream response to precipitation inputs also varied among events. Discharge began within the first hour of rainfall on 9 July, whereas streamflow initiation did not occur until six and seven hours after rainfall began on 16 and 30 September, respectively. However, high rainfall intensities were quickly followed by peak discharges during all three events, illustrating the responsiveness of this watershed to intense rainfall inputs (Figure 6.2). Most of the $\delta^{18}\text{O}\text{-H}_2\text{O}$ values in stream water indicated that stormflow was primarily generated from pre-event water stored within the watershed despite the rapid hydrograph response. This phenomenon—wherein streams respond rapidly to precipitation inputs, but the precipitation itself is not a large contributor to stormflow—has been observed elsewhere [McDonnell *et al.*, 1990, 2010; Sidle *et al.*, 2000; Buttle, 2006] and is so widespread that it constitutes a fundamental hydrologic and biogeochemical paradox of small watershed studies [Kirchner, 2003; Bishop *et al.*, 2004].

The dynamic nature of hydrologic flowpaths and hillslope-stream connectivity can affect stormflow generation and nitrate export during storms [Kirchner, 2003; Inamdar *et al.*, 2009]. Differences in the water and nitrate isotopic compositions of precipitation, soil water, and stormflow in WS4 suggest that different source areas and transport pathways influenced water and nitrate delivery to the stream during each of the three events. For example, while we lacked distributed soil water samples from WS4 during the 9 July event, the small amount of discharge (peakflow = 0.10 mm), consistency of $\delta^{18}\text{O}\text{-H}_2\text{O}$ values throughout the hydrograph (mean = $-10.1 \pm 0.1\text{‰}$), and their similarity to previous estimates of groundwater $\delta^{18}\text{O}\text{-H}_2\text{O}$ in WS4 (-9.1‰ ; [DeWalle *et al.*, 1997]) suggest that stormflow was generated primarily from groundwater and likely constrained to near-stream areas during this small event.

Similarly, nitrate contributions to the stream on 9 July were dominated by terrestrial sources rather than direct atmospheric inputs. The maximum contribution of atmospheric nitrate to the stream (12%) was quite small relative to microbial nitrate inputs, and this atmospheric contribution occurred prior to peak discharge. Rainfall intensity peaked during the first hour of this storm, which may have facilitated greater contributions of atmospheric nitrate to early discharge through wash-off of dry-deposited nitrate from vegetation surfaces. Thus, the larger proportions of atmospheric nitrate in the stream during this event do not appear to be driven by variations in subsurface hydrologic connectivity between specific watershed areas and the stream, but rather by direct routing of atmospheric nitrate to the stream via throughfall.

In contrast to the small 9 July storm, the greater variability of stream $\delta^{18}\text{O}\text{-H}_2\text{O}$ values during the 30 September event (Figure 6.2) points to contributions of water from a more variable source area across the watershed, including hillslopes. While a lack of distributed groundwater depth measurements precludes absolute confirmation that hydrologic connectivity was

established between hillslopes and the stream, several lines of evidence support the idea that variable source areas facilitated periodic rapid transport of event water to the stream during the 30 September event. First, an 8‰ decrease in precipitation $\delta^{18}\text{O}\text{-H}_2\text{O}$ values during the first seven hours of rainfall was followed by a 3‰ decline in stream water $\delta^{18}\text{O}\text{-H}_2\text{O}$ values in early discharge; stream water $\delta^{18}\text{O}\text{-H}_2\text{O}$ values subsequently decreased again by 3.5‰ between 13:00 and 15:00 (Figure 6.2). Rapid transport of this isotopically-depleted event water to the stream may have been facilitated by the establishment of transient hydrologic connections between hillslopes and the stream. Second, the $\delta^{18}\text{O}\text{-H}_2\text{O}$ isotopic compositions of A horizon soil water collected on 1 October suggest that a hydrologic connection between hillslopes and the stream may have occurred during the 30 September event (Figure 6.3). These samples contained water only contributed to lysimeters on 29 and 30 September; they therefore provide information about potential sources of stormflow. The range of soil water $\delta^{18}\text{O}\text{-H}_2\text{O}$ values encompasses the range of values observed in all but the first stream sample, suggesting that stormflow on 30 September reflected contributions from shallow and deeper groundwater reservoirs. Third, sharp declines in stream $\delta^{18}\text{O}\text{-H}_2\text{O}$ over short time periods indicate that transient hydrologic connections may have been established between watershed areas characterized by lower soil water $\delta^{18}\text{O}\text{-H}_2\text{O}$ values and the stream. The decline in stream water $\delta^{18}\text{O}\text{-H}_2\text{O}$ from -11.4‰ to -15.0‰ between 13:00 and 15:00 (Figure 6.2) is one such example.

In order for event precipitation to be transported from hillslopes to the stream on the time scale of a storm event, the hydraulic conductivity along subsurface flowpaths would need to be high enough to facilitate discharge from hillslopes to the stream [*Hibbert and Troendle, 1988*]. One factor that influences the hydraulic conductivity of soils is the soil moisture content. Rainfall during the month prior to the 30 September event totaled 81.53 mm, with rainfall input

of at least 5 mm occurring on 28 September. Soil moisture content may therefore have been high during the period of stormflow. While saturation and infiltration excess overland flow are unlikely at Fernow [Reinhart *et al.*, 1963], high antecedent moisture may have resulted in greater hydraulic conductivity and preferential flow during the 30 September storm. Such conditions would result in rapid transport of event water and shallow groundwater (with potentially high concentrations of microbial nitrate) to the stream [Sidle *et al.*, 2000], accounting for the concomitant increase in stream nitrate concentration and decrease in stormflow $\delta^{18}\text{O}\text{-H}_2\text{O}$ composition following the first discharge peak on this date.

Variable hydrologic sources and source areas notwithstanding, the consistently negative $\delta^{18}\text{O}$ and $\Delta^{17}\text{O}$ of nitrate values in stormflow on 30 September indicate that direct contributions of atmospheric nitrate to the stream did not occur during this event. The discharge-weighted mean nitrate concentration in stormflow (2.5 mg L^{-1}) was more than an order of magnitude greater than the volume-weighted mean nitrate concentration in precipitation (0.1 mg L^{-1}), supporting the idea that microbial nitrate was the dominant source in stormflow. The nitrate source dynamics observed in WS4 are consistent with those of other studies in forested watersheds throughout the eastern U.S. [Williard *et al.*, 2001; Mitchell *et al.*, 2006].

6.5 CONCLUSION

Nitrate is a highly soluble and mobile anion, making hydrologic flowpaths important vectors for nitrate transfer from landscapes to streams. Spatio-temporally heterogeneous hydrologic and biogeochemical regimes can influence the movement of water and nitrate from the landscape to

the stream, facilitating nitrate transport to streams along both shallow and deep subsurface flowpaths [Sebestyen *et al.*, 2008; Inamdar *et al.*, 2009].

By coupling hydrologic and nitrate isotope measurements, we have shown that watershed hydrology can influence nitrate source contributions and export during storm events. While the range of event water contributions to stormflow was wide during the growing season storms we sampled in WS4 (6 to 34%), atmospheric nitrate export remained below 10% during all storms, suggesting that biological N processing is extensive on this watershed and flushing of the soil nitrate pool represents the dominant mode of nitrate export during growing season storms.

Effective management of nitrogen polluted forests requires an accurate determination of stream nitrate sources and the factors influencing atmospheric nitrate processing and transport at the watershed scale. Substantial contributions of microbial nitrate to the stream draining WS4 suggest that nitrogen inputs do not exceed biological demand and that both biological and hydrological drivers (e.g., transport via throughfall versus subsurface flow) influence atmospheric nitrate contributions to streams during storms.

7.0 ECOSYSTEM PROCESSING OF ATMOSPHERIC NITRATE ALONG A NITROGEN DEPOSITION GRADIENT

7.1 INTRODUCTION

Anthropogenic production of reactive nitrogen (NH_3 , NH_4^+ , NO_x , HNO_3 , NO_3^- , and organic N compounds) now exceeds that of all natural terrestrial sources [Galloway *et al.*, 2003]. Increased inputs of reactive nitrogen have been linked to nitrogen saturation in ecosystems worldwide [Ågren and Bosatta, 1988; Aber *et al.*, 1998]. Nitrogen saturation occurs when the capacity of vegetation and soil sinks to accommodate N inputs is exceeded, and excess N is leached from the landscape to surface and ground waters as nitrate (NO_3^-) [Ågren and Bosatta, 1988; Aber *et al.*, 1998; Lovett and Goodale, 2011]. Terrestrial effects of N saturation can include decreased frost-hardiness in plants, decreased mycorrhizal fungi abundance, increased soil acidification, and greater leaching of nitrate and base cations from soils [Driscoll *et al.*, 2001; Adams *et al.*, 2007; Van Diepen *et al.*, 2007]. Excess nitrate leaching to surface and ground waters can contribute to eutrophication effects including toxic algae blooms and fish kills, as well as degraded drinking water quality [Vitousek *et al.*, 1997; Boesch *et al.*, 2001; Galloway *et al.*, 2003]. These symptoms of excess nitrogen inputs are particularly evident in the eastern United States, where the amount of atmospheric deposition has increased 5-fold over the pre-industrial baseline [Galloway *et al.*, 1984]. Sixty to 80% of this deposition occurs as nitrate [Aber *et al.*, 2003], the

sources of which are primarily fossil-fuel combustion from coal-fired power plants and automobiles [Elliott *et al.*, 2007]. Once in the atmosphere, these NO_x emissions are rapidly oxidized to multiple NO_y species (e.g., HNO₃ and particulate nitrate), that enter the terrestrial N cycle via wet and dry deposition.

There are two main sources of nitrate in eastern U.S. forests: atmospheric deposition and microbial nitrification. In forests exhibiting symptoms of N saturation, excess nitrate is not retained by terrestrial biomass, but is exported from the system via surface and ground waters [Williard *et al.*, 2001; Adams *et al.*, 2007]. Over time, nitrate concentrations in streams draining N-saturated forests can increase; indeed, long-term increases in stream nitrate concentration have been used to identify N saturation in some forested watersheds [Peterjohn *et al.*, 1996; Kothawala *et al.*, 2011]. However such long-term stream chemistry records are not available for most watersheds, complicating assessments of N saturation status at many sites. As an alternative, stable isotope-based characterizations of stream nitrate sources (e.g., $\delta^{15}\text{N}$ and $\delta^{18}\text{O}$ of nitrate) have been used to assess the N saturation status of forests [Pardo *et al.*, 2004; Barnes *et al.*, 2008]. If increased N supply relative to biological demand results in less efficient (i.e., more “leaky”) ecosystem N cycling as N saturation progresses, then assimilation of atmospheric nitrate inputs may also become less extensive. In this case, stream nitrate isotopic compositions should show evidence of unprocessed atmospheric nitrate. Due to the similarity in $\delta^{15}\text{N}$ values of atmospheric and microbial nitrate (Figure 1.2), $\delta^{15}\text{N}$ values are not typically used for nitrate source differentiation. Conversely, greater separation of $\delta^{18}\text{O}$ ranges for atmospheric and microbial nitrate (Figure 1.2) has facilitated the apportionment of nitrate contributions from these two sources using a simple two-endmember mixing model (Equation 1)

$$f_{\text{atm}} = \frac{\chi_{\text{stream}} - \chi_{\text{nitrification}}}{\chi_{\text{atm}} - \chi_{\text{nitrification}}} \quad (\text{Eq. 1})$$

where f_{atm} is the fraction of stream nitrate contributed by atmospheric deposition and χ is the $\delta^{18}\text{O}$ of nitrate value of stream, microbial nitrification, or atmospheric nitrate. This approach has been used in many studies to characterize source contributions to stream nitrate [Williard *et al.*, 2001; Burns and Kendall, 2002; Pardo *et al.*, 2004; Campbell *et al.*, 2006; Barnes *et al.*, 2008; Sebestyen *et al.*, 2008, 2014; Goodale *et al.*, 2009].

While there is a strong precedent for using $\delta^{18}\text{O}$ of nitrate for source apportionment, important limitations to this approach are being increasingly recognized. As a growing number of studies have characterized $\delta^{18}\text{O}$ values for atmospheric and microbial nitrate, their source ranges have also widened and become more similar [Kendall and Doctor, 2004; Michalski *et al.*, 2004]. In addition, mass-dependent fractionation during biological processes such as denitrification can lead to enrichment of $\delta^{15}\text{N}$ and $\delta^{18}\text{O}$ values in the residual soil nitrate pool (Figure 1.2), which can further confound isotope mass balance-based source apportionment [Michalski *et al.*, 2004].

More recently, studies have demonstrated that atmospheric nitrate is anomalously enriched in the ^{17}O isotope; this enrichment is denoted by $\Delta^{17}\text{O}$ ([Michalski *et al.*, 2003]; Figure 1.3). Values of $\Delta^{17}\text{O}$ in atmospheric nitrate generally range from +20 to +33‰, whereas microbial nitrate has $\Delta^{17}\text{O}$ values of zero or less [Michalski *et al.*, 2003; Morin *et al.*, 2009]. Importantly, $\Delta^{17}\text{O}$ is not susceptible to mass-dependent fractionation as with $\delta^{18}\text{O}$ of nitrate, making it a conservative tracer of atmospheric nitrate. When atmospheric deposition (with a positive $\Delta^{17}\text{O}$ value) is biologically assimilated and cycled, the positive $\Delta^{17}\text{O}$ signal is lost as the

nitrate is converted to organic N. When the organic N is subsequently nitrified, this microbially-produced nitrate has a $\Delta^{17}\text{O}$ value of zero or less. Thus, when streams show positive $\Delta^{17}\text{O}$ of nitrate values, this indicates that some proportion of the atmospheric nitrate deposited in the watershed was not biologically cycled prior to export to the stream. The ability to unambiguously differentiate between atmospheric and microbial nitrate sources makes $\Delta^{17}\text{O}$ a useful tool for assessing whether the extent of atmospheric nitrate processing changes with increasing ecosystem N saturation or variation in N deposition regimes.

Several cross-site comparisons have been conducted in the eastern U.S. to examine the effects of variable N deposition rates on forest N saturation [Aber *et al.*, 2003; Driscoll *et al.*, 2003; Pardo *et al.*, 2006]. These studies provide insights into the ways that N deposition and factors such as species composition, climate, and geology interact to influence forest N export dynamics. However, the key question that remains unanswered by such studies is: how are atmospheric nitrate inputs processed along gradients of nitrogen deposition? Some studies have reported positive correlations between stream nitrate concentrations and N deposition in the northeastern U.S. [Aber *et al.*, 2003], whereas others have observed no relationship [Johnson and Lindberg, 1992; Williard *et al.*, 1997]; however, the post-depositional fate of this atmospheric nitrate is unclear. In watersheds with high rates of nitrate export, do atmospheric inputs represent an excess N supply that is exported directly to the stream without biological processing? Or is elevated nitrate export from some watersheds primarily due to increased microbial activity (i.e., nitrification), indicating that the terrestrial N cycle can accommodate elevated atmospheric inputs? The answers to these questions are important, as they directly address ecosystem responses to elevated N deposition, which is largely the result of human activities.

7.2 STUDY SITES AND METHODS

7.2.1 Study Sites

This study was conducted across a long-term (1982-2007) nitrate deposition gradient that included reference watersheds at Coweeta Hydrologic Laboratory in North Carolina, Fernow Experimental Forest in West Virginia, and Hubbard Brook Experimental Forest in New Hampshire (Figure 7.1). From 1982 to 2007, annual average atmospheric nitrate deposition along this gradient ranged from $11 \text{ kg ha}^{-1} \text{ yr}^{-1}$ at Coweeta to $17 \text{ kg ha}^{-1} \text{ yr}^{-1}$ at Fernow. At all sites, one reference watershed was selected for monthly stream and precipitation sampling. All study watersheds were dominated by mixed hardwoods (with some spruce-fir dominated areas in the higher elevations of the Hubbard Brook watershed), and ranged in age from 84 to 110 years. Additional information on specific study watersheds is presented in Table 7.1.

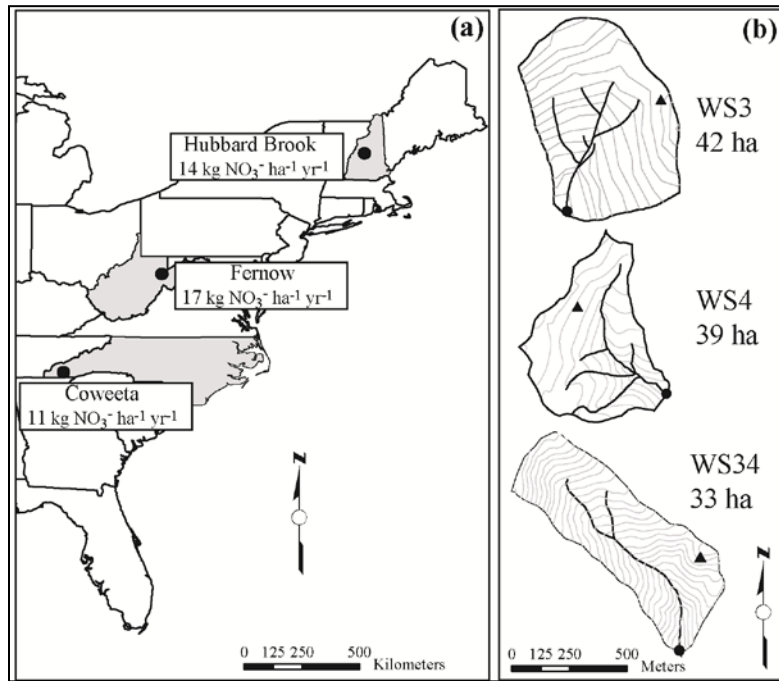


Figure 7.1. (a) Location of study sites along a long-term (1982-2007) nitrate deposition gradient. (b) Maps of study watersheds.

Solid circles denote weir locations and solid triangles denote precipitation gauge locations in each watershed.

Contour lines show 12-meter spacing.

Table 7.1. Description of study watersheds

Site (Watershed)	Forest Age (yrs)	Area (ha)	Elevation Range (m)	Aspect	Mean slope (%)	Soil depth to bedrock (cm)	Mean annual precipitation (cm)	Forest type
Coweeta (WS 34)	84	33	866-1184	SE	52	>150	200	Mixed hardwood
Fernow (WS 4)	110	39	743-867	ESE	20	92	145	Mixed hardwood
Hubbard Brook (WS 3)	~100	42	527-732	SW	21	61	140	Mixed hardwood, spruce-fir

7.2.2 Sample Collection

When sufficient sample volume was present, 1 L stream and precipitation samples were collected monthly from all study watersheds, timed to coincide with routine sample collection for long-term monitoring at study sites. Samples were collected on the same dates at all sites. Stream samples were collected just above the weir and represent instantaneous grab samples. Precipitation samples were collected from bulk precipitation collectors located in meteorological openings (maintained to minimize forest edge effects) in each study watershed (Figure 7.1). Precipitation samples represent rain and snow that had accumulated during the week prior to sample collection. Within 24 hours of collection, all samples were filtered through 0.22 μm polyethersulfone membrane filters to remove suspended solids and biological material. Filtered

samples were frozen and shipped to the University of Pittsburgh where they remained frozen until isotopic analysis.

7.2.3 Isotopic Analysis

Nitrate concentrations for all samples were measured by ion chromatography (Dionex ICS-2000) at the University of Pittsburgh. For isotopic analysis, a denitrifying bacteria, *Pseudomonas aureofaciens*, was used to convert aqueous nitrate into gaseous N₂O which was then introduced into the mass spectrometer [Sigman *et al.*, 2001; Casciotti *et al.*, 2002]. For $\Delta^{17}\text{O}$ analysis, this N₂O was thermally decomposed at 800°C into N₂ and O₂ prior to isotopic analysis following the method described by Kaiser *et al.* [2007]. Duplicate samples were analyzed for $\delta^{15}\text{N}$, $\delta^{18}\text{O}$, and $\Delta^{17}\text{O}$ of nitrate on an Isoprime Trace Gas and Gilson GX-271 autosampler coupled with an Isoprime Continuous Flow Isotope Ratio Mass Spectrometer (CF-IRMS) at the *Regional Stable Isotope Laboratory for Earth and Environmental Science* at the University of Pittsburgh. Isotope values are reported in parts per thousand relative to nitrate standards as follows:

$$\delta^{15}\text{N}, \delta^{18}\text{O}, \text{ and } \delta^{17}\text{O} (\text{‰}) = \left[\left(\frac{R_{\text{sample}}}{R_{\text{standard}}} \right) - 1 \right] \times 1000 \quad (\text{Eq. 2})$$

where $R = {}^{15}\text{N}/{}^{14}\text{N}$, ${}^{18}\text{O}/{}^{16}\text{O}$, or ${}^{17}\text{O}/{}^{16}\text{O}$. The mass-independent oxygen isotope anomaly of nitrate ($\Delta^{17}\text{O}\text{-NO}_3^-$) is likewise reported in parts per thousand and calculated using the equation:

$$\Delta^{17}\text{O} (\text{‰}) = \delta^{17}\text{O} - 0.52 \times \delta^{18}\text{O} \quad (\text{Eq. 3})$$

Samples with low nitrate concentrations were pre-concentrated prior to bacterial conversion to N₂O. Pre-concentration was accomplished by calculating the sample volume necessary to obtain a final concentration of 20 nmol (for $\delta^{15}\text{N}$ and $\delta^{18}\text{O}$ analysis) or 200 nmol (for $\Delta^{17}\text{O}$ analysis) in a 5 mL sample. Appropriate sample volumes were measured into 10% hydrochloric acid-washed Pyrex or Teflon beakers and placed in a drying oven at 60°C until all liquid was evaporated. The interior of each beaker was then rinsed with 10mL of 18 M Ω water to reconstitute duplicate samples to the appropriate concentration. Samples were prepared for isotopic analysis following the bacterial denitrifier method as described above. International reference standards were similarly pre-concentrated and used for correction of pre-concentrated samples.

$\delta^{15}\text{N}$ and $\delta^{18}\text{O}$ values were corrected using international reference standards USGS-32, USGS-34, USGS-35, and N3; USGS-34 and USGS-35 were used to correct $\Delta^{17}\text{O}$ values. These standards were also used to correct for linearity and instrument drift. Standard deviations for international reference standards were 0.2‰, 0.5‰, and 0.2‰ for $\delta^{15}\text{N}$, $\delta^{18}\text{O}$, and $\Delta^{17}\text{O}$, respectively.

There is the potential for isobaric interference of the $\delta^{15}\text{N}$ signal in samples with high $\Delta^{17}\text{O}$ values, such as precipitation. Corrections for mass-independent contributions of $\Delta^{17}\text{O}$ to m/z 45 were evaluated following the relationship described in *Coplen et al.* [2004], where a 1‰ increase in $\delta^{15}\text{N}$ corresponds to an 18.8‰ increase in $\Delta^{17}\text{O}$. Corrected $\delta^{15}\text{N}$ values were 0.6‰ to 1.9‰ lower than uncorrected values, depending on the mass-independent contribution of $\Delta^{17}\text{O}$ in the sample. Because this correction factor is small relative to the range of precipitation $\delta^{15}\text{N}$ values observed and because we could not apply the correction to some samples due to a lack of $\Delta^{17}\text{O}$ data, the $\delta^{15}\text{N}$ values presented here do not include the mass-independent $\Delta^{17}\text{O}$ correction.

While values of corrected $\delta^{15}\text{N}$ data are slightly lower than the data presented here, the temporal trends in $\delta^{15}\text{N}$ values presented here are not strongly influenced by the omission of the mass-independent $\Delta^{17}\text{O}$ correction.

7.2.4 Statistical Analysis

We used analysis of variance to test for significant differences in mean nitrate concentrations, $\delta^{15}\text{N}$, $\delta^{18}\text{O}$, and $\Delta^{17}\text{O}$ values among sites, seasons, and sample types. When significant differences were indicated, we applied Tukey's Honestly Significant Difference test to determine which means were significantly different ($\alpha=0.05$). To control for the inflation of Type I error rate with multiple comparisons, the experiment-wise error rate was held at $\alpha=0.05$ when comparing means among the three study sites. As a result, site means were significantly different at $p < 0.0167$. All statistical analyses were conducted using SAS [SAS Institute, Inc., 2011].

7.3 RESULTS

Mean nitrate concentrations in precipitation did not differ significantly among sites and there were no clear temporal trends in precipitation nitrate concentrations at any of the sites (Figure 7.2). Mean precipitation $\delta^{15}\text{N}$ values were significantly higher ($p=0.0004$) at Fernow than at Coweeta and Hubbard Brook, whereas no significant differences in mean nitrate oxygen isotopic composition ($\delta^{18}\text{O}$ and $\Delta^{17}\text{O}$) were observed among sites (Table 7.2). There were no consistent

temporal trends in precipitation $\delta^{15}\text{N}$; conversely, similar seasonal trends in $\delta^{18}\text{O}$ and $\Delta^{17}\text{O}$ were apparent among sites, with higher values during the colder months and lower values during the warmer months (Figure 7.2).

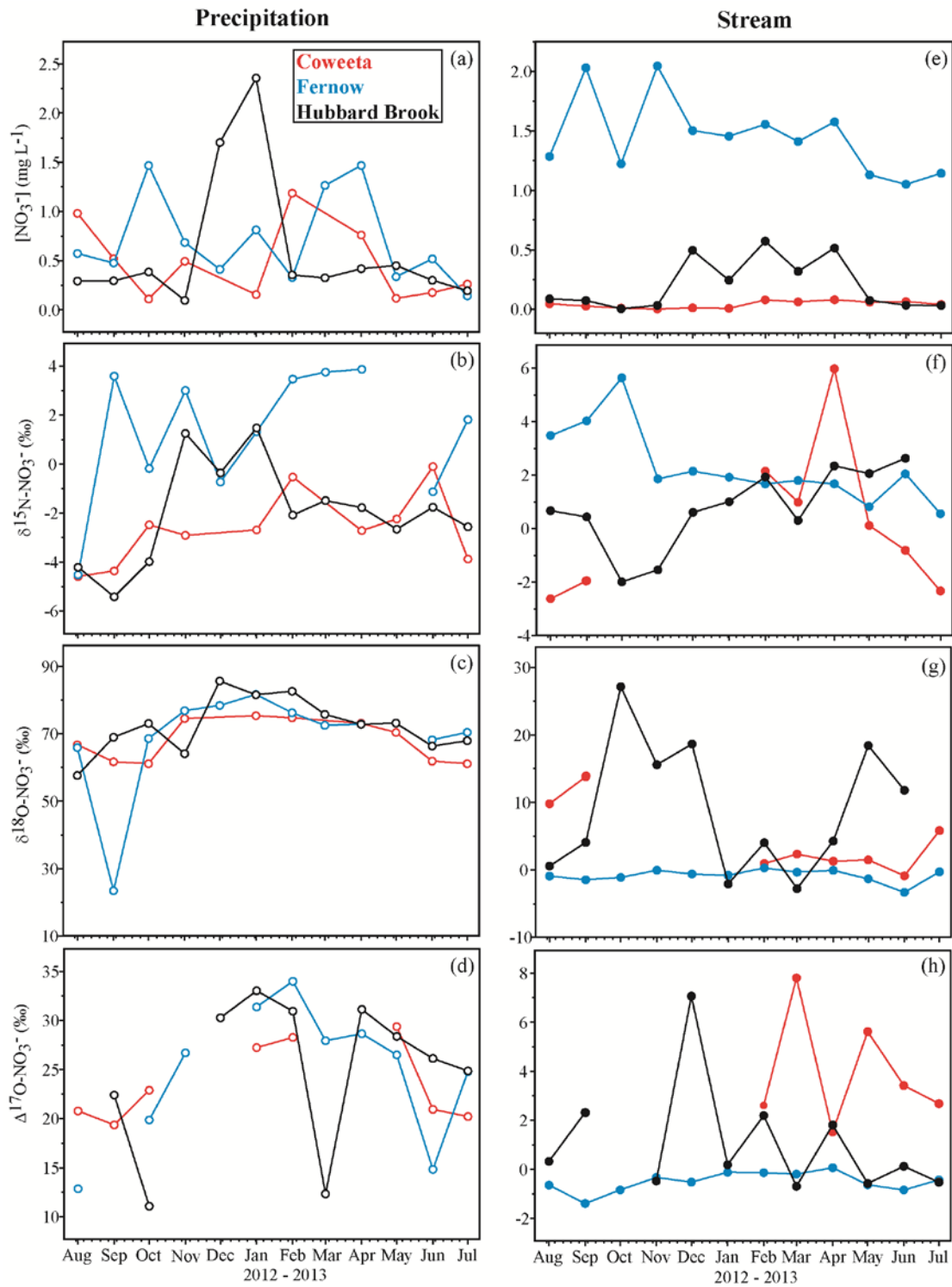


Figure 7.2. Monthly concentrations (a and e), $\delta^{15}\text{N}$ (b and f), $\delta^{18}\text{O}$ (c and g), and $\Delta^{17}\text{O}$ (d and h) values of nitrate in precipitation (open circles) and streams (solid circles) at Coweeta (in red), Fernow (in blue), and Hubbard Brook (in black) Experimental Forests.

Table 7.2. Mean concentrations and isotope values of nitrate in precipitation and stream water for study watersheds at Coweeta (CWT), Fernow (FEF), and Hubbard Brook (HBR) Experimental Forests.

The experiment-wise error rate was held at $\alpha=0.05$ for multiple comparisons; site means followed by different letters are significantly different at $p < 0.0167$.

Site	Precipitation				Stream			
	$[NO_3^-]$ ($mg L^{-1}$)	$\delta^{15}N$ (‰)	$\delta^{18}O$ (‰)	$\Delta^{17}O$ (‰)	$[NO_3^-]$ ($mg L^{-1}$)	$\delta^{15}N$ (‰)	$\delta^{18}O$ (‰)	$\Delta^{17}O$ (‰)
CWT (WS34)	0.5 ($n=10$)	-2.7 ^b ($n=10$)	+68.1 ($n=10$)	+23.6 ($n=8$)	0.1 ^b ($n=12$)	+0.2 ($n=8$)	+4.3 ^{ab} ($n=8$)	+3.9 ^a ($n=6$)
FEF (WS4)	0.7 ($n=12$)	+1.3 ^a ($n=11$)	+68.7 ($n=11$)	+24.8 ($n=10$)	1.5 ^a ($n=12$)	+2.3 ($n=12$)	-0.8 ^b ($n=12$)	-0.5 ^b ($n=12$)
HBR (WS3)	0.6 ($n=12$)	-2.0 ^b ($n=12$)	+72.5 ($n=12$)	+25.1 ($n=10$)	0.2 ^b ($n=12$)	+0.8 ($n=11$)	+9.1 ^a ($n=11$)	+1.1 ^b ($n=11$)
p-value*	0.6064	0.0004	0.5839	0.8940	<0.0001	0.0489	0.0039	0.0002

Mean stream nitrate concentrations were significantly higher at Fernow than Coweeta and Hubbard Brook ($p < 0.0001$; Table 7.2). While there were no strong seasonal trends in stream nitrate concentration at Fernow or Coweeta, concentrations at Hubbard Brook were elevated during the dormant season (from December through April) relative to the rest of the year. Mean stream nitrate $\delta^{15}N$ values were not significantly different and there were no consistent temporal trends in stream nitrate $\delta^{15}N$ among sites (Figure 7.2). Mean $\delta^{18}O$ and $\Delta^{17}O$ of stream nitrate were significantly different among sites (Table 7.2), and temporal trends were also different among the sites. At Fernow, both $\delta^{18}O$ and $\Delta^{17}O$ values of stream nitrate remained near zero during every month of the study (range = -3.3‰ to +0.3‰ for $\delta^{18}O$ and -1.4‰ to +0.1‰ for $\Delta^{17}O$). In contrast, the limited dataset of $\delta^{18}O$ values at Coweeta showed values ranging from -

0.9‰ to +13.8‰, while the widest range of stream nitrate $\delta^{18}\text{O}$ values occurred at Hubbard Brook (-2.8‰ to +27.2‰). Hubbard Brook also showed the greatest range in $\Delta^{17}\text{O}$ of stream nitrate, from -0.7‰ to +7.1‰. At Coweeta, stream nitrate concentrations during the first six months of the study (August 2012 through January 2013) were too low for $\Delta^{17}\text{O}$ analysis. $\Delta^{17}\text{O}$ values in samples from February through July 2013 were all positive, ranging from +1.5‰ to +7.8‰, indicating the presence of atmospheric nitrate in every stream sample.

There was strong differentiation between precipitation and stream nitrate concentrations and isotopic compositions at all sites. The mean concentration of precipitation nitrate was significantly greater than that of stream nitrate at Coweeta, whereas the mean stream nitrate concentration was significantly higher than in precipitation at Fernow (Table 7.3). Mean precipitation $\delta^{15}\text{N}$ values were significantly lower than stream values at Coweeta and Hubbard Brook, while mean precipitation nitrate $\delta^{18}\text{O}$ and $\Delta^{17}\text{O}$ values were significantly higher than stream nitrate values at all sites (Table 7.3).

Table 7.3. Mean concentrations and isotope values of nitrate in precipitation and stream water at individual study sites.

Precipitation and stream means followed by different letters are significantly different at $p < 0.05$.

	Precipitation	Stream	p-value
<i>Coweeta (WS34)</i>			
[NO ₃ ⁻] (mg L ⁻¹)	0.48 ^a (n=10)	0.04 ^b (n=12)	0.0008
δ ¹⁵ N (‰)	-2.7 ^b (n=10)	+0.2 ^a (n=8)	0.0152
δ ¹⁸ O (‰)	+68.1 ^a (n=10)	+4.3 ^b (n=8)	<0.0001
Δ ¹⁷ O (‰)	+23.6 ^a (n=8)	+3.9 ^b (n=6)	<0.0001
<i>Fernow (WS4)</i>			
[NO ₃ ⁻] (mg L ⁻¹)	0.71 ^b (n=12)	1.45 ^a (n=12)	<0.0001
δ ¹⁵ N (‰)	+1.3 (n=11)	+2.3 (n=12)	0.2711
δ ¹⁸ O (‰)	+68.7 ^a (n=11)	-0.8 ^b (n=12)	<0.0001
Δ ¹⁷ O (‰)	+24.8 ^a (n=10)	-0.5 ^b (n=12)	<0.0001
<i>Hubbard Brook (WS3)</i>			
[NO ₃ ⁻] (mg L ⁻¹)	0.60 (n=12)	0.21 (n=12)	0.0718
δ ¹⁵ N (‰)	-2.0 ^b (n=12)	+0.8 ^a (n=11)	0.0017
δ ¹⁸ O (‰)	+72.5 ^a (n=12)	+9.1 ^b (n=11)	<0.0001
Δ ¹⁷ O (‰)	+25.1 ^a (n=10)	+1.1 ^b (n=11)	<0.0001

There were no seasonal differences in precipitation nitrate concentrations between warm season (May-October) and cool season (November-April) periods at any site. Seasonal differences in mean $\delta^{15}\text{N}$ were only significant for precipitation nitrate at Hubbard Brook (-0.5‰ in the cool season versus -3.5‰ in the warm season; $p=0.0056$; Table 7.4). Mean cool season $\delta^{18}\text{O}$ values in precipitation nitrate were higher at all sites, but differences were only statistically significant at Coweeta and Hubbard Brook (Table 7.4). Precipitation nitrate $\Delta^{17}\text{O}$ means were also higher during the cool season at all sites, but only significantly so at Fernow (+29.7‰ in the cool season versus +19.8‰ in the warm season; $p=0.0101$; Table 7.4). In streams, the only significant seasonal difference in mean nitrate concentrations occurred at Hubbard Brook (0.36 mg L^{-1} during the cool season versus 0.05 mg L^{-1} during the warm season; $p=0.0044$; Table 7.4). Significant seasonal differences in mean $\delta^{15}\text{N}$ of stream nitrate were only observed at Coweeta (+3.1‰ in the cool season versus -1.5‰ in the warm season; $p=0.0121$; Table 7.4), and mean stream nitrate $\delta^{18}\text{O}$ values only showed significant season differences at Fernow (-0.3‰ in the cool season versus -1.6‰ in the warm season; $p=0.0291$; Table 7.4). Mean stream nitrate $\Delta^{17}\text{O}$ values were higher at all sites during the cool season, but differences were only statistically significant at Fernow (-0.2‰ in the cool season versus -0.8‰ in the warm season; $p=0.0051$; Table 7.4).

Table 7.4. Mean cool (November-April) and warm (May-October) seasons precipitation and stream nitrate concentrations and isotope values.

Cool and warm season means followed by different letters are significantly different at $p < 0.05$.

	Precipitation		p-value	Stream		p-value
	Cool	Warm		Cool	Warm	
<i>Coweeta (WS34)</i>						
[NO ₃ ⁻] (mg L ⁻¹)	0.7 (n=4)	0.4 (n=6)	0.2710	0.1 (n=6)	0.1 (n=6)	0.9248
δ ¹⁵ N (‰)	-2.2 (n=4)	-3.0 (n=6)	0.4667	+3.1 ^a (n=3)	-1.5 ^b (n=5)	0.0121
δ ¹⁸ O (‰)	+74.5 ^a (n=4)	+63.9 ^b (n=6)	0.0007	+1.5 (n=3)	+6.0 (n=5)	0.2579
Δ ¹⁷ O (‰)	+27.8 (n=2)	+22.3 (n=6)	0.0938	+4.0 (n=3)	+3.9 (n=3)	0.9765
<i>Fernow (WS4)</i>						
[NO ₃ ⁻] (mg L ⁻¹)	0.8 (n=6)	0.6 (n=6)	0.3823	1.6 (n=6)	1.3 (n=6)	0.1359
δ ¹⁵ N (‰)	+2.5 (n=6)	-0.1 (n=5)	0.1208	+1.9 (n=6)	+2.8 (n=6)	0.2935
δ ¹⁸ O (‰)	+76.5 (n=6)	+59.3 (n=5)	0.0681	-0.3 ^a (n=6)	-1.4 ^b (n=6)	0.0291
Δ ¹⁷ O (‰)	+29.7 ^a (n=5)	+19.8 ^b (n=5)	0.0101	-0.2 ^a (n=6)	-0.8 ^b (n=6)	0.0051
<i>Hubbard Brook (WS3)</i>						
[NO ₃ ⁻] (mg L ⁻¹)	0.9 (n=6)	0.3 (n=6)	0.1719	0.4 ^a (n=5)	0.1 ^b (n=5)	0.0044
δ ¹⁵ N (‰)	-0.5a (n=6)	-3.5b (n=6)	0.0056	+0.8 (n=6)	+0.8 (n=5)	0.9865
δ ¹⁸ O (‰)	+77.1 ^a (n=6)	+67.5 ^b (n=6)	0.0431	+6.3 (n=6)	+12.4 (n=5)	0.3291
Δ ¹⁷ O (‰)	+27.5 (n=5)	+22.6 (n=5)	0.3399	+1.7 (n=6)	+0.3 (n=5)	0.3539

7.4 DISCUSSION

7.4.1 Atmospheric Nitrate Processing and Export

The study sites differed markedly in the degree to which atmospheric N deposition inputs were biologically processed prior to export in streams. Using the two-endmember mixing model (Equation 1), where χ is $\Delta^{17}\text{O}$ of nitrate and the nitrification and precipitation endmember values are zero [Michalski *et al.*, 2004] and +34‰ (representing the highest precipitation $\Delta^{17}\text{O}$ value measured at any site during the study period), respectively, we calculated the proportions of atmospheric nitrate in monthly stream samples at all sites. The highest proportions of atmospheric nitrate export occurred at Coweeta (however, nitrate concentrations were too low for $\Delta^{17}\text{O}$ analysis during some months), while the lowest proportions were observed at Fernow throughout the study period. Proportions of atmospheric nitrate in streams ranged from zero to 0.2% at Fernow, zero to 21% at Hubbard Brook, and 4% to 23% at Coweeta (for February through July 2013) (Figure 7.3). These results were unexpected, as consistently low nitrate concentrations in the stream at Coweeta suggest that this watershed is nitrogen-limited and that biological nitrate demand is therefore high. The fact that some proportion of atmospheric nitrate bypassed biological processing in every stream sample at this low N deposition site indicates that demand from biological N sinks (i.e., vegetation and/or soil microbes) is too low to prevent direct export of some atmospherically deposited nitrate. In contrast, nearly complete biological cycling of atmospheric nitrate inputs at Fernow suggests strong demand from biological N sinks at this high N deposition site, even though elevated stream nitrate concentrations indicate that the nitrate retention capacity of these sinks is low.

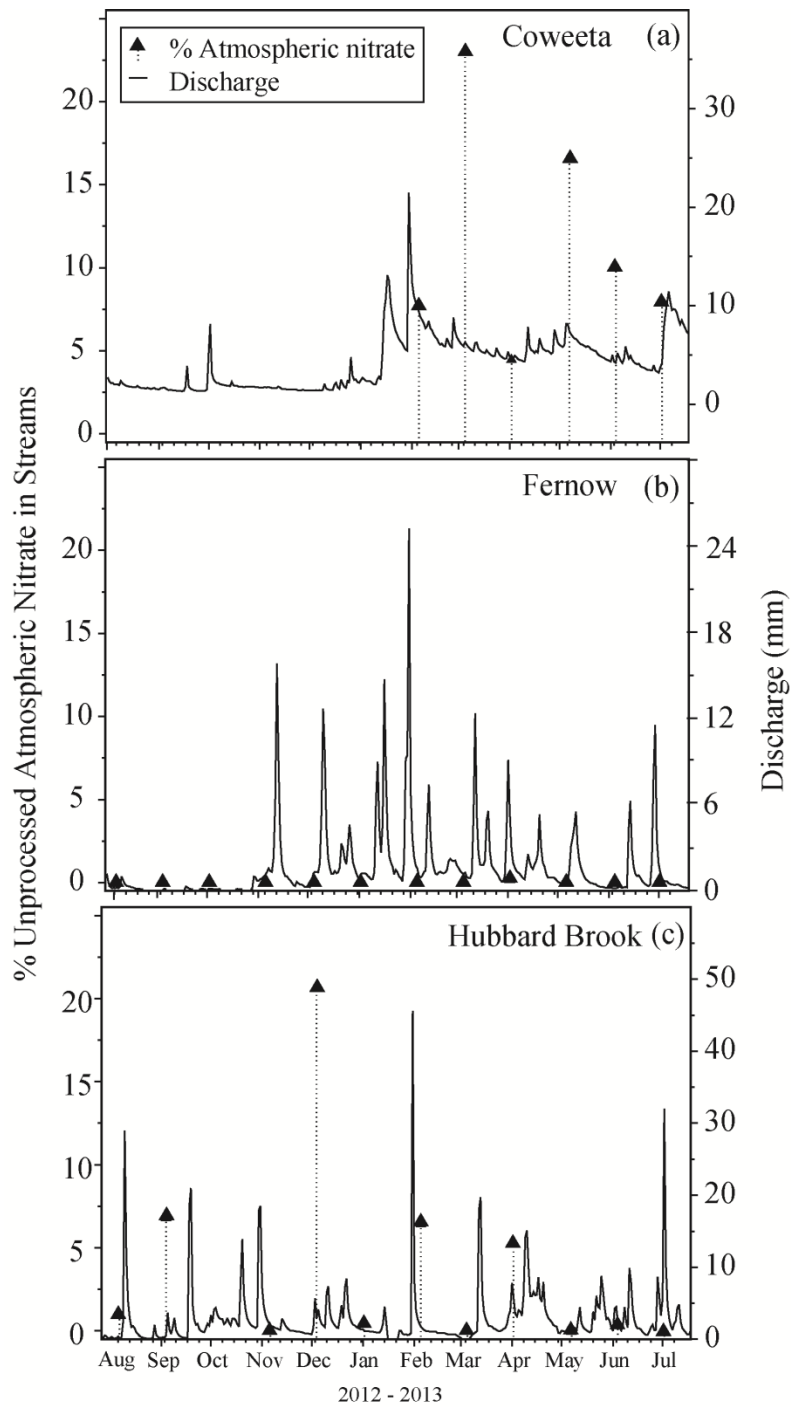


Figure 7.3. Proportions of atmospheric nitrate calculated using observed $\Delta^{17}\text{O}$ values and daily discharge in reference watersheds at (a) Coweeta, (b) Fernow and (c) Hubbard Brook Experimental Forests. Note that discharge axes differ among sites.

The complex relationships demonstrated by the sites in this study with respect to the deposition, biological processing, and retention of nitrate demonstrate the need for a better understanding of the factors driving ecosystem responses to atmospheric N deposition. The balance between ecosystem carbon and nitrogen pools may be one such factor, strongly affecting the extent to which atmospheric N inputs are biologically processed. Previous studies have documented both beneficial and detrimental effects of elevated N deposition on forest carbon pools, with increased ecosystem carbon sequestration attributed to greater N availability in some studies [Magnani *et al.*, 2007; Thomas *et al.*, 2010]. In other studies, elevated stream nitrate export was attributed to decreased heterotrophic bacterial demand for ammonium and increased competition from nitrifying bacteria in low C:N (C:N < 20) soils [Williard *et al.*, 1997; Nave *et al.*, 2009]. Although the mean O horizon C:N ratio in WS4 at Fernow is 23.8 (n=15; [Adams *et al.*, 2006]), high rates of nitrification relative to mineralization (nearly 100%; [Gilliam *et al.*, 2001]) suggest strong competition from nitrifying bacteria for substrate ammonium at this site. Such microbial N cycling dynamics likely contribute to the high proportions of microbial nitrate observed in the stream draining WS4. Similar dynamics may operate in WS3 at Hubbard Brook, where a low mean O horizon C:N ratio (20.8; [Ross *et al.*, 2011]) may have facilitated the large microbial source contributions to stream nitrate (> 93%) observed at this site on all but one sampling date.

In addition to biological demand, physically-based drivers such as watershed geomorphology and hydrologic status may also influence the extent of atmospheric nitrate export from forests. The highest proportions of atmospheric nitrate in streams at Coweeta (23%), Hubbard Brook (21%), and Fernow (0.2%) all occurred on sampling dates coincident with stormflow (Figure 7.3). That peak atmospheric nitrate export occurred during stormflow

conditions at all sites along the N deposition gradient is noteworthy, and suggestive of watershed hydrologic status as an important regulator of atmospheric nitrate export. Substantial contributions of atmospheric nitrate to streams on other dates at Coweeta (ranging from 10-17%) were also coincident with stormflow (Figure 7.3). Other studies have reported elevated atmospheric nitrate export during hydrologic events (particularly snowmelt events) relative to periods of baseflow [Spoelstra et al., 2001; Sebastyen et al., 2008; Goodale et al., 2009; Pellerin et al., 2012]. During lower flows, atmospheric nitrate comprised less than 8% of total stream nitrate in the study watersheds at Coweeta, Fernow, and Hubbard Brook; this is consistent with many previous studies in the eastern U.S. that reported average atmospheric nitrate contributions to streams of less than 10% during baseflow [Williard et al., 2001; Burns and Kendall, 2002; Sebastyen et al., 2008; Goodale et al., 2009; Pellerin et al., 2012]. More frequent sampling or targeted storm event sampling at our study sites would have clarified the relationship between watershed hydrologic status and atmospheric nitrate export and is an important area of future research.

Landscape differences within the study watersheds may also have contributed to the patterns of atmospheric nitrate export we observed. Landscape and soil characteristics that promote rapid water movement through watersheds can lead to greater atmospheric nitrate delivery to streams [Durka et al., 1994]. Helliwell et al. [2007] suggested that rapid hydrologic routing likely outweighs N retention in steep watersheds, whereas greater soil water residence times in watersheds with shallower slopes increase soil N pools and enhance nitrification. The mean slope steepness of WS34 at Coweeta (52%) is more than two times greater than that of WS4 at Fernow (20%) or WS3 at Hubbard Brook (21%). Steep slopes and greater mean annual precipitation at Coweeta (Table 7.1) may have facilitated rapid routing of water and atmospheric

nitrate to the stream in this watershed. By influencing the rate of atmospheric nitrate transport through watersheds, physical attributes such as landscape geomorphology may also limit the opportunity for biological processes to act on atmospheric deposition inputs. It is therefore important to consider how such differences in landform may regulate atmospheric nitrate processing under various hydrologic and N deposition regimes.

7.4.2 Seasonal Patterns of Precipitation Nitrate Isotopes

Mean precipitation nitrate $\delta^{15}\text{N}$, $\delta^{18}\text{O}$, and $\Delta^{17}\text{O}$ values were higher during the cool season than the warm season at all sites (Table 7.4). Other studies have reported similar seasonal patterns in precipitation nitrate isotopes [Durka *et al.*, 1994; Williard *et al.*, 2001; Hastings *et al.*, 2003; Pardo *et al.*, 2004]. While temporal variability in $\delta^{15}\text{N}$ of nitrate has been attributed to variation in nitrate sources [Hastings *et al.*, 2003; Elliott *et al.*, 2007; Yang *et al.*, 2013], seasonality of $\delta^{18}\text{O}$ and $\Delta^{17}\text{O}$ of nitrate is typically explained by variability in the dominant oxidation pathways of atmospheric nitrate [Hastings *et al.*, 2003; Michalski *et al.*, 2003]. Oxidation of NO_x to nitrate via ozone (O_3) is more prevalent during the cool season, whereas oxidation via the hydroxyl (OH) or peroxy radicals ($\text{HO}_2 + \text{RO}_2$) becomes more important during the warmer months [Hastings *et al.*, 2003; Michalski *et al.*, 2003]. Ozone is characterized by both high $\delta^{18}\text{O}$ (+80‰ to +120‰) and $\Delta^{17}\text{O}$ (+30‰ to +50‰) values [Michalski *et al.*, 2013]; these isotopic enrichments are imparted to atmospheric nitrate when NO_x oxidation proceeds via ozone. In contrast, atmospheric nitrate formed via oxidation by hydroxyl or peroxy radicals is characterized by lower $\delta^{18}\text{O}$ and $\Delta^{17}\text{O}$ values, more closely reflecting the oxygen isotopic compositions of tropospheric water vapor, from which the hydroxyl radical derives its oxygen

($\delta^{18}\text{O-OH} = -30\text{‰}$ to $+2\text{‰}$ and $\Delta^{17}\text{O-OH} = 0\text{‰}$; [Hastings *et al.*, 2003]) or atmospheric O_2 , from which peroxy radicals derive their oxygen atoms ($\delta^{18}\text{O-O}_2 = +23.9\text{‰}$; [Fang *et al.*, 2011b]). These differences in the isotopic composition of atmospheric oxidants have been used to infer the importance of each oxidation pathway to seasonal atmospheric nitrate formation dynamics [Hastings *et al.*, 2003; Michalski *et al.*, 2003]. That the temporal patterns in $\delta^{18}\text{O}$ and $\Delta^{17}\text{O}$ values of precipitation nitrate were similar at all sites suggest that a common factor— such as seasonal variation in atmospheric oxidation chemistry— influenced precipitation nitrate isotope dynamics.

In three of the months during the study, precipitation samples collected at Hubbard Brook and Fernow did not follow this seasonal trend in $\Delta^{17}\text{O}$ values (Figure 7.2). Indeed, the range of $\Delta^{17}\text{O}$ values in these samples ($+11.1\text{‰}$ to $+14.8\text{‰}$) was well outside the range generally reported for atmospheric nitrate ($+20\text{‰}$ to $+33\text{‰}$; [Michalski *et al.*, 2003; Morin *et al.*, 2009]), suggesting that some other factor may have influenced the isotopic composition of these precipitation samples. Using an isotope mass balance model (ISO-RACM), [Michalski and Xu, 2010] predicted atmospheric $\Delta^{17}\text{O}$ of nitrate values resulting from various NO_x oxidation pathways. According to their model, $\Delta^{17}\text{O}$ values below $+15\text{‰}$ occurred under atmospheric conditions of low ozone and high biogenic VOC mixing ratios; however the authors suggested that such conditions were unlikely to be observed in the troposphere [Michalski and Xu, 2010]. At two of the study sites (Fernow and Hubbard Brook) we observed $\Delta^{17}\text{O}$ of nitrate values less than $+15\text{‰}$; these low values occurred during the growing season, when emission of biogenic VOCs would have been possible at these densely-forested sites. Yang *et al.* [2013] attributed very low $\delta^{18}\text{O}$ values of atmospheric nitrate ($\sim +17\text{‰}$) in the South China Sea to oxidation of NO to NO_2 by peroxy radicals, which derive their oxygen atoms from atmospheric O_2 and are therefore

expected to have much lower $\delta^{18}\text{O}$ values than those of ozone [Fang *et al.*, 2011b]. Oxidation pathways not proceeding via ozone would also be expected to yield low $\Delta^{17}\text{O}$ values of atmospheric nitrate, and may explain the periodically low values observed at Hubbard Brook at Fernow. In addition, Rose and Elliott [manuscript in preparation; see also Chapter 5] suggested that $\Delta^{17}\text{O}$ values as low as +11.2‰ in precipitation nitrate observed during storms at Fernow may have resulted from rapid oxidation and re-deposition as nitrate of biogenic NO_x emitted during soil wet-up (biogenic NO_x should have a $\Delta^{17}\text{O}$ value of zero, as it is formed by mass-dependent fractionating processes). While we did not measure biogenic NO_x emissions or ozone and VOC mixing ratios during this study, future research focusing on these atmospheric dynamics would provide critical insights into the sources and processes driving atmospheric nitrate formation and deposition in these forested systems.

7.5 CONCLUSION

The results presented here demonstrate the complexities of atmospheric nitrate processing and export in forested systems and provide new insights into ecosystem nitrogen saturation dynamics. In the low N deposition watershed at Coweeta, consistently low stream nitrate concentrations imply that N supply and biological demand are well-balanced, while consistently high stream nitrate concentrations in the high N deposition watershed at Fernow (which are 36 times higher than those at Coweeta, on average) suggest that N supply exceeds biological demand. However, the relationship between atmospheric nitrate supply and biological demand as indicated by stream nitrate stable isotopes is in contrast with these concentration-based

assessments. Rather than a balance between nitrate inputs and outputs, stream nitrate stable isotopes at Coweeta point to incomplete biological assimilation of atmospheric nitrate inputs, whereas isotope-based source apportionment of stream nitrate at Fernow indicates that atmospheric nitrate inputs are extensively biologically cycled prior to export. That the extents of atmospheric nitrate processing and export differ both within sites as well as among sites located along the nitrate deposition gradient in this study indicates that conceptual models of nitrogen saturation should consider not only the balance between N supply and biological demand [*Aber et al.*, 1989, 1998] but also the capacity of ecosystems to retain N added via atmospheric deposition [*Lovett and Goodale*, 2011].

8.0 CONCLUSIONS

This dissertation has presented research examining the fate and transport of atmospheric nitrate deposition in forested watersheds of the Appalachian Mountain Range. Based on triple nitrate isotope analysis of natural waters, the novel results of this work enhance our understanding of the effects of nitrate inputs resulting from anthropogenic activities on terrestrial and aquatic systems.

Chapter 2 explored the roles of hydrological, geomorphological, and biogeochemical processes in the cycling and export of atmospheric nitrate in watersheds. These physical drivers are often under-appreciated in watershed-scale studies of N biogeochemistry, but can serve as important regulators of nitrate export in general and atmospheric nitrate export in particular.

In Chapter 3, we showed that, despite differences in mean stream nitrate concentrations, export of unprocessed atmospheric nitrate was low in three hardwood-dominated watersheds at Fernow Experimental Forest and high in a conifer-dominated stand with persistently low stream nitrate concentrations. Unprocessed atmospheric nitrate comprised less than 15% of nitrate export in weekly stream samples from the hardwood-dominated watersheds, based on $\Delta^{17}\text{O}$ of nitrate measurements. In contrast, high $\Delta^{17}\text{O}$ values in the N-limited conifer stand indicated 32% to 72% contributions of atmospheric nitrate to the stream. These results demonstrate extensive atmospheric nitrate cycling in the hardwood watersheds regardless of N saturation stage, whereas

the conifer stand exported high proportions of unprocessed atmospheric nitrate despite near-zero stream nitrate concentrations. However, elevated export of atmospheric nitrate in all study watersheds during a snowmelt event suggests that hydrologic events may facilitate periodic direct routing of atmospheric nitrate to streams.

In Chapter 4, we examined spatial and temporal heterogeneity of soil water nitrate concentrations and sources across WS4 at Fernow Experimental Forest. Low soil water nitrate concentrations on the south-facing aspect were associated with high proportions of atmospheric nitrate, whereas high soil water nitrate concentrations on the east-facing portion of the watershed were largely attributable to microbial nitrification. While nitrate source dynamics were highly variable at the intra-watershed scale, characterization of stream nitrate sources at the watershed outlet identified microbial nitrification as the dominant source of nitrate exported from the watershed. This disparity between nitrate source dynamics at the intra- and whole-watershed scales has implications for the determination of nitrogen saturation status and the factors that influence nitrate transport from landscapes to streams, such as hydrologic regime and watershed geomorphology.

The research presented in Chapter 5 represents the first characterization of intra-event precipitation nitrate isotope dynamics using triple nitrate isotopes ($\delta^{15}\text{N}$, $\delta^{18}\text{O}$, and $\Delta^{17}\text{O}$). We examined the intra-storm variability of precipitation nitrate stable isotopic composition during six growing season storms sampled during 2010 at Fernow Experimental Forest. We reported highly variable $\delta^{15}\text{N}$, $\delta^{18}\text{O}$, and $\Delta^{17}\text{O}$ values in precipitation over short time periods (~hourly) and explored possible explanations for this isotopic variability. During one event, $\delta^{15}\text{N}$ and $\delta^{18}\text{O}$ of nitrate increased by 16‰ and 11‰, respectively, over two hours. On two other dates, $\Delta^{17}\text{O}$ of nitrate values varied by more than 9‰ in one hour. Several factors may contribute to this intra-

storm isotopic variability, including temporal variation in atmospheric NO_x production from multiple sources, variability in NO_x oxidation pathways during atmospheric nitrate formation, and rainout/washout processes. Pulses of biogenic NO_x emitted at the study site may be an important and overlooked NO_x source, particularly during events with drier antecedent moisture conditions. This suggests that a portion of wet nitrate deposition may come from intra-site recycling rather than external sources.

Chapter 6 examined high-temporal resolution dynamics of stream nitrate export during three of the storms presented in Chapter 5. Whereas atmospheric nitrate contributions to stormflow were less than 12% during the three storms, mean event water contributions to stormflow ranged from 6 to 34%, suggesting that fast routing of precipitation inputs to the stream may have occurred periodically during some events. Trends in $\delta^{18}\text{O}$ of water in stormflow during the largest event on 30 September support the establishment of a transient hydrologic connection between hillslopes and the stream. These differences in atmospheric and terrestrial water and nitrate source contributions to stormflow demonstrate that while microbial nitrification is the most important source of stream nitrate in WS4, rapid movement of event water through watershed areas can be an important regulator of nitrate export during storms.

Chapter 7 expanded the examination of atmospheric nitrate transport and fate from the single-site level to a larger geographic context, spanning a ~1700 km nitrate deposition gradient along the Appalachian Mountain Range. The results of this work showed that concentration- and isotope-based assessments of ecosystem N saturation status may often conflict with one another. Seasonal trends and mean values of precipitation nitrate $\delta^{15}\text{N}$, $\delta^{18}\text{O}$, and $\Delta^{17}\text{O}$ were generally similar among the sites. In contrast, the concentrations, $\delta^{18}\text{O}$, and $\Delta^{17}\text{O}$ values of stream nitrate differed significantly among the sites. Despite having the highest long-term annual average rate

of atmospheric nitrate deposition and mean stream nitrate concentration during the study period, the watershed at Fernow consistently exported the lowest proportions of atmospheric nitrate in streamflow. In contrast, the study watershed at Coweeta had the lowest long-term annual average rate of atmospheric nitrate deposition and mean stream nitrate concentration during the study period, but exported the highest proportions of atmospheric nitrate. The relationship between atmospheric nitrate supply and biological demand as indicated by stream nitrate stable isotopes is therefore in contrast with concentration-based assessments. These results demonstrate the complexities of atmospheric nitrate processing and export from forested systems and provide new insights into ecosystem N saturation dynamics.

The results of this work demonstrate the dynamic nature of forested systems with respect to the processing and retention of atmospheric N additions. We have shown that, while the capacity of natural systems to biologically cycle allochthonous nitrate can be quite large, their capacity to retain those inputs is more limited. These new insights have important implications for our understanding of anthropogenic effects on natural systems in N-polluted regions and for the mitigation of elevated nitrate export to surface waters.

APPENDIX A

DATA TABLE FOR WEEKLY STREAM AND PRECIPITATION SAMPLES

Table A-1 Nitrate concentration, nitrate isotope, and water isotope data for weekly stream and precipitation samples

Data for Watersheds 4, 5, 6, and 7 refer to stream samples; data for NADP precipitation refer to precipitation samples collected at Fernow for the National Atmospheric Deposition Program. Entries with no data indicate nitrate concentrations below the instrument detection limit or insufficient sample volume for isotope analysis.

Watershed	Year	Month	Day	[NO ₃ ⁻] (mg L ⁻¹)	δ ¹⁵ N- NO ₃ ⁻ (‰)	δ ¹⁸ O- NO ₃ ⁻ (‰)	Δ ¹⁷ O- NO ₃ ⁻ (‰)	δ ² H- H ₂ O (‰)	δ ¹⁸ O- H ₂ O (‰)
4	2010	1	5	2.1	2.0	2.5	0.6	-61.1	-9.3
4	2010	1	12	3.5	2.0	3.5	0.6	-58.1	-9.6
4	2010	1	19	2.5	1.9	3.8	1.1	-65.7	-10.1
4	2010	1	26	2.6	1.8	3.0	0.5	-65.7	-10.5
4	2010	2	2	2.1	1.8	-2.3	0.5	-59.5	-9.9
4	2010	2	9	2.0	1.7	-3.4	0.3	-64.7	-9.9
4	2010	2	16	2.0	1.8	2.2	0.8	-64.3	-10.0

Watershed	Year	Month	Day	[NO ₃ ⁻] (mg L ⁻¹)	δ ¹⁵ N- NO ₃ ⁻ (‰)	δ ¹⁸ O- NO ₃ ⁻ (‰)	Δ ¹⁷ O- NO ₃ ⁻ (‰)	δ ² H- H ₂ O (‰)	δ ¹⁸ O- H ₂ O (‰)
4	2010	2	23	2.1	1.6	6.1	3.2	-66.8	-10.7
4	2010	3	2	2.0	1.8	-1.3	0.7	-64.2	-10.6
4	2010	3	9	1.8	1.9	1.3	1.6	-63.8	-10.3
4	2010	3	16	2.2	1.8	1.7	2.1	-80.5	-12.3
4	2010	3	23	2.0	1.9	-0.2	1.4	-75.0	-11.4
4	2010	3	30	1.9	1.8	-0.3	1.1	-74.8	-11.5
4	2010	4	6	1.8	1.8	-2.1	0.7	-72.6	-11.0
4	2010	4	13	1.8	2.2	-2.8	0.4	-66.7	-11.0
4	2010	4	20	1.6	2.1	-2.8	1.0	-69.2	-11.0
4	2010	4	27	1.5	2.5	-2.3	0.4	-69.3	-10.9
4	2010	5	4	1.8	2.6	-1.1	0.3	-73.3	-11.4
4	2010	5	11	1.5	2.5	-3.2	0.5	-71.6	-10.9
4	2010	5	18	1.4	2.7	-2.9	0.2	-66.3	-10.7
4	2010	5	24	1.4	2.4	-3.1	0.3	-70.2	-11.0
4	2010	6	1	1.3	2.7	-2.1	0.6	-70.3	-10.7
4	2010	6	8	1.5	2.4	-2.6	0.2	-69.1	-11.0
4	2010	6	15	1.4	2.3	-3.8	-0.5	-70.8	-11.2
4	2010	6	22	1.4	2.5	-7.1	-0.8	-68.7	-10.8
4	2010	6	29	1.3	3.6	-7.4	-1.0	-67.2	-9.8
4	2010	7	6	1.4	4.3	-7.9	-1.2	-66.3	-10.3
4	2010	11	30	1.9	2.8	-3.1	-0.3	-66.0	-10.3
4	2010	12	6	2.3			-0.2	-68.8	-11.0
4	2010	12	13	2.0	2.5	-0.7	0.5	-72.7	-10.9
4	2010	12	21	2.0	2.3	-3.2	-0.3	-68.3	-10.9
4	2010	12	28	1.9	1.5	-4.5	0.0	-70.9	-9.8
5	2010	1	5	1.1	1.7	2.1		-61.0	-9.2
5	2010	1	12	1.2	1.5	1.1	0.4	-57.2	-9.4
5	2010	1	19	1.2	1.9	3.8	0.4	-66.0	-9.9
5	2010	1	26	1.2	1.6	2.3	0.6	-68.4	-10.2
5	2010	2	2	1.1	1.3	0.8		-59.8	-9.5

Watershed	Year	Month	Day	[NO ₃ ⁻] (mg L ⁻¹)	δ ¹⁵ N- NO ₃ ⁻ (‰)	δ ¹⁸ O- NO ₃ ⁻ (‰)	Δ ¹⁷ O- NO ₃ ⁻ (‰)	δ ² H- H ₂ O (‰)	δ ¹⁸ O- H ₂ O (‰)
5	2010	2	9	1.2	1.2	0.2	-0.1	-61.4	-10.1
5	2010	2	16	1.2	1.0	0.8	1.0	-63.1	-10.1
5	2010	2	23	1.4	1.5	13.4	5.6	-70.1	-10.9
5	2010	3	2	1.1	1.6	-2.3	0.8	-61.8	-10.1
5	2010	3	9	1.2	1.8	0.8	1.3	-64.1	-10.1
5	2010	3	16	1.0	1.6	2.7	2.6	-79.2	-12.4
5	2010	3	23	0.9	1.6	-0.9	0.7	-74.5	-11.7
5	2010	3	30	0.9	1.5	-1.7	0.6	-77.9	-11.6
5	2010	4	6	0.9	1.2	-4.1	0.3	-70.3	-10.7
5	2010	4	13	0.9	2.1	-4.0	-0.1	-72.3	-11.0
5	2010	4	20	0.8	2.3	-3.9	0.1	-79.9	-10.2
5	2010	4	27	0.9	2.5	-3.4	0.3	-73.1	-10.7
5	2010	5	4	0.9	2.6	-2.3	0.2	-82.8	-11.0
5	2010	5	11	0.8	1.8	-6.0	-0.1	-73.2	-10.3
5	2010	5	18	0.8	1.9	-4.9	-0.3	-71.9	-10.3
5	2010	5	24	0.7	2.5	-4.4	-0.4	-75.6	-10.9
5	2010	6	1	0.6	2.2	-3.6	0.9	-68.0	-10.0
5	2010	6	8	0.9	2.6	-2.0	-0.3	-73.3	-10.5
5	2010	6	15	0.8	2.2	-5.2	-0.8	-72.1	-10.7
5	2010	6	22	0.9	2.6	-7.6	-0.9	-68.1	-10.3
5	2010	6	29	0.7	3.2	-7.1	-0.8	-64.5	-9.4
5	2010	7	6	0.8	3.3	-9.4	-0.9	-66.4	-10.0
5	2010	8	24	0.9	5.0	-4.7	-0.7	-55.5	-8.2
5	2010	9	28	1.4	4.5	-4.7	-1.2	-53.5	-8.1
5	2010	10	5	0.9	4.1	-4.8	-1.0	-66.0	-9.4
5	2010	11	9	1.0	2.8	-4.6	-0.6	-70.7	-10.4
5	2010	11	16	0.7	2.8	-4.8	-0.6	-70.9	-10.4
5	2010	11	23	0.8	2.7	-4.7	-0.6	-69.2	-10.6
5	2010	11	30	1.0	2.5	-3.5	-0.1	-69.0	-9.9
5	2010	12	6	1.1	2.0	-2.8	-0.2	-73.3	-10.8

Watershed	Year	Month	Day	[NO ₃] (mg L ⁻¹)	δ ¹⁵ N- NO ₃ ⁻ (‰)	δ ¹⁸ O- NO ₃ ⁻ (‰)	Δ ¹⁷ O- NO ₃ ⁻ (‰)	δ ² H- H ₂ O (‰)	δ ¹⁸ O- H ₂ O (‰)
5	2010	12	13	1.2	2.2	-1.1	1.1	-76.0	-10.8
5	2010	12	21	1.1	1.8	-4.5	-0.1	-68.2	-10.7
5	2010	12	28	1.1	1.7	-4.8	0.0	-69.4	-10.9
6	2010	1	5	0.0	-1.1	49.6		-57.2	-8.3
6	2010	1	12	0.0	2.6	50.1		-51.7	-8.3
6	2010	1	19	0.0				-57.4	-8.7
6	2010	1	26	0.0				-61.8	-9.1
6	2010	2	2					-56.5	-8.7
6	2010	2	9	0.0	-1.6	40.9		-56.7	-8.8
6	2010	2	16	0.0	2.6	45.1		-58.5	-8.8
6	2010	2	23	0.1	3.8	72.8	23.9	-59.9	-9.1
6	2010	3	2	0.0	0.5	49.2		-50.6	-9.0
6	2010	3	9	0.0	-2.1	42.5		-56.8	-8.8
6	2010	3	16					-63.6	-9.9
6	2010	3	23	0.0				-64.2	-10.1
6	2010	3	30					-65.8	-9.9
6	2010	4	6	0.0				-61.0	-9.5
6	2010	4	13	0.0	-0.8	38.0		-58.8	-9.2
6	2010	4	20	0.0				-55.2	-9.1
6	2010	4	27	0.0				-58.4	-9.1
6	2010	5	4	0.0				-56.4	-8.9
6	2010	5	18	0.0	0.9	25.7		-57.1	-8.2
6	2010	5	24	0.0	2.9	26.8		-58.2	-9.0
6	2010	6	1	0.1			6.6	-54.9	-8.9
6	2010	6	8	0.0				-55.1	-9.0
6	2010	6	15	0.0	1.7	27.5		-61.8	-9.1
6	2010	6	22	0.0			1.7	-63.0	-9.4
6	2010	6	29	0.1	-2.9	-5.3	1.4	-53.0	-8.6
6	2010	11	30	0.0				-63.2	-9.0
6	2010	12	6					-61.7	-9.7

Watershed	Year	Month	Day	[NO ₃] (mg L ⁻¹)	δ ¹⁵ N- NO ₃ ⁻ (‰)	δ ¹⁸ O- NO ₃ ⁻ (‰)	Δ ¹⁷ O- NO ₃ ⁻ (‰)	δ ² H- H ₂ O (‰)	δ ¹⁸ O- H ₂ O (‰)
6	2010	12	13					-63.0	-10.0
6	2010	12	21	0.0				-60.1	-9.6
7	2010	1	5	4.2	2.1	1.5	-0.9	-61.2	-9.6
7	2010	1	12	4.4	2.2	1.5	0.2	-62.3	-9.6
7	2010	1	19	3.8	2.1	2.2	0.0	-64.8	-9.7
7	2010	1	26	4.2	2.1	2.0	0.1	-62.2	-9.9
7	2010	2	2	4.2	2.3	-3.3	0.0	-64.1	-9.7
7	2010	2	9	4.4	2.2	1.4	-0.1	-62.8	-9.9
7	2010	2	16	4.1	1.8	-1.1	0.0	-61.1	-10.0
7	2010	2	23	4.1	2.0	4.0	3.0	-71.6	-10.8
7	2010	3	2	5.0	2.3	-1.8	0.4	-64.3	-10.0
7	2010	3	9	3.4	2.2	-1.1	0.4	-76.9	-10.3
7	2010	3	16	3.7	2.0	-0.9	0.7	-73.7	-11.5
7	2010	3	23	4.3	2.0	-1.9	0.5	-73.8	-11.1
7	2010	3	30	3.9	2.0	-1.9	0.0	-74.3	-11.0
7	2010	4	6	3.9	2.5	-3.0	0.1	-70.2	-10.7
7	2010	4	13	3.9	1.6	-5.4	0.3	-66.8	-10.4
7	2010	4	20	3.4	2.5	-3.6	0.3	-70.3	-10.6
7	2010	4	27	3.2	2.7	-3.0	0.0	-68.1	-10.7
7	2010	5	4	2.9	2.9	-2.4	-0.1	-70.8	-10.8
7	2010	5	11	3.4	3.0	-3.1	0.0	-66.3	-10.2
7	2010	5	18	3.1	2.9	-3.5	-1.0	-64.4	-10.5
7	2010	5	24	3.1	2.7	-3.2	0.1	-75.4	-10.6
7	2010	6	1	2.7	2.7	-3.4	-0.1	-66.2	-10.2
7	2010	6	8	2.9	2.8	-3.2	-0.2	-67.7	-10.6
7	2010	6	15	3.0	2.4	-4.5	-0.7	-73.3	-10.5
7	2010	6	22	3.0	3.5	-6.2	-0.8	-69.4	-10.4
7	2010	6	29	3.2	4.4	-5.4	-1.0	-63.1	-9.8
7	2010	7	6	3.7	4.0	-7.5	-1.4	-64.1	-9.6
7	2010	7	13	3.9	5.2	-6.1	-1.0	-62.0	-9.7

Watershed	Year	Month	Day	[NO ₃ ⁻] (mg L ⁻¹)	δ ¹⁵ N- NO ₃ ⁻ (‰)	δ ¹⁸ O- NO ₃ ⁻ (‰)	Δ ¹⁷ O- NO ₃ ⁻ (‰)	δ ² H- H ₂ O (‰)	δ ¹⁸ O- H ₂ O (‰)
7	2010	7	20	3.8	5.4	-5.8	-1.2	-60.1	-9.4
7	2010	7	27	4.0	5.4	-6.4	-1.3	342.9	-8.9
7	2010	8	24	4.2	5.9	-4.3		-57.4	-8.6
7	2010	9	28	8.4			-1.2	-61.0	-8.6
7	2010	10	5	3.3	4.0	-5.2	-0.9	-69.8	-10.3
7	2010	11	9	3.0	3.4	-4.6	-0.5	-69.4	-10.1
7	2010	11	16	2.5	3.6	-4.2	-0.6	-66.0	-9.7
7	2010	11	23	3.1	3.3	-4.4	-0.8	-71.1	-10.3
7	2010	11	30	3.4	2.8	-4.0	-0.5	-66.9	-10.0
7	2010	12	6	3.9	2.5	-3.6	-0.6	-67.4	-10.5
7	2010	12	13	3.0	2.5	-2.5	-0.3	-72.7	-11.0
7	2010	12	21	3.8	2.5	-3.7	-0.7	-77.5	-10.5
7	2010	12	28	3.7	2.7	-3.8	-0.8	-67.6	-10.6
NADP	2010	2	9	0.3	0.3	81.7			
precipitation									
NADP	2010	2	16	1.2	-0.9	71.3			
precipitation									
NADP	2010	3	2	3.0	1.5	70.4	27.7		
precipitation									
NADP	2010	3	16	1.4	4.6	55.9	16.5		
precipitation									
NADP	2010	3	23	0.1	1.7	62.8	24.5		
precipitation									
NADP	2010	3	30	0.8	-0.4	67.9	23.6		
precipitation									
NADP	2010	4	13	0.7	0.9	67.4	25.5		
precipitation									
NADP	2010	4	20	1.1	-2.1	71.2	26.3		
precipitation									
NADP	2010	4	27	1.3	-1.8	73.9	23.9		
precipitation									

Watershed	Year	Month	Day	[NO₃⁻] (mg L⁻¹)	δ¹⁵N- NO₃⁻ (‰)	δ¹⁸O- NO₃⁻ (‰)	Δ¹⁷O- NO₃⁻ (‰)	δ²H- H₂O (‰)	δ¹⁸O- H₂O (‰)
NADP precipitation	2010	5	4	0.3	-1.4	60.4			
NADP precipitation	2010	5	11	0.6	-6.0	61.4	18.7		
NADP precipitation	2010	5	18	0.7	2.1	65.8	23.2		
NADP precipitation	2010	5	25	0.6	0.3	68.3	19.1		
NADP precipitation	2010	6	1	0.8	-0.1	53.9	13.8		
NADP precipitation	2010	6	8	0.7	-3.7	64.1	21.5		
NADP precipitation	2010	6	15	1.2	-2.9	65.2	21.7		
NADP precipitation	2010	6	22	0.6	-2.1	64.6	18.8		
NADP precipitation	2010	6	29	1.3	-1.4	65.3	19.6		
NADP precipitation	2010	7	13	0.3	2.0	65.8			
NADP precipitation	2010	7	20	0.5	0.6	65.1	18.6		
NADP precipitation	2010	7	27	0.4	-0.9	64.0	19.3		
NADP precipitation	2010	8	3	0.9	1.1	67.8	19.8		
NADP precipitation	2010	8	10	1.0	-0.7	50.0	12.8		
NADP precipitation	2010	8	24	0.7	0.8	64.7	22.3		
NADP precipitation	2010	9	14	0.9	-1.8	68.0	21.9		

Watershed	Year	Month	Day	[NO₃⁻] (mg L⁻¹)	δ¹⁵N- NO₃⁻ (‰)	δ¹⁸O- NO₃⁻ (‰)	Δ¹⁷O- NO₃⁻ (‰)	δ²H- H₂O (‰)	δ¹⁸O- H₂O (‰)
NADP precipitation	2010	9	21	0.4	-2.4	64.9	21.6		
NADP precipitation	2010	9	28	0.4	-0.7	43.0	15.6		
NADP precipitation	2010	10	5	0.5	2.6	51.1	18.1		
NADP precipitation	2010	10	12	0.9	4.7	61.5	22.6		
NADP precipitation	2010	10	19	1.6	-1.1	53.6	19.1		
NADP precipitation	2010	11	2	0.3	2.6	66.3	21.3		
NADP precipitation	2010	11	9	0.4	3.8	60.6	20.8		
NADP precipitation	2010	11	16	1.2	-1.8	63.6	23.8		
NADP precipitation	2010	11	23	0.6	1.3	40.3	13.2		
NADP precipitation	2010	11	30	0.3	2.1	77.3	28.6		
NADP precipitation	2010	12	7	0.2	5.1	52.5	12.3		
NADP precipitation	2010	12	14	0.4	-0.5	70.5	29.1		
NADP precipitation	2010	12	21	0.3	0.4	71.1	24.5		
NADP precipitation	2011	1	11	2.9	4.9	78.1	29.4		
NADP precipitation	2011	1	18	1.6	0.9	82.2	29.4		
NADP precipitation	2011	1	25	1.8	2.4	69.7	22.5		

Watershed	Year	Month	Day	[NO₃⁻] (mg L⁻¹)	δ¹⁵N- NO₃⁻ (‰)	δ¹⁸O- NO₃⁻ (‰)	Δ¹⁷O- NO₃⁻ (‰)	δ²H- H₂O (‰)	δ¹⁸O- H₂O (‰)
NADP precipitation	2011	2	1	1.1	2.3	80.1	31.3		
NADP precipitation	2011	2	8	0.5	1.9	78.4	28.6		

APPENDIX B

DATA TABLE FOR MONTHLY LYSIMETER SAMPLES

Table B-1 Nitrate concentration, nitrate isotope, and water isotope data for monthly soil solution samples

Data refer to monthly soil solution samples collected from zero-tension lysimeter throughout Fernow Watershed 4. Entries with no data indicate nitrate concentrations below the instrument detection limit, missing sample, or insufficient sample volume for isotope analysis.

Year	Month	Day	Lysimeter Number	Soil Horizon	[NO ₃ ⁻] (mg L ⁻¹)	δ ¹⁵ N- NO ₃ ⁻ (‰)	δ ¹⁸ O- NO ₃ ⁻ (‰)	Δ ¹⁷ O- NO ₃ ⁻ (‰)	δ ² H- H ₂ O (‰)	δ ¹⁸ O- H ₂ O (‰)
2010	1	21	3	A	0.3	3.8	65.1	20.4		
2010	1	21	7	A	2.2	4.6	77.7	31.6		
2010	1	21	8	A	0.2	5.0	79.7			
2010	1	21	9	A	3.0	-2.6	5.8	3.4		
2010	1	21	10	A	0.0					
2010	1	21	13	A	4.2	1.8	-0.5	-0.1		
2010	1	21	14	A	2.0	3.4	48.0	19.7		
2010	1	21	3	B	0.3	3.2	63.4	20.4		

Year	Month	Day	Lysimeter Number	Soil Horizon	[NO ₃ ⁻] (mg L ⁻¹)	δ ¹⁵ N- NO ₃ ⁻ (‰)	δ ¹⁸ O- NO ₃ ⁻ (‰)	Δ ¹⁷ O- NO ₃ ⁻ (‰)	δ ² H- H ₂ O (‰)	δ ¹⁸ O- H ₂ O (‰)
2010	1	21	6	B	0.0					
2010	1	21	10	B	0.0					
2010	1	21	11	B	0.1					
2010	1	21	13	B	4.3	2.0	-0.2	-0.6		
2010	1	21	6	C	0.0					
2010	1	21	9	C	0.3	2.9	5.2	0.6		
2010	1	21	12	C	0.3	1.4	9.4	5.3		
2010	1	21	15	C	2.0	2.5	3.0	1.1		
2010	3	17	1	A	3.3	1.1	22.3		-122.7	-17.7
2010	3	17	2	A	1.5	0.7	-2.8	0.0	-95.0	-14.0
2010	3	17	4	A	0.2	6.0	76.4	28.0		
2010	3	17	7	A	0.6	4.3	76.5	23.6	-134.5	-19.3
2010	3	17	9	A	1.8	1.0	5.9	4.2	-101.7	-15.1
2010	3	17	10	A	0.3	0.7	21.1	7.9	-91.6	-14.2
2010	3	17	11	A	1.0	-0.2	5.4	5.0	-112.3	-16.9
2010	3	17	12	A	3.0	1.0	3.9	3.2	-106.8	-16.0
2010	3	17	13	A	11.4	0.2	-0.6	0.5	-110.9	-15.4
2010	3	17	14	A	1.7	2.7	41.4	17.4	-114.4	-17.0
2010	3	17	1	B	0.7	1.7	-1.9	-0.6	-69.6	-10.9
2010	3	17	2	B	1.0	1.7	4.5	0.6	-64.7	-10.3
2010	3	17	3	B	1.4	0.4	17.2		-103.9	-15.4
2010	3	17	7	B	0.2	4.3	75.3	18.1	-124.3	-17.7
2010	3	17	8	B					-73.9	-10.8
2010	3	17	9	B	0.2	-1.7	0.3	-0.2	-70.0	-11.0
2010	3	17	10	B	0.0				-88.6	-13.2
2010	3	17	11	B	0.0				-90.6	-12.4
2010	3	17	12	B	0.2	3.1	2.8	1.0	-53.9	-8.9
2010	3	17	13	B	12.4	0.1	-0.6	1.3	-110.5	-16.5
2010	3	17	5	C					-74.7	-11.6
2010	3	17	7	C					-55.6	-9.0

Year	Month	Day	Lysimeter Number	Soil Horizon	[NO ₃ ⁻] (mg L ⁻¹)	δ ¹⁵ N- NO ₃ ⁻ (‰)	δ ¹⁸ O- NO ₃ ⁻ (‰)	Δ ¹⁷ O- NO ₃ ⁻ (‰)	δ ² H- H ₂ O (‰)	δ ¹⁸ O- H ₂ O (‰)
2010	3	17	9	C	0.6	3.0	4.6	1.2	-69.5	-11.2
2010	3	17	10	C	0.3	0.0	2.6	1.8	-83.8	-11.8
2010	3	17	12	C	0.4	0.7	5.4	2.2	-70.2	-11.0
2010	3	17	15	C	3.0	1.8	6.5	3.1	-93.8	-14.0
2010	4	26	11	A	1.0	0.6	11.7	5.8	-120.9	-17.4
2010	4	26	5	C					-88.3	-13.4
2010	4	26	9	C	0.6	2.7	7.9	2.7	-99.9	-14.7
2010	4	26	12	C	0.3	0.8	5.4	1.9	-77.9	-12.1
2010	4	26	15	C	2.5	2.0	7.0	3.2	-87.6	-13.5
2010	7	30	3	A	0.2	2.5	63.4	16.4	-33.7	-6.1
2010	9	17	1	A	2.8	-0.6	10.5	2.0	-30.1	-6.8
2010	9	17	2	A	3.5	-1.7	10.0	1.0	-27.6	-6.3
2010	9	17	3	A	0.4	-0.4	48.3	14.2	-25.0	-5.8
2010	9	17	8	A	0.3	0.8	61.6	17.7		
2010	9	17	9	A	3.4	-6.9	3.4	0.7	-29.1	-6.3
2010	9	17	10	A	0.9	-4.0	22.1	5.8	-29.6	-6.4
2010	9	17	11	A	0.5	-1.9	38.4	11.9		
2010	9	17	15	A	0.3	0.6	22.6	6.0	-27.5	-6.1
2010	9	17	12	C	2.2	0.2	7.3	0.9		
2010	10	01	1	A	1.1	1.9	3.4	-0.8	-86.1	-12.0
2010	10	01	2	A	1.0	-1.1	3.2	-1.0		
2010	10	01	3	A	0.1				-128.8	-17.7
2010	10	01	5	A	0.1					
2010	10	01	7	A	0.0				-111.4	-15.9
2010	10	01	8	A	0.2			0.5	-137.0	-19.0
2010	10	01	9	A	1.5	1.6	0.9	-0.6	-92.5	-13.3
2010	10	01	10	A	0.2	-0.4	9.3	1.5	-69.1	-10.4
2010	10	01	11	A					-120.8	-17.1
2010	10	01	14	A	0.3	3.1	4.8	0.1	-102.5	-14.4
2011	2	14	1	A	2.87	1.9	15.2	7.7	-79.9	-12.3

Year	Month	Day	Lysimeter Number	Soil Horizon	[NO ₃ ⁻] (mg L ⁻¹)	δ ¹⁵ N- NO ₃ ⁻ (‰)	δ ¹⁸ O- NO ₃ ⁻ (‰)	Δ ¹⁷ O- NO ₃ ⁻ (‰)	δ ² H- H ₂ O (‰)	δ ¹⁸ O- H ₂ O (‰)
2011	2	14	3	A	0.40	2.3	-1.7	0.4	-59.8	-9.6
2011	2	14	5	A	0.12	0.9	-6.1	0.1	-60.5	-9.6
2011	2	14	7	A	0.3	3.9	81.4	29.8	-92.8	-13.8
2011	2	14	8	A	0.7	6.6	76.6		-95.6	-14.2
2011	2	14	9	A	0.6	0.1	-6.4	0.4	-66.7	-10.2
2011	2	14	10	A					-61.5	-9.5
2011	2	14	11	A	0.0				-54.7	-9.4
2011	2	14	12	A	0.8	3.5	-5.0	0.6	-60.5	-9.4
2011	2	14	14	A	1.3	4.0	-5.0	-0.5	-63.1	-9.8
2011	2	14	15	A	8.5	2.8	1.7	1.2	-70.9	-11.8
2011	2	14	1	B	2.4	4.0	-1.4	-0.6	-62.4	-10.0
2011	2	14	2	B	1.2	1.7	13.7	4.6	-83.4	-13.1
2011	2	14	3	B	1.4	0.0	13.6	3.5	-80.6	-12.0
2011	2	14	5	B	0.0				-60.8	-9.3
2011	2	14	6	B	0.1				-73.4	-10.9
2011	2	14	7	B	0.2	8.2	76.6	20.8	-88.9	-13.5
2011	2	14	8	B	0.0				-70.8	-10.6
2011	2	14	9	B	0.1				-60.1	-9.3
2011	2	14	10	B					-63.5	-9.9
2011	2	14	11	B					-65.6	-10.3
2011	2	14	12	B	0.2	3.8	-3.8	5.3	-62.7	-9.4
2011	2	14	13	B	8.2	2.7	-1.4	-0.8	-63.7	-10.3
2011	2	14	6	C	0.0				-92.2	-13.5
2011	2	14	7	C	0.0				-95.0	-13.8
2011	2	14	9	C	0.0				-80.0	-11.8
2011	2	14	10	C	0.9	-5.4	1.0	-0.4	-63.5	-9.0
2011	2	14	12	C	0.9	1.5	27.6	10.8	-68.6	-11.0
2011	2	14	15	C	2.9	2.4	4.1	2.4	-89.4	-10.6

APPENDIX C

DATA TABLE FOR HOURLY STORM EVENT PRECIPITATION SAMPLES

Table C-1 Precipitation amount, nitrate concentration, nitrate isotope, and water isotope data for hourly precipitation samples

Data refer to precipitation samples collected hourly at the base of Fernow Watershed 4 during six growing season storms. Time data refer to the end of the sampling period (e.g., a time of 19:00 represents precipitation accumulated between 18:00 and 19:00). Entries with no data indicate nitrate concentrations below the instrument detection limit or insufficient sample volume for isotope analysis.

Year	Month	Day	Time	Precip (mm)	[NO ₃ ⁻] (mg L ⁻¹)	δ ¹⁵ N- NO ₃ ⁻ (‰)	δ ¹⁸ O- NO ₃ ⁻ (‰)	Δ ¹⁷ O- NO ₃ ⁻ (‰)	δ ² H- H ₂ O (‰)	δ ¹⁸ O- H ₂ O (‰)
2010	07	09	19:00	9.23	0.7	1.5	64.2	19.6	-40.1	-6.5
2010	07	09	20:00	3.43	0.6	0.3	66.3	18.6	-44.0	-7.0
2010	07	09	21:00	3.16	0.2	-1.2	65.3	13.0	-54.0	-8.8
2010	07	09	22:00	0.79	0.3	-1.0	62.0			
2010	07	09	23:00	0.26	0.2	-2.0	70.2	22.0	-59.6	-9.6

Year	Month	Day	Time	Precip (mm)	[NO ₃ ⁻] (mg L ⁻¹)	δ ¹⁵ N- NO ₃ ⁻ (‰)	δ ¹⁸ O- NO ₃ ⁻ (‰)	Δ ¹⁷ O- NO ₃ ⁻ (‰)	δ ² H- H ₂ O (‰)	δ ¹⁸ O- H ₂ O (‰)
2010	07	10	0:00	1.05						
2010	07	10	1:00	0.26	2.6	14.0	80.8	25.6		
2010	07	10	2:00	0.26	2.1	13.1	82.0	26.8		
2010	07	10	3:00	0.00	2.8	6.5	76.2			
2010	07	10	4:00	0.00						
2010	09	11	23:55	0.00	1.0	-3.9	60.3	12.8	-43.9	-7.6
2010	09	12	1:55	0.28	1.8	-4.3	46.6	13.9		
2010	09	12	2:55	0.28	1.6	-3.1	65.3	22.1	-36.9	-6.9
2010	09	12	3:55	0.28	1.6	-2.0	68.5	23.4	-38.9	-6.9
2010	09	12	5:55	0.55	2.0	-3.9	43.0	14.2		
2010	09	16	16:00	3.95	0.2	-1.7	55.1	16.4	-26.4	-6.3
2010	09	16	17:00	2.11	0.4	-2.7	65.7	14.3	-20.7	-5.5
2010	09	16	18:00	0.26	1.2	-3.1	65.6	11.2	-13.2	-5.0
2010	09	16	19:00	0.26	1.6	-3.5	66.4	20.4	-10.7	-4.5
2010	09	16	21:00	19.75	0.6	-3.5	61.4	14.6	-37.6	-7.5
2010	09	16	22:00	0.26	0.5	-4.5	68.0	14.7	-36.5	-7.4
2010	09	26	19:30	1.31	0.4	0.0	64.9	19.6		
2010	09	26	21:00	1.31	1.2	3.9	70.4	23.5		
2010	09	26	23:00	0.26	1.6	4.9	72.9	25.4	-59.7	-9.4
2010	09	27	4:00	1.31	0.7	0.6	73.8	24.0	-41.9	-7.5
2010	09	27	6:00	0.52	0.3	-4.5	73.0	26.4	-39.0	-7.3
2010	09	27	8:00	0.52	0.2	-1.8	74.0	24.1	-44.4	-7.5
2010	09	27	9:00	0.52	0.2	-1.3	72.1	29.0		
2010	09	27	13:00	0.26	0.7	-9.7	59.8	20.3	-44.7	-7.2
2010	09	27	14:00	0.26	0.8	-12.4	56.4	19.9		
2010	09	28	0:00	3.92	0.2	-6.6	67.9	24.3	-73.1	-10.2
2010	09	28	1:00	0.26	0.2	-1.9	77.2	22.1	-64.1	-9.5
2010	09	28	2:00	1.57	0.1	-1.2	76.0	26.1	-60.4	-9.1
2010	09	28	3:00	0.52	0.1	-0.4	67.5	26.0	-74.7	-11.2
2010	09	28	4:00	1.04	0.1	-1.1	67.1	22.1	-79.8	-11.4

Year	Month	Day	Time	Precip (mm)	[NO ₃ ⁻] (mg L ⁻¹)	δ ¹⁵ N- NO ₃ ⁻ (‰)	δ ¹⁸ O- NO ₃ ⁻ (‰)	Δ ¹⁷ O- NO ₃ ⁻ (‰)	δ ² H- H ₂ O (‰)	δ ¹⁸ O- H ₂ O (‰)
2010	09	28	6:00	0.26	0.3	1.2	78.3	30.6	-73.6	-10.2
2010	09	28	10:00	0.26	0.4	1.3	73.7	28.3		
2010	09	30	2:00	1.30	0.5	-0.1	70.5	23.1		
2010	09	30	3:00	1.30	0.1	-6.5	58.5	23.2		
2010	09	30	4:00	1.30	0.0	1.0	68.6		-116.1	-14.9
2010	09	30	5:00	3.90	0.0	-0.9	70.7			
2010	09	30	6:00	1.30	0.0	-3.9	64.7		-142.4	-18.1
2010	09	30	7:00	5.21	0.0	4.5	73.0		-139.5	-18.2
2010	09	30	8:00	6.51	0.0	2.8	74.0		-145.5	-19.5
2010	09	30	9:00	13.02	0.0	2.9	60.8			
2010	09	30	10:00	11.71	0.0	5.3	55.4		-168.5	-22.2
2010	09	30	11:00	2.60	0.0	-2.9	56.6		-172.8	-23.1
2010	09	30	12:00	0.26	0.1	-1.8	58.1	17.4	-170.7	-22.8
2010	09	30	14:00	2.60	0.3	0.6	58.8	20.4	-170.3	-22.4
2010	09	30	15:00	1.30	0.7	11.7	66.7	22.3	-169.8	-22.3
2010	09	30	17:00	2.60	0.8	13.0	67.3	23.6		
2010	09	30	18:00	1.04	0.5	10.4	73.0	24.0		
2010	09	30	19:00	0.26	0.5	11.7	84.3	26.5		

APPENDIX D

DATA TABLE FOR HOURLY STORM EVENT STREAM SAMPLES

Table D-1 Discharge amount, nitrate concentration, nitrate isotope, and water isotope data for hourly stream samples

Data refer to stream samples collected hourly at the base of Fernow Watershed 4 during three growing season storms. Entries with no data indicate nitrate concentrations below the instrument detection limit or insufficient sample volume for isotope analysis.

Year	Month	Day	Time	Discharge (mm)	[NO ₃ ⁻] (mg L ⁻¹)	δ ¹⁵ N- NO ₃ ⁻ (‰)	δ ¹⁸ O- NO ₃ ⁻ (‰)	Δ ¹⁷ O- NO ₃ ⁻ (‰)	δ ² H- H ₂ O (‰)	δ ¹⁸ O- H ₂ O (‰)
2010	07	09	20:42	0.10	2.0	2.2	3.0	1.5	-61.4	-9.9
2010	07	09	21:42	0.12	2.1	2.5	0.8	0.4	-61.4	-10.0
2010	07	09	22:42	0.09	2.0	2.6	0.2	0.5	-61.4	-10.2
2010	07	09	23:42	0.09	2.1	3.0	-0.7	0.3	-62.0	-10.1
2010	07	10	0:42	0.09	2.0	3.9	-0.3	0.0	-65.6	-10.0
2010	07	10	1:42	0.09	1.9	3.3	-0.7	0.1	-62.7	-10.2
2010	07	10	2:42	0.09	2.0	3.4	-1.2	-0.1	-70.0	-10.2
2010	07	10	3:42	0.09	1.9	4.0	-1.2	-0.3	-62.7	-10.4

Year	Month	Day	Time	Discharge (mm)	[NO ₃ ⁻] (mg L ⁻¹)	δ ¹⁵ N- NO ₃ ⁻ (‰)	δ ¹⁸ O- NO ₃ ⁻ (‰)	Δ ¹⁷ O- NO ₃ ⁻ (‰)	δ ² H- H ₂ O (‰)	δ ¹⁸ O- H ₂ O (‰)
2010	07	10	4:42	0.09	1.8	3.7	-1.1	-0.2	-65.0	-10.2
2010	07	10	5:42	0.04	1.8	3.7	-1.7	-0.4	-64.9	-10.0
2010	07	10	6:42	0.04	1.8	3.7	-1.8	-0.1	-63.8	-10.2
2010	07	10	7:42	0.04	1.7	4.7	-4.5	0.3	-64.7	-10.0
2010	07	10	8:42	0.04	1.7	4.7	-2.1	0.1	-68.0	-10.2
2010	07	10	9:42	0.04	1.7	4.8	-2.3	-0.3	-64.1	-10.1
2010	07	10	10:42	0.04	1.7	4.5	-2.8	0.2	-66.6	-10.1
2010	07	10	11:42	0.04	1.7	4.7	-2.7	-0.9	-64.7	-9.9
2010	07	10	12:42	0.04	1.7	4.7	-2.8	-0.5	-68.1	-10.2
2010	07	10	13:42	0.04	1.6	5.0	-3.2	-0.5	-64.2	-9.9
2010	07	10	14:42	0.04	1.6	4.9	-3.9	-0.2	-64.4	-10.0
2010	07	10	15:42	0.04	1.6	4.9	-2.9	-0.3		
2010	07	10	16:42	0.04					-67.0	-10.2
2010	07	10	17:42	0.04	1.7	4.6	-3.4	-0.5	-65.2	-10.4
2010	07	10	18:42	0.04	1.7	4.5	-3.9	-0.3		
2010	09	16	18:00	0.00	10.8	1.4	-1.8	-0.2		
2010	09	16	19:00	0.00	9.4	1.4	-2.1	0.1	-43.2	-7.5
2010	09	16	20:00	0.04	9.4	1.9	-4.2	0.0		
2010	09	16	21:00	0.34	9.0	1.7	-2.6	-0.2	-43.3	-7.3
2010	09	16	22:00	1.02	9.5	1.6	-1.5	0.0		
2010	09	16	23:00	0.48	4.6	1.4	1.7	-0.2		
2010	09	17	0:00	0.27	5.1	2.0	1.9	-0.1		
2010	09	17	1:00	0.27	5.1	2.0	1.0	-0.3	-48.5	-7.9
2010	09	17	2:00	0.14	5.2	2.1	1.2	0.0		
2010	09	17	3:00	0.14	5.1	1.8	0.1	0.0	-44.1	-7.8
2010	09	17	4:00	0.08	5.2	2.2	1.1	0.1	-44.3	-7.6
2010	09	17	5:00	0.08	5.1	1.7	0.8	0.0	-45.9	-7.8
2010	09	17	6:00	0.07	5.2	1.8	0.8	-0.6	-44.4	-7.6
2010	09	17	7:00	0.07	5.1	1.6	0.8	0.2	-43.1	-7.9
2010	09	17	8:00	0.05	5.2	1.9	1.1	0.0	-43.7	-7.6

Year	Month	Day	Time	Discharge (mm)	[NO ₃ ⁻] (mg L ⁻¹)	δ ¹⁵ N- NO ₃ ⁻ (‰)	δ ¹⁸ O- NO ₃ ⁻ (‰)	Δ ¹⁷ O- NO ₃ ⁻ (‰)	δ ² H- H ₂ O (‰)	δ ¹⁸ O- H ₂ O (‰)
2010	09	17	9:00	0.05	5.2	1.9	-2.2	-0.3	-47.7	-7.9
2010	09	17	10:00	0.05	5.1	1.8	0.8	0.6		
2010	09	17	11:00	0.07	5.1	2.4	1.4	0.1	-44.1	-7.8
2010	09	17	12:00	0.08	5.0	1.4	-0.8	0.0	-44.4	-7.7
2010	09	30	9:00	1.59	2.2	2.0	-3.6	-0.7	-71.9	-10.3
2010	09	30	10:00	2.14	2.0	2.4	-2.3	-0.7	-81.0	-11.5
2010	09	30	11:00	1.32	3.3	2.1	-1.3	-0.6	-91.4	-12.7
2010	09	30	12:00	0.60	3.7	2.0	-1.5	-0.6	-75.3	-13.1
2010	09	30	13:00	0.92	3.8	2.2	-1.2	-0.3	-81.9	-11.4
2010	09	30	14:00	0.87	3.7	2.1	-3.8	-0.9	-81.7	-12.4
2010	09	30	15:00	0.70	3.4	2.2	-2.2	-0.6	-111.3	-15.0
2010	09	30	16:00	0.50	3.2	2.3	-1.8	-1.0	-81.5	-12.0
2010	09	30	17:00	0.50	3.0	2.4	-2.1	-1.0	-79.2	-11.2
2010	09	30	18:00	0.43	2.9	2.3	-2.4	-0.9	-82.6	-11.8
2010	09	30	19:00	0.43	2.8	2.9	-1.6	-0.9	-78.6	-11.3
2010	09	30	20:00	0.35	2.7	2.9	-1.1	-0.8	-83.3	-11.7
2010	09	30	21:00	0.35	2.6	3.0	-1.0	-0.5	-77.2	-11.2
2010	09	30	22:00	0.28	2.5	3.3	-0.5	-1.1	-77.8	-11.7
2010	09	30	23:00	0.28	2.5	3.0	-1.5	-0.7	-76.8	-11.1
2010	10	01	0:00	0.26	2.5	3.2	-2.5	-0.9	-76.4	-11.0
2010	10	01	1:00	0.26	2.4	3.4	-2.5	-0.5		
2010	10	01	2:00	0.26	2.4	3.4	-2.5	-0.3	-79.6	-11.4
2010	10	01	3:00	0.26	2.7	3.7	-2.2	-0.6	-74.3	-11.0
2010	10	01	4:00	0.26	2.5	3.6	-2.2	-0.6	-76.7	-11.2
2010	10	01	5:00	0.26	2.5	3.7	-2.3	-0.4	-73.2	-11.0
2010	10	01	6:00	0.26	2.4	3.5	-2.3	-0.8	-79.2	-11.3
2010	10	01	7:00	0.26	2.4	3.5	-2.0	-0.7	-72.9	-10.8
2010	10	01	8:00	0.26	2.4	3.5	-2.2	-0.3	-77.9	-11.2
2010	10	01	9:00	0.26	2.4	3.7	-2.2	-0.6	-72.4	-10.8
2010	10	01	10:00	0.19	2.3	3.7	-2.2	-0.9	-72.8	-11.2

Year	Month	Day	Time	Discharge (mm)	[NO ₃ ⁻] (mg L ⁻¹)	δ ¹⁵ N- NO ₃ ⁻ (‰)	δ ¹⁸ O- NO ₃ ⁻ (‰)	Δ ¹⁷ O- NO ₃ ⁻ (‰)	δ ² H- H ₂ O (‰)	δ ¹⁸ O- H ₂ O (‰)
2010	10	01	11:00	0.19	2.3	3.8	-3.2	-0.1	-72.0	-10.9

APPENDIX E

DATA TABLE FOR MONTHLY STREAM AND PRECIPITATION SAMPLES

Table E-1 Nitrate concentration, nitrate isotope, and water isotope data for monthly precipitation and stream samples

Data refer to stream and precipitation samples collected once per month at Coweeta Watershed 34, Fernow Watershed 4, and Hubbard Brook Watershed 3. Stream samples were collected at the base of each watershed and precipitation samples were sub-sampled from a bulk precipitation collector located within each watershed. Precipitation samples reflect accumulation during the previous week. Entries with no data indicate nitrate concentrations below the instrument detection limit or insufficient sample volume for isotope analysis.

Site	Water-shed	Year	Month	Day	Sample Type	[NO ₃ ⁻] (mg L ⁻¹)	δ ¹⁵ N- NO ₃ ⁻ (‰)	δ ¹⁸ O- NO ₃ ⁻ (‰)	Δ ¹⁷ O- NO ₃ ⁻ (‰)	δ ² H- H ₂ O (‰)	δ ¹⁸ O- H ₂ O (‰)
Coweeta	34	2012	8	7	Precip	0.9	-4.6	66.8	20.8	-5.3	-1.9
Coweeta	34	2012	9	4	Precip	0.5	-4.4	61.7	19.4	-11.3	-3.7
Coweeta	34	2012	10	2	Precip	0.1	-2.5	61.2	22.9	-18.7	-5.4

Site	Water-shed	Year	Month	Day	Sample Type	[NO ₃ ⁻] (mg L ⁻¹)	δ ¹⁵ N- NO ₃ ⁻ (‰)	δ ¹⁸ O- NO ₃ ⁻ (‰)	Δ ¹⁷ O- NO ₃ ⁻ (‰)	δ ² H- H ₂ O (‰)	δ ¹⁸ O- H ₂ O (‰)
Coweeta	34	2012	11	6	Precip	0.5	-2.9	74.5		-78.2	-12.9
Coweeta	34	2013	1	2	Precip	0.2	-2.7	75.4	27.2	-64.6	-10.6
Coweeta	34	2013	2	5	Precip	1.2	-0.5	74.8	28.3	-71.7	-11.8
Coweeta	34	2013	4	2	Precip	0.8	-2.7	73.1		-35.8	-7.9
Coweeta	34	2013	5	7	Precip	0.1	-2.2	70.4	29.4	-25.6	-6.1
Coweeta	34	2013	6	4	Precip	0.2	-0.1	61.9	20.9	-24.0	-5.3
Coweeta	34	2013	7	2	Precip	0.3	-3.9	61.1	20.2	-18.7	-5.4
Coweeta	34	2012	8	7	Stream	0.1	-2.6	9.8		-30.9	-6.2
Coweeta	34	2012	9	4	Stream	0.0	-1.9	13.8		-32.1	-6.3
Coweeta	34	2012	10	2	Stream	0.0				-23.7	-5.5
Coweeta	34	2012	11	6	Stream	0.0				-32.7	-6.3
Coweeta	34	2012	12	4	Stream	0.0				-24.4	-6.3
Coweeta	34	2013	1	2	Stream	0.0				-27.4	-6.3
Coweeta	34	2013	2	5	Stream	0.1	2.2	1.0	2.6	-26.9	-5.9
Coweeta	34	2013	3	5	Stream	0.1	1.0	2.3	7.8	-28.5	-6.0
Coweeta	34	2013	4	2	Stream	0.1	6.0	1.3	1.5	-30.4	-6.0
Coweeta	34	2013	5	7	Stream	0.1	0.1	1.5	5.6	-28.2	-6.0
Coweeta	34	2013	6	4	Stream	0.1	-0.8	-0.9	3.4	-29.3	-6.2
Coweeta	34	2013	7	2	Stream	0.1	-2.3	5.8	2.7	-31.2	-6.3
Fernow	4	2012	8	7	Precip	0.6	-4.5	65.9	12.9	-19.7	-4.2
Fernow	4	2012	9	4	Precip	0.5	3.6	23.4		-88.0	-13.8
Fernow	4	2012	10	2	Precip	1.5	-0.2	68.6	19.9	-30.1	-6.9
Fernow	4	2012	11	6	Precip	0.7	3.0	76.9	26.7	-97.3	-13.9
Fernow	4	2012	12	4	Precip	0.4	-0.7	78.4		-38.8	-6.9
Fernow	4	2013	1	2	Precip	0.8	1.3	81.7	31.4	-96.6	-13.9
Fernow	4	2013	2	5	Precip	0.3	3.5	76.3	34.0	-101.5	-13.9
Fernow	4	2013	3	5	Precip	1.3	3.8	72.5	27.9	-112.4	-15.5
Fernow	4	2013	4	2	Precip	1.5	3.9	72.9	28.7	-101.8	-13.8
Fernow	4	2013	5	7	Precip	0.3			26.5	-57.3	-8.9
Fernow	4	2013	6	4	Precip	0.5	-1.1	68.2	14.8	-51.3	-7.6

Site	Water-shed	Year	Month	Day	Sample Type	[NO ₃ ⁻] (mg L ⁻¹)	δ ¹⁵ N- NO ₃ ⁻ (‰)	δ ¹⁸ O- NO ₃ ⁻ (‰)	Δ ¹⁷ O- NO ₃ ⁻ (‰)	δ ² H- H ₂ O (‰)	δ ¹⁸ O- H ₂ O (‰)
Fernow	4	2013	7	2	Precip	0.1	1.8	70.4	24.8	-37.8	-5.6
Fernow	4	2012	8	7	Stream	1.3	3.5	-0.9	-0.6	-52.9	-8.4
Fernow	4	2012	9	4	Stream	2.0	4.0	-1.5	-1.4	-65.4	-9.7
Fernow	4	2012	10	2	Stream	1.2	5.6	-1.1	-0.8	-57.0	-8.8
Fernow	4	2012	11	6	Stream	2.1	1.9	-0.1	-0.3	-64.9	-9.6
Fernow	4	2012	12	4	Stream	1.5	2.2	-0.6	-0.5	-57.8	-8.8
Fernow	4	2013	1	2	Stream	1.5	1.9	-0.8	-0.1	-63.7	-9.6
Fernow	4	2013	2	5	Stream	1.6	1.7	0.3	-0.1	-69.7	-10.1
Fernow	4	2013	3	5	Stream	1.4	1.8	-0.3	-0.2	-69.5	-10.1
Fernow	4	2013	4	2	Stream	1.6	1.7	-0.1	0.1	-77.1	-10.9
Fernow	4	2013	5	7	Stream	1.1	0.8	-1.3	-0.6	-68.7	-10.3
Fernow	4	2013	6	4	Stream	1.1	2.1	-3.3	-0.8	-70.6	-10.2
Fernow	4	2013	7	2	Stream	1.1	0.6	-0.3	-0.4	-68.1	-10.2
Hubbard Brook	3	2012	8	7	Precip	0.3	-4.2	57.6		-36.5	-6.4
Hubbard Brook	3	2012	9	4	Precip	0.3	-5.4	68.9	22.4	-50.5	-7.9
Hubbard Brook	3	2012	10	2	Precip	0.4	-4.0	73.1	11.1	-79.6	-11.8
Hubbard Brook	3	2012	11	6	Precip	0.1	1.3	64.1		-32.6	-6.5
Hubbard Brook	3	2012	12	4	Precip	1.7	-0.4	85.7	30.3	-59.9	-9.8
Hubbard Brook	3	2013	1	2	Precip	2.4	1.5	81.6	33.0	-122.7	-17.2
Hubbard Brook	3	2013	2	5	Precip	0.4	-2.1	82.7	31.0	-54.8	-8.4
Hubbard Brook	3	2013	3	5	Precip	0.3	-1.5	75.8	12.3	-117.9	-14.9
Hubbard Brook	3	2013	4	2	Precip	0.4	-1.8	72.8	31.1	-121.3	-17.0
Hubbard Brook	3	2013	5	7	Precip	0.5	-2.7	73.2	28.4	-50.1	-7.6
Hubbard Brook	3	2013	6	4	Precip	0.3	-1.8	66.4	26.1	-34.8	-5.9
Hubbard Brook	3	2013	7	2	Precip	0.2	-2.6	67.9	24.9	-48.4	-7.2
Hubbard Brook	3	2012	8	7	Stream	0.1	0.7	0.6	0.3	-55.4	-8.6
Hubbard Brook	3	2012	9	4	Stream	0.1	0.4	4.1	2.3	-51.6	-8.3
Hubbard Brook	3	2012	10	2	Stream	0.0	-2.0	27.2		-45.9	-7.6
Hubbard Brook	3	2012	11	6	Stream	0.0	-1.5	15.6	-0.5	-46.2	-7.6
Hubbard Brook	3	2012	12	4	Stream	0.5	0.6	18.7	7.1	-49.1	-8.3

Site	Water-shed	Year	Month	Day	Sample Type	[NO ₃ ⁻] (mg L ⁻¹)	δ ¹⁵ N- NO ₃ ⁻ (‰)	δ ¹⁸ O- NO ₃ ⁻ (‰)	Δ ¹⁷ O- NO ₃ ⁻ (‰)	δ ² H- H ₂ O (‰)	δ ¹⁸ O- H ₂ O (‰)
Hubbard Brook	3	2013	1	2	Stream	0.2	1.0	-2.1	0.2	-51.1	-8.7
Hubbard Brook	3	2013	2	5	Stream	0.6	1.9	4.0	2.2	-57.2	-9.1
Hubbard Brook	3	2013	3	5	Stream	0.3	0.3	-2.8	-0.7	-49.1	-9.1
Hubbard Brook	3	2013	4	2	Stream	0.5	2.4	4.3	1.8	-62.9	-10.0
Hubbard Brook	3	2013	5	7	Stream	0.1	2.1	18.4	-0.6	-62.2	-10.0
Hubbard Brook	3	2013	6	4	Stream	0.0	2.6	11.8	0.1	-58.8	-9.6
Hubbard Brook	3	2013	7	2	Stream	0.0			-0.5	-57.8	-9.0

BIBLIOGRAPHY

- Aber, J., W. McDowell, K. Nadelhoffer, A. Magill, G. Berntson, M. Kamakea, S. McNulty, W. Currie, L. Rustad, and I. Fernandez (1998), Nitrogen saturation in temperate forest ecosystems, *BioScience*, 48(11), 921–934.
- Aber, J., C. L. Goodale, S. Ollinger, M. L. Smith, A. Magill, M. E. Martin, R. A. Hallet, and J. L. Stoddard (2003), Is nitrogen deposition altering the nitrogen status of northeastern forests?, *BioScience*, 53(4), 375–389, doi:10.1641/0006-3568(2003)053[0375:INDATN]2.0.CO;2.
- Aber, J. D., K. J. Nadelhoffer, P. Steudler, and J. M. Melillo (1989), Nitrogen saturation in northern forest ecosystems., *BioScience*, 39(6), 378–386.
- Adams, M. B. (1999), Acidic deposition and sustainable forest management in the central Appalachians, USA, *For. Ecol. Manag.*, 122(1), 17–28, doi:10.1016/S0378-1127(99)00029-8.
- Adams, M. B., D. R. DeWalle, W. T. Peterjohn, F. S. Gilliam, W. E. Sharpe, and K. W. Williard (2006), Soil chemical response to experimental acidification treatments, in *The Fernow Watershed Acidification Study*, pp. 41–69, Springer.
- Adams, M. B., J. N. Kochenderfer, and P. J. Edwards (2007), The Fernow watershed acidification study: ecosystem acidification, nitrogen saturation and base cation leaching, *Water Air Soil Pollut. Focus*, 7(1-3), 267–273, doi:10.1007/s11267-006-9062-1.
- Ågren, G. I., and E. Bosatta (1988), Nitrogen saturation of terrestrial ecosystems, *Environ. Pollut.*, 54(3), 185–197, doi:10.1016/0269-7491(88)90111-X.
- Alexander, B., M. G. Hastings, D. J. Allman, J. Dachs, J. A. Thornton, and S. A. Kunasek (2009), Quantifying atmospheric nitrate formation pathways based on a global model of the oxygen isotopic composition (^{17}O) of atmospheric nitrate, *Atmospheric Chem. Phys.*, 9, 5043–5056, doi:10.5194/acp-9-5043-2009.
- Ammann, M., R. Siegwolf, F. Pichlmayer, M. Suter, M. Saurer, and C. Brunold (1999), Estimating the uptake of traffic-derived NO_2 from ^{15}N abundance in Norway spruce needles, *Oecologia*, 118(2), 124–131.

- Argerich, A., S. L. Johnson, S. D. Sebestyen, C. C. Rhoades, E. Greathouse, J. D. Knoepp, M. B. Adams, G. E. Likens, J. L. Campbell, and W. H. McDowell (2013), Trends in stream nitrogen concentrations for forested reference catchments across the USA, *Environ. Res. Lett.*, 8(1), 014039, doi:10.1088/1748-9326/8/1/014039.
- Bain, D. J., M. B. Green, J. L. Campbell, J. F. Chamblee, S. Chaoka, J. M. Fraterrigo, S. S. Kaushal, S. L. Martin, T. E. Jordan, and A. J. Parolari (2012), Legacy effects in material flux: structural catchment changes predate long-term studies, *Bioscience*, 62(6), 575–584.
- Band, L. E., P. Patterson, R. Nemani, and S. W. Running (1993), Forest ecosystem processes at the watershed scale: incorporating hillslope hydrology, *Agric. For. Meteorol.*, 63(1), 93–126.
- Barnes, R. T., P. A. Raymond, and K. L. Casciotti (2008), Dual isotope analyses indicate efficient processing of atmospheric nitrate by forested watersheds in the northeastern US, *Biogeochemistry*, 90(1), 15–27, doi:10.1007/s10533-008-9227-2.
- Bauer, B., and M. Reynolds (2008), Recovering data from scanned graphs: performance of Frantz's g3data software, *Behav. Res. Methods*, 40(3), 858–868.
- Bernhardt, E. S., G. E. Likens, D. C. Buso, and C. T. Driscoll (2003), In-stream uptake dampens effects of major forest disturbance on watershed nitrogen export, *Proc. Natl. Acad. Sci.*, 100(18), 10304–10308.
- Bernhardt, E. S., G. E. Likens, R. O. Hall, D. C. Buso, S. G. Fisher, T. M. Burton, J. L. Meyer, W. H. McDowell, M. S. Mayer, and W. B. Bowden (2005), Can't see the forest for the stream? In-stream processing and terrestrial nitrogen exports, *Bioscience*, 55(3), 219–230.
- Bishop, K., J. Seibert, S. Köhler, and H. Laudon (2004), Resolving the double paradox of rapidly mobilized old water with highly variable responses in runoff chemistry, *Hydrol. Process.*, 18(1), 185–189.
- Boesch, D. F., R. B. Brinsfield, and R. E. Magnien (2001), Chesapeake Bay eutrophication: scientific understanding, ecosystem restoration, and challenges for agriculture., *J. Environ. Qual.*, 30(2), 303–320.
- Böhlke, J. K., and J. M. Denver (1995), Combined use of groundwater dating, chemical, and isotopic analyses to resolve the history and fate of nitrate contamination in two agricultural watersheds, Atlantic coastal plain, Maryland, *Water Resour. Res.*, 31(9), 2319–2339, doi:10.1029/95WR01584.
- Britto, D. T., and H. J. Kronzucker (2006), Plant nitrogen transport and its regulation in changing soil environments, *J. Crop Improv.*, 15(2), 1–23.

- Brookshire, J., S. Gerber, J. R. Webster, J. M. Vose, and W. T. Swank (2011), Direct effects of temperature on forest nitrogen cycling revealed through analysis of long-term watershed records, *Glob. Change Biol.*, *17*(1), 297–308.
- Brown, S. S., J. E. Dibb, H. Stark, M. Aldener, M. Vozella, S. Whitlow, E. J. Williams, B. M. Lerner, R. Jakoubek, and A. M. Middlebrook (2004), Nighttime removal of NO_x in the summer marine boundary layer, *Geophys. Res. Lett.*, *31*(7), L07108, doi:10.1029/2004GL019412.
- Buchwald, C., and K. L. Casciotti (2010), Oxygen isotopic fractionation and exchange during bacterial nitrite oxidation, *Limnol. Oceanogr.*, *55*(3), 1064–1074, doi:10.4319/lo.2010.55.3.1064.
- Buda, A. R., and D. R. DeWalle (2009a), Dynamics of stream nitrate sources and flow pathways during stormflows on urban, forest and agricultural watersheds in central Pennsylvania, USA, *Hydrol. Process.*, *23*(23), 3292–3305.
- Buda, A. R., and D. R. DeWalle (2009b), Using atmospheric chemistry and storm track information to explain the variation of nitrate stable isotopes in precipitation at a site in central Pennsylvania, USA, *Atmos. Environ.*, *43*(29), 4453–4464, doi:10.1016/j.atmosenv.2009.06.027.
- Burch, H., P. Waldner, and B. Fritschi (1996), Variation of pH and concentration of nutrients and minerals during rain-events, in *Ecohydrological Processes in Small Basins. 6th Conference of the European Network of Experimental and Representative Basins (ERB), Strassbourg*, pp. 59–64.
- Burns, D. A. (1998), Retention of NO₃⁻ in an upland streamenvironment: a mass balance approach, *Biogeochemistry*, *40*(1), 73–96.
- Burns, D. A., and C. Kendall (2002), Analysis of δ¹⁵N and δ¹⁸O to differentiate NO₃⁻ sources in runoff at two watersheds in the Catskill Mountains of New York, *Water Resour. Res.*, *38*(5), 9–1, doi:10.1029/2001WR000292.
- Burns, D. A., P. S. Murdoch, G. B. Lawrence, and R. L. Michel (1998), Effect of groundwater springs on N O₃⁻ concentrations during summer in Catskill Mountain streams, *Water Resour. Res.*, *34*(8), 1987–1996, doi:10.1029/98WR01282.
- Burns, D. A., J. J. McDonnell, R. P. Hooper, N. E. Peters, J. E. Freer, C. Kendall, and K. Beven (2001), Quantifying contributions to storm runoff through end-member mixing analysis and hydrologic measurements at the Panola Mountain Research Watershed (Georgia, USA), *Hydrol. Process.*, *15*(10), 1903–1924.
- Burns, D. A., E. W. Boyer, E. M. Elliott, and C. Kendall (2009), Sources and transformations of nitrate from streams draining varying land uses: evidence from dual isotope analysis, *J. Environ. Qual.*, *38*(3), 1149–1159, doi:10.2134/jeq2008.0371.

- Burns, D. A., J. A. Lynch, B. J. Cosby, M. E. Fenn, J. S. Baron, and U.S. EPA Clean Air Markets Division (2011), *National Acid Precipitation Assessment Program Report to Congress 2011: An Integrated Assessment*, National Science and Technology Council, Washington, DC.
- Buttle, J. M. (2006), Isotope hydrograph separation of runoff sources, *Encycl. Hydrol. Sci.*, (10), 116, doi:10.1002/0470848944.hsa120.
- Bytnerowicz, A., and M. E. Fenn (1996), Nitrogen deposition in California forests: a review, *Environ. Pollut.*, 92(2), 127–146, doi:10.1016/0269-7491(95)00106-9.
- Campbell, D. H., C. Kendall, C. C. Y. Chang, S. R. Silva, and K. A. Tonnessen (2002), Pathways for nitrate release from an alpine watershed: determination using $\delta^{15}\text{N}$ and $\delta^{18}\text{O}$, *Water Resour. Res.*, 38(5), 10–1–10–9, doi:10.1029/2001WR000294.
- Campbell, J. L., M. J. Mitchell, P. M. Groffman, L. M. Christenson, and J. P. Hardy (2005), Winter in northeastern North America: a critical period for ecological processes, *Front. Ecol. Environ.*, 3(6), 314–322, doi:10.1890/1540-9295(2005)003%5B0314:WINNAA%5D2.0.CO;2.
- Campbell, J. L., M. J. Mitchell, and B. Mayer (2006), Isotopic assessment of NO_3^- and SO_4^{2-} mobility during winter in two adjacent watersheds in the Adirondack Mountains, New York, *J. Geophys. Res. Biogeosciences*, 111(G4), doi:10.1029/2006JG000208.
- Cape, J. N., Y. S. Tang, N. Van Dijk, L. Love, M. A. Sutton, and S. C. F. Palmer (2004), Concentrations of ammonia and nitrogen dioxide at roadside verges, and their contribution to nitrogen deposition, *Environ. Pollut.*, 132(3), 469–478, doi:10.1016/j.envpol.2004.05.009.
- Casciotti, K. L., D. M. Sigman, M. G. Hastings, J. K. Böhlke, and A. Hilkert (2002), Measurement of the oxygen isotopic composition of nitrate in seawater and freshwater using the denitrifier method, *Anal. Chem.*, 74(19), 4905–4912.
- Casciotti, K. L., M. McIlvin, and C. Buchwald (2010), Oxygen isotopic exchange and fractionation during bacterial ammonia oxidation, *Limnol. Oceanogr.*, 55(2), 753, doi:10.4319/lo.2010.55.2.0753.
- Chang, C. C., J. Langston, M. Riggs, D. H. Campbell, S. R. Silva, and C. Kendall (1999), A method for nitrate collection for $\delta^{15}\text{N}$ and $\delta^{18}\text{O}$ analysis from waters with low nitrate concentrations, *Can. J. Fish. Aquat. Sci.*, 56(10), 1856–1864.
- Christ, M. J., W. T. Peterjohn, J. R. Cumming, and M. B. Adams (2002), Nitrification potentials and landscape, soil and vegetation characteristics in two central Appalachian watersheds differing in NO_3^- export, *For. Ecol. Manag.*, 159(3), 145–158.
- Church, M. R. (1997), Hydrochemistry of forested catchments, *Annu. Rev. Earth Planet. Sci.*, 25(1), 23–59.

- Cirno, C. P., and J. J. McDonnell (1997), Linking the hydrologic and biogeochemical controls of nitrogen transport in near-stream zones of temperate-forested catchments: a review, *J. Hydrol.*, 199(1), 88–120, doi:10.1016/S0022-1694(96)03286-6.
- Clark, C. M., and D. Tilman (2008), Loss of plant species after chronic low-level nitrogen deposition to prairie grasslands, *Nature*, 451(7179), 712–715, doi:10.1016/S0022-1694(96)03286-6.
- Cliff, S. S., and M. H. Thiemens (1997), The $^{18}\text{O}/^{16}\text{O}$ and $^{17}\text{O}/^{16}\text{O}$ ratios in atmospheric nitrous oxide: a mass-independent anomaly, *Science*, 278(5344), 1774–1776, doi:10.1126/science.278.5344.1774.
- Collier, M. D., M. N. Fotelli, M. Nahm, S. Kopriva, H. Rennenberg, D. E. Hanke, and A. Gessler (2003), Regulation of nitrogen uptake by *Fagus sylvatica* on a whole plant level—interactions between cytokinins and soluble N compounds, *Plant Cell Environ.*, 26(9), 1549–1560.
- Compton, J. E., L. S. Watrud, L. Arlene Porteous, and S. DeGroot (2004), Response of soil microbial biomass and community composition to chronic nitrogen additions at Harvard Forest, *For. Ecol. Manag.*, 196(1), 143–158.
- Coplen, T. B., J. K. Böhlke, and K. L. Casciotti (2004), Using dual-bacterial denitrification to improve $\delta^{15}\text{N}$ determinations of nitrates containing mass-independent ^{17}O , *Rapid Commun. Mass Spectrom.*, 18(3), 245–250, doi:10.1002/rcm.1318.
- Corre, M. D., and N. P. Lamersdorf (2004), Reversal of nitrogen saturation after long-term deposition reduction: impact on soil nitrogen cycling, *Ecology*, 85(11), 3090–3104.
- Costa, A. W., G. Michalski, A. J. Schauer, B. Alexander, E. J. Steig, and P. B. Shepson (2011), Analysis of atmospheric inputs of nitrate to a temperate forest ecosystem from $\Delta^{17}\text{O}$ isotope ratio measurements, *Geophys. Res. Lett.*, 38(15), L15805, doi:10.1029/2011GL047539.
- Creed, I. F., and L. E. Band (1998), Export of nitrogen from catchments within a temperate forest: evidence for a unifying mechanism regulated by variable source area dynamics, *Water Resour. Res.*, 34(11), 3105–3120.
- Creed, I. F., L. E. Band, N. W. Foster, I. K. Morrison, J. A. Nicolson, R. S. Semkin, and D. S. Jeffries (1996), Regulation of nitrate-N release from temperate forests: a test of the N flushing hypothesis, *Water Resour. Res.*, 32(11), 3337–3354, doi:10.1029/96WR02399.
- Curtis, C. J., C. D. Evans, C. L. Goodale, and T. H. Heaton (2011), What have stable isotope studies revealed about the nature and mechanisms of N saturation and nitrate leaching from semi-natural catchments?, *Ecosystems*, 14(6), 1021–1037, doi:10.1007/s10021-011-9461-7.

- Davidson, E. A. (1992), Pulses of nitric oxide and nitrous oxide flux following wetting of dry soil: an assessment of probable sources and importance relative to annual fluxes, *Ecol. Bull.*, 149–155.
- Davidson, E. A., and W. Kinglerlee (1997), A global inventory of nitric oxide emissions from soils, *Nutr. Cycl. Agroecosystems*, 48(1), 37–50.
- Davidson, E. A., M. Keller, H. E. Erickson, L. V. Verchot, and E. Veldkamp (2000), Testing a conceptual model of soil emissions of nitrous and nitric oxides, *BioScience*, 50(8), 667–680.
- Dejwakh, N. R., T. Meixner, G. Michalski, and J. McIntosh (2012), Using ^{17}O to investigate nitrate sources and sinks in a semi-arid groundwater system, *Environ. Sci. Technol.*, 46(2), 745–751.
- Dewalle, D. R., W. E. Sharpe, and P. J. Edwards (1988), Biogeochemistry of two Appalachian deciduous forest sites in relation to episodic stream acidification, *Water. Air. Soil Pollut.*, 40(1-2), 143–156.
- DeWalle, D. R., P. J. Edwards, B. R. Swistock, R. Aravena, and R. J. Drimmie (1997), Seasonal isotope hydrology of three Appalachian forest catchments, *Hydrol. Process.*, 11(15), 1895–1906, doi:10.1002/(SICI)1099-1085(199712)11:15<1895::AID-HYP538>3.0.CO;2-#.
- Van Diepen, L. T., E. A. Lilleskov, K. S. Pregitzer, and R. M. Miller (2007), Decline of arbuscular mycorrhizal fungi in northern hardwood forests exposed to chronic nitrogen additions, *New Phytol.*, 176(1), 175–183.
- Dise, N. B., J. J. Rothwell, V. Gauci, C. van der Salm, and W. de Vries (2009), Predicting dissolved inorganic nitrogen leaching in European forests using two independent databases, *Sci. Total Environ.*, 407(5), 1798–1808, doi:10.1016/j.scitotenv.2008.11.003.
- Driscoll, C. T., G. B. Lawrence, A. J. Bulger, T. J. Butler, C. S. Cronan, C. Eagar, K. F. Lambert, G. E. Likens, J. L. Stoddard, and K. C. Weathers (2001), Acidic deposition in the northeastern United States: sources and inputs, ecosystem effects, and management strategies, *BioScience*, 51(3), 180–198.
- Driscoll, C. T. et al. (2003), Nitrogen pollution in the northeastern United States: sources, effects, and management options, *BioScience*, 53(4), 357–374, doi:10.1641/0006-3568(2003)053[0357:NPITNU]2.0.CO;2.
- Dunne, T., and R. D. Black (1970), Partial area contributions to storm runoff in a small New England watershed, *Water Resour. Res.*, 6(5), 1296–1311.
- Dunne, T., and R. D. Black (1971), Runoff processes during snowmelt, *Water Resour. Res.*, 7(5), 1160–1172.

- Durka, W., E. D. Schulze, G. Gebauer, and S. Voerkellust (1994), Effects of forest decline on uptake and leaching of deposited nitrate determined from ^{15}N and ^{18}O measurements, *Nature*, 372, 22.
- Edwards, P. J., and J. D. Helvey (1991), Long-term ionic increases from a central Appalachian forested watershed, *J. Env. Qual.*, 20(1), 250–255.
- Elliott, E. M., C. Kendall, S. D. Wankel, D. A. Burns, E. W. Boyer, K. Harlin, D. J. Bain, and T. J. Butler (2007), Nitrogen isotopes as indicators of NO_x source contributions to atmospheric nitrate deposition across the midwestern and northeastern United States, *Environ. Sci. Technol.*, 41(22), 7661–7667.
- Elliott, E. M., C. Kendall, E. W. Boyer, D. A. Burns, G. G. Lear, H. E. Golden, K. Harlin, A. Bytnerowicz, T. J. Butler, and R. Glatz (2009), Dual nitrate isotopes in dry deposition: utility for partitioning NO_x source contributions to landscape nitrogen deposition, *J. Geophys. Res.*, 114(G4), G04020.
- Evans, C., C. Reynolds, C. Curtis, H. Crook, D. Norris, and S. Brittain (2005), A conceptual model of spatially heterogeneous nitrogen leaching from a Welsh moorland catchment, *Water Air Soil Pollut. Focus*, 4(6), 97–105, doi:10.1007/s11267-005-3019-7.
- Fang, Y., P. Gundersen, R. Vogt, K. Koba, F. Chen, X. Chen, and M. Yoh (2011a), Atmospheric deposition and leaching of nitrogen in Chinese forest ecosystems, *J. For. Res.*, 16(5), 341–350, doi:10.1007/s10310-011-0267-4.
- Fang, Y. T., K. Koba, X. M. Wang, D. Z. Wen, J. Li, Y. Takebayashi, X. Y. Liu, and M. Yoh (2011b), Anthropogenic imprints on nitrogen and oxygen isotopic composition of precipitation nitrate in a nitrogen-polluted city in southern China, *Atmospheric Chem. Phys.*, 11(3), 1313–1325.
- Felix, J. D., and E. M. Elliott (2013), The agricultural history of human-nitrogen interactions as recorded in ice core $\delta^{15}\text{N}\text{-NO}_3^-$, *Geophys. Res. Lett.*, doi:10.1002/grl.50209.
- Felix, J. D., E. M. Elliott, and S. L. Shaw (2012), Nitrogen isotopic composition of coal-fired power plant NO_x : influence of emission controls and implications for global emission inventories, *Environ. Sci. Technol.*, 46(6), 3528–3535, doi:10.1021/es203355v.
- Fenn, M. E., R. Haeuber, G. S. Tonnesen, J. S. Baron, S. Grossman-Clarke, D. Hope, D. A. Jaffe, S. Copeland, L. Geiser, and H. M. Rueth (2003), Nitrogen emissions, deposition, and monitoring in the western United States, *BioScience*, 53(4), 391–403.
- Fenn, M. E., S. Jovan, F. Yuan, L. Geiser, T. Meixner, and B. S. Gimeno (2008), Empirical and simulated critical loads for nitrogen deposition in California mixed conifer forests, *Environ. Pollut.*, 155(3), 492–511, doi:10.1016/j.envpol.2008.03.019.
- Flum, T., and S. C. Nodvin (1995), Factors affecting streamwater chemistry in the Great Smoky Mountains, USA, *Water. Air. Soil Pollut.*, 85(3), 1707–1712.

- Fortescue, J. A. (1980), *Environmental geochemistry. A holistic approach.*, Springer-Verlag. 347p.
- Frey, S. D., M. Knorr, J. L. Parrent, and R. T. Simpson (2004), Chronic nitrogen enrichment affects the structure and function of the soil microbial community in temperate hardwood and pine forests, *For. Ecol. Manag.*, 196(1), 159–171, doi:10.1016/j.foreco.2004.03.018.
- Freyer, H. D. (1991), Seasonal variation of $^{15}\text{N}/^{14}\text{N}$ ratios in atmospheric nitrate species, *Tellus B*, 43(1), 30–44, doi:10.1034/j.1600-0889.1991.00003.x.
- Freyer, H. D., D. Kley, A. Volz-Thomas, and K. Kobel (1993), On the interaction of isotopic exchange processes with photochemical reactions in atmospheric oxides of nitrogen, *J. Geophys. Res. Atmospheres 1984–2012*, 98(D8), 14791–14796.
- Galloway, J. N., G. E. Likens, and M. E. Hawley (1984), Acid precipitation: natural versus anthropogenic components, *Science*, 226(4676), 829–831.
- Galloway, J. N., J. D. Aber, J. W. Erisman, S. P. Seitzinger, R. W. Howarth, E. B. Cowling, and B. J. Cosby (2003), The nitrogen cascade, *BioScience*, 53(4), 341–356.
- Galloway, J. N., A. R. Townsend, J. W. Erisman, M. Bekunda, Z. Cai, J. R. Freney, L. A. Martinelli, S. P. Seitzinger, and M. A. Sutton (2008), Transformation of the nitrogen cycle: recent trends, questions, and potential solutions, *Science*, 320(5878), 889–892, doi:10.1126/science.1136674.
- Ganzeveld, L. N., J. Lelieveld, F. J. Dentener, M. C. Krol, A. J. Bouwman, and G. J. Roelofs (2002), Global soil-biogenic NO_x emissions and the role of canopy processes, *J. Geophys. Res.*, 107(D16), 4298, doi:0.1029/2001JD001289.
- Gardner, K. K., B. L. McGlynn, and L. A. Marshall (2011), Quantifying watershed sensitivity to spatially variable N loading and the relative importance of watershed N retention mechanisms, *Water Resour. Res.*, 47(8), W08524, doi:10.1029/2010WR009738.
- Gessler, A., S. Schneider, D. Von Sengbusch, P. Weber, U. Hanemann, C. Huber, A. Rothe, K. Kreutzer, and H. Rennenberg (1998), Field and laboratory experiments on net uptake of nitrate and ammonium by the roots of spruce (*Picea abies*) and beech (*Fagus sylvatica*) trees, *New Phytol.*, 138(2), 275–285.
- Ghude, S. D., D. M. Lal, and G. Beig (2010), Rain-induced soil NO_x emission from India during the onset of the summer monsoon: a satellite perspective, *J. Geophys. Res.*, 115(D16), D16304, doi:10.1029/2009JD013367.
- Gilliam, F. S., B. M. Yurish, and M. B. Adams (2001), Temporal and spatial variation of nitrogen transformations in nitrogen-saturated soils of a central Appalachian hardwood forest, *Can. J. For. Res.*, 31(10), 1768–1785, doi:10.1139/x01-106.

- Gold, A. J., P. M. Groffman, K. Addy, D. Q. Kellogg, M. Stolt, and A. E. Rosenblatt (2001), Landscape attributes as controls on groundwater nitrate removal capacity of riparian zones, *JAWRA J. Am. Water Resour. Assoc.*, 37(6), 1457–1464.
- Goodale, C. L., S. A. Thomas, G. Fredriksen, E. M. Elliott, K. M. Flinn, T. J. Butler, and M. T. Walter (2009), Unusual seasonal patterns and inferred processes of nitrogen retention in forested headwaters of the Upper Susquehanna River, *Biogeochemistry*, 93(3), 197–218, doi:10.1007/s10533-009-9298-8.
- Grennfelt, P., and H. Hultberg (1986), Effects of nitrogen deposition on the acidification of terrestrial and aquatic ecosystems, *Water, Air, Soil Pollut.*, 30(3-4), 945–963, doi:10.1007/978-94-009-3385-9_96.
- Gress, S. E., T. D. Nichols, C. C. Northcraft, and W. T. Peterjohn (2007), Nutrient limitation in soils exhibiting differing nitrogen availabilities: what lies beyond nitrogen saturation?, *Ecology*, 88(1), 119–130.
- Groffman, P. M., and J. M. Tiedje (1989), Denitrification in north temperate forest soils: spatial and temporal patterns at the landscape and seasonal scales, *Soil Biol. Biochem.*, 21(5), 613–620, doi:10.1016/0038-0717(89)90053-9.
- Guenet, B., M. Danger, L. Abbadie, and G. Lacroix (2010), Priming effect: bridging the gap between terrestrial and aquatic ecology, *Ecology*, 91(10), 2850–2861.
- Hales, H. C., D. S. Ross, and A. Lini (2007), Isotopic signature of nitrate in two contrasting watersheds of Brush Brook, Vermont, USA, *Biogeochemistry*, 84(1), 51–66, doi:10.1007/s10533-007-9074-6.
- Hastings, M. G., D. M. Sigman, and F. Lipschultz (2003), Isotopic evidence for source changes of nitrate in rain at Bermuda, *J. Geophys. Res.*, 108(D24), 4790, doi:10.1029/2003JD003789.
- Heaton, T. H. E. (1990), $^{15}\text{N}/^{14}\text{N}$ ratios of NO_x from vehicle engines and coal-fired power stations, *Tellus B*, 42(3), 304–307.
- Hedin, L. O., J. C. von Fischer, N. E. Ostrom, B. P. Kennedy, M. G. Brown, and G. P. Robertson (1998), Thermodynamic constraints on nitrogen transformations and other biogeochemical processes at soil-stream interfaces, *Ecology*, 79(2), 684–703.
- Helliwell, R. C., M. C. Coull, J. J. L. Davies, C. D. Evans, D. Norris, R. C. Ferrier, A. Jenkins, and B. Reynolds (2007), The role of catchment characteristics in determining surface water nitrogen in four upland regions in the UK., *Hydrol. Earth Syst. Sci.*, 11(1).
- Hibbert, A. R., and C. A. Troendle (1988), Streamflow generation by variable source area, in *Forest hydrology and ecology at Coweeta*, pp. 111–127, Springer.

- Hill, A. R., K. J. Devito, S. Campagnolo, and K. Sanmugas (2000), Subsurface denitrification in a forest riparian zone: interactions between hydrology and supplies of nitrate and organic carbon, *Biogeochemistry*, 51(2), 193–223, doi:10.1023/A:1006476514038.
- Hoering, T. (1957), The isotopic composition of the ammonia and the nitrate ion in rain, *Geochim. Cosmochim. Acta*, 12(1), 97–102.
- Högberg, P. (1997), Tansley Review No. 95 ^{15}N natural abundance in soil-plant systems, *New Phytol.*, 137(2), 179–203.
- Horváth, L., E. Führer, and K. Lajtha (2006), Nitric oxide and nitrous oxide emission from Hungarian forest soils; linked with atmospheric N-deposition, *Atmos. Environ.*, 40(40), 7786–7795.
- Hudman, R. C., N. E. Moore, R. V. Martin, A. R. Russell, A. K. Mebust, L. C. Valin, and R. C. Cohen (2012), A mechanistic model of global soil nitric oxide emissions: implementation and space based-constraints, *Atmos Chem Phys Discuss*, 12, 3555–3594.
- Inamdar, S., J. Rupp, and M. Mitchell (2009), Groundwater flushing of solutes at wetland and hillslope positions during storm events in a small glaciated catchment in western New York, USA, *Hydrol. Process.*, 23(13), 1912–1926, doi:10.1002/hyp.7322.
- Jaeglé, L., R. V. Martin, K. Chance, L. Steinberger, T. P. Kurosu, D. J. Jacob, A. I. Modi, V. Yoboué, L. Sigha-Nkamdjou, and C. Galy-Lacaux (2004), Satellite mapping of rain-induced nitric oxide emissions from soils, *J Geophys Res*, 109(D21), D21310.
- Jaeglé, L., L. Steinberger, R. V. Martin, and K. Chance (2005), Global partitioning of NO_x sources using satellite observations: Relative roles of fossil fuel combustion, biomass burning and soil emissions, *Faraday Discuss*, 130, 407–423.
- Janssens, I. A., W. Dieleman, S. Luysaert, J.-A. Subke, M. Reichstein, R. Ceulemans, P. Ciais, A. J. Dolman, J. Grace, and G. Matteucci (2010), Reduction of forest soil respiration in response to nitrogen deposition, *Nat. Geosci.*, 3(5), 315–322.
- Jencso, K. G., B. L. McGlynn, M. N. Gooseff, S. M. Wondzell, K. E. Bencala, and L. A. Marshall (2009), Hydrologic connectivity between landscapes and streams: transferring reach-and plot-scale understanding to the catchment scale, *Water Resour. Res.*, 45(4), W04428.
- Johnson, D. W., and S. E. Lindberg (1992), *Atmospheric deposition and forest nutrient cycling. A synthesis of the Integrated Forest Study.*, Springer-Verlag. 707p.
- Jordan, F. L., J. J. L. Cantera, M. E. Fenn, and L. Y. Stein (2005), Autotrophic ammonia-oxidizing bacteria contribute minimally to nitrification in a nitrogen-impacted forested ecosystem, *Appl. Environ. Microbiol.*, 71(1), 197–206.

- Kaiser, J., M. G. Hastings, B. Z. Houlton, T. Röckmann, and D. M. Sigman (2007), Triple oxygen isotope analysis of nitrate using the denitrifier method and thermal decomposition of N₂O, *Anal. Chem.*, 79(2), 599–607.
- Kaye, J. P., and S. C. Hart (1997), Competition for nitrogen between plants and soil microorganisms, *Trends Ecol. Evol.*, 12(4), 139–143.
- Kelly, C., S. Schoenholtz, and M. Adams (2011), Soil properties associated with net nitrification following watershed conversion from Appalachian hardwoods to Norway spruce, *Plant Soil*, 344(1-2), 361–376, doi:10.1007/s11104-011-0755-5.
- Kelly, C. N. (2010), Carbon and nitrogen cycling in watersheds of contrasting vegetation types in the Fernow Experimental Forest, West Virginia, Doctoral Dissertation, University Libraries, Virginia Polytechnic Institute and State University.
- Kendall, C. (1998), Tracing nitrogen sources and cycling in catchments, in *Isotope tracers in catchment hydrology*, edited by C. Kendall and J. J. McDonnell, pp. 519–576, Elsevier, Amsterdam.
- Kendall, C., and D. H. Doctor (2004), Stable isotope applications in hydrologic studies, in *Surface and Ground Water, Weathering, and Soils*, vol. 5, edited by H. D. Holland and K. K. Turekian, pp. 319–364, Elsevier, Amsterdam.
- Kendall, C., E. M. Elliott, and S. D. Wankel (2007), Tracing anthropogenic inputs of nitrogen to ecosystems, in *Stable isotopes in ecology and environmental science*, vol. 2, edited by R. Michener and K. Lajtha, pp. 375–449, Blackwell Publishing, Oxford.
- Kirchner, J. W. (2003), A double paradox in catchment hydrology and geochemistry, *Hydrol. Process.*, 17(4), 871–874.
- Kirchner, M., G. Jakobi, E. Feicht, M. Bernhardt, and A. Fischer (2005), Elevated NH₃ and NO₂ air concentrations and nitrogen deposition rates in the vicinity of a highway in Southern Bavaria, *Atmos. Environ.*, 39(25), 4531–4542.
- Koba, K., N. Tokuchi, E. Wada, T. Nakajima, and G. Iwatsubo (1997), Intermittent denitrification: The application of a ¹⁵N natural abundance method to a forested ecosystem, *Geochim. Cosmochim. Acta*, 61(23), 5043–5050, doi:10.1016/S0016-7037(97)00284-6.
- Koba, K. et al. (2012), The ¹⁵N natural abundance of the N lost from an N-saturated subtropical forest in southern China, *J. Geophys. Res. Biogeosciences*, 117(G2), G02015, doi:10.1029/2010JG001615.
- Kochenderfer, J. N. (2007), Fernow and the Appalachian hardwood region, in *The Fernow Watershed Acidification Study*, pp. 17–39, Springer, Dordrecht, The Netherlands.

- Kohzu, A., M. Watanabe, S. Hayashi, A. Imai, Y. Nakajima, K. Osaka, and S. Miura (2013), Analysis of nitrate production, mixing, and consumption processes in mountain streams around Mt. Tsukuba using the oxygen and nitrogen isotope ratios of nitrate, *Jpn. J. Limnol.*, 73, 1–16.
- Koopmans, L. H., D. B. Owen, and J. I. Rosenblatt (1964), Confidence intervals for the coefficient of variation for the normal and log normal distributions, *Biometrika*, 51(1-2), 25–32.
- Kothawala, D. N., S. A. Watmough, M. N. Futter, L. Zhang, and P. J. Dillon (2011), Stream nitrate responds rapidly to decreasing nitrate deposition, *Ecosystems*, 14(2), 274–286.
- Li, D., and X. Wang (2008), Nitrogen isotopic signature of soil-released nitric oxide (NO) after fertilizer application, *Atmos. Environ.*, 42(19), 4747–4754.
- Lindberg, S. E., G. M. Lovett, D. D. Richter, and D. W. Johnson (1986), Atmospheric deposition and canopy interactions of major ions in a forest, *Science*, 231, 141–145.
- Linn, D. M., and J. W. Doran (1984), Effect of water-filled pore space on carbon dioxide and nitrous oxide production in tilled and nontilled soils, *Soil Sci. Soc. Am. J.*, 48(6), 1267–1272.
- Lohse, K. A., and P. Matson (2005), Consequences of nitrogen additions for soil losses from wet tropical forests, *Ecol. Appl.*, 15(5), 1629–1648.
- Lovett, G., and C. Goodale (2011), A new conceptual model of nitrogen saturation based on experimental nitrogen addition to an oak forest, *Ecosystems*, 14(4), 615–631, doi:10.1007/s10021-011-9432-z.
- Lovett, G. M., and S. E. Lindberg (1986), Dry deposition of nitrate to a deciduous forest, *Biogeochemistry*, 2(2), 137–148.
- Lovett, G. M., and H. Rueth (1999), Soil nitrogen transformations in beech and maple stands along a nitrogen deposition gradient, *Ecol. Appl.*, 9(4), 1330–1344.
- Lovett, G. M., K. C. Weathers, and M. A. Arthur (2002), Control of nitrogen loss from forested watersheds by soil carbon:nitrogen ratio and tree species composition, *Ecosystems*, 5(7), 0712–0718.
- Lovett, G. M., K. C. Weathers, M. A. Arthur, and J. C. Schultz (2004), Nitrogen cycling in a northern hardwood forest: do species matter?, *Biogeochemistry*, 67(3), 289–308.
- Magill, A. H., J. D. Aber, J. J. Hendricks, R. D. Bowden, J. M. Melillo, and P. A. Steudler (1997), Biogeochemical response of forest ecosystems to simulated chronic nitrogen deposition, *Ecol. Appl.*, 7(2), 402–415.

- Magill, A. H., J. D. Aber, W. S. Currie, K. J. Nadelhoffer, M. E. Martin, W. H. McDowell, J. M. Melillo, and P. Steudler (2004), Ecosystem response to 15 years of chronic nitrogen additions at the Harvard Forest LTER, Massachusetts, USA, *For. Ecol. Manag.*, 196(1), 7–28.
- Magnani, F., M. Mencuccini, M. Borghetti, P. Berbigier, F. Berninger, S. Delzon, A. Grelle, P. Hari, P. G. Jarvis, and P. Kolarik (2007), The human footprint in the carbon cycle of temperate and boreal forests, *Nature*, 447(7146), 849–851.
- Marschner, H., M. Häussling, and E. George (1991), Ammonium and nitrate uptake rates and rhizosphere pH in non-mycorrhizal roots of Norway spruce [*Picea abies* (L.) Karst.], *Trees*, 5(1), 14–21.
- McDonnell, J. J., M. Bonell, M. K. Stewart, and A. J. Pearce (1990), Deuterium variations in storm rainfall: implications for stream hydrograph separation, *Water Resour. Res.*, 26(3), 455–458.
- McDonnell, J. J., K. McGuire, P. Aggarwal, K. J. Beven, D. Biondi, G. Destouni, S. Dunn, A. James, J. Kirchner, and P. Kraft (2010), How old is streamwater? Open questions in catchment transit time conceptualization, modelling and analysis, *Hydrol. Process.*, 24(12), 1745–1754.
- McGlynn, B. L., J. J. McDonnell, J. B. Shanley, and C. Kendall (1999), Riparian zone flowpath dynamics during snowmelt in a small headwater catchment, *J. Hydrol.*, 222(1), 75–92, doi:10.1016/S0022-1694(99)00102-X.
- McNeil, B. E., J. M. Read, and C. T. Driscoll (2007), Foliar nitrogen responses to elevated atmospheric nitrogen deposition in nine temperate forest canopy species, *Environ. Sci. Technol.*, 41(15), 5191–5197.
- Michalski, G., and F. Xu (2010), Isotope modeling of nitric acid formation in the atmosphere using ISO-RACM: testing the importance of NO oxidation, heterogeneous reactions, and trace gas chemistry, *Atmospheric Chem. Phys. Discuss.*, 10(3), 6829–6869.
- Michalski, G., Z. Scott, M. Kabling, and M. H. Thiemens (2003), First measurements and modeling of $\Delta^{17}\text{O}$ in atmospheric nitrate, *Geophys. Res. Lett.*, 30(16), 1870.
- Michalski, G., T. Meixner, M. Fenn, L. Hernandez, A. Sirulnik, E. Allen, and M. Thiemens (2004), Tracing atmospheric nitrate deposition in a complex semiarid ecosystem using $\Delta^{17}\text{O}$, *Environ. Sci. Technol.*, 38(7), 2175–2181, doi:10.1021/es034980+.
- Michalski, G., S. K. Bhattacharya, and G. Girsch (2013), NO_x cycle and tropospheric ozone isotope anomaly: an experimental investigation, *Atmospheric Chem. Phys. Discuss.*, 13(4), 9443–9483.

- Min, X., M. Y. Siddiqi, R. D. Guy, A. D. M. Glass, and H. J. Kronzucker (1998), Induction of nitrate uptake and nitrate reductase activity in trembling aspen and lodgepole pine, *Plant Cell Environ.*, 21(10), 1039–1046.
- Mitchell, M. J. (2001), Linkages of nitrate losses in watersheds to hydrological processes, *Hydrol. Process.*, 15(17), 3305–3307.
- Mitchell, M. J., G. Iwatsubo, K. Ohrui, and Y. Nakagawa (1997), Nitrogen saturation in Japanese forests: an evaluation, *For. Ecol. Manag.*, 97(1), 39–51, doi:10.1016/S0378-1127(97)00047-9.
- Mitchell, M. J., K. B. Piatek, S. Christopher, B. Mayer, C. Kendall, and P. McHale (2006), Solute sources in stream water during consecutive fall storms in a northern hardwood forest watershed: a combined hydrological, chemical and isotopic approach, *Biogeochemistry*, 78(2), 217–246.
- Morin, S., J. Savarino, M. M. Frey, F. Domine, H.-W. Jacobi, L. Kaleschke, and J. M. Martins (2009), Comprehensive isotopic composition of atmospheric nitrate in the Atlantic Ocean boundary layer from 65 S to 79 N, *J. Geophys. Res. Atmospheres 1984–2012*, 114(D5).
- Morin, S., R. Sander, and J. Savarino (2011), Simulation of the diurnal variations of the oxygen isotope anomaly ($\Delta^{17}\text{O}$) of reactive atmospheric species, *Atmospheric Chem. Phys.*, 11(8), 3653–3671.
- Morino, Y., Y. Kondo, N. Takegawa, Y. Miyazaki, K. Kita, Y. Komazaki, M. Fukuda, T. Miyakawa, N. Moteki, and D. R. Worsnop (2006), Partitioning of HNO_3 and particulate nitrate over Tokyo: effect of vertical mixing, *J. Geophys. Res. Atmospheres 1984–2012*, 111(D15).
- Murdoch, P. S., and J. L. Stoddard (1992), The role of nitrate in the acidification of streams in the Catskill Mountains of New York, *Water Resour. Res.*, 28(10), 2707–2720.
- Nakamura, T., K. Osaka, Y. Hiraga, and F. Kazama (2011), Nitrogen and oxygen isotope composition of nitrate in streamwater of Fuji River basin, *J. Jpn. Assoc. Hydrol. Sci.*, 41(3), 79–89.
- National Atmospheric Deposition Program (2011), *National Atmospheric Deposition Program 2010 Annual Summary*, Illinois State Water Survey, Urbana IL.
- National Atmospheric Deposition Program (2014), Annual National Trends Network Maps, Available from: nadp.isws.illinois.edu (Accessed 19 June 2014)
- National Oceanic and Atmospheric Administration (NOAA) (2010a), National Climatic Data Center, State of the Climate: Wildfires for July 2010, Available from: <http://www.ncdc.noaa.gov/sotc/fire/2010/7> (Accessed 12 December 2012)

- National Oceanic and Atmospheric Administration (NOAA) (2010b), National Climatic Data Center, State of the Climate: Wildfires for September 2010, Available from: <http://www.ncdc.noaa.gov/sotc/fire/2010/9> (Accessed 12 December 2012)
- Nave, L. E., E. D. Vance, C. W. Swanston, and P. S. Curtis (2009), Impacts of elevated N inputs on north temperate forest soil C storage, C/N, and net N-mineralization, *Geoderma*, 153(1), 231–240.
- Nolan, B., K. Hitt, and B. Ruddy (2002), Probability of nitrate contamination of recently recharged groundwaters in the conterminous United States., *Environ. Sci. Technol.*, 36(10), 2138–45.
- Norton, J. M., and J. M. Stark (2011), Regulation and measurement of nitrification in terrestrial systems, *Methods Enzym.*, 486, 343–368.
- Ogawa, A., H. Shibata, K. Suzuki, M. J. Mitchell, and Y. Ikegami (2006), Relationship of topography to surface water chemistry with particular focus on nitrogen and organic carbon solutes within a forested watershed in Hokkaido, Japan, *Hydrol. Process.*, 20(2), 251–265.
- Ohte, N. (2012), Implications of seasonal variation in nitrate export from forested ecosystems: a review from the hydrological perspective of ecosystem dynamics, *Ecol. Res.*, 27(4), 657–665.
- Ohte, N., S. D. Sebestyen, J. B. Shanley, D. H. Doctor, C. Kendall, S. D. Wankel, and E. W. Boyer (2004), Tracing sources of nitrate in snowmelt runoff using a high-resolution isotopic technique, *Geophys. Res. Lett.*, 31(21), L21506, doi:10.1029/2004GL020908.
- Ohte, N., I. Tayasu, A. Kohzu, C. Yoshimizu, K. Osaka, A. Makabe, K. Koba, N. Yoshida, and T. Nagata (2010), Spatial distribution of nitrate sources of rivers in the Lake Biwa watershed, Japan: controlling factors revealed by nitrogen and oxygen isotope values, *Water Resour. Res.*, 46(7), W07505.
- Osaka, K., N. Ohte, K. Koba, C. Yoshimizu, M. Katsuyama, M. Tani, I. Tayasu, and T. Nagata (2010), Hydrological influences on spatiotemporal variations of $\delta^{15}\text{N}$ and $\delta^{18}\text{O}$ of nitrate in a forested headwater catchment in central Japan: Denitrification plays a critical role in groundwater, *J. Geophys. Res. Biogeosciences*, 115(G2), G02021, doi:10.1029/2009JG000977.
- Pacific, V., K. Jencso, and B. McGlynn (2010), Variable flushing mechanisms and landscape structure control stream DOC export during snowmelt in a set of nested catchments, *Biogeochemistry*, 99(1-3), 193–211, doi:10.1007/s10533-009-9401-1.
- Pardo, L. H., C. Kendall, J. Pett-Ridge, and C. C. Y. Chang (2004), Evaluating the source of streamwater nitrate using $\delta^{15}\text{N}$ and $\delta^{18}\text{O}$ in nitrate in two watersheds in New Hampshire, USA, *Hydrol. Process.*, 18(14), 2699–2712, doi:10.1002/hyp.5576.

- Pardo, L. H. et al. (2006), Regional assessment of N saturation using foliar and root $\delta^{15}\text{N}$, *Biogeochemistry*, 80(2), 143–171, doi:10.1007/s10533-006-9015-9.
- Pardo, L. H., M. J. Robin-Abbott, and C. T. Driscoll (2011), Assessment of nitrogen deposition effects and empirical critical loads of nitrogen for ecoregions of the United States, *Gen Tech Rep NRS-80 Newtown Sq. PA US Dep. Agric. For. Serv. North. Res. Stn. 291 P.*
- Parker, G. G. (1983), Throughfall and stemflow in the forest nutrient cycle, *Adv. Ecol. Res.*, 13, 57–133.
- Pellerin, B. A., J. F. Saraceno, J. B. Shanley, S. D. Sebestyen, G. R. Aiken, W. M. Wollheim, and B. A. Bergamaschi (2012), Taking the pulse of snowmelt: in situ sensors reveal seasonal, event and diurnal patterns of nitrate and dissolved organic matter variability in an upland forest stream, *Biogeochemistry*, 108(1), 183–198.
- Perakis, S. S., J. E. Compton, and L. O. Hedin (2005), Nitrogen retention across a gradient of 15N additions to an unpolluted temperate forest soil in Chile, *Ecology*, 86(1), 96–105.
- Peterjohn, W. T., M. B. Adams, and F. S. Gilliam (1996), Symptoms of nitrogen saturation in two central Appalachian hardwood forest ecosystems, *Biogeochemistry*, 35(3), 507–522.
- Peterjohn, W. T., C. J. Foster, M. J. Christ, and M. B. Adams (1999), Patterns of nitrogen availability within a forested watershed exhibiting symptoms of nitrogen saturation, *For. Ecol. Manag.*, 119(1-3), 247–257, doi:doi: DOI: 10.1016/S0378-1127(98)00526-X.
- Piatek, K., M. Mitchell, S. Silva, and C. Kendall (2005), Sources of nitrate in snowmelt discharge: evidence from water chemistry and stable isotopes of nitrate, *Water. Air. Soil Pollut.*, 165(1-4), 13–35, doi:10.1007/s11270-005-4641-8.
- Piatek, K. B., P. Munasinghe, W. T. Peterjohn, M. B. Adams, and J. R. Cumming (2010), A decrease in oak litter mass changes nutrient dynamics in the litter layer of a central hardwood forest, *North. J. Appl. For.*, 27(3), 97–104.
- Rastetter, E. B., B. L. Kwiatkowski, and R. B. McKane (2005), A stable isotope simulator that can be coupled to existing mass balance models, *Ecol. Appl.*, 15(5), 1772–1782, doi:10.1890/04-0643.
- Redling, K., E. Elliott, D. Bain, and J. Sherwell (2013), Highway contributions to reactive nitrogen deposition: tracing the fate of vehicular NO_x using stable isotopes and plant biomonitors, *Biogeochemistry*, 116, 261–274.
- Reinhart, K. G., A. Eschner, and G. R. Trimble (1963), Effect on streamflow of four forest practices in the mountains of West Virginia, *Res. Pap. NE-1.*
- Revesz, K., and J.-K. Böhlke (2002), Comparison of ^{18}O measurements in nitrate by different combustion techniques, *Anal. Chem.*, 74(20), 5410–5413.

- Robinson, D. (2001), $\delta^{15}\text{N}$ as an integrator of the nitrogen cycle, *Trends Ecol. Evol.*, 16(3), 153–162.
- Ross, D. S., G. B. Lawrence, and G. Fredriksen (2004), Mineralization and nitrification patterns at eight northeastern USA forested research sites, *For. Ecol. Manag.*, 188(1), 317–335.
- Ross, D. S., S. W. Bailey, G. B. Lawrence, J. B. Shanley, G. Fredriksen, A. E. Jamison, and P. A. Brousseau (2011), Near-surface soil carbon, carbon/nitrogen ratio, and tree species are tightly linked across northeastern United States watersheds, *For. Sci.*, 57(6), 460–469.
- van der Salm, C., W. De Vries, G. J. Reinds, and N. B. Dise (2007), N leaching across European forests: derivation and validation of empirical relationships using data from intensive monitoring plots, *For. Ecol. Manag.*, 238(1), 81–91.
- SAS Institute, Inc. (2011), *SAS/STAT user's guide: Statistics, Release 9.3 edition.*, SAS Institute, Inc., Cary, NC.
- Savarino, J., J. Kaiser, S. Morin, D. M. Sigman, and M. H. Thieme (2007), Nitrogen and oxygen isotopic constraints on the origin of atmospheric nitrate in coastal Antarctica, *Atmospheric Chem. Phys.*, 7(8), 1925–1945.
- Schiff, S. L., K. J. Devito, R. J. Elgood, P. M. McCrindle, J. Spoelstra, and P. Dillon (2002), Two adjacent forested catchments: dramatically different NO_3^- export, *Water Resour. Res.*, 38(12), 1292, doi:10.1029/2000WR000170.
- De Schrijver, A., G. Geudens, L. Augusto, J. Staelens, J. Mertens, K. Wuyts, L. Gielis, and K. Verheyen (2007), The effect of forest type on throughfall deposition and seepage flux: a review, *Oecologia*, 153(3), 663–674.
- Sebestyen, S. D., E. W. Boyer, J. B. Shanley, C. Kendall, D. H. Doctor, G. R. Aiken, and N. Ohte (2008), Sources, transformations, and hydrological processes that control stream nitrate and dissolved organic matter concentrations during snowmelt in an upland forest, *Water Resour. Res.*, 44, W12410.
- Sebestyen, S. D., J. B. Shanley, E. W. Boyer, C. Kendall, and D. H. Doctor (2014), Coupled hydrological and biogeochemical processes controlling variability of nitrogen species in streamflow during autumn in an upland forest, *Water Resour. Res.*, doi:10.1002/2013WR013670.
- Seinfeld, J. H., and S. N. Pandis (2006), *Atmospheric Chemistry and Physics*, John Wiley & Sons, Hoboken, NJ. 1326 p.
- Seitzinger, S., J. A. Harrison, J. K. Böhlke, A. F. Bouwman, R. Lowrance, B. Peterson, C. Tobias, and G. V. Drecht (2006), Denitrification across landscapes and waterscapes: a synthesis, *Ecol. Appl.*, 16(6), 2064–2090.

- Shearer, G., and D. H. Kohl (1986), N₂-fixation in field settings: estimations based on natural ¹⁵N abundance, *Funct. Plant Biol.*, 13(6), 699–756.
- Sidle, R. C., Y. Tsuboyama, S. Noguchi, I. Hosoda, M. Fujieda, and T. Shimizu (2000), Stormflow generation in steep forested headwaters: a linked hydrogeomorphic paradigm, *Hydrol. Process.*, 14(3), 369–385.
- Sigman, D. M., K. L. Casciotti, M. Andreani, C. Barford, M. Galanter, and J. K. Böhlke (2001), A bacterial method for the nitrogen isotopic analysis of nitrate in seawater and freshwater, *Anal. Chem.*, 73(17), 4145–4153.
- Snider, D. M., J. Spoelstra, S. L. Schiff, and J. J. Venkiteswaran (2010), Stable oxygen isotope ratios of nitrate produced from nitrification: ¹⁸O-labeled water incubations of agricultural and temperate forest soils, *Environ. Sci. Technol.*, 44(14), 5358–5364.
- Speiran, G. K. (2010), Effects of groundwater-flow paths on nitrate concentrations across two riparian forest corridors, *JAWRA J. Am. Water Resour. Assoc.*, 46(2), 246–260.
- Spoelstra, J., S. L. Schiff, R. J. Elgood, R. G. Semkin, and D. S. Jeffries (2001), Tracing the sources of exported nitrate in the Turkey Lakes Watershed using ¹⁵N/¹⁴N and ¹⁸O/¹⁶O isotopic ratios, *Ecosystems*, 4(6), 536–544, doi:10.1007/s10021-001-0027-y.
- Spoelstra, J., S. L. Schiff, P. W. Hazlett, D. S. Jeffries, and R. G. Semkin (2007), The isotopic composition of nitrate produced from nitrification in a hardwood forest floor, *Geochim. Cosmochim. Acta*, 71(15), 3757–3771.
- Stark, J. (1996), Modeling the temperature response of nitrification, *Biogeochemistry*, 35(3), 433–445, doi:10.1007/BF02183035.
- Stark, J. M., and M. K. Firestone (1995), Mechanisms for soil moisture effects on activity of nitrifying bacteria, *Appl. Environ. Microbiol.*, 61(1), 218–221.
- Stark, J. M., and S. C. Hart (1997), High rates of nitrification and nitrate turnover in undisturbed coniferous forests, *Nature*, 385(6611), 61–64, doi:10.1038/385061a0.
- Stark, J. M., D. R. Smart, S. C. Hart, and K. A. Haubensak (2002), Regulation of nitric oxide emissions from forest and rangeland soils of western North America, *Ecology*, 83(8), 2278–2292.
- Steinkamp, J., L. N. Ganzeveld, W. Wilcke, and M. G. Lawrence (2008), Influence of modelled soil biogenic NO emissions on related trace gases and the atmospheric oxidizing efficiency, *Atmospheric Chem. Phys. Discuss.*, 8(3), 10227–10255.
- Stoddard, J. L. (1994), Long-term changes in watershed retention of nitrogen. Its causes and aquatic consequences, in *Environmental Chemistry of Lakes and Reservoirs*, edited by L. Baker, pp. 223–284, American Chemical Society, Washington, DC.

- Tabayashi, Y., and K. Koba (2011), Heterogeneous atmospheric nitrogen deposition effects upon the nitrate concentration of stream waters in a forested mountain area, *Water, Air, Soil Pollut.*, 216(1-4), 105–115.
- Tague, C. L., and L. E. Band (2004), RHESSys: Regional Hydro-Ecologic Simulation System--an object-oriented approach to spatially distributed modeling of carbon, water, and nutrient cycling., *Earth Interact.*, 8(1).
- Taylor, P. G., and A. R. Townsend (2010), Stoichiometric control of organic carbon–nitrate relationships from soils to the sea, *Nature*, 464(7292), 1178–1181.
- Taylor, S. B. (1999), Geomorphic controls on sediment-transport efficiency in the central Appalachians: a comparative analysis of three watersheds underlain by the Acadian Clastic Wedge, West Virginia University Libraries.
- Templer, P. H., and T. E. Dawson (2004), Nitrogen uptake by four tree species of the Catskill Mountains, New York: implications for forest N dynamics, *Plant Soil*, 262(1-2), 251–261.
- Templer, P. H., and T. M. McCann (2010), Effects of the hemlock woolly adelgid on nitrogen losses from urban and rural northern forest ecosystems, *Ecosystems*, 13(8), 1215–1226.
- Templer, P. H., G. M. Lovett, K. C. Weathers, S. E. Findlay, and T. E. Dawson (2005), Influence of tree species on forest nitrogen retention in the Catskill Mountains, New York, USA, *Ecosystems*, 8(1), 1–16.
- Templer, P. H., M. A. Arthur, G. M. Lovett, and K. C. Weathers (2007), Plant and soil natural abundance $\delta^{15}\text{N}$: indicators of relative rates of nitrogen cycling in temperate forest ecosystems, *Oecologia*, 153(2), 399–406.
- Thomas, R. Q., C. D. Canham, K. C. Weathers, and C. L. Goodale (2010), Increased tree carbon storage in response to nitrogen deposition in the US, *Nat. Geosci.*, 3(1), 13–17.
- Tietema, A. (1998), Microbial carbon and nitrogen dynamics in coniferous forest floor material collected along a European nitrogen deposition gradient, *Whole Ecosyst. Exp. NITREX EXMAN Proj.*, 101(1–3), 29–36, doi:10.1016/S0378-1127(97)00122-9.
- Tobari, Y., K. Koba, K. Fukushima, N. Tokuchi, N. Ohte, R. Tateno, S. Toyoda, T. Yoshioka, and N. Yoshida (2010), Contribution of atmospheric nitrate to stream-water nitrate in Japanese coniferous forests revealed by the oxygen isotope ratio of nitrate, *Rapid Commun. Mass Spectrom.*, 24(9), 1281–1286.
- Todd, R. L., W. T. Swank, J. E. Douglass, P. C. Kerr, D. L. Brockway, and C. D. Monk (1975), The relationship between nitrate concentration in the southern Appalachian Mountain streams and terrestrial nitrifiers, *Agro-Ecosyst.*, 2(2), 127–132.

- Tsunogai, U., D. Komatsu, S. Daita, G. Kazemi, F. Nakagawa, I. Noguchi, and J. Zhang (2010), Tracing the fate of atmospheric nitrate deposited onto a forest ecosystem in Eastern Asia using $\Delta^{17}\text{O}$, *Atmos Chem Phys Discuss*, 10, 1809–1820.
- U.S. EPA CASTNET (2012), *2010 Annual Report*, Annual Report, U.S. Environmental Protection Agency.
- Ullah, S., and T. R. Moore (2009), Soil drainage and vegetation controls of nitrogen transformation rates in forest soils, southern Quebec, *J. Geophys. Res.*, 114(G1), G01014.
- Venterea, R. T., P. M. Groffman, M. S. Castro, L. V. Verchot, I. J. Fernandez, and M. B. Adams (2004), Soil emissions of nitric oxide in two forest watersheds subjected to elevated N inputs, *For. Ecol. Manag.*, 196(2), 335–349.
- Vicars, W. C. et al. (2013), Spatial and diurnal variability in reactive nitrogen oxide chemistry as reflected in the isotopic composition of atmospheric nitrate: Results from the CalNex 2010 field study, *J. Geophys. Res. Atmospheres*, 118(18), 10,567–10,588, doi:10.1002/jgrd.50680.
- Vidon, P., C. Allan, D. Burns, T. P. Duval, N. Gurwick, S. Inamdar, R. Lowrance, J. Okay, D. Scott, and S. Sebestyen (2010), Hot spots and hot moments in riparian zones: potential for improved water quality management, *J. Am. Water Resour. Assoc.*, 46(2), 278–298.
- Vidon, P. G. F., and A. R. Hill (2004), Landscape controls on nitrate removal in stream riparian zones, *Water Resour. Res.*, 40(3), W03201, doi:10.1029/2003WR002473.
- Vitousek, P. M., and W. A. Reiners (1975), Ecosystem succession and nutrient retention: a hypothesis, *BioScience*, 376–381.
- Vitousek, P. M., J. D. Aber, R. W. Howarth, G. E. Likens, P. A. Matson, D. W. Schindler, W. H. Schlesinger, and D. G. Tilman (1997), Human alteration of the global nitrogen cycle: sources and consequences, *Ecol. Appl.*, 7(3), 737–750.
- Wang, Y., M. B. McElroy, R. V. Martin, D. G. Streets, Q. Zhang, and T. M. Fu (2007), Seasonal variability of NO_x emissions over east China constrained by satellite observations: Implications for combustion and microbial sources, *J. Geophys. Res.*, 112(D6), D06301.
- Wankel, S. D., Y. Chen, C. Kendall, A. F. Post, and A. Paytan (2010), Sources of aerosol nitrate to the Gulf of Aqaba: Evidence from $\delta^{15}\text{N}$ and $\delta^{18}\text{O}$ of nitrate and trace metal chemistry, *Mar. Chem.*, 120(1), 90–99.
- Webb, J. R., B. J. Cosby, F. A. Deviney, J. N. Galloway, S. W. Maben, and A. J. Bulger (2004), Are brook trout streams in western Virginia and Shenandoah National Park recovering from acidification?, *Environ. Sci. Technol.*, 38(15), 4091–4096.

- Williard, K. W., D. R. DeWalle, P. J. Edwards, and R. R. Schnabel (1997), Indicators of nitrate export from forested watersheds of the mid-Appalachians, United States of America, *Glob. Biogeochem. Cycles*, 11(4), 649–656.
- Williard, K. W., D. R. DeWalle, P. J. Edwards, and W. E. Sharpe (2001), ^{18}O isotopic separation of stream nitrate sources in mid-Appalachian forested watersheds, *J. Hydrol.*, 252(1), 174–188.
- Xue, D., B. De Baets, J. Botte, J. Vermeulen, O. Van Cleemput, and P. Boeckx (2010), Comparison of the silver nitrate and bacterial denitrification methods for the determination of nitrogen and oxygen isotope ratios of nitrate in surface water, *Rapid Commun. Mass Spectrom.*, 24(6), 833–840.
- Yang, J.-Y., S.-C. Hsu, M. Dai, S.-Y. Hsiao, and S.-J. Kao (2013), Isotopic composition of water-soluble nitrate in bulk atmospheric deposition at Dongsha Island: sources and implications of external N supply to the northern South China Sea, *Biogeosciences Discuss.*, 10(6), 9661–9695.
- Zarnetske, J. P., R. Haggerty, S. M. Wondzell, and M. A. Baker (2011), Labile dissolved organic carbon supply limits hyporheic denitrification, *J. Geophys. Res. Biogeosciences* 2005–2012, 116(G4).
- Zhang, Y., J. Liu, Y. Mu, S. Pei, X. Lun, and F. Chai (2011), Emissions of nitrous oxide, nitrogen oxides and ammonia from a maize field in the North China Plain, *Atmos. Environ.*, 45(17), 2956–2961.